Terms and Conditions of Use of Digitised Theses from Trinity College Library Dublin

Copyright statement

All material supplied by Trinity College Library is protected by copyright (under the Copyright and Related Rights Act, 2000 as amended) and other relevant Intellectual Property Rights. By accessing and using a Digitised Thesis from Trinity College Library you acknowledge that all Intellectual Property Rights in any Works supplied are the sole and exclusive property of the copyright and/or other IPR holder. Specific copyright holders may not be explicitly identified. Use of materials from other sources within a thesis should not be construed as a claim over them.

A non-exclusive, non-transferable licence is hereby granted to those using or reproducing, in whole or in part, the material for valid purposes, providing the copyright owners are acknowledged using the normal conventions. Where specific permission to use material is required, this is identified and such permission must be sought from the copyright holder or agency cited.

Liability statement

By using a Digitised Thesis, I accept that Trinity College Dublin bears no legal responsibility for the accuracy, legality or comprehensiveness of materials contained within the thesis, and that Trinity College Dublin accepts no liability for indirect, consequential, or incidental, damages or losses arising from use of the thesis for whatever reason. Information located in a thesis may be subject to specific use constraints, details of which may not be explicitly described. It is the responsibility of potential and actual users to be aware of such constraints and to abide by them. By making use of material from a digitised thesis, you accept these copyright and disclaimer provisions. Where it is brought to the attention of Trinity College Library that there may be a breach of copyright or other restraint, it is the policy to withdraw or take down access to a thesis while the issue is being resolved.

Access Agreement

By using a Digitised Thesis from Trinity College Library you are bound by the following Terms & Conditions. Please read them carefully.

I have read and I understand the following statement: All material supplied via a Digitised Thesis from Trinity College Library is protected by copyright and other intellectual property rights, and duplication or sale of all or part of any of a thesis is not permitted, except that material may be duplicated by you for your research use or for educational purposes in electronic or print form providing the copyright owners are acknowledged using the normal conventions. You must obtain permission for any other use. Electronic or print copies may not be offered, whether for sale or otherwise to anyone. This copy has been supplied on the understanding that it is copyright material and that no quotation from the thesis may be published without proper acknowledgement.

An Examination of the Parameters Involved in the Design of a Continuous Flow Solar Disinfection Process

Submitted in fulfilment of the requirements for the award of the degree of
Doctor of Philosophy

By

Orlaith Ann McLoughlin

B.A., B.A.I. Civil Structural and Environmental Engineering
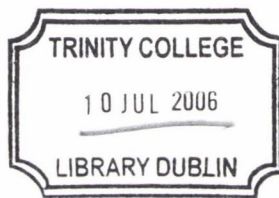
Under the supervision of

Laurence Gill (Trinity College, Dublin)

Department of Civil, Structural and Environmental Engineering

Trinity College, Dublin

2006

Declaration

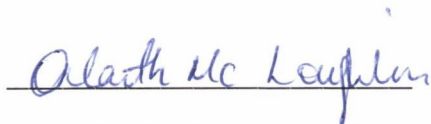I declare that the present work has not been submitted as an exercise for a degree at any other university. This thesis consists entirely of my own work except where references indicate otherwise.

I agree that the library of the University of Dublin, Trinity College, Dublin, may lend or copy this thesis upon request.

Orlaith Ann McLoughlin

This thesis is dedicated to the memory of Professor Simon Perry

Acknowledgements

Abstract

The aim of this research was to assess a number of parameters that affect the continuous flow solar disinfection process. Solar disinfection involves harnessing natural sunlight in order to inactivate microbial pathogens from drinking water sources. Most previous research has involved a batch system using transparent containers to expose contaminated water to natural solar radiation. During the course of this project a number of continuous flow reactors were used- small-scale reactors using reflectors of different shapes, Parabolic, Compound Parabolic and V-groove, along with a pilot-scale reactor, which was Compound Parabolic.

Initially a number of experiments were performed using the small-scale parabolic reactor and simulated solar radiation. *Escherichia coli* K-12 was used as the test organism in all experiments (with the exception of those trials assessing the relative resistance of different pathogens to solar disinfection). Parameters examined included flow regime, the incident solar radiation intensity, the effect of these different intensities on different organisms, a comparison of tubing type and a comparison between batch process solar disinfection and continuous flow solar disinfection. Each set of experiments was assessed by determining the inactivation kinetics under each condition and comparing these against a baseline condition.

A comparison of different small-scale reactors was made under simulated solar radiation, natural solar radiation of high intensity in southern Spain and natural solar radiation of low intensity in Ireland. Each of the three reactors, each of 1 litre capacity was compared to a non-reflective reactor, which acted as a baseline. The order of efficiency of the four reactors used was found to be the Compound Parabolic, the Parabolic and the V-groove with the non-reflective reactor being least efficient in all cases. A comparison between simulated and natural solar radiation showed inactivation kinetics to be much enhanced under natural solar conditions. The small-scale reactors of capacity 1 litre were also compared with a pilot-scale reactor, which had a capacity of 35 litres. This showed that the small-scale Compound Parabolic reactor was more efficient when disinfection efficiency was assessed with respect to dose. A comparison between two different collector areas was also made using the pilot-scale reactor where, contrary to previous studies, a smaller illuminated area yielded more efficient results.

Titanium dioxide (TiO_2) was used as a photocatalyst in order to enhance the solar disinfection process in both the pilot-scale (using a suspended catalyst) and the small-scale Compound Parabolic (using a fixed catalyst on glass and paper) reactors. The

catalyst was shown to induce a slight enhancement to the solar disinfection process. The regrowth capacity of the *E. coli* K-12 was also assessed in both the solar disinfection and solar photocatalytic disinfection process. No regrowth was apparent in either system.

The effect of increased temperature and different volumes on the solar disinfection process was also assessed. It was found that a synergistic effect between temperature and solar radiation was apparent at temperatures in excess of 45°. It was found that a 1 litre volume produced more efficient inactivation kinetics than a 0.4 litre volume in the same amount of time. This also contradicts the literature and suggests that there may be a mechanism other than dose acting on the bacteria.

Several of the experimental results throughout the thesis indicated that a mechanism other than the classical UV dose dependent kinetics might be operating on the system. One proposed explanation was that the recirculation of the bacteria into the reservoir (effectively a dark zone) in a continuous flow reactor might induce a stress on the bacteria. The proposed stroboscopic mechanism was also examined by a series of "flashes" or dark zones being introduced into both reactors (batch and continuous flow) to examine the effect. It was found that a both a series of short flashes and a long dark period enhanced the solar disinfection kinetics, suggesting that an optimum balance exists between frequency of flash, length of flash and a following dark period.

Finally, an effort was made to use the inactivation kinetics found during this project to design a full-scale system for water supply for a village in a developing country. A series of design charts were compiled suitable for field use in developing countries.

The use of continuous flow solar disinfection is a novel and appropriate way to harness the sun's energy to produce clean water, it is of interest particularly in developing countries which tend to have an abundance of sunshine.

Table of Contents

3   Materials and Methods

4   Simulated Solar Radiation

5   Comparison of Solar Disinfection Reactors

6 Solar Photocatalytic Disinfection

7 Other Factors which Effect the Solar Disinfection Process

8 The Stroboscopic Mechanism

CHAPTER 1

INTRODUCTION

1.1 Introduction

"Access to safe water is a fundamental human need and, therefore, a basic human right. Contaminated water jeopardises both the physical and social health of all people. It is an affront to human dignity"

Kofi Annan, 2002.

The combination of safe drinking water and hygienic sanitation facilities is a precondition for health. Yet one person in six, more than one billion people have little or no choice than to use potentially harmful sources of water. As a consequence, 2.2 million people in developing countries, most of them children, die each year from diseases associated with a lack of safe drinking water, inadequate sanitation and poor hygiene. The World Health Organisation (WHO) global estimate of the number of deaths from infectious diarrhoeas in the year 2001 amounts to 2 million for all age groups with a heavy toll among children under five - an estimated 1.4 million deaths. The cluster of ill-health is even more insidious in its impact on the economics of countries and on livelihoods at household level. Water-associated diseases hit the poor in a disproportionate way and this burden of ill health maintains the vicious cycle in which poverty leads to more ill-health and more ill-health implies further impoverishment (UNESCO, 2003). Most countries with no access to improved drinking water sources lie in the tropical belt where there is an abundance of sunshine and so are ideally suited to simple technologies which harness the sun in order to provide clean water.

1.2 Solar Disinfection

The potential for solar-based drinking water treatment processes has been explored by researchers since 1878 by Downes and Blunt and research has intensified since the 1990s (Acra *et al.*, 1989; Vidal and Diaz, 2000; Goswami, 1995, 1997; Cooper and Goswami, 1998 a, b) with studies focusing on both solar distillation and solar disinfection.

Solar distillation uses sunlight to heat water and produce water vapour, which is then condensed back to water. Impurities such as salts, heavy metals and bacteria will not evaporate and are left behind. Although solar water distillation is effective and solar energy is clean, safe and viable in many countries, it has not found widespread use due to high capital investment (Simate, 2001). Systems that directly heat water have been found

to be effective in the inactivation of *Salmonella typhimurium*, *Streptococcus faecalis* and *Escherichia coli* (Jørgenson *et al.*, 1998).

The germicidal effect of sunlight has long been known. Between 1877 and 1895 a remarkable set of studies revealed that sunlight, especially the UV-violet-blue rays, was capable of killing many different types of bacteria (Hockberger, 2000). Solar disinfection occurs when a photon of sunlight (of an appropriate wavelength) is absorbed by a molecule present in the contaminated water. This causes a photochemical reaction which disrupts the components of that molecule, usually its DNA. The focus of most solar disinfection studies has been batch systems such as SODIS. This method involves storing contaminated water in transparent vessels such as bottles or bags and exposing them to sunlight for periods of up to eight hours. This technique has shown to be effective against a wide range of organisms such as *E. coli*, *S. typhimurium* and *V. cholerae* (Ibáñez *et al.*, 2003; Sommer *et al.*, 1992). The SODIS treatment method is based on the synergistic effect of both water temperature and UVA radiation (EAWAG). The uptake of this technology has been spreading and proving successful. For example, between December 1995 and March 1996 a controlled field trial was carried out in Kenya to assess the health benefit of using SODIS bottles which found that solar treatment of drinking water was found to significantly reduce episodes of diarrhoea (Conroy *et al.*, 1996).

Photocatalysis may be defined as the acceleration of a photoreaction by the presence of a catalyst (Blanco, 2003). There have been several attempts to enhance the solar disinfection process by encouraging these photocatalytic processes in the water by the addition of titanium dioxide (TiO_2) and a number of researchers have used TiO_2 to enhance the batch solar disinfection process (Salih, 2002; Watts, 1995; Matsunga, 1995; Huang, 2000; Ibanez, 2003; Dunlop *et al.*, 2002) in both suspended and fixed forms.

To date research into continuous flow systems for disinfection purposes has been limited with two main studies carried out by Acra *et al.* (1990) and Vidal and Diaz (2000). In the past solar continuous flow systems have mainly been used for detoxification of chemicals by photocatalytic processes. Both studies reported that sunlight was effective in the inactivation of faecal coliforms, *S. faecalis* and *E. coli* (Acra *et al.*, 1989; Vidal and Diaz, 2000).

The aim of this project was to characterise the solar disinfection process in order to design a continuous flow system for use in developing countries.

1.3 Scope of this Thesis

This project aims to assess the many parameters associated with solar disinfection and to compare different solar disinfection processes and reactors. Below is an outline of this thesis with a short description of each section.

Section 2 describes the problems associated with drinking water in the developing world as well as conventional techniques used to improve drinking water quality. This is followed by a discussion on previous studies on the solar disinfection process including enhancements with TiO_2.

Section 3 begins with a discussion on solar collector technology and materials which are useful in solar reactors. A full description of all the solar disinfection reactors used in this project and the materials used in their fabrication is made along with describing the experimental set-up of the trials included in this project. Analytical and statistical methods are also described.

Section 4 describes preliminary experiments carried out under simulated sunlight including assessment of flow regime, simulated solar intensity, indicator organisms and tubing type. A comparison between batch process solar disinfection and continuous flow solar disinfection is also made. All experiments in this section were carried out using a small-scale parabolic solar disinfection reactor.

Section 5 describes experiments which compare different solar disinfection reactors. These include efficiency comparisons under both simulated and natural sunlight (both in Ireland and southern Spain) using different small-scale reactors each with a different reflector profile; a Compound Parabolic, Parabolic, V-groove and Non-reflecting reactor. A comparison of disinfection under simulated and natural solar radiation is also made. A comparison between the small-scale Compound Parabolic reactor and a larger pilot-scale reactor is made as well as an assessment of the effect of changing the area of reactor exposed to sunlight.

Section 6 explores the concept of the introduction of a photocatalyst (TiO_2) into the solar disinfection process. TiO_2 is assessed in suspended form as well as in two separate fixed

forms. An assessment of the regrowth capacity of solar inactivated bacteria is also made in both a photocatalytic system and one with no catalyst included.

Section 7 discusses other factors which could affect the solar disinfection process such as change in reactor volume or change in temperature within the system.

Section 8 discusses the effect of dark zones within a reactor. Experiments were carried out with different dark-illuminated ratios in order to assess whether mechanisms other than dose affect the solar disinfection process.

Section 9 provides a simplified method for the design of a full-scale system based on the results found in the previous sections.

Section 10 is a summary of the conclusions drawn in each section as well as recommendations for future work.

CHAPTER 2
LITERATURE REVIEW

2.1 Introduction

In wealthier parts of the world, the connection between water, hygiene and health is taken for granted. But for the less fortunate majority, access to clean and adequate water is a daily struggle. The importance of promoting and protecting health has risen to the top of the political agenda and much progress has been made. However millions are still deprived of a basic human right and huge challenges remain in fulfilling the numerous promises made.

Every day, diarrhoeal diseases cause an estimated 5500 deaths, mostly among children under five. The World Health Organisation (WHO) global estimate of the number of deaths from infectious diarrhoeas in the year 2001 amounts to 2 million for all age groups, with a heavy toll among children under five- an estimated 1.4 million deaths. The cluster of ill health is even more insidious in its impact on the economics of countries and on livelihoods at household level. Water-associated diseases hit the poor in a disproportionate way and this burden of ill health maintains the vicious cycle in which poverty leads to more ill health, and more ill health implies future impoverishment (UNESCO, 2003).

The Millennium Development Goals (MDGs), adopted at the Millennium Summit of the United Nations in September 2000, call for a dramatic reduction in poverty and marked improvements in the health of the poor. The importance of the MDGs in health is, in one sense, self-evident. Improving the health and longevity of the poor is an end in itself, a fundamental goal of economic development. But it is also a means to achieving the other development goals relating to poverty reduction (WHO, 2000).

One of the goals set by the United Nations Millennium Declaration is to ensure environmental sustainability. Significantly, one of the three key targets defined to achieve this goal is to halve, by 2015, the proportion of people without sustainable access to safe drinking water. Taking into account the projected growth of the world population these targets imply that an additional 1.5 billion people will require access to some form of improved water supply by 2015. Even to maintain the proportional level of coverage in urban areas in the year 2000 until 2015 will require an estimated 953 million people to gain access to water supply. Meeting the 2015 target of halving the fraction of the population without sustainable access to drinking water globally means providing services for an additional 100 million people each year (274000/day) from 2000 to 2015. By comparison,

during the decade of the 1990s an estimated total of 901 million people gained access to water supply. With the exception of sub-Saharan Africa, all regions will have achieved or will be close to achieving this target (UNESCO, 2003).

The definition of health as contained in the 1948 Constitution of WHO has withstood the ravages of time: 'health is a complete state of physical, mental and social well-being, and not merely the absence of disease and infirmity'. Having one's basic needs in terms of water met and being able to rely on a sustainable livelihood are crucial elements of social well-being, and contribute substantially to physical and mental well being as well. Water and health are intrinsically linked. There are basically two types of links that facilitate the cause-effect relationships between water management issues and impacts on health: water as the conveyance medium of pathogens (disease causing organisms) and water providing the habitat for vectors and intermediate hosts of pathogens (UNESCO, 2003).

2.2 Water and Public Health

2.2.1 Introduction

The diseases associated with water, sanitation and hygiene include infectious diarrhoea (which in turn includes cholera, salmonellosis, shigellosis and amoebiasis), typhoid and paratyphoid fevers, acute hepatitis A, acute hepatitis E and F, fluorosis, arsenicosis, legionellosis, schistosomiasis, trachoma, dracunculiasis, scabies, dengue, malaria and yellow fever. The transmission routes and solutions to these diseases are outlined below along with some common water-related diseases.

2.2.2 Classification of Transmission Mechanisms

Before the water related infections can be classified, the four distinct types of water related route by which a disease may be transmitted from one person to another must be defined (Cairncross and Feachem, 2000):

- Water-borne route

Water-borne transmission occurs when the pathogen is in water which is drunk by a person or animal which may then become infected. Potentially water-borne diseases include the

classical infections, notably cholera and typhoid, but also a wide range of other diseases, such as infectious hepatitis, diarrhoeas and dysenteries. All water-borne diseases can also be transmitted by any route which permits faecal material to pass into the mouth (a faecal-oral route). Water-borne transmission is merely a special case of drinking faecal material in water, and any disease which can be water-borne can also be transmitted by other faecal-oral routes.

- Water-washed route

Many infections of the intestinal tract and of the skin may be significantly reduced following improvements in domestic and personal hygiene. These improvements in hygiene often hinge upon the increased availability of water and the use for hygienic purposes of increased volumes of water. A water-washed disease may be formally defined as one whose transmission will be reduced following an increase in the volume of water used, irrespective of the quality of that water.

Water washed diseases are of three main types. Firstly, infections of the intestinal tract, such as diarrhoeal diseases, which are important causes of serious illness and death especially among young children in poor countries. These include cholera, bacillary dysentery and other diseases previously mentioned under water-borne diseases. These diseases are all faecal-oral in their transmission route and are therefore either water-borne or water-washed. The second type of water-washed infection is that of the skin or eyes. Bacterial skin sepsis, scabies and fungal infections of the skin are extremely prevalent in many hot climates, while eye infections such as trachoma are also common and may lead to blindness. These infections are related to poor hygiene and it is anticipated that they will be reduced by increasing the volume of water used for personal hygiene. The third type of water-washed infection is also not faecal-oral and therefore can never be water-borne. These are infections carried by lice which may be reduced by improving personal hygiene and therefore reducing the probability of infestation of the body and clothes with these arthropods. Louse-borne epidemic typhus is mainly transmitted by body lice, which cannot persist on people who regularly launder their clothes. Louse-borne relapsing fever may also respond to changes in hygiene linked to increased use of water for washing.

- Water-based route

A water-based disease is one whose pathogen spends a part of its life cycle in a water snail or other aquatic animal. All these diseases are due to infection by parasitic worms (helmiths), which depend on aquatic intermediate hosts to complete their life cycles. The degree of sickness depends upon the number of adult worms which are infecting the patient and so the importance of the disease must be measured in terms of the intensity of infection as well as the number of people infected. An important example is schistosomiasis in which water, polluted by excreta, contains aquatic snails in which the schistosome worms develop until they are shed into the water as infective cercariae and re-infect man through his skin.

Another water-based disease is Guinea worm (*Dracunculus medinensis*), which is found in West Africa and has a unique transmission route. The mature female worm, about 0.5m long, lies under the skin (usually on the leg) and creates a painful blister. When the blister is immersed in water or water is splashed onto it, as is often done to soothe the pain, the worm releases thousands of microscopic larvae. If the larvae are washed into a pond or a shallow well, they are eaten by cyclopoids, which then become infected, and they develop inside these new hosts. Cyclopoids are tiny crustaceans that are found in many small bodies of water. They are only 0.8mm long, and so are easily consumed inadvertently in water from an infected pond or well. Infected cyclopoids tend to sink to the bottom, so the risk is greatest when only a shallow depth of water remains. The cyclopoids themselves are not dangerous to drink, but any Dracunculus worms they contain will develop further in the human host and any fertilized female will make her way to the legs and form a new blister a year later, ready to start a new cycle.

Although a water-based disease, Guinea worm is the only infection which is exclusively transmitted in drinking water. It kills few people but causes debilitating pain, usually in planting season, so can have far reaching economic effects by reducing the ability to work of most of the population. Provision of safe water supplies is the primary measure to control the disease, especially in communities where 20% or more of the population is regularly infected. When annual influence has been reduced to 10% or less, most of the cases are likely to be caused by the casual use of infected water sources away from the home, while working, visiting or travelling. In such cases or in very small villages where

safe water supplies are not yet affordable, the inhabitants must be encouraged to filter their drinking water through a cloth to remove the cyclopoids, to avoid unsafe drinking water, and to ensure that people with blisters do not enter drinking-water sources.

The other diseases in this category are acquired by eating insufficiently cooked fish, crabs, crayfish or aquatic vegetation, which are clearly unrelated to drinking water.

- Insect vector route

The fourth and final route is for water related diseases to be spread by insects which either breed in water or bite near water. Malaria, yellow fever, dengue and onchocerciasis (river blindness), for example, are transmitted by insects which breed in water while West African sleeping sickness (Trypanosomes) is transmitted by the riverine tsetse fly which bites near water.

Table 2.1 lists these four water-related transmission routes and links them to their appropriate preventative strategies.

Transmission route	Preventative Strategies
Water-borne	Improve quality of drinking water
	Prevent casual use of unprotected sources
Water-washed	Increase water quantity used
	Improve accessibility and reliability of domestic water supply
	Improve hygiene
Water-based	Reduce need for contact with infected water
	Control snail populations
	Reduce contamination of surface waters
Water-related insect vector	Improve surface water management
	Destroy breeding sites of insects
	Reduce need to visit breeding sites
	Use mosquito netting

Table 2.1: Water-related Transmission Routes (Cairncross and Feachem, 2000).

2.2.3   Pathogenic Organisms

The term pathogenic is applied to those organisms, which either produce or are involved in the production of a disease. Three different groups of pathogenic microorganisms can be transmitted via drinking water- bacteria, viruses and protozoa.

Bacteria are the most widely distributed life forms. Pathogenic bacteria range in length from approximately 0.4 to 14µm and 0.2 to 1.2µm in width (Figure 2.1(a)). Key bacterial pathogens responsible for waterborne disease include *Legionella*, *Salmonella typhi*, *Shigella* and *Vibrio cholerae*.

Viruses are inactive when outside of a living host cell. Viruses that are linked to waterborne disease have protein coats that provide protection from environmental hazards. They range in size from 0.02 to 0.09µm but unlike bacteria and protozoa they contain only one type of nucleic acid (RNA or DNA) (Figure 2.1 (b)). Key viral pathogens include hepatitis A and Norwalk virus.

Protozoa are much larger than bacteria and viruses (10-300µm) (Figure 2.1 (b)). In order to survive harsh environmental conditions, some species can secrete a protective covering and form a resting stage called a cyst. Encystment can protect protozoa from drinking water disinfection efforts and facilitate the spread of disease. Key protozoan pathogens include Giardia and Cryptosporidium (USEPA, 1993).
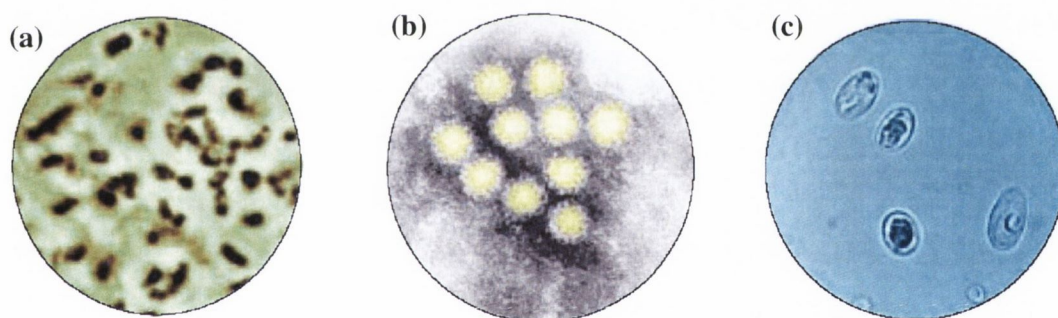
Figure 2.1: Bacteria (a), Virus (b) and Protozoa (c) (USEPA, 1993).

2.2.4   Bacterial Diseases

The various serotypes, which make up the genus *Salmonella*, are the most important group of bacteria affecting the public health of humans and animals. Raw or treated wastewater as well as abattoirs can contaminate water resources and *Salmonella* is commonly present in raw waters. Typical symptoms of salmonellosis are acute gastroenteritis, abdominal cramps, fever, and nausea. Diseases associated with it are typhoid fever (*Salmonella typhi*)

and paratyphoid (*Salmonella paratyphi* A, B or C). *Salmonella typhi* occasionally continues to proliferate in the gall bladder of a few patients who have recovered from the primary infection, and these carriers continue to excrete the organisms in their faeces for long periods (Twort *et al.*, 2000).

Bacillary dysentery is caused by bacteria of the genus *Shigella- Sh. dysenteriae* 1, *Sh. Flexneri*, *Sh. Boydii* and *Sh. Sonnei* are some of the subspecies. The bacterial genus is rather similar in their epidemiology to *Salmonella*. Infection can be contracted via water contaminated human faeces or ingestion of food contaminated by food handlers. It arises from contamination by sewage in drinking water (USEPA, 1999; Twort *et al.*, 2000).

Cholera is caused by the bacterium *Vibrio cholerae*. Major waterborne outbreaks occur in developing countries, which do not have adequate sanitation and where water supplies are continuously contaminated with sewage. An infected person or symptomless carrier of the disease excretes up to 10^{13} bacteria daily, enough to theoretically infect 10^7 people. Up to 10^6-10^7 organisms are required to cause the illness so it is transmitted primarily by drinking water or by eating food which has been washed with contaminated water. It is an intestinal disease with symptoms such as sudden diarrhoea, vomiting, dehydration and sometimes complete collapse. Without immediate medical attention the disease has >60% mortality rate, the patient dying within a few hours of first showing symptoms.

Opportunistic bacteria are usually found as part of the normal heterotrophic bacterial flora of aquatic systems. These organisms are not normally a threat to healthy individuals but can lead to infection in certain circumstances, such as immuno-compromised persons. Of these, those of particular concern include campylobacter, *E. coli*, mycobacteria, legionella pneumophila and aeromonads. This study will be concerned with *E. coli* from this group.

E. coli causes haemorrhagic, haemolytic-uraemic syndrome and is a major cause of kidney disease in children. It is generally associated with food in particular beef and milk but in recent years has been implicated in a number of waterborne outbreaks. The number of organisms required to initiate infection is thought to be <100 and at present there is no specific treatment for the disease (USEPA, 1999).

Campylobacteriosis is caused by bacteria associated with the excrement from wild fowl, which causes gastro intestinal illness. *Campylobacters* are frequently found in sewage and can survive for several weeks at cold temperatures in surface waters (Twort *et al.*, 2000).

2.2.5 Viral Diseases

Viruses of most concern for drinking water are those which cause gastrointestinal illness (enteric viruses) which includes entereroviruses, rotavirus, asteroviruses, calciviruses and Hepatitis A. Viral contamination arises when sewage containing pathogenic viruses contaminates surface and ground waters, which are subsequently used as drinking water. Most viruses are able to remain viable for several weeks in water at low temperatures as long as there is some organic matter present. Rotavirus is a major contributor to child diarrhoea syndrome. This causes death in some six million children in developing countries each year (USEPA, 1999).

Viruses differ from bacteria in that they are smaller and can multiply only within suitable host cells, in which they produce changes, which give rise to a range of diseases.

2.2.6 Protozoan Diseases

Giardia lamblia is a flagellated protozoan that is a significant cause of gastroenteritis ranging from mild to severe and being significantly more common in children than in adults. Transmission of *giardia* cysts may be by faecal contamination of hands, food or water supplies. Giardiasis is caused by the ingestion of cysts by a susceptible host. The cysts are 7 to 10µm wide and 8 to 12µm long and can survive for many days in a cool aquatic environment. There is no way of preventing infection except by adequate water treatment, i.e. filtration and source protection.

Cryptosporidium parvum is a coccidian protozoan. Cryptosporidiosis is acquired by ingesting viable oocysts. Clinical symptoms include influenza like illness, diarrhoea, malaise and abdominal pain. Generally this is a disease that is not fatal among healthy individuals however in young malnourished children it can cause severe dehydration and sometimes death. Water treatment such as slow sand filtration is critical in the removal of these protozoa. The parasite has a complex life cycle, which takes place within the body of the host and can include repeated cycles of infection. Infective oocysts of the parasite, which are 4 to 6µm in diameter, are then shed in vast numbers in the faeces of infected animals and humans. These oocysts are often found in surface waters, particularly in areas associated with intensive animal grazing and are also found occasionally in groundwater sources.

2.3   Principles of Disinfection

2.3.1   Introduction

While many of the pathogens described above are of little or no threat in the developed world, they are life threatening in regions of the developing world where adequate water treatment is not available. A barrier approach is the key strategy for controlling the health risks posed by microbes in drinking waters. This involves the treatment of wastewaters to remove microbes that cause disease as well as the treatment of raw waters including disinfection.

The term disinfection means the destruction of infective organisms in water to such low levels that no infection of disease results when the water is used for domestic purposes including drinking. Disinfection is most commonly accomplished by the use of chemical agents, radiation, mechanical means and physical agents (Twort *et al.*, 2000).

Chemical agents that have been used as disinfectants include chlorine and its compounds; bromine; iodine; ozone; phenol and phenolic compounds; alcohols; heavy metals and related compounds; dyes; soaps and detergents; quaternary ammonium compounds; hydrogen peroxide and various alkalies and acids. Of these the most common disinfectants are the oxidising chemicals, chlorine being the most widely used.

The major types of radiation are electromagnetic, acoustic and particle. Gamma rays are emitted from radioisotopes such as cobalt 60. Because of their penetration power, gamma rays have been used to disinfect both water and wastewater.

Bacteria and other organisms are also removed by mechanical means during wastewater treatment. The removals accomplished are generally a by-product of the primary function of processes such as screening and sedimentation.

Physical agents that can be used are heat and light. Heating water to boiling point will destroy major disease –producing nonspore-forming bacteria. Heat is commonly used in the dairy or beverage industry, but is not a feasible means of disinfecting large quantities of water because of the high cost. Ultraviolet rays are a good disinfectant; these rays can be both artificial (lamp) and natural (sunlight) (Metcalf and Eddy, 1991).

The three primary mechanisms of pathogen inactivation are to:

- Destroy or impair cellular structural organisation by attacking major cell constituents, such as destroying the cell wall or impairing the functions of semi-permeable membranes;

- Interfere with energy-yielding metabolism through enzyme substrates in combination with prosthetic groups of enzymes, thus rendering enzymes non-functional; and

- Interfere with biosynthesis and growth by preventing synthesis of normal proteins, nucleic acids, coenzymes, or the cell wall.

Depending on the disinfectant and microorganism type, combinations of these mechanisms can also be responsible for pathogen inactivation. In water treatment, it is believed that the primary factors controlling disinfection efficiency are: the ability of the disinfectant to oxidise or rupture the cell wall and the ability of the disinfectant to diffuse into the cell and interfere with cellular activity (USEPA, 1999).

Three common disinfectants, chlorine, ozone and UV, radiation are described below.

2.3.2 Chlorine

Chlorine is one of the most commonly used disinfectants throughout the world due to the following attributes:

- Effectively inactivates a wide range of pathogens commonly found in water;

- Leaves a residual in the water that is easily measured and controlled;

- Is economical;

- Has an extensive track record of successful use in improving water treatment operations.

There are, however, some concerns regarding chlorine usage that may impact on its uses such as: chlorine reacts with many naturally occurring organic and inorganic compounds in water to produce undesirable disinfection by-products (DBPs); hazards associated with using chlorine require special treatment and response programs; and high chlorine doses can cause taste and odour problems (USEPA, 1999).

Chlorination may be performed using chlorine gas or other chlorinated compounds that may be in liquid or solid form. Chlorine gas may be generated by a number of processes including the electrolysis of alkaline brine or hydrochloric acid, the reaction between sodium chloride and nitric acid or the oxidation of hydrochloric acid. Since chlorine is a stable compound, chlorine gas, sodium hypochlorite and calcium hypochlorite are typically produced off-site by a chemical manufacturer.

The precise action by which chlorine kills bacteria in water is uncertain but it is believed that the chlorine compounds formed when chlorine is added to water rupture bacterial membranes an inhibit vital enzymic activities resulting in bacterial death (Twort *et al.*, 2000). In bacteria chlorine adversely effects cell respiration, transport and possibly DNA activity. Several environmental factors influence the inactivation efficiency of chlorine including water temperature, pH, contact time, mixing, turbidity and concentration of available chlorine.

Since its introduction, numerous investigations have been made to determine the germicidal efficiency of chlorine. Although there are widespread differences in the susceptibility of various pathogens, the general order of increasing chlorine disinfection difficulty are bacteria, viruses, and protozoa as their thick outer shells make protozoa resistant to chlorine (Twort *et al.*, 2000; USEPA, 1999).

Advantages of using chlorine include:

- Oxidises soluble iron, manganese and sulphides.

- Enhances colour removal.

- May enhance coagulation and filtration of particulate contaminants.

- Is an effective biocide.

- Is the easiest and least expensive disinfection method.

- Is the most widely used disinfection method and therefore, the best known.

- Is available as calcium and sodium hypochlorite, being easier and safer to use than chlorine gas.

- Provides a residual.

Some disadvantages of using chlorine as a disinfectant are (Twort *et al.*; 2000, USEPA, 1999; Metcalf and Eddy, 2003):

- May cause deterioration in coagulation or filtration of dissolved organic substances.

- Forms halogen-substituted by-products (some of which are known carcinogens).

- Finished water could have taste and odour problems, depending on the water quality and dosage.

- Chlorine gas is a hazardous corrosive gas.

- Special leak contaminant and scrubber facilities could be required for chlorine gas.

- Is less effective at high pH.

- Forms oxygenated by-products that are biodegradable and which can enhance subsequent biological growth if a chlorine residual is not maintained.

2.3.3 *Ozone*

Ozone was first used for drinking water treatment in 1893 in the Netherlands. It is primarily used in water treatment for disinfection and oxidation. Ozone exists as a gas at room temperature; it is highly corrosive and toxic. Ozone is a powerful oxidant, second only to the hydroxyl free radical, among chemicals typically used in water treatment.

Ozone has a high germicidal effectiveness against a wide range of pathogenic organisms including bacteria, protozoa and viruses. Because of its high germicidal efficiency, ozone can be used to meet high inactivation required by water treatment with or without filters. However, ozone cannot be used as a secondary disinfectant because the ozone residual decays too rapidly.

Inactivation of bacteria by ozone is attributed to an oxidation reaction. The first site to be attacked appears to be the bacterial membrane either through the glycoproteins or glycolipids or through certain amino acids such as tryptophan. In addition ozone disrupts enzymatic activity of bacteria by acting on the sulfhydryl groups of certain enzymes. Beyond the cell membrane and cell wall, ozone may act on the nuclear material within the cell and has been found to affect both purines and pyrimidines in nucleic acids (USEPA,

1999).

The bactericidal effect of ozone is rapid, with usual contact time being between 4 and 10 minutes with dosages of the order of 2-3mg/l. It has shown to be more effective than chlorine in killing viruses, cysts and oocysts when a residual of 0.2 to 0.4mg/l is maintained for four minutes after the initial ozone demand is satisfied (Twort *et al.*, 2000)

Advantages of using ozone include (USEPA, 1999; Twort *et al.*, 2000; Metcalf and Eddy, 2003):

- Ozone is more effective than chlorine, chloramines and chlorine dioxide for inactivation of viruses, Cryptosporidium and Giardia.

- Ozone oxidises iron, manganese and sulphides.

- Ozone can sometimes enhance the clarification process and turbidity removal.

- Ozone controls colour, taste and odours.

- Ozone requires a very short contact time.

- In the absence of bromide, halogen-substitutes DBPs are not formed.

- Upon decomposition, the only residual is dissolved oxygen.

- Biocidal activity is not influenced by pH.

Disadvantages include:

- DBPs are formed in the presence of bromide.

- The initial cost of ozonation equipment is high.

- The generation of ozone requires high energy and should be generated on-site

- Ozone is highly corrosive and toxic.

- Ozone decays rapidly at high pH and warm temperatures.

- Ozone provides no residual.

- Ozone requires a high level of maintenance and operator skill.

2.3.4 Ultraviolet Radiation (UV)

Unlike most disinfectants, ultraviolet (UV) radiation does not inactivate microorganisms by chemical interaction. UV radiation inactivates organisms by absorption of the light which causes a photochemical reaction that alters molecular components essential to cell function. As UV rays penetrate the cell wall of the microorganism, the energy reacts with nucleic acids and other vital cell components, resulting in injury or death of the exposed cells. UV radiation quickly dissipates into water to be absorbed or reflected off material within the water and as a result no residual is produced.

UV radiation energy waves are the range of electromagnetic waves 100 to 400nm long. The division of UV radiation may be classified as Vacuum UV (100-200nm), UVC (200-280nm), UVB (280-315nm) and UVA (315-400nm). In terms of germicidal effects, the optimum UV range is between 245 and 285nm (USEPA, 1999). UV disinfection utilises either low-pressure lamps that emit maximum energy output at a wavelength of 253.7nm, or medium pressure lamps that emit energy at wavelengths from 180 to 1370nm. Low pressure lamps are used in low flow or domestic applications, they deliver about 85-90% of the energy input at 253.7nm. In medium pressure lamps only about a third of the energy input is delivered between 240 and 280nm but the energy intensity is about 50 times greater than that for low pressure lamps. The energy consumption of UV radiation using low-pressure lamps is typically of the order of 10 to 20Wh/m^3 of water treated and up to twice that for medium pressure lamps (Twort *et al.*, 2000). The lamps typically used in UV disinfection consist of a quartz tube filled with an inert gas, such as argon, and small quantities of mercury. UV lamps operate in much the same way as fluorescent lamps; radiation is emitted from electron flow through ionised mercury vapour to produce UV energy in most units. The difference between the two lamps is that the fluorescent lamp bulb is coated with phosphorous, which converts the UV radiation to visable light. The UV lamp is not coated, so it transmits the UV radiation generated by the arc (USEPA, 1999).

The degree to which the destruction or inactivation of microorganisms occurs by UV radiation is directly related to the UV dose. The UV dosage is calculated as:

$$D = I \times t \tag{2.1}$$

where D is the UV dose in mWs/cm^2, I is the intensity in mW/cm^2 and t is exposure time in seconds. When microorganisms are exposed to UV radiation, a constant fraction of the

living population is inactivated during each progressive increment in time. This dose-response relationship for germicidal effect indicates that high intensity UV energy over a shorter period of time would provide the same kill as a lower intensity UV energy at a proportionally longer period of time. The exposure time for disinfection varies between 0.5-5 seconds depending on the level of microorganisms present and the optical transmissivity of the water. The minimum UV dosage level for effective bacterial disinfection (>3-log removal) is specified as $16mWs/cm^2$ at 253.7nm by the US Department of Health. When viricidal action is required this dose increases to levels of 30-$40mWs/cm^2$. UV radiation has also been shown to be effective at inactivating *Cryptosporidium* oocysts with doses of $40mWs/cm^2$ producing a 4-log inactivation (Twort *et al.*, 2000).

As opposed to most alternative disinfectants, UV is a physical process that requires a contact time on the order of seconds to accomplish pathogen inactivation. As with any disinfectant, UV has its limitations. For example, because it is a physical rather than a chemical disinfectant, it does not provide a residual to control pathogen proliferation and biofilm formation in the distribution system.

UV radiation is efficient at inactivating vegetative and sporous forms of bacteria, viruses and other pathogenic microorganisms. Electromagnetic radiation in the wavelengths ranging from 240 to 280nm effectively inactivates microorganisms by irreparably damaging their nucleic acid. The most potent wavelength for damaging DNA is approximately 254nm. Other wavelengths, such as 200nm, have been shown to exhibit peak absorbance in aqueous solutions of DNA, however there is no practical application for UV inactivation of microorganisms in the wavelength range from 190 to 210nm. The germicidal effects of UV light involve photochemical damage to RNA and DNA within the microorganisms. DNA and RNA carry genetic information necessary for reproduction; therefore damage to either of these substances can effectively sterilise the organism. Damage often results from the formation of photo-products. Cytosine (DNA and RNA), thymine (DNA) and uracil (RNA) are the three primary types of pyrimidine molecules, which are effected by UV radiation. The most common photo-products arising form damage by UV radiation are thymine dimers, in which two adjacent thymines become covalently joined by cyclobutane. Replication of the nucleic acid becomes very difficult

once the pyrimidine molecules are bonded together due to the distortion of the DNA helical structure by UV radiation. Moreover if replication does occur, mutant cells that are unable to replicate will be produced. When the bacterial cell is unable to multiply it is assumed to be killed (Kalisvaart, 2001). Figure 1 is a schematic of the germicidal inactivation observed with UV radiation. Two phenomena of key importance when using UV disinfection in water treatment are the dark repair mechanisms and the capability of certain organisms to photoreactivate following exposure to certain light wavelengths.
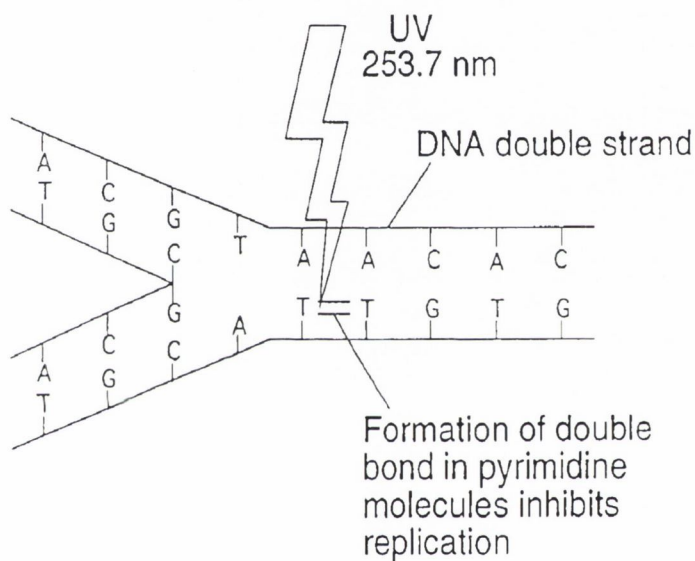
Figure 2.2: Germicidal Inactivation by UV Radiation (USEPA, 1999)

Bacterial cells have evolved three main types of repair mechanisms in response to DNA damage (Lewin, 1997). Direct repair involves a simple reversal of a structural alteration such as photoreactivation where the enzyme photolyse, activated by visible light, cleaves the links responsible for the formation of thymine dimers. Excision repair systems cleave DNA near the site of damage, remove the damaged strand, and synthesise a complementary strand to replace the excised material. Mismatch repair occurs when base pairs are no longer matched correctly, for example, cytosine and thymine. In mismatch repair, "new" and "old" strands are identified and the newly synthesised strand is preferentially corrected.

The repair mechanisms in microorganisms are not universal and some microorganisms have shown to be unable to repair themselves, these include: *Bacillus subtilis*, *Cryptosporidium parvum*, Poliovirus and MS2 phage. Organisms that have shown to be capable of photoreactivation include: *E. coli*, *Salmonella typhi*, *Salmonella typhimurium* and *Vibrio cholerae*.

The types of disinfection described above are effective in the developed world where public health is the prime concern of engineers and politicians over cost and energy. In order to meet the MDGs we must strive to find appropriate technologies suitable for less developed countries. The criteria that need to be met in order for a technology to be considered appropriate are outlined in the next section.

2.4 Appropriate Technology

Appropriate technologies represent a less capital intensive, more human orientated form of technological innovation and act as an impetus for development and improvement of standard of living in developing countries. A technology is appropriate because people have found it suitable to their needs. Appropriate technologies do not have a negative effect on the natural environment or the health and well being of the indigenous population (Linnell, 1995).

The philosophy for appropriate technology movement is to provide an opportunity for smooth transition between "labour-intensive" and "capital-intensive" industries.

The concept was first written about by E.F. Schumacher (1973) in his book "Small is Beautiful: Economics as if People Mattered" where he describes appropriate technology as "making the use of the best of modern knowledge and experience, conducive to decentralisation, compatible with the laws of ecology, gentle in the use of scarce resources and designed to serve the human person instead of making him a servant of machines".

National and local governments as well as people and community groups strive to introduce forms of technology that are efficient and fit within fiscal limitations, this is true in both developed and developing countries. The depth of importance of choosing the most important technology is magnified in developing countries where the margin of error is narrow due to limited resources. There are certain criteria used to judge the

appropriateness of a technology (Wicklein, 1998):

1. Systems Independence

This relates to the ability of a technical device to stand-alone and do its job without any supporting facilities and devices to aid its function. It refers mainly to cost, i.e. if the cost is compounded because of the need to use supporting devices then the technology may be unattainable for the people who need it most. Evaluation of a technology must include the technological device in question but also supporting materials and equipment for its full operation. Technological advances should be selected only if supporting facilities and devices are already in place or if moderate changes and improvements or existing systems are required for implementation.

2. Image of Modernity

Technologies need to be perceived as modern and progressive within their context-humanity has an innate desire to feel important and be perceived as worthwhile. Successful technology brings both satisfaction of need and perceived degree of sophistication such that social status is elevated. When an image of modernity is incorporated, there is an appeal to dignity and pride to meet with acceptance by the people who can benefit from it the most.

3. Individual Technology v's Collective Technology

This is related to societal or cultural standards in which the proposed technology would be operating. Some cultures advocate strong commitment to group processes where the benefit of the whole is held in higher esteem than the individual accomplishment. Some cultures place high priority on individual responsibility and accomplishment. If a cultural group has a strong allegiance to local community, regional technology may be more system-dependent as overall group could take greater responsibility for the operation of a large system. A society which is geared towards individuals or single-family units need technology which is more system independent, i.e. designed so an individual could operate and afford the system.

4. Cost of Technology

The majority of technologies although developed with cost as the central consideration are still too expensive for most people in developing countries to afford. Cost must be such that people in developing regions can afford it. One of the major difficulties in reducing production costs of appropriate technologies is that many of the technologies are developed for a one-of-a-kind use within specific location under specific social and cultural limitations. Advantages of mass production are severely restricted because of this.

5. Risk Factor

The development of any new technology carries with it a chance of either success or failure. The risk can be internal or external. Internal risk involves the way in which the technology will fit into a local production system whereas external risk involves the needed support systems, which may be required to keep the technology functioning properly. Economically and politically it is unhealthy to try to remove all risks, some risks are healthy for growth and development of locally implemented appropriate technologies. It is essential to provide challenge to local economic and production systems. This helps technology to take root and gain ownership at a local level.

6. Evolutionary Capacity of a Technology

Technologies are preferred to have design capacities that allow for continuation of development. They should have the capability to expand and be reconfigured to accomplish a higher volume of work and/or more sophisticated production processes. Technology can grow with the society it benefits and not just exist as a relatively short-lived solution. The nature of the technology might eventually allow users to compete economically at regional, national and international levels, which is the ultimate goal of any developing country. Without this capability the technological device elevates its owners and users /to a new static level of poverty.

7. Single Purpose and Multi-Purpose Technology

It is advisable to develop appropriate technologies that provide for a variety of applications because of the extreme poverty of people in developing countries. Technologies, which

perform multiple specific purposes are beneficial to those who cannot afford to purchase individual single function pieces of equipment.

An ideal appropriate technology does not exist. The best approach is to design appropriate technology by balancing the above criteria with specific human needs. The application of these criteria in no way belittles developing countries; appropriateness is just as relevant in advanced technical settings as in developing technical settings.

An important factor in the choosing of a technology for a region is community participation. Communities must participate in the initial planning, the choice of appropriate technology, the location of facilities, the operation and maintenance program, financing options, replacement schedule etc. This ensures that schemes are sustainable both economically and environmentally (Geraghty & Temnewo, 2000).

The use of appropriate technology is particularly important in providing basic human needs such as water supplies and sanitation to people in developing countries. Water supply and sanitation in developed countries is dominated by sophisticated engineering. Large scale, costly and ambitious projects exported overseas by the aid community in the name of progress imbued by a spirit of professional and scientific superiority makes them little different from their colonial predecessors. The International Drinking Water and Sanitation Decade (1980-1990) sought to challenge the powerful and high tech image of progress on which the Western environment and social transformations have been based. It attracted donors to provide resources, know-how and better co-ordination of their aid programmes. Sophisticated technology could not satisfy these health needs so they built upon Schumacher's appropriate technology theory. This included low-cost solutions such as communal hand pumps and pit latrines which were effective substitutes for complex piped systems and avoided reliance on scarce expensive inputs thus caring for a wider population. Focus was on diversity rather than homogeneity, flexibility rather than bureaucratic rigidity. Simplified production processes reduced production costs and implementation costs were lowered by community participation (Bell & Franceys, 1995).

The Dublin Statement on Water and Sustainable Development (1992) also supported the theory of appropriate technology, focusing on four principles to ensure sustainability of water projects. The four principles were:

- Fresh water is a finite and vulnerable resource, essential to sustain life, development and the environment

- Water development and management should be based on a participatory approach, involving users, planners and policy-makers at all levels

- Women play a central part in the provision, management and safeguarding of water

- Water has an economic value in all its competing uses and should be recognised as an economic good.

The International Drinking Water and Sanitation Decade highlighted the problem of providing these basic needs to people in developing countries but the improvements made did not come anywhere near reaching there targets. 70% of people in developing countries have no adequate sanitation facilities whereas in some parts of Africa the population without safe drinking water can be up to 75% (DeBoer, 2000).

According to Falkenmark (1998) poverty eradication involves at least three components that are directly of indirectly water related: morbidity reduction through health protecting activities (safe water supply and sanitation), security in access to food either through achieving national self reliance through water consuming crop production or through purchasing of food which depends on access to a secured family income, family income which depends on employment opportunities in sustainable industrial or cash crop production, both water dependent.

In summary, an appropriate technology is:

- Low in capital costs,

- Uses local materials,

- Creates jobs employing local skills and labour,

- Makes technology understandable to people using it,

- Involves decentralisation of renewable resources and supposes that people can and will work together to bring improvements to communities recognising that in most of the world decisions are made by groups rather than individuals (Linnell, 1995).

An example of an appropriate technology that has been successful is South Africa's Play-pump which simplifies the chore of fetching water in rural areas. The Play-pump is a specifically designed and patented playground roundabout that drives conventional borehole pumps, keeping costs and maintenance to an absolute minimum, while entertaining children. It is capable of producing 1400l/hr at 16rpm from a depth of 40m. As children spin water is pumped from underground into a 2500 litre tank with a tap providing easy access to the water. Four billboards are attached to the tank, two of which are used for health messages with the other two rented out as advertising, which in turn provides the revenue required for maintenance (Play-pump, 2005).

It essential that all the criteria necessary for an appropriate technology are met when designing new technologies for developing countries. This thesis focuses on the design of an appropriate solar disinfection system for use in developing countries.

2.5   Solar Energy

This section begins by discussing sunlight in general and its propagation through the atmosphere to the earth's surface followed by a review of previous work where the sun's energy has been harnessed for water purification purposes.

2.5.1   Sunlight

The term electromagnetic energy comprises all types of energy that travels from its source through space in the form of harmonic waves along straight paths at the uniform speed of light ($3x10^8$m/s). Radiation is the term that pertains to the emission and propagation of electromagnetic energy in the form of waves (Acra *et al.*, 1989).

There are many types of electromagnetic energy, but consideration of the subject is necessarily limited to those of solar origin that provide pertinent background information for the proper utilisation of solar radiation for disinfection purposes. It should be recognised that solar radiation constitutes only a portion of the entire electromagnetic energy spectrum. Electromagnetic radiation, as well as solar radiation, is commonly classified on the basis of radiation wavelength into several regions or bands. The wavelength bands of solar radiation, both visable and invisible, are described in Table 2.2 below.

Band	Wavelength (nm)	Atmospheric Effects
Gamma ray	<0.03	Completely absorbed by atmosphere
X-Ray	0.03-3	Completely absorbed by the upper atmosphere
Ultraviolet, UV		
UVB	3-300	Completely absorbed by oxygen. Nitrogen, and ozone in the upper atmosphere
UVA	300-400	Transmitted through the atmosphere but atmospheric scattering is severe
Visable	400-700	Transmitted through the atmosphere with moderate scattering of the shorter wavelengths
Infrared, IR		
Reflected IR	700-3000	Mostly reflected radiation
Thermal IR	3000-14000	Absorption at specific wavelengths by carbon dioxide, ozone and water vapour, with two major atmospheric windows

Table 2.2: Electromagnetic Energy (Acra *et al.*, 1989)

2.5.2 *Propagation of Solar Energy*

The sun continuously radiates enormous amounts of solar energy at wavelengths that cover the ultraviolet, visable and infrared bands. The maximum intensity of the emitted solar energy occurs at a wavelength of about 555nm, which falls within the band of green visable light.

Solar radiation moves freely in outer space because of the vacuum, unless its path is obstructed by planets, satellites, meteorites or other space objects. Whatever portion reaches the earth and its surrounding atmosphere may encounter a variety of atmospheric or terrestrial objects. When solar radiation strikes any object whether in the form of a gas, liquid or solid, changes in its magnitude, direction and wavelength are expected to occur depending upon the nature and characteristics of the intervening object (Acra *et al.*, 1989). These changes may come as a result of any of the following possible phenomena:

- Radiation may be transmitted through a transparent object with a change in speed and direction.

- Radiation may be partially or completely absorbed by an object, the components thus absorbed being dependent on the wavelength of the specific radiation and the characteristics of the object.

- Radiation may be scattered by being deflected in all directions, a common example being the scattering of sunlight as it traverses the atmosphere.

- Radiation may be reflected by being returned from the surface of an object in an unchanged form except for the deviation whereby the angle of reflection would be equal and opposite to the angle of incidence.

Outer Space

The enormous amount of energy continuously emitted by the sun is dispersed into outer space in all directions. Only a small fraction of this energy is intercepted by the earth and other solar planets. The solar energy reaching the periphery of the earth's atmosphere is considered to be constant for all practical purposes, and is known as the solar constant. Because of the difficulty in achieving accurate measurements, the exact value of the solar constant is not known with certainty but is believed to be 1360W/m^2 (Şen, 2004). The solar constant value is estimated on the basis of the solar radiation received on a unit area exposed perpendicularly to the rays of the sun at an average distance between the sun and the earth. In passing through outer space, which is characterised by vacuum, the different types of solar energy remain intact and are not modified until the radiation reaches the top of the earth's atmosphere. In outer space, therefore, one would expect to encounter the types of radiation listed in Table 2.2, which are: gamma ray, X-ray, ultraviolet and infrared radiations (Acra *et al.*, 1989).

Atmospheric Effects

Not all of the solar radiation received at the periphery of the atmosphere reaches the surfaces of the earth. This is because the earth's atmosphere plays an important role in selectively controlling the passage towards the earth's surface of the various components of solar radiation. A considerable portion of solar radiation is reflected back into outer space

upon striking the uppermost layers of the atmosphere, and also from the tops of the clouds. In the course of penetration through the atmosphere, some of the incoming radiation is either absorbed or scattered in all directions by atmospheric gases, vapours and dust particles. The scattered portion is also called diffuse radiation and the radiation arriving on the ground directly in line from the sun is called direct radiation (Şen, 2004). There are two processes known to be involved in atmospheric scattering of solar radiation. These are termed selective scattering and non-selective scattering. These two processes are determined by the different sizes of particles in the atmosphere.

Selective scattering is so named because radiations with shorter wavelengths are selectively scattered much more extensively than those with longer wavelengths. It is caused by atmospheric gases or particles that are smaller in dimension than the wavelength of a particular radiation. Such scattering could be caused by gas molecules, smoke, fumes, and haze. Under clear atmospheric conditions, therefore, selective scattering would be much less severe than when the atmosphere is extensively polluted form anthropogenic sources. Selective atmospheric scattering is, broadly speaking, inversely proportional to the wavelength of radiation and, therefore, decreases in the following order of magnitude: far UV>near UV>violet>blue>green>yellow>orange>red>infrared. Accordingly, the most severely scattered radiation s that which falls in the ultraviolet, violet and blue bands of the spectrum. The scattering effect on radiation in these three bands is roughly ten times as great as on the red rays of sunlight (Acra *et al.*, 1989).

Non-selective scattering occurring in the lower atmosphere is caused by dust, fog and clouds with particle sizes more than ten times the wavelength of the components of solar radiation. Since the amount of scattering is equal for all wavelengths, clouds and fog appear white although their water particles are colourless. Atmospheric gases also absorb solar energy at certain wavelength intervals called absorption bands, in contrast to the wavelength regions characterised by high transmittance of solar radiation called atmospheric transmission bands, or atmospheric windows. The degree of absorption of solar radiation passing through the outer atmosphere depends upon the component rays of sunlight and their wavelengths. The gamma rays, X-rays and UV radiation less than 200nm in wavelength are absorbed by oxygen and nitrogen. Most of the radiation with a range of wavelengths from 200nm to 300nm is absorbed by the ozone (O_3) layer in the

upper atmosphere. These absorption phenomena are essential for living things because prolonged exposure to radiation of wavelengths shorter than 300nm destroys living tissue. Solar radiation in the red and infrared regions of the spectrum at wavelengths greater than 700nm is absorbed to some extent by carbon dioxide, ozone and water present in the atmosphere in the form of vapour and condensed droplets. In fact, the water droplets present in clouds not only absorb rays of long wavelengths, but also scatter some of the solar radiation of short wavelengths (Acra *et al.*, 1989).

Ground Level

As a result of the atmospheric phenomena involving reflection, scattering, and absorption of radiation, the quantity of solar energy that ultimately reaches the earth's surface is much reduced in intensity as it traverses the atmosphere. The amount of reduction varies with the radiation wavelength, and depends on the length of the atmospheric path through which the solar radiation traverses. The intensity of the direct beams of sunlight thus depends on the altitude of the sun, and also varies with such factors as latitude, season, cloud coverage and atmospheric pollutants.

The total radiation received at ground level includes both direct radiation and indirect (or diffuse) radiation. Diffuse radiation is the component of total radiation caused by atmospheric scattering and reflection of the incident radiation on the ground. Absorbed, diffused and direct radiation types are presented in Figure 2.3 below, where solar radiation from the sun at the top of the atmosphere is assumed as 100 units.
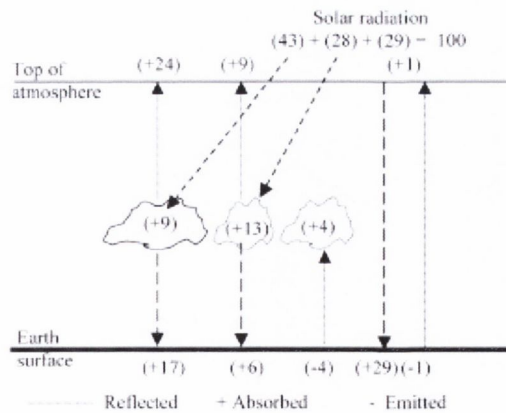
Figure 2.3: Direct, diffuse and absorbed radiation (Şen, 2004)

Reflection from the ground is primarily visable light with a maximum radiation peak at a wavelength of 555nm (green light). The relatively small amount of energy radiated from the earth at an average ambient temperature of 17°C at its surface consists of infrared radiation with a peak concentration at 970nm. This invisible radiation is dominant at night. During daylight hours, the amount of diffuse radiation may be as much as 10% of the total solar radiation at noon even when the sky is clear. This value may rise to about 20% in the early morning and late afternoon. The UV component does not exceed 5% of the total incident radiation at sea level under cloudless atmospheric conditions (Acra et al., 1989). At high altitudes, the intensity of UVR is significantly higher than at sea level. With increasing height the overhead atmosphere becomes thinner and the attenuation of the UV radiation from atmospheric constituents such as aerosols and clouds is decreasing (Dvorkin and Steinberger, 1999; Alexandris et al., 1999). The spectral distribution of solar energy at sea level is roughly 3, 44 and 53% in the UV, visable and infrared regions, respectively. In practice these variables need to be taken into consideration for the use of solar energy (Acra et al., 1990).

In conclusion, therefore, it is evident that in cloudy weather the total radiation received at ground level is greatly reduced, the amount of reduction being dependent on cloud coverage and cloud thickness. Under extreme cloud conditions a significant proportion of the incident radiation would be in the form of scattered or diffuse light. Chen et al. (2004) found that greater attenuation is found for clouds whose base lies below 300m with reductions being up to 65%, whereas clouds between 300 and 100m reduced UVB doses by 56%. In addition, lesser solar radiation is expected during the early and late hours of the day. These facts are of practical value for the proper utilisation of solar radiation for such purposes as destruction of microorganisms.

2.5.3   *World Distribution of Solar Radiation*

It is common knowledge that solar radiation is unevenly distributed, and that it varies in intensity from one geographic location to another depending on latitude, season and time of day. Until recently, valid records for solar radiation have been very scanty in the vast majority of the developing countries. In the absence of such useful information as a guide for the proper exploitation of solar energy, only general hints can be offered regarding the

geographic areas with favourable conditions for solar energy applications.

For convenience and simplicity, the geographic distribution of total solar radiation on a global scale is divided in terms of intensity into four broad belts around the earth. These are illustrated in Figure 2.4 and also briefly described below with respect to the northern hemisphere, with the understanding that the same conditions apply to the corresponding belts in the southern hemisphere (Acra *et al.*, 1989):
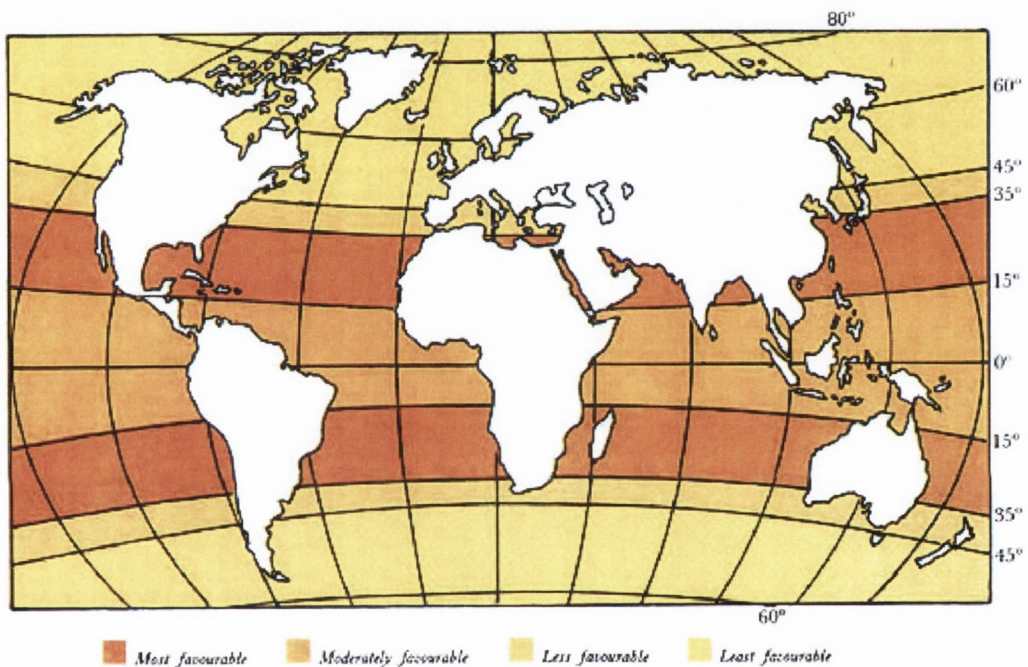
Figure 2.4: World Distribution of Solar Radiation (Acra *et al.*, 1989)

- *The most favourable belt.* This belt, lying between latitudes 15°N and 35°N, embraces the regions that are naturally endowed with the most favourable conditions for solar energy applications. These semi-arid regions are characterised by having the greatest amount of solar radiation, more than 90% of which comes as direct radiation because of the limited cloud coverage and rainfall (less than 250mm per year). Moreover, there is usually over 3000 hours of sunshine per year.

- *Moderately favourable belt.* This belt lies between the equator and latitude 15°N, and is the next most favourable region for the purpose of solar energy applications. Because humidity is high and cloud cover is frequent, the proportion of scattered radiation is quite high. There is a total of about 2500 hours of sunshine per year. The solar intensity is almost uniform throughout the year as the seasonal variations are only slight.

- *Less favourable belt.* This belt lies between latitude 35°N and 45°N. Although the average solar radiation intensity is roughly about the same as for the other two belts, there are marked seasonal variations in both radiation intensities and daylight hours. During the winter months solar radiation is relatively lower than in the rest of the year.

- *Least favourable belt.* The regions in the belt lie beyond latitude 45°N. They include the USSR, and the greater parts of northern Europe and North America. Here about half of the total radiation is diffuse radiation, with a higher proportion in winter than in summer primarily because of the rather frequent and extensive cloud cover.

Solar intensities in Ireland, Spain, Sudan and Ghana (one in each belt) are shown in Table 2.3 for different times of year.

Location	Solar Intensity @ midday (kW/m^2)		Latitude	Longitude
	June	December		
Dublin, Ireland	0.56	0.12	53	6
Madrid, Spain	0.82	0.33	40	3
Khartoum, Sudan	0.72	0.51	15	32
Accra, Ghana	0.59	0.48	5	0

Table 2.3: Solar Intensities at different times of year at different latitudes (NASA, 2005)

It is important to note that the majority of developing countries fall within the more favourable regions between latitudes 35°N and 35°S. For this reason they can count on solar radiation as a steadfast source of energy that can be readily exploited cheaply by both rural and urban households for a multitude of purposes, including solar disinfection of

drinking water.

2.6   Solar Distillation

2.6.1   *Lethal Effect of Heat on Bacteria*

High temperatures have profound effects on the structural and physiological properties of sporulating and non-sporulating bacteria, with membranes, RNA, DNA, ribosomes, protein and enzymes all affected. Nevertheless it is apparent that no single event is responsible for cell death (Russell, 2003). Bacteria vary considerably in their temperature response, depending on the type of bacteria i.e. whether they are sporulating or non-sporulating. Some bacteria have the ability to form a protective coating called a spore when subjected to adverse conditions such as heat. *E. coli*, *Salmonella sp.* and *Streptococci* are example of non-sporulating bacteria, whereas *Bacillus species* and *Clostridium perfringens* have the ability to form spores.

- Non-Sporulating Bacteria

All the major cellular components are affected, namely the outer cell layers (and especially the outer membrane in Gram-negative bacteria), cytoplasmic membrane, ribosomal RNA, proteins, among them enzymes and DNA. There is a rapid induction of intracellular heat-shock proteins that provide cells with the means to attempt to mitigate the effects of high temperatures. Extracellular alarmones may be produced to warn organisms of impending disaster. Exposure of cultures to increasing temperatures may enable the cells to adapt to higher, normally rapidly lethal temperatures (Russell, 2003).

- Bacterial Spores

Marked structural and physiological changes occur during sporulation, germination and outgrowth with significant changes in susceptibility to high temperatures. During sporulation, heat resistance develops, whereas during early germination depolymerisation of the cortex takes place and heat sensitivity is regained.

Moist heat damages the spore membranes and there is protein denaturation and strand breakage. General stress proteins, some specific to heat shock, arise when sporulation proceeds at a normal temperature after previous cell exposure to a higher temperature. Dry heat is mutagenic i.e. it causes a change to the cell's DNA (Russell, 2003).

These temperature effects can be promoted in various ways using solar distillation techniques.

2.6.2   *Application of Sunlight to Promote a Heating Effect*

The sun's energy can be used to heat water to pasteurisation temperature in a number of devices. The simplest solar water purification devices are the solar box and the solar still. A solar box consists of a cardboard or wooden box with an insulated bottom and sides and a glass or clear plastic lid. The inside surfaces should be painted black. A covered pot with water (ideally also black) is placed inside. The pot remains in the box until the water is at 65° for a few minutes. Generally, a solar box can pasteurise about a gallon of water in 3 hours on a very sunny day. Pasteurisation can kill bacteria, viruses and cysts, heating water up to 65° for six minutes will kill all bacteria, viruses and parasites present (Rolla, 1998).

Solar distillation uses sunlight to heat water and produce water vapour, which is then condensed back to water, impurities such as salts, minerals, heavy metals and bacteria will not evaporate and are left behind (Simate, 2001). The basic operation of a solar still is that water to be distilled is contained in an enclosure which has the top cover made of glass or some other transparent material and the cover is inclined at an angle. Direct sunlight heats up the water in the basin through the bottom of the basin and this causes the water to evaporate. The water vapour then condenses on the glass cover since the cover is in contact with the cooler outside air. The resulting liquid water runs under the glass cover and is collected.

In 1995 a simple reflective solar cooker, the Cookit, was developed by Solar Cookers International (SCI; Sacramento California) and subsequently introduced as a cooking device in three refugee camps in Kenya and Ethiopia. For cooking the foiled reflective panels of the Cookit direct sunshine onto a dark pot, which is enclosed in a clear polypropylene, bag and cooks the food. It was discovered when using Cookit on sunny days a plastic bag was not needed to enclose a black jar for heating water to pasteurisation temperatures (at least 65°C) (Safapour and Metcalf, 1998).

In 1998 Jorgensen *et al.* developed a device for direct heating of water by solar radiation in a flow through system of copper pipes. The solar water device heats water by using solar radiation directly in a flow-through system of copper pipes arranged in parallel with two

horizontal header pipes and several vertical riser pipes. The water is led into the lower horizontal pipe and from here it rises by convection to the upper horizontal pipe. The pipes are connected by soft soldering and covered by aluminium plates. The tubes and plates are painted black, mounted in an aluminium box and covered with a transparent double layer polycarbonate plate, coated to resist UV radiation. When the temperature of the water reaches 75°C a valve opens and the water can flow out of the system. Daily production was found to be about 50 litres of decontaminated water per metre squared of reactor.

2.7   Solar Disinfection

2.7.1   *History of Solar Disinfection*

The germicidal effect of sunlight has long been known. Between 1877 and 1895 a remarkable set of studies revealed that sunlight, especially the UV-violet-blue rays, was capable of killing many different types of bacteria (Hockberger, 2000). Downes and Blunt (1877-1878) reported that the growth of bacteria was inhibited by exposure to sunlight. This was demonstrated by placing glass test tubes containing Pasteur solution on a windowsill and exposing them to London air (source of contamination). The tubes that were exposed to daily sunlight remained free from contamination whereas tubes that had been shielded form sunlight became contaminated within a few days.

Wavelength sensitivity was evaluated by placing the test tubes in boxes made of coloured glass. Contamination was noticeably absent in the deep blue and clear boxes whereas contamination proceeded as normal within the blood red and yellow boxes.

In 1885 Saturnin Arloing investigated the effect of sunlight on *Bacillus anthacis*. He also developed an improved strategy for delivering sunlight to the sample; he employed a heliostat that allowed the light to remain focused on its target throughout the day. Under these conditions growth of the bacteria was prevented for weeks after as little as two hours of direct sunlight (Hockberger, 2000)

In 1892-95 Marshal Ward began his studies of solar toxicity also using *B. anthracis*. He inoculated agar and gelatin containing glass Petri dishes with bacteria, mounted each dish several inches above a mirror that was used to reflect sunlight to the underside of the dish. A black stencil was affixed to the underside of the dish providing a cutout of an alphanumeric symbol by which to gauge bacterial growth. After exposure followed by 48h

in the dark, anthrax colonies grew everywhere except where light had penetrated the symbol (Hockberger, 2000).

Ward also performed a series of experiments to test the wavelength sensitivity of the response. He cut a hole in the top of the dish and covered it with a thin quartz cover slip to allow UV transmission. Next, he used a lens-slit-lens combination to fill the face of a prism with light from an electric arc lamp, maximising the efficiency and stability of the illumination. The spectral output of the prism was directed onto the quartz window creating a rectangular pattern on the agar plate. He marked the pattern and then covered the entire plate (excluding the window) in black paper, wrapped in aluminium foil and covered in white paper. This reduced reflections inside the dish and minimised absorption on the outside. There was virtually identical inhibition of growth throughout the UV-violet-blue region with a sharp cut-off at the borderline between blue and green light. There was no evidence of any effect in any other region of the visable or the infrared spectrum.

These initial findings have then led to further, more recent investigation into simple methods of disinfecting drinking water using sunlight.

2.7.2 Solar Disinfection Mechanisms

Downes and Blunt (1878) also performed tests aimed at addressing the underlying molecular mechanism. They reasoned that sunlight might act either by destroying molecules inside the bacteria, or alternatively by inducing the synthesis of toxic by-products, or both. They found that the experiments they performed on Pasteur solution were unaffected by sunlight and therefore suggested that a cellular induction (initiating or increasing production of an enzyme) process was more likely.

In order to understand how UV radiation affects molecules an understanding of how radiation is absorbed by a substance is required. Photons are produced at each specific wavelength of a light source. Each photon has its own energy content, which depends upon the wavelength. When the photon is absorbed by a material, for example a microorganism, electrons in the atoms or molecules making up the material are excited. The velocity of the photons is equal to the velocity of visable light, 3×10^8 m/s, while the time needed for their absorption by atoms or molecules is about 10^{-15} seconds. The larger and more complex a molecule (for example DNA or proteins), the more different wavelengths are absorbed and

therefore the wider the absorption line spectrum (Kalisvaart, 2001).

An atom or molecule absorbing a UV photon assumes for a period of 10^{-10} to 10^{-8} seconds an excited state in which the energy of its electrons are increased by the amount of photon energy. The number of possible states for the electrons is finite - only photons of specific wavelengths can be absorbed by an isolated atomic or molecular species. The excitation energy provided by the UV photons is much higher than energy of thermal motions of molecules at physiological temperatures. Absorbing molecules therefore assume energy levels that they otherwise would never attain and thus acquire properties differing considerably form those effective in ordinary chemistry. As an excited electron returns to a lower energetic state excess energy may be disposed of in several ways (Harm, 1980):

- Emitted as a photon-fluorescence

- Dissipated as thermal energy in the course of collisions with other molecules

- May cause a photochemical reaction - immediate effects of UV radiation which are the basis for photochemical phenomena.

Cell Components absorbing Radiation below 300nm
- DNA

The majority of biological effects, especially in very small microorganisms are in the first place due to photochemical reactions in the nucleic acid DNA, which contains the genetic material of all cellular organisms. The absorption curve shows maximum absorption at 200nm with an absorption peak at 260-265nm (i.e. maximum absorption does not occur at 254nm) (Von Sonntag, 1986). In DNA the backbone molecules (sugar and phosphate) do not absorb above 210nm. Absorption by DNA and RNA above 210nm is due to absorption of nucleotide bases adenine (A), guanine (G), cytosine (C), thymine (T) and uracil (U) (found only in RNA). The absorption spectra of bases are found in the UV-C and UV-B regions. Nucleotide bases absorb photons so the result is the formation of photoproducts. The most common photoproducts are thymine dimers, which occur when two adjacent thymines become covalently joined by cyclobutane. When DNA is damaged it can no longer replicate and so the bacterial cell is unable to multiply and assumed to be killed.

- Proteins

This is relevant in the case of larger microorganisms such as fungi, protozoa and algae. UV may be unable to penetrate far beneath the surfaces of these organisms leaving the DNA scarcely affected, if at all. It is probably no accident that precisely at the point where solar radiation falls off below 300nm proteins and nucleic acids begin to absorb and be damaged by UV radiation (Jagger, 1967).

The absorption spectrum of proteins shows a peak at around 280nm. The peptide bond (-CONH-) in proteins displays some double bond characteristics; it is a relatively weak absorber and is only significant at wavelengths below 240nm. As there is a peptide bond for every amino acid residue in a protein, UV absorption below 240nm is significant.

Absorption of UV light by the amino acid cysteine makes proteins and enzymes unstable. If the dissociation energy for disulphide (S-S) bond between cysteines is reached dissociation of the tertiary structure of the protein takes place which results in denaturation of the biomolecule. This will result in a loss of the biological activity of the molecule. For example if denaturation of the enzyme polymerase takes place the microorganism losses its ability to multiply. Due to the high concentration of proteins in microorganisms (50% dry weight) absorption of UV may often influence their role in nucleic acid synthesis and chromosome structure.

Cell Components Absorbing Radiation above 300nm

The ability of wavelengths in the solar spectrum above 300nm to kill small bacteria (<10 μm) has been known for a long time (Airloing, 1885). The affected biological molecules or chromophores have not yet been identified, since proteins and nucleic acids show little or no absorption above 340nm. Hence, other chromophores with sufficient absorbency to result in the killing of small microorganisms must be targeted. Wavelengths above 300nm and in the adjacent visible range destroy the capacity of microorganisms to multiply and radiation of 350-490nm has been shown to cause leakage of ions. It has also been suggested that damage at these wavelengths is less effectively repaired than at 254nm. Germicidal effects of UVA are almost entirely due to the formation of oxygen radicals in the cytoplasm (Tortora, 1995; Kalisvaart, 2001).

Mechanism of Solar Disinfection

UVA damage occurs when UVA radiation is absorbed by photosensitizers which react with oxygen molecules producing highly reactive oxygen species which in turn react with DNA, damaging bases, breaking strands and cross linking DNA and proteins. Photosensitizers present in the water absorb UV light and are raised to an excited singlet state. This is very unstable and may return to ground state immediately with subsequent loss of energy, usually as a photon of light. If the excited state undergoes intersystem crossing i.e. a transition between singlet an triplet states, a metastable (transient but long lived) triplet state, an excited state at lower energy than the singlet state, will be produced (see Figure 2.5). This state has a longer half-life (10^{-3}- 5 seconds) allowing it to interact with neighbouring molecules before returning to ground state (Whitelam, 1986).
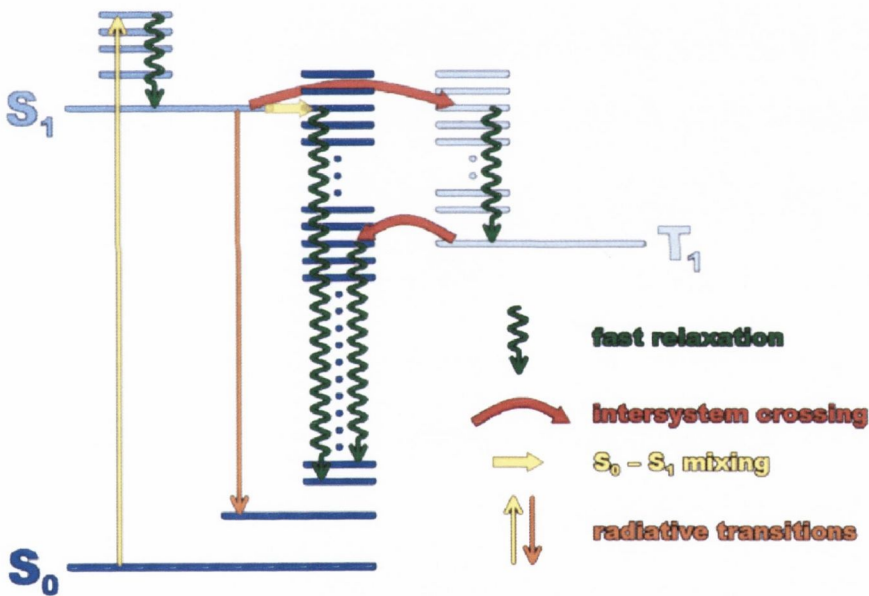
Figure 2.5: Possible Energy states of an absorbed photon (Jablonski Diagram) where S_0 is ground state, S_1 is an excited singlet state and T_1 is a triplet state.

There are two means by which the excited triplet sensitizer can interact with oxygen and generate highly reactive oxygen species.

Type I: (reaction with a substrate)

This reaction involves the transfer of an electron from a substrate with subsequent

production of a semi-reduced sensitizer and semioxidised substrate (Spikes, 1977). The semireduced sensitizer may then react with oxygen producing a highly reactive superoxide radical. The superoxide radical spontaneously dismutates to produce ground state oxygen and hydrogen peroxide. A highly reactive hydroxyl radical may then be generated from hydrogen peroxide if traces of free iron or ascorbate and thiol compounds are present.

Type II: (reaction with molecular oxygen)

These reactions involve the transfer of energy and are more common. The product of the reaction is much more reactive than those formed in type 1 reactions. An excited triplet state sensitizer simply reacts with triplet oxygen with the production of the ground state sensitizer and a highly reactive singlet state of oxygen.

Both types of reaction lead to a highly reactive oxygen species and it is these, which interfere with DNA, proteins and membranes thus causing the bactericidal action of the sun. The reactive oxygen species attack DNA causing base charges or strand breaks (Farr, 1991). Such damage may result in a block in replication and thus be lethal. Reactive oxygen species have also been shown to attack proteins altering the amino acids. Such alterations may lead to the inactivation of certain enzymes and thus affect major intercellular activities. Photosensitizers play an important role as they absorb light. Oxygen must be present to react with excited photosensitizers in order to produce reactive molecules. The higher the level of oxygen the greater the chance of an excited photosensitizer dissipating its energy to it.

In summary, the adverse effects of solar radiation on living systems are mostly attributed to the small amount of UVB that is absorbed by cellular DNA. UVA wavelengths are less efficient in inducing DNA damage because they are not absorbed by native DNA but can still produce secondary photoreactions of existing DNA photoproducts or damage DNA via indirect photosensitising reactions (Sinha and Häder, 2002). UVB causes direct DNA damage by inducing the formation of DNA photoproducts, of which cyclobutane pyrimidine dimers are the most common. Whereas UVA wavelengths cause indirect damage to cellular DNA through catalysing the formation of chemical intermediates such as reactive oxygen species such as O_2^-, H_2O_2 and OH (Rincón and Pulgarin, 2004).

2.7.3   Batch Process Solar Disinfection

Batch Process Solar Disinfection (SODIS) consists of exposing raw water to the sun for several hours. This can be done in bottles or plastic bags in order to provide a low cost individual water treatment (Sommer *et al.*, 1997). SODIS is a treatment method to eliminate the pathogens, which cause water-borne diseases. It is ideal to disinfect small quantities of water used for consumption. The treatment process depends on solar energy only, which is an old but hardly applied water purification method.

In 1991, EAWAG/SANDEC embarked on an extensive project to assess the potential of SODIS and develop an effective, sustainable, low-cost water treatment method. SODIS is a simple technology used to improve the microbiological quality of drinking water. SODIS uses solar radiation to destroy pathogenic microorganisms that cause water borne diseases. It is ideal to treat small quantities of water.

Contaminated water is filled into transparent plastic bottles and exposed to full sunlight for six hours. Sunlight treats the contaminated water through two synergistic mechanisms: UVA radiation and increased water temperature. If the water temperature rises above 50°C, the disinfection process is three times faster (EAWAG, 2005).

Inactivation of microorganisms by
UV-A-radiation and thermal
treatment
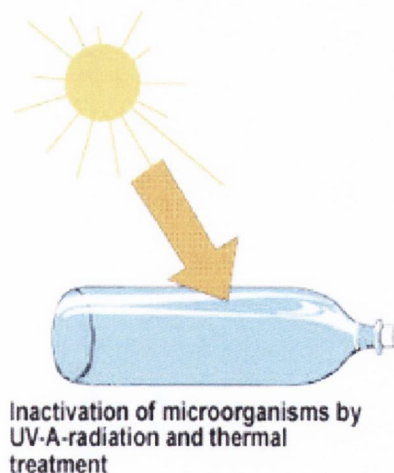
Figure 2.6: Batch Process Solar Disinfection (EAWAG, 2005)

A number of factors were found to be key in the application of SODIS (EAWAG, 2005).

- Weather

SODIS containers need to be exposed to the sun for 6 hours if the sky is clear or up to 50%

cloudy. The container needs to be exposed to the sun for 2 consecutive days if the sky is 100% cloudy. During days of continuous rainfall SODIS does not perform satisfactorily. Rainwater harvesting is recommended during these days. If a water temperature of at least 50°C is reached, an exposure time of 1 hour is sufficient.

- Water Turbidity

Suspended particles in the water reduce the penetration of solar radiation into the water and protect microorganisms from being irradiated. SODIS requires relatively clear water with turbidity less than 30NTU. Water with a higher turbidity has to be inactivated by the temperature increase rather than radiation or the water must be filtered before being exposed to the sun.

- Material and Shape of the Containers

Various types of transparent materials are good transmitters of light in the UV and visable range of the solar spectrum. Plastic bottles made from PET (Polyethyleneterephthalate) are preferred because they contain less UV-stabilisers than PVC bottles. Ageing of plastic bottles due to mechanical scratches and photoproduct production leads to a reduction in UV transmittance, which reduces the efficiency of SODIS. Heavily scratched or old, blind bottles should be replaced.

UV radiation is reduced by increasing water depth. At a water depth of 10cm and moderate turbidity of 26NTU, UV radiation is reduced by 50%. PET bottles do not have the most efficient shape for SODIS as they have a small area for sunlight exposure and have a water depth of 6-10cm. Containers with a larger exposed area per water volume would be more efficient. However, PET soft drink bottles are often easily available and thus more practical for the SODIS application.

- Oxygen

SODIS is more efficient in water containing high levels of oxygen. Aeration of the water can be achieved by shaking ¾ filled containers for about 20 seconds before they are completely filled.

Microorganisms, which have been found to be inactivated by SODIS, include pathogenic bacteria, viruses and protozoa. Table 2.4 below shows a list of pathogens that have been successfully inactivated by SODIS.

Pathogen	Illness	Reduction through SODIS ** at water temperatures of 40°C and solar exposure of 6 hours
Bakteria		
E.coli	Indikator for Water Quality & Enteritis	3-4 log (99.9 -99.99%)
Vibrio cholera	Cholera	3-4 log
Salmonella spp.	Thyphoid	3-4 log
Shigella spp.	Dysentery	3-4 log
Viruses		
Rotavirus	Diarrhoea, Dysentery	3-4 log
Polio Virus	Polio	inactivated, results not yet published
Hepatitis Virus	Hepatitis	Reduction of cases of SODIS users
Protozoa		
Giardia spp	Giardiasis	3-4 log (Infectivity of Cysts)
Cryptosporidium spp.	Cryptosporidiasis	2-3 log (Infectivity of Cysts)
Entamoeba histolitica	Dysentery	inactivated, results not yet published

Table 2.4: Inactivation of Different Organisms by SODIS (EAWAG, 2005)

Numerous studies have since been carried out to enhance the batch disinfection process by simple methods and to assess the effect of SODIS on different microorganisms, with the main indicator organism being *E. coli* K-12 (Kehoe *et al.*, 2001; Martin-Dominguez *et al.*, 2005; Reed, 1997; Reed *et al*, 2000). Photocatalytic enhancements have also been looked at and will be discussed in Section 1.6.

Kehoe *et al.*, 2001 assessed the effect of agitation, turbidity, aluminium foil reflectors and container volume on the efficiency of the batch process. To investigate the effect of agitation on inactivation kinetics 1 litre bottles were filled ¾ full and agitated by vigorous shaking for 1 minute prior to sampling. It was reported that no significant difference in inactivation rates was observed between agitated and non-agitated samples, however 1 minute agitation does not seem very efficient, oxygen transfer could be improved by continuous stirring. The study on the effect of aluminium foil reflectors was carried out using 0.5 litre bottles with aluminium kitchen foil attached to the rear outside surface of the bottles. Inactivation rates of *E. coli* were significantly improved in those bottles that were foil backed (1.85 times better). Two separate samples were used to assess the effect of turbidity on the disinfection process. In overcast conditions (mean irradiance 19mWcm^{-2}) a sample with a turbidity of 100NTU experienced a 6-log reduction in *E. coli* after 8.5 hours exposure whereas a sample with turbidity of 200NTU showed only a 3-log reduction after exposure under the same conditions. Exposures of 0.5 litres and 1.5 litre volumes showed

no significant difference in inactivation kinetics.

Reed (1997) investigated the role of oxygen in the SODIS process by exposing 2 litre bottles of contaminated water (*E. coli* and *Ent. faecalis*) to direct sunlight. Bottles were prepared such that separate samples were under anaerobic or aerobic conditions. It was shown that inactivation of *E. coli* in aerobic samples was 4 times more effective than in the anaerobic samples whereas it was 10 times more effective for *Ent. faecalis* in the aerobic samples, showing that solar disinfection is more effective under aerobic conditions. Further research by Reed *et al.* (2000) confirmed the oxygen requirement for inactivation of faecal coliforms under field conditions.

Dominguez *et al.* (2005) tested SODIS bottles with different shaped reflectors underneath to assess the effect of reflected sunlight on the disinfection process. Two different concentrating designs were used: a square concentrator and a double parabola concentrator. The reflecting surface in each case was aluminised duct tape. The authors also tested a combination of clear bottles, half black bottles and bottles which were totally painted black. The best results were observed when either concentrator was used with the half black bottle or the transparent bottle as compared to those experiments when no concentrator was used.

Between December 1995 and March 1996 a controlled field trial was carried out in Kenya to assess the health benefit of using SODIS bottles (Conroy *et al.*, 1996). 206 Maasai children aged between 5-16 in three adjoining areas of the Kajiado province in Kenya were given two 1.5 litre plastic bottles and assigned a method of water storage- full exposure to sunlight or no exposure. Every two weeks for twelve weeks the mothers of the children were asked to report any episodes of diarrhoea in their children. Water sources were monitored and tested repeatedly positive for faecal coliforms during the trial. During this study solar treatment of drinking water was associated with a reduction in diarrhoea episodes.

SODIS, while proving to be an effective technology has a number of limitations such as the volume of water that can be treated and the inherent dependency on each individual user. These limitations could be addressed by employing a centralised continuous flow system.

2.7.4   Continuous Flow Solar Disinfection

To date research into continuous flow systems for disinfection purposes has been limited with two main studies carried out by Acra *et al.* (1990) and Vidal and Diaz (2000). In the past, solar continuous flow systems have mainly been used for detoxification of chemicals by photocatalytic processes (see Section 2.8).

Acra *et al.* (1990) tested two separate solar reactors in Beirut in the late 1980s. Each reactor consisted of a storage reservoir and a solar reactor (serpentine or helical in shape) made form transparent Pyrex tubing, see Figure 2.7 below. Trial experiments were carried out in natural sunlight and results showed inactivation of *Streptococcus faecalis*, coliforms and *E. coli*. The authors recommended some factors that could increase the productivity of the reactors. These could include increasing reactor capacity or using many modular reactors and the removal of residual turbidity by settling in containers that could be readily removed for cleaning. They also felt it was essential to limit the disinfection process to that part of the day with sufficiently bright sunlight (~600W/m^2).
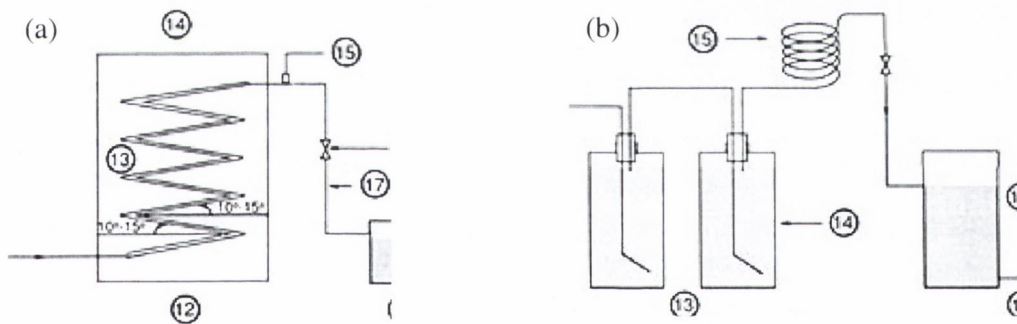
Figure 2.7: Serpentine (a) and Helical (b) shaped solar disinfection reactors (Acra *et al.*, 1990)

Vidal and Diaz (2000) performed experiments at both laboratory scale and at pilot plant level using a non-tracking compound parabolic collector. In the laboratory irradiation was carried out by a solar simulator with a 1000W Xenon arc lamp. Reaction vessels were 250ml vessels covered with Pyrex and experiments showed inactivation of *E. coli*, *Ent. faecalis* and *B. subtilis* spores. The pilot scale apparatus consisted of 12 Pyrex tubes mounted in compound parabolic reflectors orientated in an east-west orientation to maximise sunlight capture. 150 litres of water was recirculated through the photoreactor

tubes (25 litre volume) into a tank. Total inactivation of *E. coli* and *Ent. faecalis* was reported with initial concentrations varying from 1×10^2 to 1×10^5 CFU/ml. A cost analysis of the system was also made estimating an annual cost of disinfection in 2000 as $0.19/m^3$. Both of these studies indicate that continuous flow solar disinfection could be an ideal appropriate technology for use in developing countries where there is an abundance of sunlight.

2.8   Solar Photocatalysis

2.8.1   *Introduction*

Photocatalysis may be defined as the acceleration of a photoreaction by the presence of a catalyst (Blanco, 2003). Any mechanistic description of a photoreaction begins with the absorption of a photon. In the case of homogeneous photocatalytic processes the interaction of a photon-absorbing species, a substrate (R) light can lead to a chemical modification of the substrate, (R*). The photon absorbing species (C) is activated and accelerates the process by interacting through a state of excitation (C*). In the case of heterogeneous photocatalysis the interaction of a photon produces the appearance of electron/hole (e^- and h^+) pairs, the catalyst being a semi-conductor (e.g. TiO_2). In this case the excited electrons are transferred to the reducible specimen (Ox_1) at the same time that the catalyst accepts electrons from the oxidisable specimen (Red_2), which occupies the holes. In both directions the net flow of electrons is null and the catalyst remains unaltered.

$$C \rightarrow C*$$
$$C* + R \rightarrow R* + C \qquad\qquad \text{Homogeneous}$$
$$R* \rightarrow P$$

$$C \rightarrow C\left(e^- + h^+\right)$$
$$h^+ + \text{Re}\,d_2 \rightarrow Ox_2 \qquad\qquad \text{Heterogeneous}$$
$$e^- + Ox_1 \rightarrow \text{Re}\,d_1$$

The following sections will focus on heterogeneous photocatalysis and in particular the use of TiO_2 to enhance the solar disinfection process.

2.8.2   Heterogeneous Photocatalysis

The concept of heterogeneous photocatalytic degradation is simple; the use und irradiation of a stable solid semiconductor for stimulating a reaction at the solid/solution interface. By definition the solid can be recovered unchanged after many turnovers of the redox system. When a semiconductor is in contact with a liquid electrolyte solution containing a redox couple, charge transfer occurs across the interface to balance the potentials of the two phases. An electric field is formed at the surface of the semiconductor towards the interface. During photoexcitation band bending (bending of the valence bands in semiconductors due to the existence of surface charge potential formed as a result of adsorption of donor/acceptor molecules) provides the conditions for carrier separation. In the case of semiconductor particles, the two charge carriers should react at the semiconductor/electrolyte interface with the species in solution. Under steady state conditions the amount of charge transferred to the electrolyte must be equal and opposite for the two types of carriers. The semiconductor-mediated processes involve electron transfer across the interface. When electron/hole pairs are generated in a semiconductor particle the electron moves away from the surface to the bulk of the semiconductor as the hole migrates towards the surface (see Figure 2.8 below). If these charge carriers are separated fast enough they can be used for chemical reactions at the surface of the photocatalyst i.e. for the oxidation or reduction of pollutants (Blanco and Malato, 2002; Serpone and Emiline, 2002).
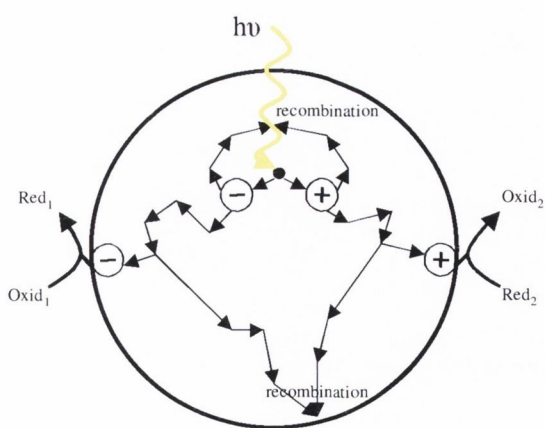
Figure 2.8: Fate of Electrons and Holes with a Particle of Illuminated Semiconductor in Contact with an Electrolyte (Blanco, 2003)

Metal oxides and sulphides represent a large class of semiconductor materials suitable for photocatalytic purposes. TiO_2 requires a band gap energy of 3.0 to be activated with the required corresponding wavelength being 390nm. This is calculated according to Planck's equation which states the radiation able to produce this gap must be of wavelength (λ) equal or lower than that calculated by $\lambda = \frac{hc}{E_g}$ where E_G is the semiconductor band gap energy, h is Planck's constant and c is the speed of light. Table 2.5 lists some semiconductor materials that have been used for photocatalytic reactions together with the wavelength required to activate the catalysts.

Material	Wavelength (nm)
CdS	497
Fe_3O_4	565
SnO_2	318
TiO_2	390
ZnO	390

Table 2.5: Semiconductor materials used in photocatalytic reactions with the wavelength required for activation.

Therefore a semiconductor particle is an ideal photocatalyst for a specific reaction if

- The products formed are highly specific

- The catalyst remains unaltered during the process

- The formation of electron/hole pairs is required (generated by the absorption of photons with energy greater than that necessary to move an electron from the valence band to the conduction band)

- Photon energy is not stored in the final products.

2.8.3   Application to Water Treatment

UV light can be used in several ways but direct photolysis can occur only when the contaminant to be destroyed absorbs the incident light efficiently. Homogeneous photocatalysis require large quantities of added oxidant. One such process is Photo-Fenton

reaction, an advanced oxidation process that has been developed to detoxify non-biodegradable wastewater. In the key reaction of the Photo-Fenton process Fe^{2+} ions are oxidised by the H_2O_2 while one equivalent OH is produced. The obtained Fe^{3+} or its complexes subsequently act as the light absorbing species that produce another radical while the initial Fe^{2+} is retained.

$$Fe^{2+} + H_2O_2 \rightarrow Fe^{3+} + OH^- + OH^\bullet$$

$$Fe^{3+} + H_2O + h\upsilon \rightarrow Fe^2 + H^+OH^\bullet$$

$$\left[Fe^{3+}L_n\right] + h\upsilon \rightarrow \left[Fe^{2+}L_{n-1}\right] + L^\bullet$$
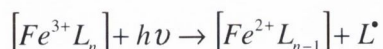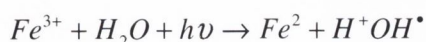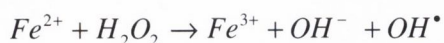
The main advantage of the Photo-Fenton process is the light sensitivity up to a wavelength of 600nm (35% of solar radiation). Disadvantages include the low pH values required and the necessity of iron hydroxide removal after the reaction (Fallmann *et al.*, 1999).

During heterogeneous photocatalysis dispersed solid particles absorb larger fractions of the UV spectrum efficiently and generate chemical oxidants in-situ from dissolved oxygen or water. These advantages make heterogeneous photocatalysis a particularly attractive method for environmental detoxification. The most important features of this process making it applicable to the treatment of contaminated aqueous effluents are:

- The process takes place at ambient temperature

- Oxidation of the organic substances into CO_2 is complete if dosage of Fenton's reagent as well as dose of photons is sufficient.

- The oxygen necessary for the reaction is obtained from the atmosphere

- The catalyst is cheap, innocuous and can be reused

- The catalyst can be attached to different types of inert matrices

$O_2^{-\cdot}$

O_2

$h\nu \geq 3.0\text{eV}$

e^-

TiO_2
Particle

h^+

H_2O

$\cdot OH + H^+$
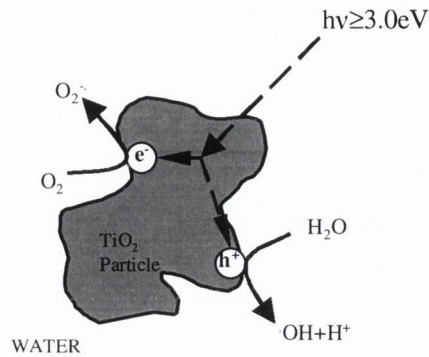
WATER

Figure 2.9: Effect of UV Radiation on a TiO$_2$ Particle Dispersed in Water

Whenever different semiconductor materials have been tested under comparable conditions for the degradation of the same compound, TiO$_2$ has generally been demonstrated to be the most active. TiO$_2$'s strong resistance to chemical and photocorrosion, its safety and low cost limits the choice of convenient alternatives. TiO$_2$ is of special interest since it can use natural sunlight, it is not photocorrosive in contrast to ZnO or Cds and not toxic in contrast to CdS. This is because it has an appropriate energetic separation between its valence and conduction bands, which can be surpassed by the energy content of a solar photon.

$$TiO_2 \rightarrow e^- + h^+ + TiO_2$$
$$e^- + h^+ + TiO_2 \rightarrow TiO_2 + heat + h\nu^i$$
$$\left(TiO_2^{iv} - O_2 - Ti^{iv}\right) - OH_2 + h_{VB}^+ \rightarrow \left(TiO_2^{iv} - O_2 - Ti^{iv}\right) - OH^\bullet + H^+$$
$$O_{2(ads)} + e^-_{CB} \rightarrow O_{2(ads)}^{-\cdot}$$
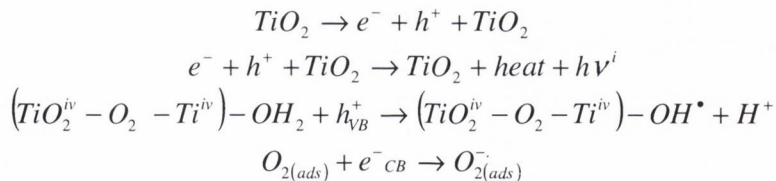
The hydroxyl radical (OH$^\cdot$) is the main oxidising specimen responsible for photooxidation of the majority of the organic compounds studied. The first effect, after absorption of near UVR, is the generation of electron/hole pairs which are separated between the conduction and valence bands. Recombination of the pairs generated is avoided if the dissolvent is oxidoreductively active (water) so that the solution also acts as a donor and acceptor of electrons. The holes oxidise water molecules attached to the TiO$_2$ surface forming OH radicals and protons. Oxygen and water are essential for photooxidation with TiO$_2$- there is no degradation in the absence of either (Blanco, 2003). Rutile and anatase are two different mineral forms of TiO$_2$ that are used in photocatalytic systems. Generally anatase is

considered to be the photoactive form while rutile is considered to have low photocatalytic activity. However, a mixture of anatase and rutile (e.g. TiO_2 Degussa P-25, consisting of 80% anatase and 20% rutile) has been shown to have better photo-activity than either by itself (Rincón and Pulgarin, 2003).

2.8.4 TiO_2 in Practice

One of the major design issues for photochemical systems is whether to use a suspended or a supported photocatalyst. Until now the majority of tests of solar photocatalytic reactors have been using small particles of TiO_2 suspended in contaminated water. The main advantages of slurry systems are:

- A low pressure drop through the reactor
- Better availability of the catalytic surface area for adsorption and reaction
- Good mass transfer of the contaminants from the fluid to the photocatalyst

The major disadvantage of systems containing suspended solids is the need to remove the TiO_2 from the cleaned water after treatment. Most TiO_2 powders contain submicron-sized particles. As a consequence, the potential inexpensive separation by sedimentation or filtration of the suspension is troublesome and treating large volumes of water is almost impossible. However, it has been reported that the process efficiency is reduced when the catalyst is fixed and for the same catalyst loading slurry reactors are more effective than fixed systems (Alfano et al., 2000). TiO_2 thin films are prepared by coating a substrate with a TiO_2 sol by different techniques such as chemical vapour deposition, chemical spray pyrolysis, electrodeposition and sol-gel method. This method is also suitable for deposition on a wide variety of substrates like stainless steel plates, alumina plates and silica and glass. A number of researchers have used TiO_2 to enhance the batch solar disinfection process (Salih, 2002; Watts, 1995; Matsunga, 1995; Huang, 2000; Ibanez, 2003; and Dunlop et al., 2002) in both suspended and fixed forms.

Salih (2002) conducted a series of experiments to determine the affect of TiO_2 on the solar disinfection process; TiO_2 was used in both suspended and immobilised form. Both applications improved the efficiency of solar disinfection although the suspended form was more successful with an enhancement factor of 1.62 as opposed to 1.34 for the immobilised form.

Rincon and Pulgarin (2003) carried out experiments using 50ml bottles and *E. coli* to examine the efficiency both of fixed/suspended TiO_2 as well as different forms of TiO_2. It was reported that TiO_2 fixed on Nafion membranes inactivated *E. coli* with efficiencies close to that observed for bacterial suspensions containing the same amount of suspended TiO_2. The radiation dose necessary for the total inactivation decreased by increasing the fixed TiO_2 concentration. Using suspended catalyst the highest photocatalytic efficiency was obtained for Degussa P-25 (rutile) comparing that of commercial Bayer and Aldrich, which contain an anatase form.

Ibanez *et al.* (2003) showed the complete destruction of *E. coli*, *P. aeruginosa*, *E. clocae* and *S. Typhimurium* using batch process solar disinfection with suspended TiO_2. Experiments were performed under simulated solar radiation with a concentration of 0.1g/l TiO_2.

CHAPTER 3

MATERIALS AND METHODS

3.1 Introduction

The objective of the following section is to discuss the materials and methods used during this project, including:

i.   The principles of solar collector systems and modifications used in order to harness collector systems for solar disinfection purposes.

ii.   A description of the solar disinfection reactors used during this process

iii. A description of the laboratory, analytical and statistical methods used during the course of this project.

3.2 Principles of Solar Collectors

3.2.1 Introduction

Solar reactor technology is that which efficiently collects solar photons and enters them in a suitable reactor to promote specific reactions. The equipment that does this is called a solar collector and has much in common with those used for solar thermal applications. As a result water detoxification systems and reactors have followed conventional solar thermal collector designs such as parabolic troughs and non-concentrating collectors (Blanco and Malato, 2002). Then the designs diverge as:

- Fluid must be exposed to solar UV radiation and therefore the absorber must be UV transparent.

- No insulation is required, as systems tend to concentrate on solar UV effects rather than temperature effects.

Traditionally solar collector systems have been classified into three types depending on the level of concentration attainable in the system (Malato *et al.*, 2004):

- Non-concentrating collectors, up to 150°C

- Medium-concentrating collectors, from 150-400°C

- High-concentrating collectors, over 400°C

Non-Concentrating Collectors are static and have no solar tracking. They are usually a flat plate aimed at the sun under a specific tilt. Their main advantage is their low-cost and simplicity.

Medium-Concentrating Collectors concentrate sunlight between 5 and 50 times and solar tracking is required. Parabolic trough collectors (PTC) and Fresnel lenses are in this group. PTCs have a parabolic reflecting surface which concentrates the radiation

on a tubular receiver located in the focus of the parabola. They can be one-axis (azimuth or elevation) or two-axis (azimuth and elevation) tracking. Fresnel lens collectors consist of refracting surfaces similar to convex lenses, which deviate the radiation at the same time that they concentrate it into a focus.

High-Concentrating Collectors have a focal point instead of a linear focus and are based on paraboloids with solar tracking. They have concentration ratios of up to 1000. Parabolic dishes and solar furnaces are examples of high concentrating collectors (CIEMAT, 2005).

Concentrating reactors have two major disadvantages compared to non-concentrating ones. The first is their inability to concentrate diffuse solar radiation, this is not important for thermal applications because it is only a small fraction of total solar radiation. However, during the detoxification of water it is the UV fraction of the solar spectrum that is required and since this is scattered by cloud cover as much as 50% can be diffuse. As non-concentrating solar collectors can make use of both direct and diffuse UV radiation their efficiency can be higher (Blanco and Malato, 2002). The second disadvantage of concentrating collectors is their complexity, cost and maintenance requirements that makes them unsuitable for use in developing countries.

3.2.2 Parabolic Trough Collectors

Solar photoreactors for detoxification purposes were originally designed for use in line-focus parabolic trough concentrators. There are two types of PTC; one axis tracking parabolic trough and two-axis tracking parabolic trough. The first engineering scale photoreactor for detoxification purposes was developed in the late 1980s in the US using one-axis PTCs and the second in Spain using two-axis PTCs. Both consisted of hundreds of square metres of collecting surface used for water detoxification using photocatalysis.

Two-axis PTCs consist of several parabolic trough collectors with the absorber in the focus. They are controlled by a two-axis tracking system, thus, the collector is always perpendicular to the solar rays, which are reflected by the parabola onto the reactor tube at the focus through which the contaminated water to be detoxified circulates. One-axis PTCs have a one-axis tracking system, as shown in Figure 3.1.

PTCs make efficient use of direct solar radiation as well as producing thermal energy, giving the possibility that the phenomena could be used in parallel. The combined UV and thermal effect could also have a positive effect on the inactivation rate, which will

be discussed further in Section 7. However, their mechanised nature make maintenance costs a consideration when proposing such a collector for use in developing countries.
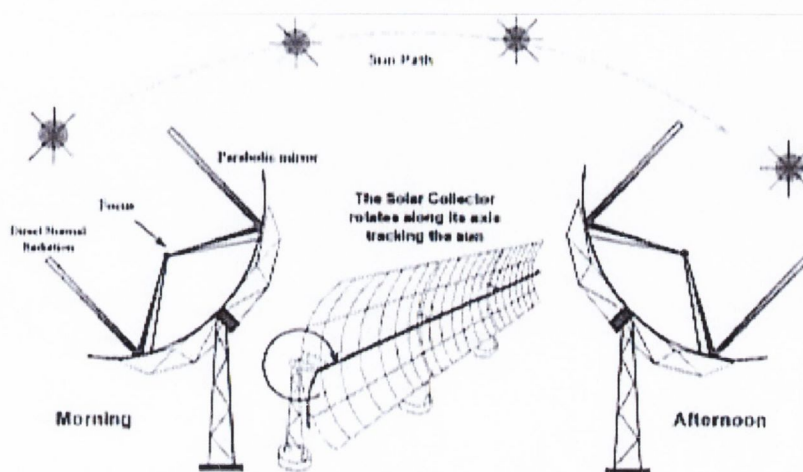
Figure 3.1: Solar ray reflection on a one-axis parabolic trough collector (CIEMAT, 2005)

3.2.3 Non-Concentrating Collectors

Non-concentrating collectors are less expensive than PTCs for a number of reasons; they have no moving parts or solar tracking devices, manufacturing costs are cheaper because their components are simpler which in turn means they have lower maintenance costs (Blanco and Malato, 2002).

A wide number of non-concentrating solar reactors have been developed for solar detoxification applications:

- *Trickle-down flat plate*, a tilted plate facing the sun over which the water to be treated falls slowly
- *Free-falling film*, same as the trickle-down flat plate but with a higher flowrate and open to the atmosphere
- *Pressurised flat plate*, consists of two plates between which water circulates
- *Tubular*, consists of many small tubes connected in parallel
- *Shallow Solar Ponds*, used as combined solar/microbiological treatment scheme.

3.2.4 Compound Parabolic Collectors

Compound Parabolic Collectors (CPCs) are low concentrating collectors that are traditionally used in thermal applications. They combine the properties of both parabolic concentrators and static flat systems. They can concentrate radiation but they are static and collect diffuse radiation. CPCs have a reflective surface following an involute around a cylindrical reactor tube. Almost all UV radiation arriving at the CPC aperture area can be collected and is available for the process in the reactor as shown in Figure 3.2 below.
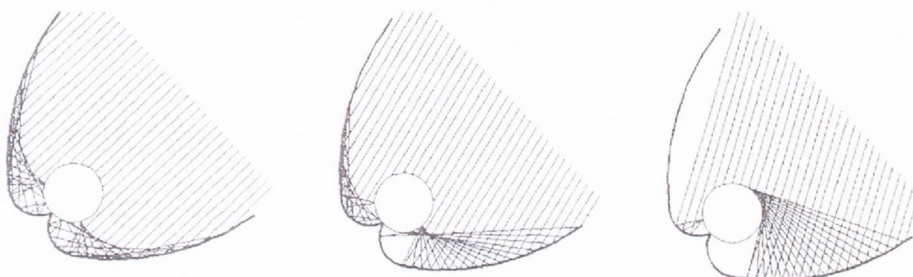
Figure 3.2: Reflection at a CPC surface

The light reflected by the CPC is distributed around the back of the tubular photoreactor illuminating most of the reactor tube circumference. Due to the ratio of CPC aperture to tube diameter, the incident radiation on the reactor is very similar to that of a non-concentrating photoreactor (i.e. the concentration ratio is one) but the performance is close to that of the simple tubular photoreactor, as the reactor tube circumference is illuminated (Blanco and Malato, 2002).

The design of the CPC reflector is based around its angle of acceptance, $2\theta_a$. The angle of acceptance is the angular range over which all rays are accepted i.e. the angular range over which the rays are reflected to the absorber. Half acceptance angles are constant for any particular design, with optimum angles between 60° and 90°.

Any point S on the reflector is defined by its distance $\rho = RS$ from the point R on the absorber surface. R is the point of contact of the tangent RS to the absorber circle. Thus, point S is also defined by the angle θ, which produces the tangent point R on the circle as well as the radius of the absorber, r. The CPC is designed so that RS is equal to the arc length AR along the circumference of the absorber. With the origin at the

centre of the absorber, the coordinates of point S (any point on the CPC reflector) are given by:

$$x = rSin\theta - \rho Cos\theta \qquad (3.1)$$

$$y = -rCos\theta - \rho Sin\theta \qquad (3.2)$$

where

$$\rho = r\theta \qquad \text{for } |\theta| \leq \theta_a + \frac{\pi}{2} \qquad (3.3)$$

and

$$\rho = r\frac{\theta + \theta_a + \dfrac{\pi}{2} - Cos(\theta - \theta_a)}{1 + Sin(\theta - \theta_a)} \qquad \text{for } \theta_a + \frac{\pi}{2} \leq |\theta| \leq \frac{3\pi}{2} - \theta_a \qquad (3.4)$$

with θ_a and θ measured in radians. The acceptance angle is defined as the angle through which a source of light can be moved and still converge at the absorber. For a CPC with a half acceptance angle of 90°, the angle of acceptance, $2\theta_a$=180°, this means that the collector accepts rays over an angular range 180° and is thus able to make this energy available to the absorber.
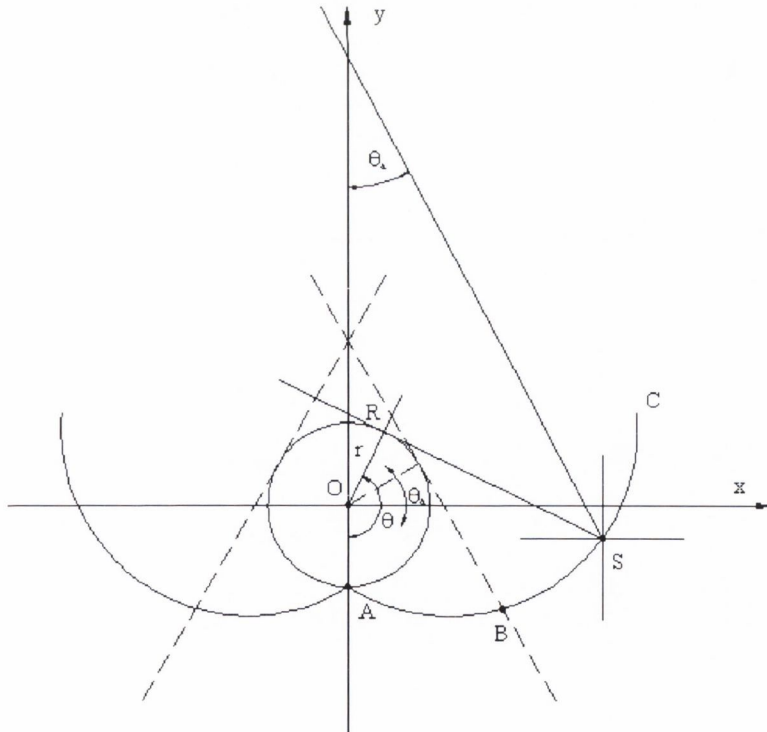
Figure 3.3: Obtaining CPC involute (CIEMAT, 2005)

58

The concentration ratio (CR) of a CPC is given by:

$$C = \frac{1}{Sin\,\theta} = \frac{A_{ap}}{2\pi r} = \frac{A_{ap}}{\pi d}$$

(3.5)

where A_{ap} is the aperture area and is the measure of the width of the aperture, therefore, the term C is dimensionless.

When $\theta_a=90°$, CR=1 and every CPC curve is an ordinary involute. When this occurs all the UV radiation that reaches the aperture area can be collected and redirected to the reactor (CIEMAT, 2005). This wide acceptance angle allows the reflector to direct both direct and diffuse sunlight onto the reactor with the additional advantage that these wide acceptance reflectors allow alignment errors of the absorber tubes. In direct sunlight wavelengths from 285-385nm comprise of only 2-3% of the energy whereas they make up 4-6% of combined diffuse and direct sunlight.

3.2.5 Reflector Surface

Materials that capture more than 50% of the incident light energy are classed as absorbers; those that reject more than 50% of the incident light are considered reflectors. Theoretically in perfect specular type reflection each ray (photon) in effect bounces off the material surface whole and intact i.e. the angle of incidence equals the angle of reflection. Most hard polished surfaces are primarily *specular* in nature. Aluminium, silver, gold and copper are the most optically useful specular materials.

Diffuse surfaces diffuse or scatter light incident from any angle and reflect it throughout a complete hemisphere in generally a cosine pattern according to Lamberts Law (1760). This pattern is produced submicroscopically by surface irregularities smaller than the wavelength of light.

Spreading surfaces break up the incident beam into a broadened reflected pencil of light through limited predetermined angles i.e. spread reflection is a combination of diffuse and specular reflection. By impressing or moulding carefully designed patterns it is possible to control the spread of light in any desired manner (Young and Freedman, 1999).

Spread   Specular   Diffuse
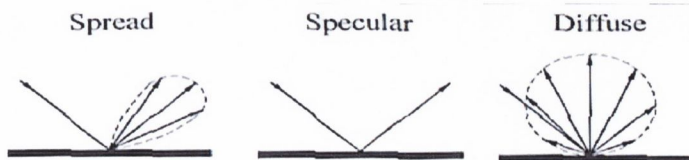
Figure 3.4:   Types of Reflection

In the case of solar applications the optical quality requirements of the reflective surface is related to the concentration required by the particular application. The higher the concentration desired the stricter the requirements for quality of parameters and the more specular the desired effect. This is an important factor of low or non-concentrating systems since lower quality requirements translate into lower manufacturing costs (CIEMAT, 2005) although there is a trade off between specular quality and the size of the reactor as the more solar radiation that is reflected the more efficient each square meter of reflector and therefore the size of the reflector could be reduced.

However the majority of solar detoxification processes require a highly reflective material in the UV range of the spectrum. Silver, most commonly used for the fabrication of conventional mirrors, is not a valid option since its efficiency is very low in the UV range (Malato *et al.*, 2005). Aluminium is the only metal surface that is highly reflective throughout the UV spectrum. Reflectivities are approximately 92% in the range 280nm to 385nm, whereas silver reflects only 25% at 280nm, (CIEMAT, 2005), see Figure 3.5 below.
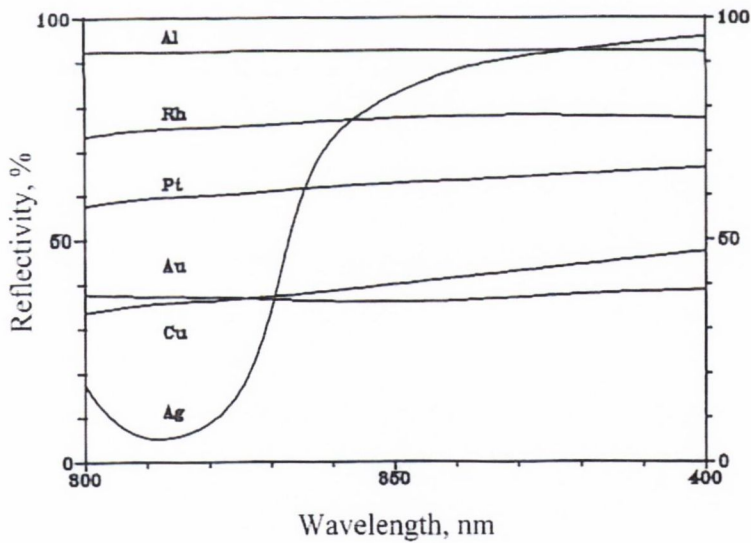
Figure 3.5: Reflectivity of different materials in the UV Range (CIEMAT, 2005).

The ideal reflective surface for solar detoxification applications must have high reflectivity in the UV range but must also have acceptable durability under outdoors conditions and be reasonably priced. At the present time the solution considered most suitable for detoxification purposes is based on anodised and electropolished

aluminium. Surfaces as aluminised plastics have been developed which may be weather resistant but lack of rigidity means that they must be attached to a rigid substrate.

The anodised process consists of creating a thin layer of aluminium oxide (Al_2O_3) on the electrolytically deposited aluminium. Fend *et al.*, reported that the reflectivity of standard anodised aluminium was only reduced by approximately 15% after exposure to solar radiation for 15 months in a cold and humid climate (where decreases are most significant). However, specular reflectance values decreased dramatically enabling the material to be used only in non-concentrating systems such as CPCs (Fend *et al.*, 1998). Thicker oxide layers (up to 50µm) are usually specified when anodised aluminium is intended for marine applications but this results in considerably lower reflectance. An interesting alternative is to cover the aluminium with a protective acrylic lacquer (resistant to corrosion). In both cases a compromise between outdoor resistance and UV reflectance must be achieved.

3.2.6 Tubular Absorber Materials

The tubular reactor must contain a working fluid and must transmit UV radiation efficiently. The selection of materials, which is both highly transmissive to UV light and resistant to its destructive effects, is limited.

Quartz has an excellent UV transmittance and chemical resistance but its high cost makes it unfeasible for low-cost applications. Fluoropolymers can only support low pressures due to their lack of rigidity; therefore the thickness of their walls has to be increased with a subsequent loss in transmittance (CIEMAT, 2005).

Glass is a natural alternative for photoreactors but is unsatisfactory due to its iron content which absorbs UV radiation. An additional negative effect called "ultraviolet solarisation" is caused by a change in valence of certain polyvalent ions that are present in the glass. Solarisation is a loss in transmission observed upon irradiation of glasses caused by impurities such as iron and manganese (Malato *et al.*, 2005). Defects are formed in the glass and often cause high absorbance in the UV and visible range (Mönke and Ehrt, 2004). One way to reduce this is to introduce 0.1% of Si in the glass melting process.
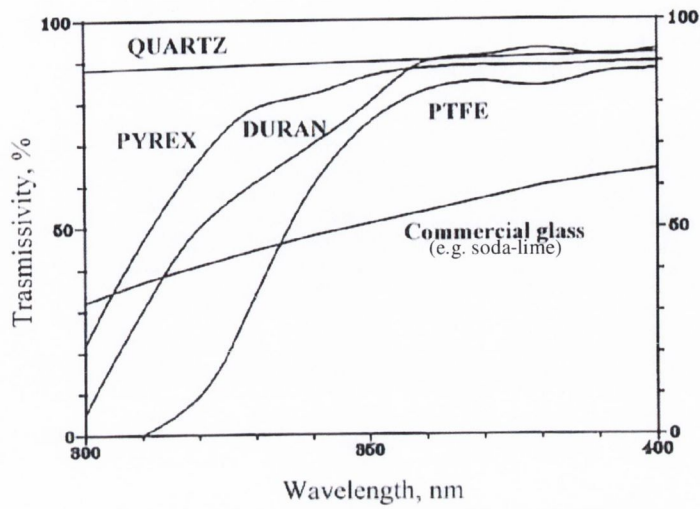
Figure 3.6: Transmissivity of different materials suitable for manufacture of photoreactor tubes.

As a result only low-iron glass such as borosilicate (Pyrex® and Duran®) is appropriate for reactors. A study by Blanco *et al.* (1999) compared different borosilicate glasses of varying iron oxide content (from <1 mg/kg to standard 250 mg/kg Fe_2O_3). UV transmissivity in the critical range between 300 and 400nm increased as the iron oxide content decreased as shown in Table 3.1. Solarisation experiments performed under artificial solar radiation showed that almost no solarisation occurred in extremely pure glass (Fe^{3+} <1 mg/kg) whereas the UV-transmissivity of the other types decreased.

Iron Content (Fe^{3+}), mg/kg	Transmissivity (300-400nm), %
0	91
50	88
100	84.5
150	83.5
200	81
250	80

Table 3.1: Transmissivity of borosilicate glass with different Fe^{3+} content (Blanco *et al.*, 1999)

3.3 Description of Solar Reactors

3.3.1 Introduction

During the course of this project five different continuous solar reactors were used in order to compare reactor efficiency under a number of conditions. Batch process experiments were also carried out using Duran® bottles. The following section describes all the reactors used.

3.3.2 Small-Scale Continuous Flow Reactors (operated in batch mode)

Four different small-scale reactors were used during this project each consisting of a reflector, tubular absorber, pump, reservoir and connectors. The reactors were static, non-tracking recirculating systems each having a different reflector profile; Compound Parabolic, Parabolic and V-groove. A non-reflecting reactor was also used in order to assess the benefits of using reflector systems. The profile of each reflector is shown in Figure 3.7 below. Reflectors were fabricated by milling a block of aluminium into the required shape and polishing the surface. Calculated aperture areas for the Compound Parabolic, V-groove and Parabolic reactors were $0.057m^2$, $0.057m^2$ and $0.042m^2$ respectively.

Each reactor had six 250mm long absorber tubes mounted at its centre. The non-reflecting reactor consisted of the six similar absorber tubes mounted above a flat matt black surface. Reactor shapes were chosen so an assessment could be made between the efficiency of shapes which were easy to fabricate and subsequently less costly (V-groove) and those of a greater reported efficiency but with a greater associated fabrication cost (Compound Parabolic).

63
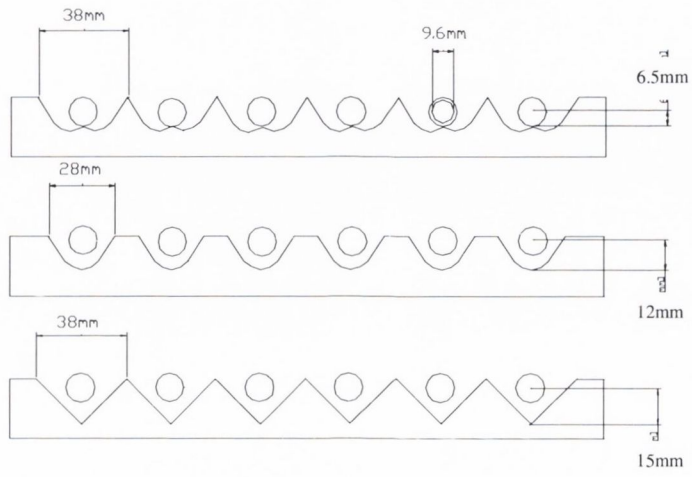
Figure 3.7:Reflector profile for the (a) Compound Parabolic, (b) Parabolic and (c) V-groove reactors.
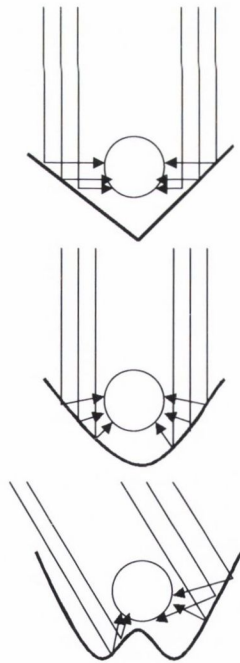
Figure 3.8: Schematic of the three reactors and their solar reflection capacities

The specular reflectivity of the milled aluminium collectors is shown in Figure 3.9 below. Sample A is a coated aluminium sheet, similar to that used in the pilot-scale reactor described in Section 3.3.3 (the coating causes the sinusoidal reflectance), sample C is the polished milled aluminium used for reactor fabrication and sample B is an unpolished aluminium sample. It should be noted that this is a plot of specular reflection at the wavelengths shown and diffuse reflectivity is not accounted for.
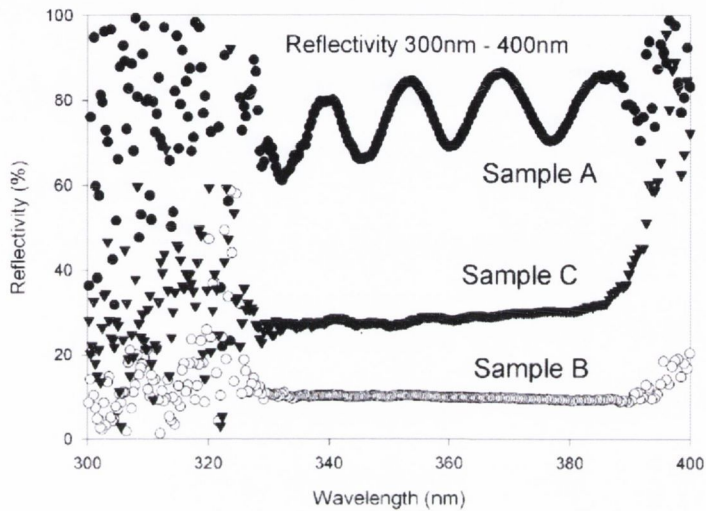
Figure 3.9: Reflectivity of Milled Aluminium in the 300nm-400nm range.

Absorber tubes were 250mm long borosilicate glass tubes of 9.6mm diameter mounted at the focal point of each reactor aperture. The tubes were connected using PVC tubing and then the system was connected to a centrifugal pump and small reservoir. A schematic of the system is shown in Figure 3.10.
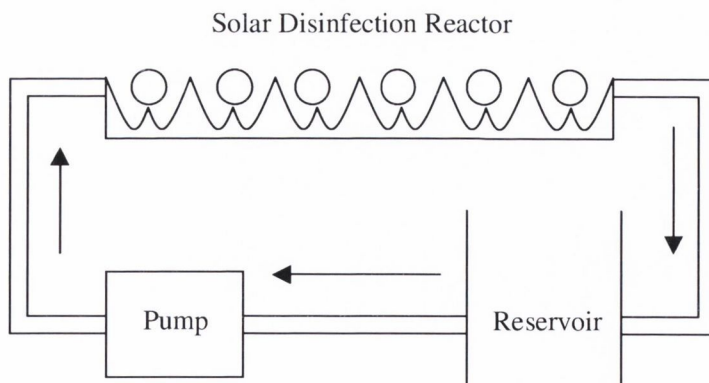
Figure 3.10: Schematic of the Solar Disinfection Reactor.

A photograph of the small-scale reactors exposed to natural solar radiation is presented in Figure 3.11 below.

Figure 3.11: Two Small-scale solar disinfection reactors exposed to natural solar radiation at PSA.

The reactors were configured as recirculating systems with a total volume of one litre.

3.3.3 Pilot-scale Reactor

The pilot-plant system used for this research was located at Plataforma Solar de Almería, southern Spain and consisted of a Compound Parabolic Collector with eight Pyrex tubes aligned in an east-west direction. Water was recirculated through a reservoir via a centrifugal pump. The CPC aperture was tilted to the same angle from the horizontal as latitude (37°) for the experiments in order to maximise sunlight capture. The characteristics of the reactor are presented in Table 3.2 below along with a photograph of the reactor in Figure 3.12.

Pilot Plant	
Total Volume	35 litres
Illuminated Volume	22.4 litres
Collector Aperture Area	3.08m^2
Inner Diameter of Tubes	29.4mm
Flowrate	20 litre/min

Table 3.2: Pilot scale Reactor Characteristics

Figure 3.12: Pilot scale reactor located at Plataforma Solar de Almería.

3.4 Solar Radiation Sources and Measurement

3.4.1 Simulated Solar Radiation

During simulated solar radiation laboratory experiments the reactors were placed directly underneath a 1000W solar simulating xenon arc lamp (Model 91190-1000W Large Area Light Source, Oriel Corporation, Stratford, CT, USA). An ellipsoidal reflector surrounds the lamp and collects over 70% of the output. This radiation is focused onto an optical integrator which produces a uniform diverging beam which is deflected 90° by a mirror to a final collimating lens. The output is a uniform collimated beam. The lamp has a short cut-off at 260nm and was fitted with an air mass 1 filter (AM 1 Direct Filter Set P/N 81074 + 81011, Oriel Corporation, Stratford, CT, USA), which simulates the equatorial solar spectrum at ground level when the sun is directly overhead. In the laboratory, radiation measurements were made using an optical power meter (model 200/10+, Coherent, Cambridge, UK). During these experiments simulated solar UV radiation intensities were kept at 31.59 W/m^2 (±1), which corresponds to a sunny noon in southern Spain. Figure 3.13 below shows the output of the solar simulator normalised to match the CIE (Commission Internationale de L'Eclairage) standard curve (Lot-Oriel).
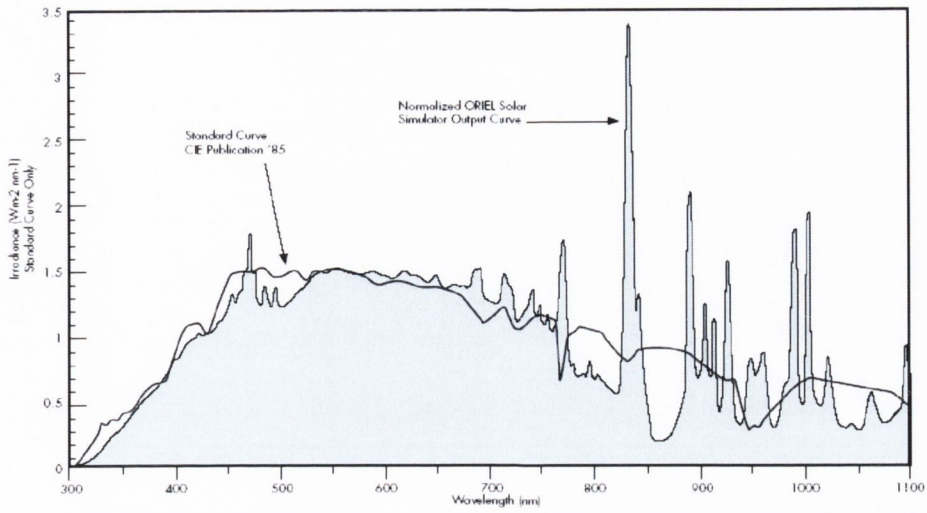
Figure 3.13: Output of Oriel Solar Simulator normalised to match the CIE standard curve.

A schematic of the 1000W simulator is presented in Figure 3.14. During experiments the solar reactor was placed directly under the beam of the simulator with the connectors and reservoir kept in the dark throughout.
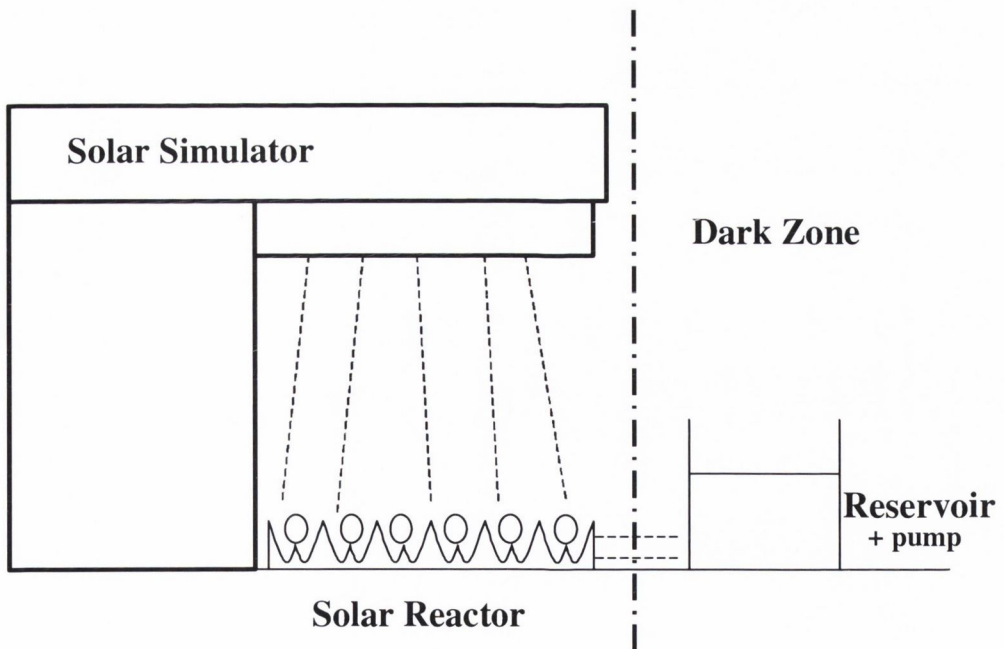
Figure 3.14: Schematic Representation of 1000W Solar Simulation Apparatus.

During batch experiments the water temperature in the bottles was kept constant at 20°C by a waterbath. During all other experiments temperature was monitored were with a thermocouple-based digital thermometer (Checktemp 2; Hanna Instruments) at the system's reservoir.

During Light/Dark ratio experiments the lamp shutter was opened and closed by using a signal generator (TTi-TGA1241, 40MHz arbitrary waveform generator, which produced a pulsed signal in order to open and close the shutter at required time intervals.

3.4.2   Natural Solar Radiation

(a) Plataforma Solar de Almería, Spain

Experiments performed under real solar conditions were carried out at Plataforma Solar de Almería in southern Spain during June and July 2003 and May 2004. Reflector apertures were tilted to the local latitudinal angle (37°) to maximise sunlight capture and positioned so that the tubes were aligned in an east-west orientation (see Figure 3.15). Solar radiation measurements at Plataforma Solar de Almería were made using a 300nm-400nm broadband UV radiometer (CUV3 Kipp and Zonen, Netherlands) located on site with an average global UV intensity 34W/m^2 (std. dev.= 2.33W/m^2) during the trials.
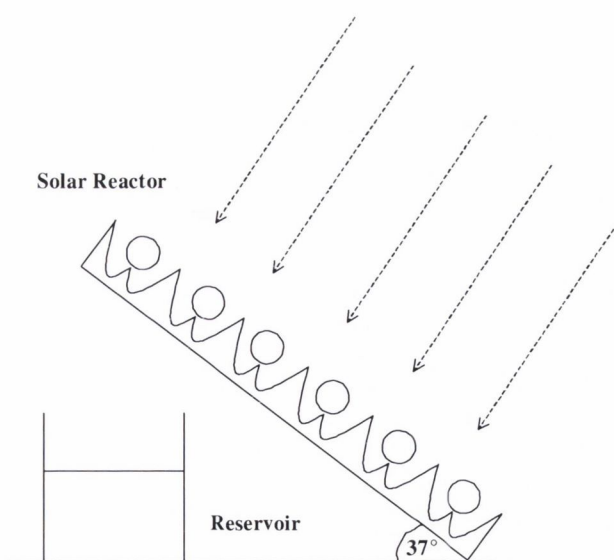
Figure 3.15: Schematic of Solar Reactor angled at 37° for use at PSA in Southern Spain

(B) Trinity College, Dublin, Ireland

Experiments were carried out on the roof of the Civil Engineering Building at Trinity College in Dublin. The reactors were set up in exactly the same way as at PSA but were angled to the local latitude (53°). Solar radiation measurements for the area were obtained from Met Eireann (solarimeter and Campbell-Stokes sunshine recorder). The average global UV intensity during the trials was ~20W/m^2.

3.5 Photocatalytic Media

3.5.1 Introduction

Titanium dioxide (TiO$_2$) was used as the photocatalyst in these experiments. The photocatalyst was prepared in three different ways as described below. Typically, photocatalysts are added into the process liquid as a suspension which has proved successful in several applications such as the breakdown of persistent organic compounds (Konstantinou and Albanis, 2003 ; Malato et al., 2002a). However, this is not considered to be a particularly attractive solution for a small-sale rural water supply system in a developing country since the TiO$_2$ will require some form of separation and recovery process at the end of the solar reactor before the water is suitable for consumption. Hence, this research has also looked at the concept of coating small 2mm diameter glass rods with TiO$_2$ which are then fixed along the centre of each reactor tube as well as fixing a TiO$_2$ coated paper inside the reactor tubes.

3.5.2 TiO$_2$ Slurry

The appropriate mass of P-25 (Degussa) TiO$_2$ (anatase:rutile=3.1; surface area 50m^2/g; non-porous particles) was pre-suspended in 200ml of distilled water and autoclaved to ensure sterility. The TiO$_2$ was then added to the solution in the reactor to obtain a uniform concentration at the desired amount (3, 6, 9 mg/l). The water in the reactor was then circulated for an adequate time to ensure a complete mix of the photocatalyst.

3.5.3 Fixed TiO$_2$ (Glass)

A stable coating of P25 TiO$_2$ onto the glass rods was achieved using the following technique. The rods were initially rinsed with distilled water and then placed into a jar filled with 1% detergent solution which was sonicated for 15 minutes. They were then rinsed with distilled water again and sonicated for a further 15 minutes. This step was repeated three times. The rods were then dried in an oven at 105°C before being

weighed. A 1% solution of Degussa P-25 TiO_2 was prepared with distilled water and sonicated for 15 minutes. Each rod was swirled in the TiO_2 solution until coated. The rods were then placed into an oven for 10 minutes until the layer dried. This step was repeated fifteen times to ensure an adequate coating. The rods were then annealed at 250°C overnight. The rods were fixed into position at the centre of the Pyrex tubes with very thin wire supports at each end before exposure to sunlight in the tests as shown in Figure 3.16.

3.5.4   Fixed TiO_2 (Paper)

The TiO_2 paper was a commercially available product from Ahlstrom[©]. The paper consisted of Degussa P-25 coated on glass fibre paper (synthetic fibres, 2mm thick) using an inorganic binder. The binder was an aqueous dispersion of colloidal SiO_2 and after washing the TiO_2 component was 19.3 g/m^2.

The paper was wrapped around 2mm glass rods and fixed into the centre of the reactor tubes using thin wire again before exposure to sunlight as shown in Figure 3.16.
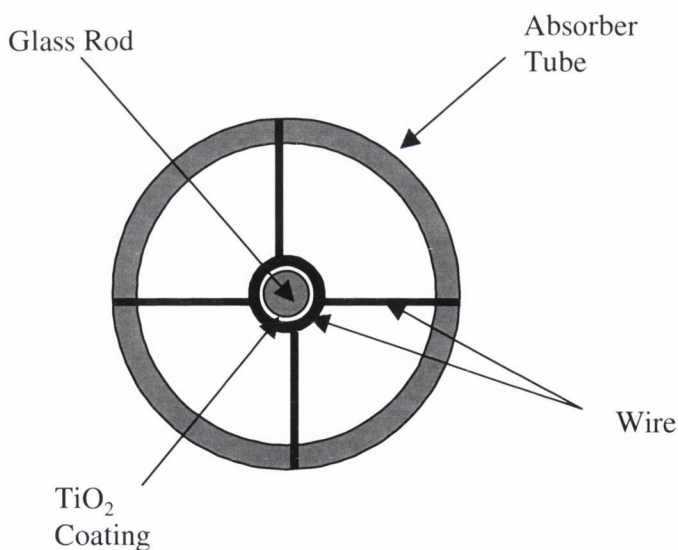
Figure 3.16: Method of Fixing TiO_2 Coated Rods into the Absorber Tubes.

3.6 Bacterial Preparation

3.6.1   Introduction

The heterotrophic plate count (HPC) is a method for estimating the number of live heterotrophic bacteria in water and measuring changes during water treatment. Colonies may arise from pairs, chains, clusters or single cells all of which are included in the term colony forming units (CFU). The spread plate method was used throughout the experiments described in the thesis. This method causes no heat shock and all colonies are on the agar surface where they can be easily distinguished from particles and bubbles (APHA, 1999).

3.6.2   Preparation of Media

Luria Bertani (LB) broth, containing Tryptone, yeast extract and NaCl in the ratio 1.0 : 0.5 : 1.0 by mass and adjusted to pH 7.0 was used as the culture medium for all bacteria. 25g of broth was dissolved in 1 litre of deionised water and the solution was shaken until the powder had dissolved. The solution was autoclaved in order to eliminate any contaminants and then transferred to sterile 50ml centrifuge tubes. Prepared tubes were stored at 4°C and used within one week of preparation.

Luria Bertani Agar, containing Tryptone, yeast extract, NaCl and agar in the ratio 1.0 : 0.5 : 1.0 : 1.5 was used as the plate medium for all experiments. The agar was prepared in deionised water and autoclaved before pouring. 25ml of the solution was poured into sterile Petri dishes and dried in a laminar flow chamber at room temperature. Plates were stored at 4°C and used within three days of preparation.

3.6.3   Preparation of Bacteria

Discrete colonies of an *Escherichia coli* K-12, (*E. coli* K-12), (or *Salmonella Typhimurium*) streaked plate were transferred to 50ml of sterile LB broth and incubated statically at 37°C for 18 hours to yield a stationary phase culture. The culture was centrifuged at room temperature at 3000rpm (855 x g) for 12 minutes. The supernatant was discarded and the pellet was resuspended in 50ml of sterile water and recentrifuged. This process was repeated twice to ensure the removal of all trace nutrients. Finally the pellet was resuspended in a total of 5ml of sterile water, diluting the pellet to a concentration of ~1x 10^9CFU/ml. The required concentration for each experiment was prepared by adding the desired amount of this solution to the required amount of sterile

water e.g. 1ml added to 1litre of sterile water to achieve an initial concentration of 1x 10^6 CFU/ml.

3.6.4 Bacterial Enumeration

The standard plate count method was used in all experiments. Samples were taken at discrete time intervals and appropriate serial dilutions were carried out in sterile water. 20μl of diluted was dropped onto a dried sterile plate in duplicate (see Figure 3.17). Plates were left at room temperature for the duration of each experiment and then incubated at 37°C for 18 hours. More than 50 colonies per drop were deemed unacceptable, as colonies were too close to each other to be distinguished. Therefore a higher dilution was used in such cases. The total count was converted to colony forming units per ml (CFU/ml) using equation (x) below.

$$\left[\frac{A+B}{2}\right] \times 50 \times Dilution = CFU / ml$$

Less than 10 colonies per drop were also unacceptable for statistical reasons. In such cases, 250μl of the sample was transferred to a plate using the spread plate technique. The colonies were counted after incubation and multiplied by four to convert to CFU/ml.
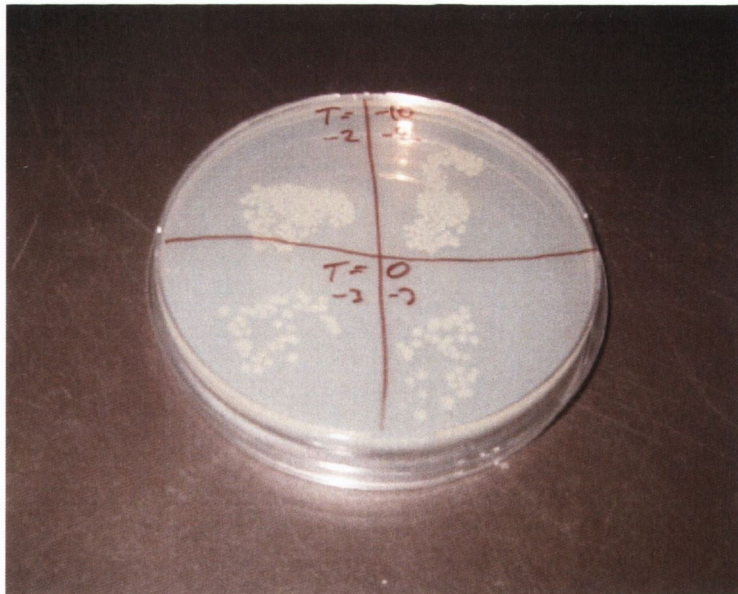
Figure 3.17: Agar plate with *E. coli* K-12 colonies: dilutions of 10^{-2} and 10^{-3} shown.

3.7 Determination of Inactivation Kinetics

3.7.1 Calculation of Decay Constants

First order decay constants were calculated according to the standard principles of disinfection kinetics (Eq. 3.6) based on the exponential decline of organisms, as described by Chick's Law (Chick, 1908).

$$\frac{dN}{dt} = -kN \rightarrow N_t = N_0 e^{-kt} \tag{3.6}$$

where :

N_t = number of viable organisms at time, t

N_0 = number of viable organisms at time zero

k = inactivation rate constant

t = time

Rearranging:

$$\ln\frac{N_t}{N_0} = kt \tag{3.7}$$

Therefore, a plot of ln (N_t/N_0) versus time should result in a straight line with slope equal to k (min^{-1}). Experimental rate constants were calculated by linear regression.

3.7.2 Calculation of Illumination Time

During the experiment the water recirculates through the reactor into the reservoir which is effectively a dark zone. Illuminated time can be calculated as the volume inside the reactor as a function of total system volume.

V_{total} = 1litre

V_{illum} = 0.1925litre

V_{dark} = 0.2075litre

V_{res} =0.6000litre

Therefore, the experimental time multiplied by 0.1925 is the amount of time each sample spends exposed to the solar radiation. For example, during one hour of experimental time, the total exposure time (illumination time) is 11.55min.

Inactivation constants have also been calculated as a function of illumination time, substituting t in Eq. 3.7 for t_{illum} to give,

$$\ln\frac{N_t}{N_0} = kt_{illum} \tag{3.8}$$

Therefore, a plot of ln (N_t/N_0) versus illuminated time should result in a straight line with slope equal to k (min^{-1}).

3.7.3 Calculation of Dose

Calculation of inactivation kinetics using experimental time or illumination time mask the fact that the solar intensities in natural sunlight are continually changing due to varying cloud cover and time of day. In order to take this into account the cumulative irradiated UV energy received per litre of sample was calculated as per equation 3.9 below (Malato *et al.*, 2002a).

$$Q_{UV_n} = Q_{UV_{n-1}} + \frac{\Delta t_n UV_{GN} A}{V_T} \qquad \Delta t_n = t_n - t_{n-1} \qquad (3.9)$$

where :

$Q_{UV, n}$, $Q_{UV,n-1}$ = cumulative irradiated UV energy received per litre of sample at times n and n-1

Δt_n =   time interval between two sampling times

UV_{GN} =   average incident radiation on the irradiated area

A =   irradiated area

V_T =   total circulating volume

Therefore, a plot of ln (N_t/N_0) versus Q (kJ) should result in a straight line with slope equal to k (kJ^{-1}).

While comparing different reactors a modification of Equation x was used to take into account the varying area of the reflectors i.e. the Parabolic reflector has a smaller irradiated area than the Compound Parabolic or V-groove reflector. The area term in the equation was modified to the absorber area, which is equal for all reactors so a % enhancement for each reflector could be calculated (Eq. 3.10).

$$Q_{aUV_n} = Q_{aUV_{n-1}} + \frac{\Delta t_n UV_{GN} A_a}{V_T} \qquad \Delta t_n = t_n - t_{n-1} \qquad (3.10)$$

where :

$Q_{aUV, n}$, $Q_{aUV,n-1}$ = cumulative irradiated UV energy received per litre of sample at times n and n-1

Δt_n =   time interval between two sampling times

UV_{GN} =   average incident radiation on the irradiated area

A_a =   absorber area

V_T =   total circulating volume

Again a plot of ln (N_t/N_0) versus Q_a (kJ) should result in a straight line with slope equal to k (kJ^{-1}).

While comparing different reactors with different exposure times a modification of Eq. 3.10 was used to take into account the varying area of the reflectors and the difference in illumination time i.e. the small-scale reactors had a different illumination time to the pilot-scale reactor (Eq. 3.11).

$$Q_{aillumUV_n} = Q_{aillumUV_{n-1}} + \frac{\Delta t_{n\,illum} UV_{GN} A_a}{V_T} \qquad\qquad \Delta t_{n\,illum} = t_{n\,illum} - t_{n_{illum}-1} \qquad (3.11)$$

where :

$Q_{aillumUV, n}$, $Q_{aillumUV,n-1}$ = cumulative irradiated UV energy received per litre of sample at times n and n-1

Δt_{nillum} = time interval between two sampling times

UV_{GN} = average incident radiation on the irradiated area

A_a = absorber area

V_T = total circulating volume

A plot of ln (N_t/N_0) versus Q_{aillum} (kJ) should result in a straight line with slope equal to k (kJ^{-1}).

CHAPTER 4

SIMULATED SOLAR RADIATION

4.1 Introduction

The aim of these preliminary studies was to

i.   Investigate the effect of flow regime on the solar disinfection process

ii. Compare the effect of different solar intensities on the solar disinfection process

iii. Assess the use of *Escherichia coli* K-12 as an indicator with comparison to the more resistant organism *Salmonella typhimurium*.

iv. Compare the effect of using glass tubing against pyrex tubing as the pipe material in a solar reactor

v.   Assess the difference in inactivation rate between batch and continuous flow disinfection (operating in batch mode) processes.

Throughout these experiments the parabolic collector was used to compare the different parameters. All tests were performed at the Royal College of Surgeons, Ireland using the 1000W Xenon arc solar simulator as described in Section 3.4.1.

4.2 Flow Regime

4.2.1 Introduction

The purpose of these experiments was to investigate the effect of different flow regimes on the solar disinfection process. Flow regimes are classified by Reynolds (Re) number, which is defined as:

$$Re = \frac{\rho v D}{\mu} \tag{1}$$

where ρ is the mass density of the liquid (kg/m^3), v is its mean velocity (m/s), μ its dynamic viscosity (kg/ms) and D (m) is the diameter of the pipe. By calculating the dimensionless Reynolds number of the flow its nature can be determined.

For water in pipes:

Laminar flow: Re < 2000

Transitional flow: Re = 2000 to 4000

Turbulent flow: Re > 4000

In laminar flow viscous effects dominate and all of the streamlines are parallel to each other; the flow is very smooth, uniform and steady. In turbulent flow the streamlines are random and the flow is uneven, such that at any particular point in the pipeline, the velocity fluctuates from one instant to the next. This allows for complete mixing of the fluid within the pipe. Between laminar and turbulent flow there is an ill-defined transition region (Hamill, 2001). The turbulent flow regime has been used in all

research previously carried out in continuous flow solar disinfection (Acra *et al*, 1989, Vidal and Diaz, 2000, Rincón and Pulgarin, 2004). This allows for complete mixing of the solution within the pipe and an even distribution of solar radiation to all bacteria. The advantage of using laminar flow would be that in a full scale single pass system the slower the flow the shorter the system would need to be to achieve the required solar UV dose as pipe diameter could be much larger.

4.2.2 Experimental Set-up

The flowrate in the parabolic reactor was controlled by means of a valve. Three different flowrates were tested, each corresponding to a different flow regime. The flowrates, velocities and corresponding Reynolds numbers are shown in Table 4.1 below. The volume of water in each case was kept constant, each test using one litre of sterile water inoculated with a 1×10^6 CFU/ml concentration of *E. coli* K-12. All tests were carried out using simulated solar radiation in the laboratory using the 1000W Xenon arc lamp as described in Section 3.4.1, adjusted to give an optical irradiance of 31W/m^2 simulated solar UV radiation, which corresponds to a total global radiation of 900W/m^2. Sampling was carried out every 15 minutes with controls left in the dark throughout the experiment. The samples were enumerated as outlined in Section 3.6.4 and inactivation kinetics determined as described in Section 3.7. All of the tests were repeated at least four times.

Flow Regime	Flowrate (l/min)	Velocity (m/s)	Re. no
Laminar	0.61	0.14	1180
Transitional	1.6	0.37	3119
Turbulent	2.2	0.51	4299

Table 4.1: Flow regime characteristics with their associated Reynolds numbers.

4.2.3 Results and Discussion

Representative data from the laboratory trials using the parabolic reactor and three different flow regimes are presented in Figure 4.1. All plots show an average of at least four experiments.

(a)

(b)
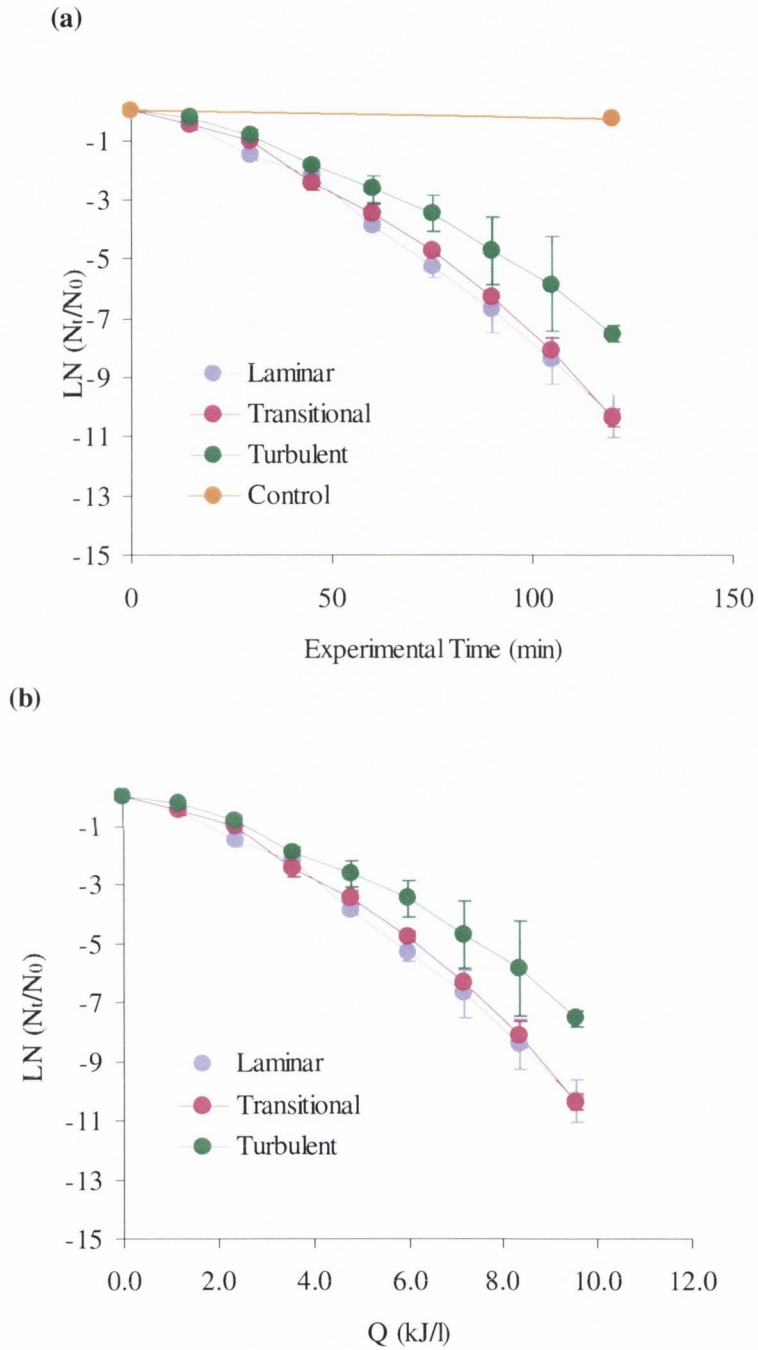
Figure 4.1: Comparison of Laminar, Transitional and Turbulent flow regimes plotted as (a) inactivation of *E. coli* K-12 against experimental time and (b) inactivation of *E. coli* K-12 against cumulative simulated solar UV dose, Q. The error bars represent the standard error of the mean.

79

All experiments showed at least a >3-log reduction of *E. coli* K-12 within the 120 minute experimental time. Inactivation rate constants were calculated according to the standard principles of disinfection kinetics (Section 3.6). The inactivation rate constant calculated for the turbulent flow regime was $0.07min^{-1}$ (±0.03, 95% CI), with similar rate constants for the laminar, $0.08min^{-1}$ (±0.01, 95% CI), and transitional, $0.07min^{-1}$ (±0.02, 95% CI), flow regimes. Inactivation rate constants were also calculated using the actual illumination time, as described in Section 3.7.2, as well as the cumulative simulated solar UV dose, Q. These calculated inactivation rate constants are shown in Table 4.2 below. It should be noted that the differences between rate constants for each different flow regime was insignificant which could be due to the fact that the Reynolds number in all experiments was still quite low.

Simulated solar UV doses required to achieve inactivation were similar for the three flow regimes where $3.6kJ_{uv}$/litre was required to achieve a 1-log reduction. The average water temperature during these experiments was 28°C.

Flow Regime	k_Q (kJ^{-1})	k_t (min^{-1})	$k_{tillum.}$ (min^{-1})
Laminar	1.13	0.08	0.44
Transitional	1.09	0.07	0.43
Turbulent	0.94	0.07	0.32

Table 4.2: Inactivation rate constants calculated using cumulative simulated solar UV dose, experimental time and illumination time for the laminar, transitional and turbulent flow regimes.

The system was hydraulically analysed by RTD analysis, it is a continuous flow reactor operating in batch mode with recirculation by pumping. In order to confirm these characteristics and to assess the mixing capacity of each flow regime, Residence Time Distribution (RTD) analysis was performed by means of a tracer study. Rhodamine WT dye was added to the reservoir and the system was set running at one of each of the three flowrates described above. The concentration of Rhodamine was monitored at the outlet from the reactor using a SCUFA (Self-Contained Underwater Fluorescence Apparatus) in order to assess the mixing capacity of the system at each flowrate. The results are shown in Figure 4.2 below. During the laminar flow regime experiment complete mixing occurred in 140 seconds whereas during the transitional and turbulent flow regime experiments complete mixing of the Rhodamine dye within the system occurred within 73 and 48 seconds respectively.
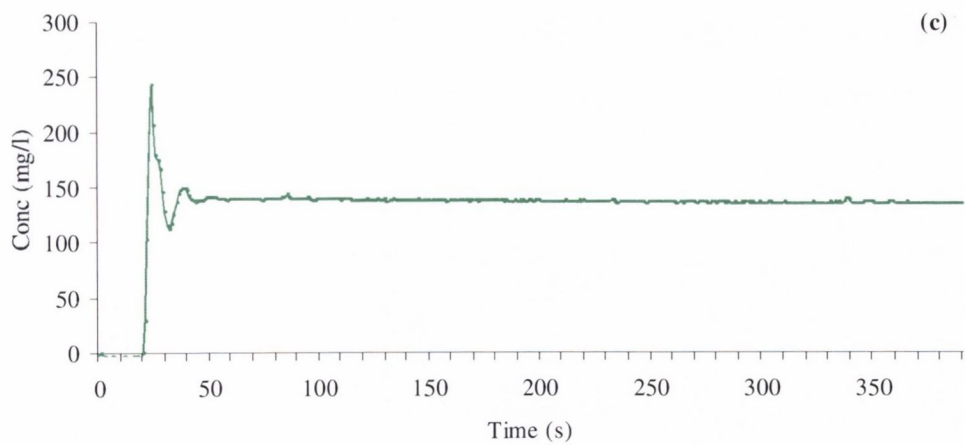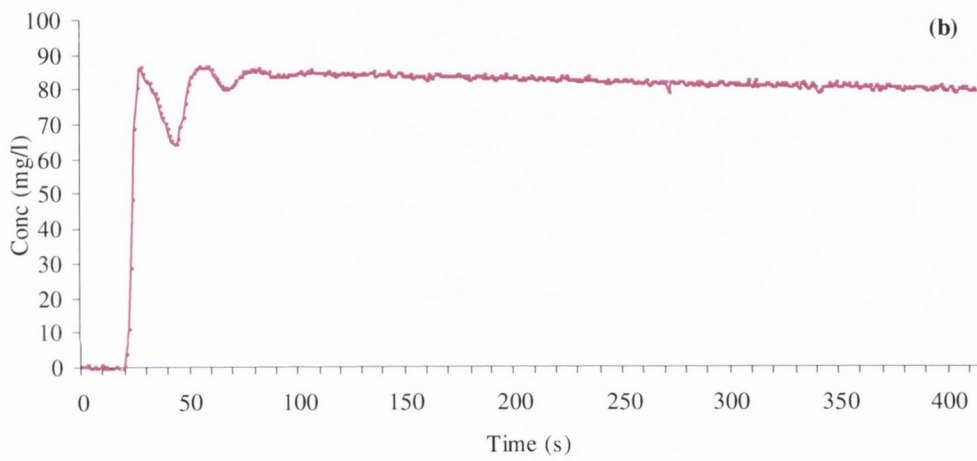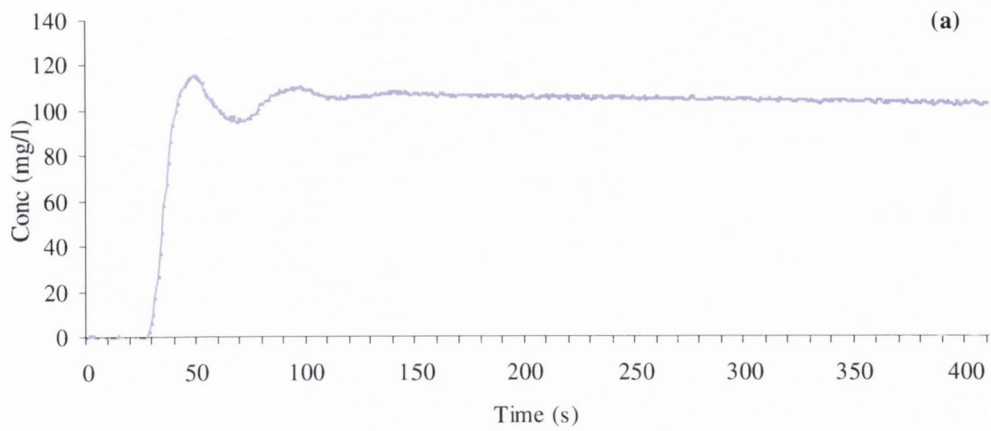
Figure 4.2: RTD analysis results for (a) laminar, (b) transitional and (c) turbulent flow regimes with plots showing Rhodamine concentration against time.

In this case the lower the flowrate the longer the volume of water will take to reach the reservoir per revolution i.e. during the turbulent flow regime experiments the total volume has made more revolutions than during the laminar regime. In the design of a single-pass scaled-up system no reservoir will exist so the flowrate alone will determine the mixing capacity of the system so it would be preferable to design using a turbulent flow regime. It should also be noted that due to the tight bends in the connectors the flow is accelerated even in the laminar or turbulent regimes. It was decided that the turbulent flow regime would be used for all the following experiments, as the mixing capacity of such a system would ensure that all organisms would receive an even dose.

4.3 Simulated Solar Intensity

4.3.1 Introduction

Solar intensity changes at different times of day as well as from region to region depending on latitude. The following set of experiments were carried out to distinguish the disinfection rate at different solar UV intensities, thus, testing the applicability of the process for different regions as well as identifying the disinfection kinetics at different times of day. The concept of dose and its applicability as a parameter to standardise solar disinfection is also discussed. UV dose is the product of UV irradiance (incident intensity) and the time of exposure of the water to the radiation. The minimal dosage level for effective bacterial disinfection using artificial mercury vapour lamps (>3-log removal) is generally agreed as $16mWs/cm^2$ at the reference wavelength of 253.7nm (specified by the US Department of Health). It is recommended that this dosage should be increased for other pathogenic organisms for example up to $58mWs/cm^2$ for *B. Subtilis* spores (Twort *et al.*, 2000). However, when using solar UV radiation there is no generalised standard dose as longer wavelengths are harnessed to cause microbial inactivation, but from the general principles of disinfection it would be expected that exposure to a high solar UV intensity for a short time would produce the same inactivation results as longer exposure at a low solar UV intensity.

4.3.2 Experimental Set-up

Simulated solar intensity could be varied by adjusting the 1000W Xenon arc lamp until the required optical irradiance was reached. Contaminated water was admitted into the parabolic reactor and exposed to three different simulated solar intensities, $9.5W_{uv}/m^2$, $17.5W_{uv}/m^2$, $31.59W_{uv}/m^2$, which correspond to total global radiation intensities of

$270W/m^2$, $500W/m^2$ and $900W/m^2$. The volume of water in each scenario was kept constant, each test using one litre of sterile (autoclaved) water inoculated with a 1×10^6 CFU/ml concentration of *E. coli* K-12. The flowrate was kept constant at 2.8 litres/min i.e. a turbulent flow regime. Sampling was carried out every 15 minutes with controls left in the dark throughout the experiment. The samples were enumerated as outlined in Section 3.6.4 and inactivation kinetics determined as described in Section 3.7. All of the tests were repeated at least four times.

4.3.3 Results and Discussion

Representative data from the laboratory trials using the parabolic reactor and three different optical irradiances are presented in Figure 4.3. All plots show an average of at least four experiments.

Calculated inactivation rate constants are shown in Table 4.3 below for experimental time, illumination time and cumulative simulated solar UV dose. Inactivation at an optical intensity of $9.5W_{uv}/m^2$ showed only a 2-log reduction in the concentration of *E. coli* K-12 of the water sample during the two-hour exposure time, corresponding to an inactivation rate constant of $0.046min^{-1}$ (± 0.0135, 95%CI). Inactivation rate constants were found to be $0.062min^{-1}$ (± 0.0107, 95%CI), for an optical irradiance of $17.5W_{uv}/m^2$ and $0.067min^{-1}$ (± 0.032, 95%CI) for an optical irradiance of $31.6W_{uv}/m^2$

Intensity (W/m^2)	k_Q (kJ^{-1})	k_t (min^{-1})	$k_{t\,illum.}$ (min^{-1})
9.5	1.93	0.050	0.21
17.5	1.42	0.062	0.30
35.6	0.94	0.067	0.32

Table 4.3: Inactivation rate constants calculated using cumulative simulated solar UV dose, experimental time and illumination time for simulated solar intensities of $9.5W_{uv}/m^2$, $17.5W_{uv}/m^2$ and $31.6W_{uv}/m^2$.
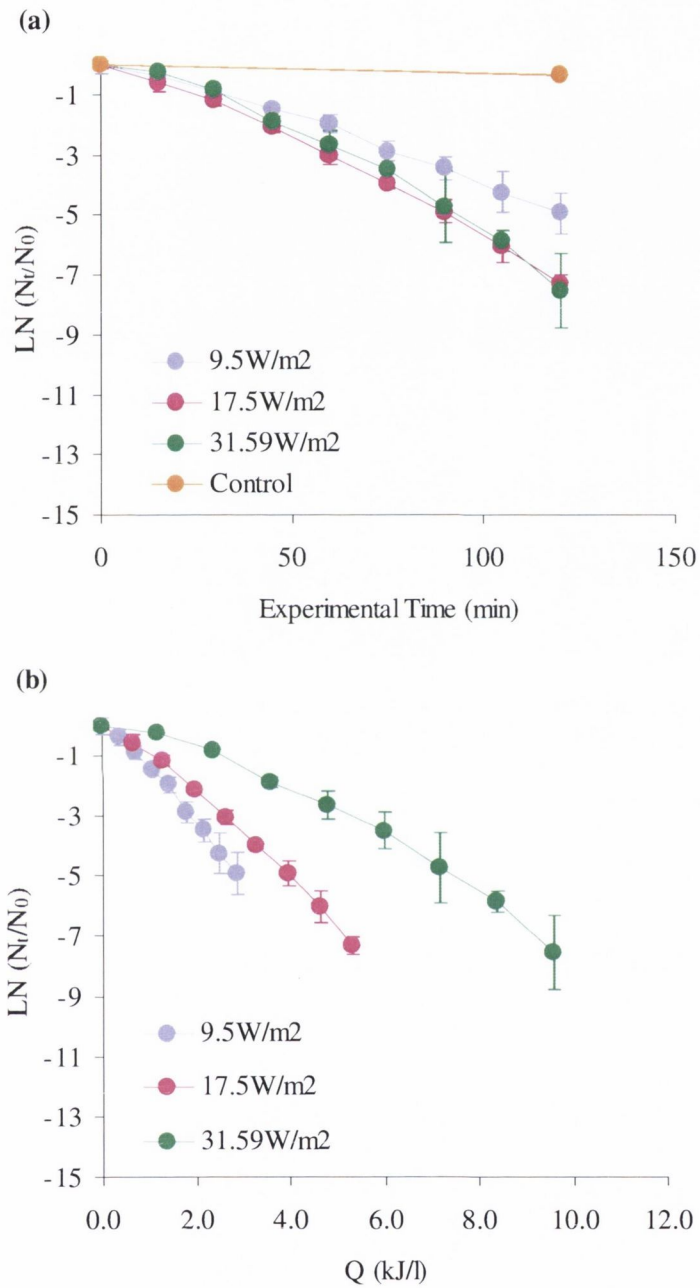
Figure 4.3: Comparison of three optical irradiances, $9.5W_{uv}/m^2$, $17.5W_{uv}/m^2$, $31.6W_{uv}/m^2$, plotted as (a) inactivation of *E.coli* K-12 against experimental time (min) and (b) inactivation of *E.coli* K-12 against cumulative simulated solar UV dose, Q, (kJ/l).

84

It can be seen from Figure 4.3(a) that almost identical bacterial inactivation kinetics with respect to time occurred with optical irradiances of $17.5W_{uv}/m^2$ and $31.6W_{uv}/m^2$, whereas exposure to $9.5W_{uv}/m^2$ produced a similar trend, while having a slower rate. From Figure 4.2(b) it can be seen that while the cumulative simulated solar radiation doses (Eqt. 3.9) were obviously much lower for lower intensities the total log removal was also less for the samples exposed to an intensity of $9.5W_{uv}/m^2$ during the two-hour experimental time, which agrees with conventional UV disinfection theory. However, both the samples exposed to $17.5W_{uv}/m^2$ and $31.6W_{uv}/m^2$ had an equal log removal (>3 log) during the two-hour experimental time (the gradient of the plotted lines (Figure 4.3(b)) being different). This suggests that inactivation kinetics are similar when samples are exposed above certain threshold irradiances or that the rate of inactivation is not linearly proportional to dose as can be seen when these results are plotted as inactivation rate against intensity (Figure 4.4). The inactivation rate increases sharply up to about $20W_{UV}/m^2$ and the increase is much slower.
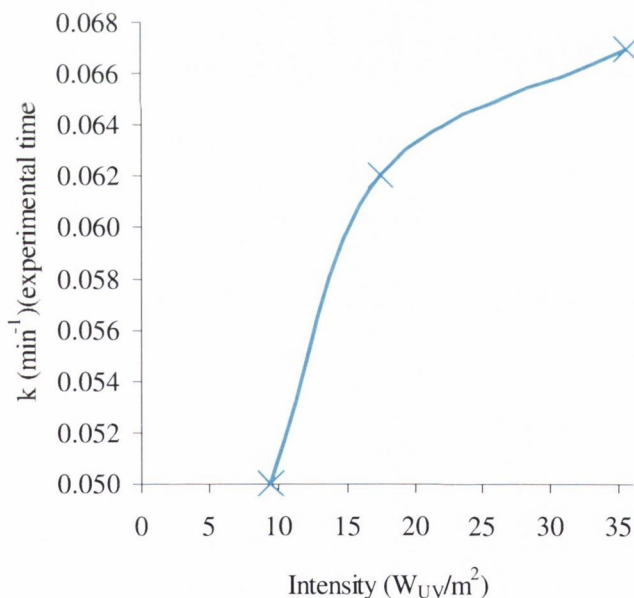
Figure 4.4: Inactivation rate, k (experimental time) plotted against intensity of exposure.

From these experiments it can be seen that there is not a lineal dependence between bacterial inactivation rate and light intensity. It can be seen from Figure 4.3(b) that the calculated inactivation rate calculated under low intensity ($9.5W/m^2$) simulated solar

85

radiation is greater than those calculated for higher intensities. It has been reported that this non-linear relationship between light intensity and deactivation of bacteria during photocatalysis could be due to excessive $\cdot$OH radical generation at high solar radiation intensities leading to self-recombination (Rincón and Pulgarin, 2003).

4.4 Comparison of Indicator Organisms

4.4.1 Introduction

No single organism can serve as an adequate indicator for all types of water and all routes of exposure. *Escherichia coli* K-12 is the indicator organism used throughout this thesis, however, the experiments described below compare the relative resistance of *E. coli* K-12 and *Salmonella typhimurium* in order to assess the validity of using *E. coli* K-12 as an indicator as well as determining if the relative resistance stays constant at both low and high intensities.

4.4.2 Experimental Set-up

At the beginning of each experiment 1 litre of water inoculated with either *E. coli* K-12 or *S. typhimurium* was admitted into the reservoir of the reactor. Initial bacterial concentrations were approximately 10^6CFU/ml in all experiments. The water was recirculated within the reactor at 2.8 litres/min and exposed to the simulated sunlight for 2 hours, with samples being taken at 15-minute intervals. Control samples were left in the dark throughout all experiments to ensure inactivation was due to exposure to simulated solar radiation alone. Experiments were repeated at two simulated solar radiation intensities, 9.5W/m^2 and 31.6W/m^2. The samples were enumerated as outlined in Section 3.6.4 and inactivation kinetics determined as described in Section 3.7. All of the experiments were repeated at least four times.

4.4.3 Results and Discussion

Representative data from the laboratory trials using the parabolic reactor and two different indicator organisms are presented in Figure 4.5 and Figure 4.6 at the intensities 9.5W/m^2 and 31.6W/m^2 respectively. All plots show an average of at least four experiments.

(a)

(b)
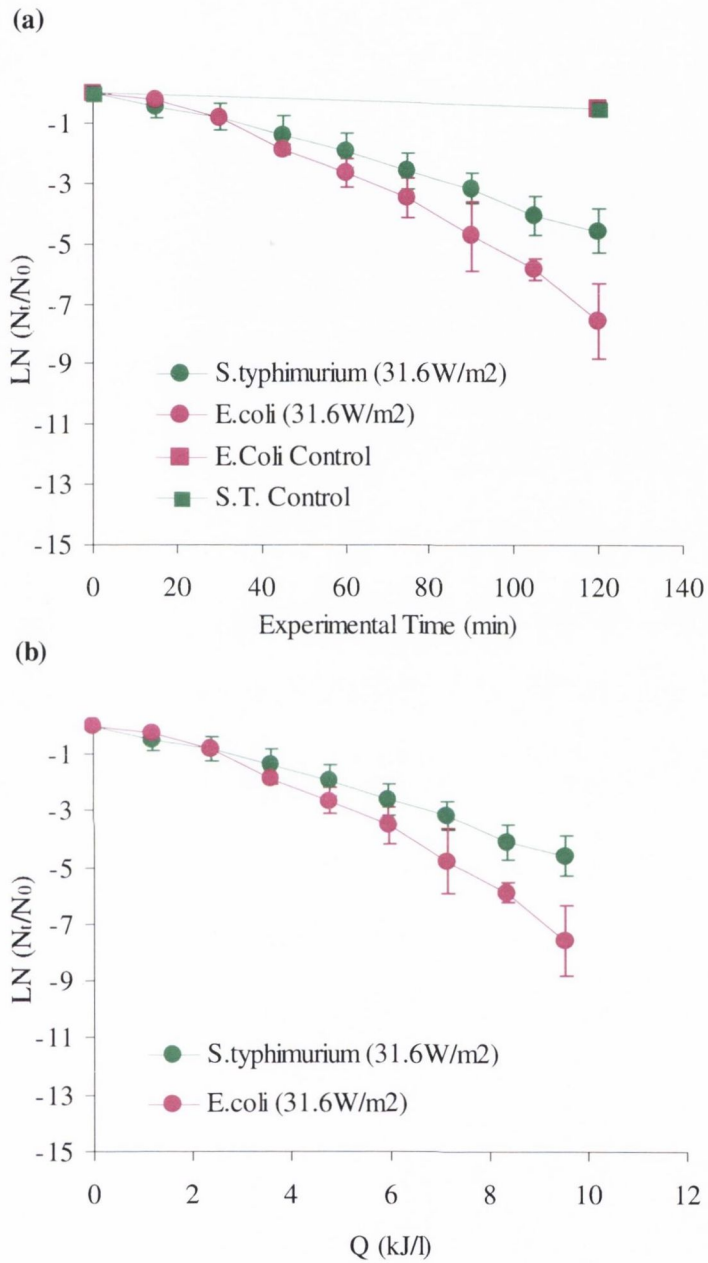
Figure 4.5: Comparison of two indicator organisms, *E. coli K-12* and *S. typhimurium*, plotted as (a) inactivation of organism against experimental time (min) and (b) inactivation of organism against cumulative simulated solar UV dose, Q, (kJ/l) at a simulated solar optical irradiance of 31.59W/m².

(a)

(b)
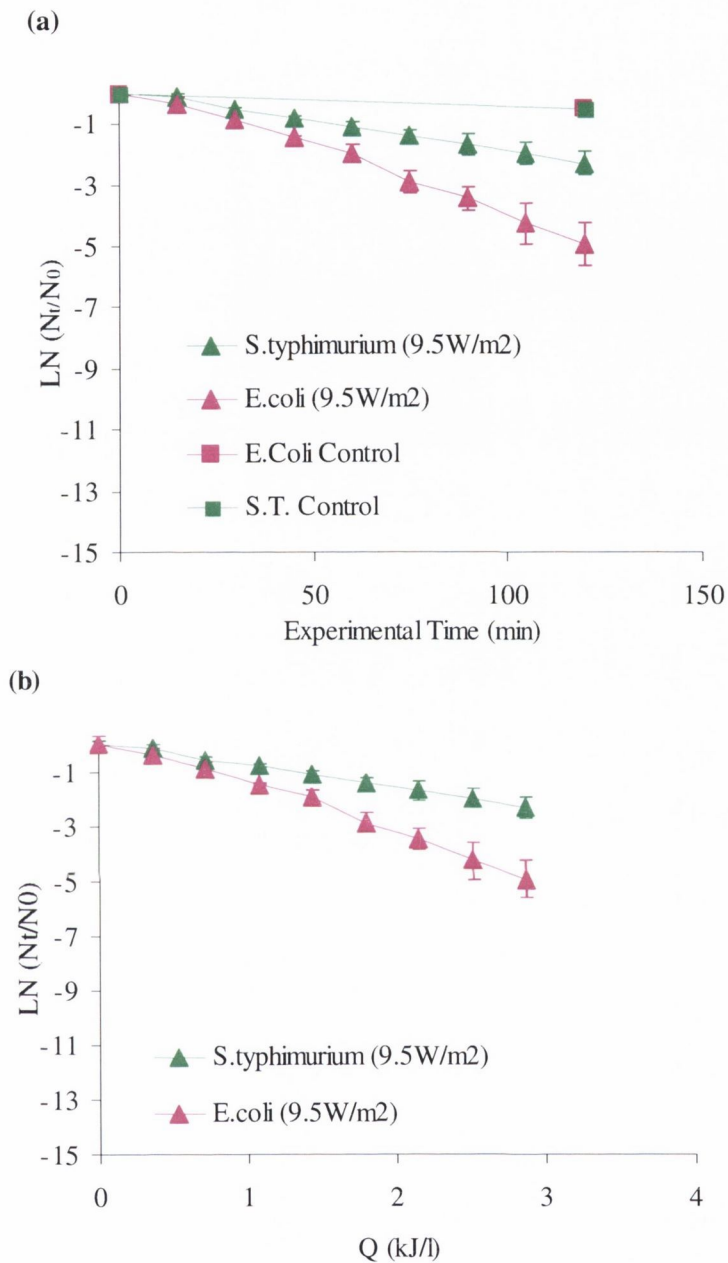
Figure 4.6: Comparison of two indicator organisms, *E. coli K-12* and *S. typhimurium*, plotted as (a) inactivation of organism against experimental time (min) and (b) inactivation of organism against cumulative simulated solar UV dose, Q, (kJ/l) at a simulated solar optical irradiance of $9.5W/m^2$.

Exposure at an optical intensity of $31.6W_{uv}/m^2$ showed >3-log reduction in the concentration of *E. coli* K-12 of the water sample during the two hour exposure time, corresponding to an inactivation rate constant of $0.067min^{-1}$ (±0.032, 95%CI). Exposure of *S. typhimurium* at the same optical intensity and over the same exposure time produced only a 2-log reduction, corresponding to an inactivation rate constant of $0.043min^{-1}$ (±0.013, 95% CI). The calculated inactivation rate constants are shown in Table 4.4 below for experimental time, illumination time and cumulative simulated solar UV dose.

Indicator	Intensity (W/m²)	k_Q (kJ⁻¹)	k_t (min⁻¹)	$k_{tillum.}$ (min⁻¹)
E. coli	31.6	0.94	0.067	0.32
S. typhimurium	31.6	0.54	0.043	0.19
E. coli	9.5	1.93	0.050	0.21
S. typhimurium	9.5	0.88	0.020	0.10

Table 4.4: Inactivation rate constants calculated using cumulative simulated solar UV dose, experimental time and illumination time for *E.coli K-12* and *S. Typhimurium* at simulated solar intensities of $9.5W_{uv}/m^2$ and $31.6W_{uv}/m^2$.

Exposure at an optical intensity of $9.5W_{uv}/m^2$ showed >2-log reduction in the concentration of *E. coli* K-12 of the water sample during the two hour exposure time, corresponding to an inactivation rate constant of $0.046min^{-1}$ (±0.0135, 95%CI). Exposure of *S. typhimurium* at the same optical intensity and over the same exposure time produced only a 1-log reduction, corresponding to an inactivation rate constant of $0.021min^{-1}$ (±0.011, 95% CI). These experiments carried out at both simulated solar UV intensities, suggest that *S. typhimurium* is more resistant to solar radiation than *E.coli* K-12 by a factor of 1.9 (±0.2). The experiments again confirm the non-linearity between bacterial inactivation and light intensity as discussed in Section 4.3.3.

Kehoe *et al.* (2004) calculated a decay constant of $0.17kJ^{-1}$ for *S. typhimurium* when using a batch process and simulated solar radiation, which is less than the value calculated in the above experiments of $0.54kJ^{-1}$, this is possibly due to the batch experiments having a greater depth of water for the radiation to pass through. Previous work by the same researchers has shown that the infectivity of *S. typhimurium* in a mouse population was reduced by exposing cells to simulated solar radiation for 1.5hrs (Smith *et al.*, 2000). Other researchers have demonstrated that the addition of titanium

dioxide slurry to the batch process solar disinfection process increases inactivation of *S. typhimurium*. Ibanez et al. (2003) reported inactivation rate constants of 0.29min^{-1} for both *E. coli* K-12 and *S. typhimurium* when a 0.1g/l TiO_2 solution was added to the bacterial suspension (note: the use of a photocatalyst to enhance the solar disinfection process is investigated in Section 6.

As shown experimentally above the relative resistance of *S. typhimurium* compared with *E. coli* K-12 did not change at the two different intensities, $31.59\text{W}_{UV}/\text{m2}$ and $9.5\text{W}_{UV}/\text{m}^2$, with all calculated inactivation rates were between 0.5 and 0.6 times those calculated for *E.coli* K-12.

4.5 Further Indicator Comparisons based on Literature

Several investigators around the world have carried out studies on the solar disinfection of different microorganisms, most using batch reactors under either solar simulator lamps or out in real sunlight. However, there have been few attempts to make direct comparisons between these studies since they have been carried out under different conditions and analysed according to different methodologies. The majority of research reported in the literature has been on single target microorganisms with a number of the studies favouring using *E. coli*. The relative resistance of the different microorganisms to solar disinfection needs to be investigated in order for the disinfection efficiency of a reactor to be more accurately established in real environmental situations where several microorganisms are likely to be in a water source simultaneously. Hence, an examination into several of these previous studies (Smith *et al.*, 2000, Lonen *et al.*, 2005, Sommer *et al.*, 1997, Salih, 2002, Ibáñez *et al.*, 2003, Kehoe *et al.*, 2004, Reed, 2004, Rincón and Pulgarin, 2004 and Walker *et al.*, 2004) augmented by the results presented in this thesis has been made in order effectively to rank the broad solar UV resistance between the different microorganisms. This study has only used the results from batch reactor trials as these are the most numerous but the relative differences between microorganisms can be translated up to the specific continuous flow system designs.

Initially, the comparative resistances between different organisms which had been carried out under similar conditions in the same study were established according to their reported disinfection kinetics with respect to time or UV dose. The disinfection kinetics in each study were then calculated according to dose (Eqt. 3.9) and compared against the base organism, *E. coli*, which was given a relative disinfection efficiency of

unity to provide the link to step between the different studies. *E. coli* was chosen since it has been used as the reference coliform enteric bacterium organism in many studies and is also the main organism that has been used in the continuous flow reactor experiments described in this thesis. Hence, the comparison between organisms have been normalised with respect to performance against *E. coli* under the same conditions according to the equation below (4.1).

$$\left[\frac{1}{k_Q}\right] : \left[\frac{1}{k_{Q_{E.coli}}}\right] = \frac{k_{E.coli}}{k} = \mathrm{Re}\,lativeSolarDi\sin fection\,\mathrm{Re}\,sis\tan ce \qquad (4.1)$$

It should be noted that studies carried out at temperatures higher than 40°C were excluded from the analysis due to potential synergistic disinfection effects between UVA and such temperatures, as described later in Section 7. Any experiments using photocatalytic enhancements were also discounted due to the different disinfection mechanisms associated with this process, as described in Section 6.

The results of this analysis are shown on Figure 4.7. The ranges of relative disinfection sensitivities on individual organisms reflect the results from more than one study by different researchers. Reasonable agreement in the trends with respect to *E. coli* was achieved, indicating the validity of the approach. The average baseline kinetic of the *E. coli* from ten different batch studies was k = 0.67 litre/kJ$_{UV}$ with a standard deviation of 0.32 litre/kJ$_{UV}$.
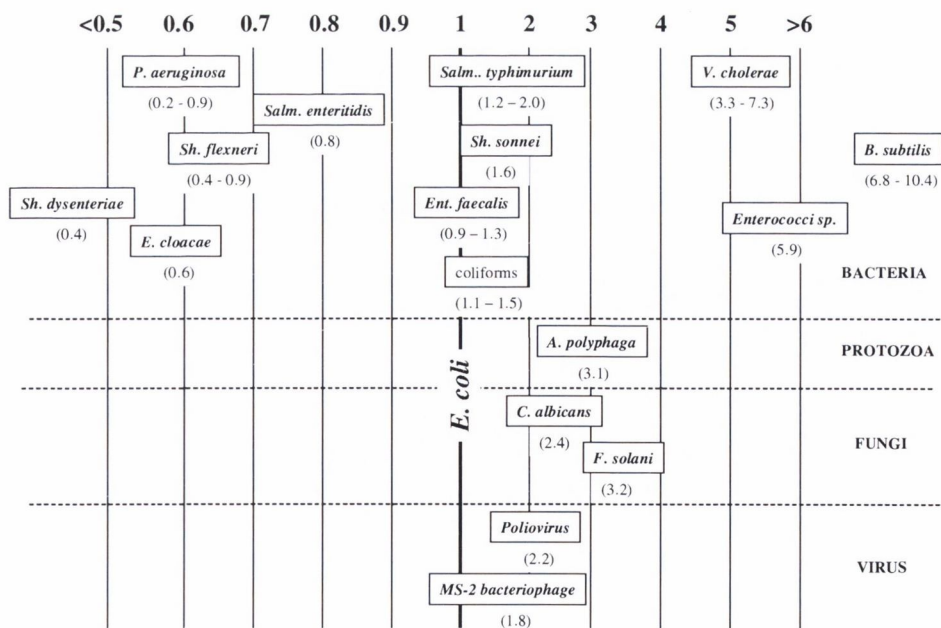
Figure 4.7. Relative solar disinfection resistance of various microorganisms in comparison to *E. coli*

Many of the Gram-negative bacteria appear to be of a broadly similar sensitivity to solar disinfection as *E. coli* with the exception of *Vibrio cholera* (which causes cholera) which seems to be considerably more resistant. *Pseudomonas aeruginosa* (responsible for opportunistic infections of the skin eye and ear) and *Enterobacter cloacae* (causing urinary and respiratory tract infections) require about half the UV dose compared to *E. coli*. The *Shigella* species, linked with diarrheal diseases or dysentery (*Sh. Dysenteriae*) and *Salmonella enteritidis* (causing gastroenteritis) are also relatively easier to disinfect than *E. coli* although *S. typhurmuriumn* and *Sh. Sonnei* appear to be slightly more resistant. The Gram-positive bacteria however, represented by the Enterococci sp., (*Enterococcus faecalis*), and *Bacillus subtilis* appear to be consistently more difficult to disinfect than *E. coli*. In particular, solar disinfection for the spore forming *Bacillus subtilis* does not appear to be particularly effective.

The protozoan *Acanthamoeba polyphaga* is found in most soil / aquatic environments and is considered very resistant compared to other cyst forming protozoa. The disinfection efficiency reported on Fig. 4.7 is for the reduction in trophozoites but it should be noted that the same study found no significant reduction in cysts under solar irradiation. Another concern with protozoa is that the cysts can act as a reservoir for pathogenic bacteria, acting as a form of environmental macrophage, since they are protected by the cyst during irradiation (Barker and Brown, 1994). This has been shown for pathogenic bacteria such as *Camplyobacter jejuni* (Axelsson-Olsson *et al.*, 2005) and *V. cholerae* (Thom and Draser, 1992). However, inactivation of *Cryptosporidium parvum* oocysts has recently been looked at (Méndez-Hermida *et al.*, 2005) reporting a 100% reduction in oocyst infectivity after 12 hours under a solar simulator. The fungal pathogens *Candida albicans* and *Fusarium solani* are more resistant than *E. coli* although water is generally not a primary route for such fungal infections. Finally, the viruses studied (poliovirus and MS-2 bacteriophage) appear to be more about twice as resistant to solar disinfection than the reference *E. coli*; MS-2 bacteriophage is considered to be one of the most environmentally resistant viruses of the F-specific RNA bacetriophages however.

It should be appreciated that most experiments have targeted just one organism and most, with few exceptions (Rincón and Pulgarin, 2003, 2004), have not looked at the

reduction in disinfection effectiveness in real water due to turbidity, chemical parameters and other microorganisms. It should also be noted that the difference in physiological state of the target organism (i.e. whether in exponential or stationary phase) (Rincón and Pulgarin, 2004) has been shown to have a large effect on the disinfection kinetic response. Hence, the design for the real world must have a significant safety factor attached above the retention time needed for the target organism.

4.6 Comparison of Tubing Materials

4.6.1 Introduction

The tubular absorber in a solar disinfection reactor must be able to transmit UV radiation efficiently as well as being resistant to its destructive effects. It must also be inert with regard to aggressive chemicals such as ·OH radicals (Malato *et al.*, 2004) created by the photocatalysis process.

Colourless glass is opaque to radiation below 320nm and to radiation above 700nm, with maximum transmission at 400nm. As explained in Section 3.1.6. quartz has excellent UV transmittance but its cost make its use for a low-cost process unfeasible. Borosilicate glass is appropriate due to its low iron content and durability. The following experiments compare the use of ordinary glass (soda lime) tubing with borosilicate glass (Pyrex) tubing as the absorber component of the parabolic solar reactor.

4.6.2 Experimental Set-up

The Pyrex tubing was fixed at the focal point of the parabolic reactor. At the beginning of each experiment 1 litre of water inoculated with *E.coli* K-12 or was admitted into the reservoir of the reactor. Initial bacterial concentrations were approximately 10^6CFU/ml in all experiments. The water was recirculated with the reactor exposed to the simulated sunlight for 2 hours, with samples being taken at 15-minute intervals. Control samples were left in the dark throughout all experiments to ensure inactivation was due to exposure to simulated solar radiation alone. Experiments were repeated using the soda lime glass tubing. The samples were enumerated as outlined in Section 3.6.4 and inactivation kinetics determined as described in Section 3.7. All of the experiments were repeated at least four times.

4.6.3 Results and Discussion

Representative data from the laboratory trials using the parabolic reactor and two different tubing types are presented in Figure 4.8. All plots show an average of at least four experiments.

Calculated inactivation rate constants are shown in Table 4.5 below for experimental time, illumination time and cumulative simulated solar UV dose. Exposure at an optical intensity of $31.6W_{uv}/m^2$ showed >3-log reduction in the concentration of *E. coli* K-12 of the water sample circulated within the Pyrex tubing during the two hour exposure time, corresponding to an inactivation rate constant of $0.07min^{-1}$, (±0.032, 95%CI). As seen in Figure 4.4 experiments performed with the ordinary soda-lime glass tubing yielded almost identical results with an inactivation rate constant calculated as $0.07min^{-1}$ (±0.007, 95%CI).

Tubing Type	k_Q (kJ^{-1})	k_t (min^{-1})	$k_{tillum.}$ (min^{-1})
Pyrex	0.94	0.07	0.32
Soda Lime	0.94	0.07	0.32

Table 4.5: Inactivation rate constants calculated using cumulative simulated solar UV dose, experimental time and illumination time for *E. coli K-12* at simulated solar intensities of $31.6W_{uv}/m^2$ with two different tubing types inserted into the reactor.

When melted (during fabrication), borosilicate glass is characterised by a high transmission in the UV and is therefore attractive in optical applications, which require transmittance in this range (Mönke and Ehrt, 2004). From the results shown above it can be seen that the ordinary glass performed equally with the borosilicate (Pyrex) glass. As discussed in Section 3.2.6 the ability of normal glass to transmit UV is dependent on its iron-content but there is also the additional negative effect of "ultraviolet solarisation" (Malato *et al.*, 2004). Solarisation is a loss in transmission observed upon irradiation of glasses caused by impurities such as iron and manganese. Defects are formed in the glass and often cause high absorbance in the UV and visible range (Mönke and Ehrt, 2004). This process has been described in more detail in Section 3.2.6. These defects occur over time which is probably the reason why no difference can be noted between inactivation using the two different types of tubing. If possible a borosilicate glass with a low-iron content should be employed in a scaled up-reactor

(a)

(b)
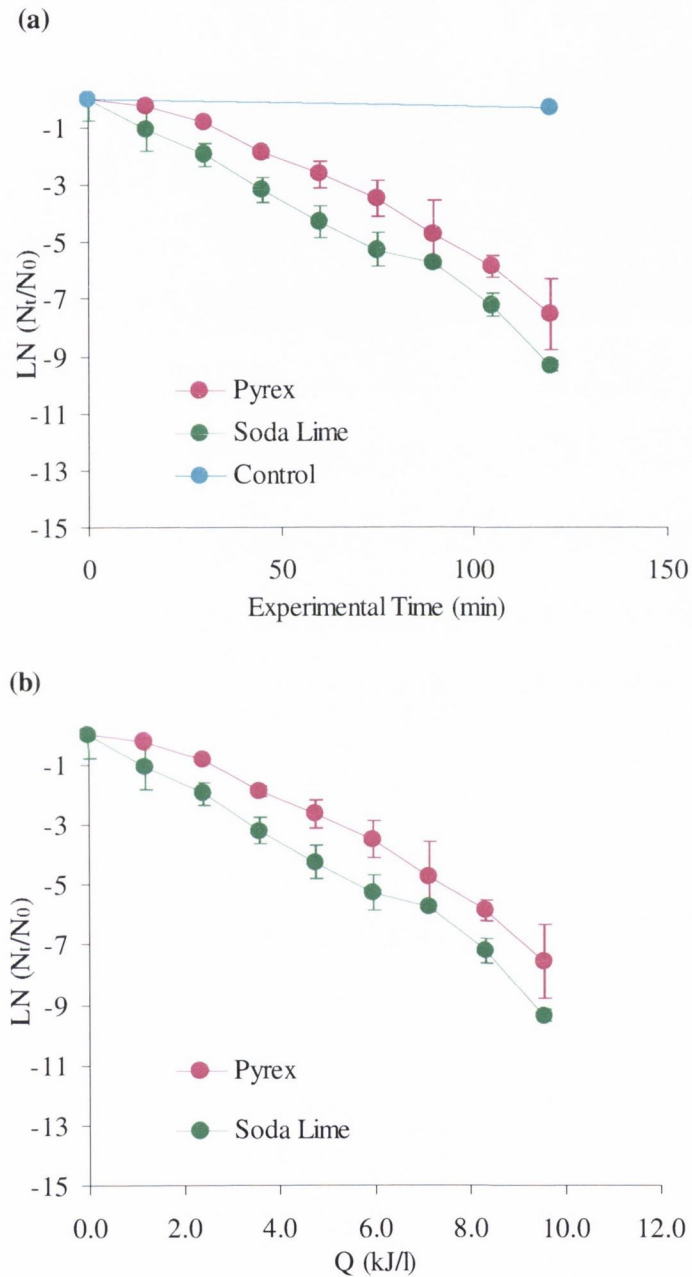
Figure 4.8: Comparison of two tubing types, Pyrex and soda lime glass plotted as (a) inactivation of *E. coli* K-12 against experimental time (min) and (b) inactivation of *E. coli* K-12 against cumulative simulated solar UV dose, Q, (kJ/l) at a simulated solar optical irradiance of $31.6W/m^2$.

4.7 Comparison between UV Disinfection in non-agitated (batch) reactors and in the continuous flow reactor operating in batch mode (with recirculation by pumping)

4.7.1 Introduction

As discussed in Section 2.7.3 Batch Process Solar Disinfection (SODIS) consists of exposing raw water to the sun in a rigid container for several hours in order to provide a low-cost water treatment. SODIS has proved successful in the inactivation of many microorganisms in small quantities of water. The following experiments compare this well characterised process with the continuous flow process.

4.7.2 Experimental Set-up

During batch experiments one-litre bottles made of borosilicate glass (Duran[©]) were filled with water and then inoculated with *E. coli* K-12 with an initial concentration of 1×10^6CFU/ml. The bottles were then placed under the solar simulator and exposed for 2 hours. Samples were taken every 15 minutes and experiments were repeated at least twice.

At the beginning of each continuous flow experiment 1 litre of water inoculated with *E. coli* K-12 or was admitted into the reservoir of the reactor. Initial bacterial concentrations were approximately 10^6CFU/ml in all experiments. The water was recirculated with the reactor exposed to the simulated sunlight for 2 hours, with samples being taken at 15-minute intervals. The experiments were repeated at least four times.

Control samples were left in the dark throughout all experiments to ensure inactivation was due to exposure to simulated solar radiation alone.   The samples were enumerated as outlined in Section 3.6.4 and inactivation kinetics determined as described in Section 3.7.

4.7.3 Results and Discussion

Representative data from the laboratory trials using the parabolic reactor and two different tubing types are presented in Figure 4.9.   All plots show an average of all experiments.
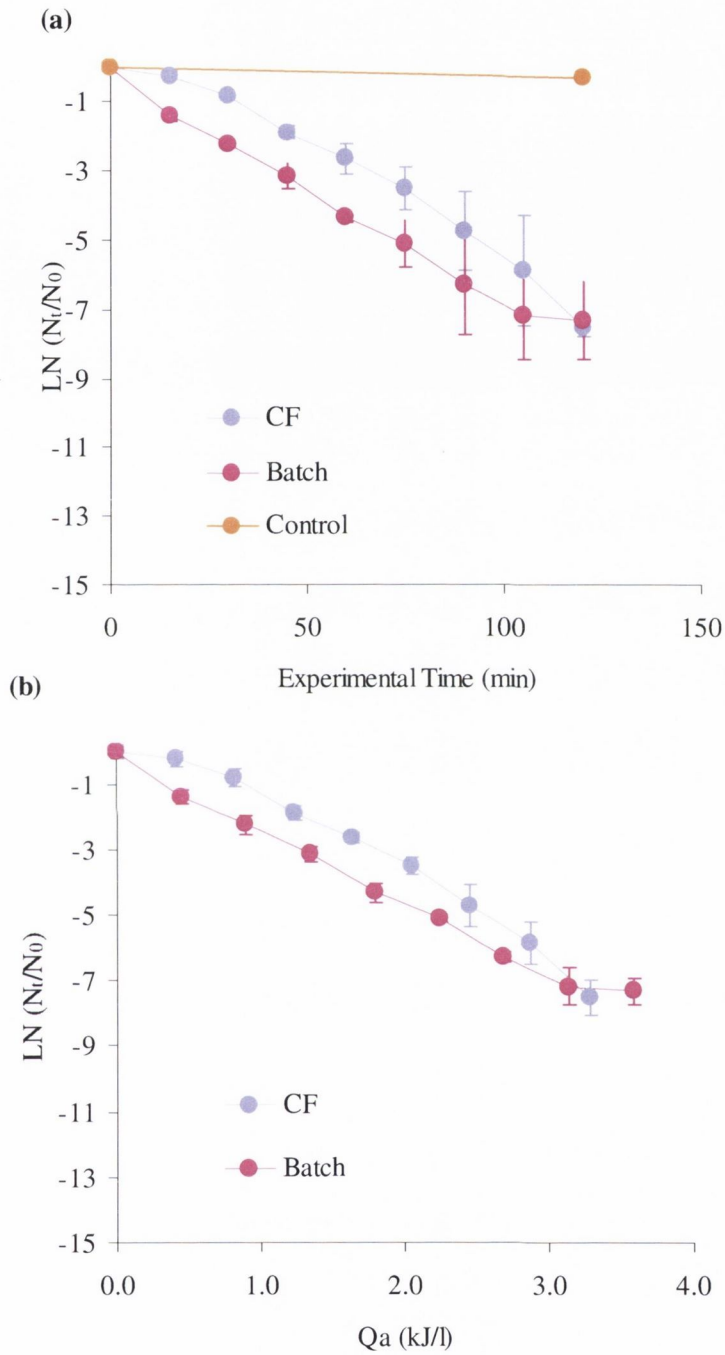
Figure 4.9: Comparison of batch process and continuous flow disinfection plotted as (a) inactivation of *E. coli* K-12 against experimental time (min) and (b) inactivation of *E. coli* K-12 against cumulative simulated solar UV dose, Q, (kJ/l) at a simulated solar optical irradiance of 31.6W/m^2.

97

Calculated inactivation rate constants are shown in Table 4.6 below for experimental time, illumination time and cumulative simulated solar UV dose. Exposure at an optical intensity of $31.6W_{uv}/m^2$ showed >3-log reduction in the concentration of *E. coli* K-12 of the water sample circulated within the continuous flow reactor during the two hour exposure time, corresponding to an inactivation rate constant of $0.067min^{-1}$, (±0.032, 95%CI). As seen in Figure 4.7 experiments performed using the batch process yielded almost identical results with an inactivation rate constant calculated as $0.066min^{-1}$ (±0.037, 95%CI).

Process	k_{Qa} (kJ^{-1})	k_{Qa} (kJ^{-1})	k_t (min^{-1})	$k_{tillum.}$ (min^{-1})
Batch	2.23	2.23	0.066	0.07
Continuous	2.74	0.94	0.067	0.31

Table 4.6: Inactivation rate constants calculated using cumulative simulated solar UV dose, experimental time and illumination time for *E. coli K-12* at simulated solar intensities of $31.6W_{uv}/m^2$ using two different solar disinfection processes.

Dose inactivation rates were calculated using Eq 3.9, which takes account of the different irradiated areas between the 1-litre bottle and the tubes of the CF reactor. The plan area of the bottle was calculated to be $0.01575m^2$ while the plan area of the absorber tubes in the reactor was calculated to be $0.0144m^2$. Therefore if inactivation rate constants are calculated according to actual absorber area (Eq. 3.10) the CF system is found to be 22% more efficient.

It would be expected that the reactor flowing at 2.8l/min is a more efficient design than an ordinary Pyrex bottle due to its shallower depth and reflector area. This does not seem to be the case if the bacterial inactivation graphs are plotted against true experimental time as shown in Figure 4.9(a). However if comparisons are made against actual exposure time (illuminated time), which remains the same as the experimental time for the bottle but is only 4.3s in the light and 17.1seconds in the dark per revolution in the continuous flow reactor then the advantage of the continuous flow reactor is evident. Results are plotted as inactivation of *E. coli* K-12 as a function of illumination time in Figure 4.10. The rate constant for the batch process was identical to that calculated for experimental time as the bottle is kept continuously exposed to the solar radiation (0.066 illuminated min^{-1} (±0.037, 95%CI)) whereas the inactivation rate constant for calculated for the continuous flow process was 0.31 illuminatedmin^{-1}.
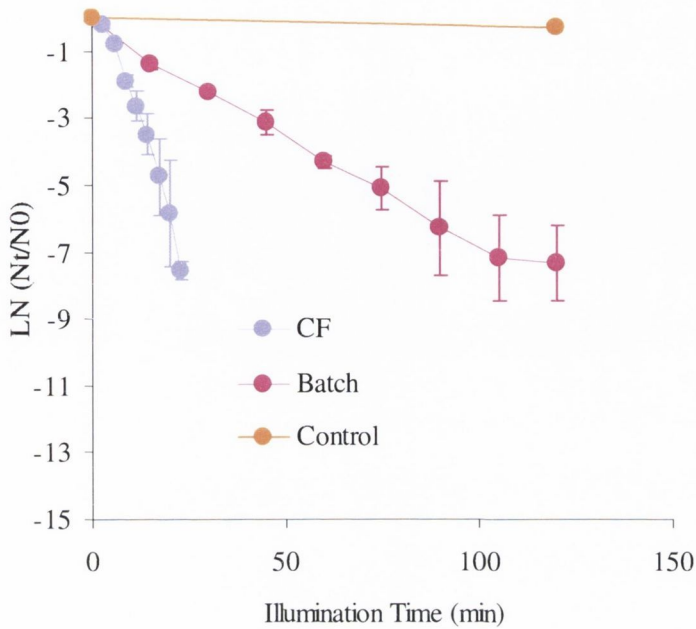
Figure 4.10: Comparison of batch process and continuous flow disinfection plotted as inactivation of *E. coli* K-12 against illumination time (min)

It should be noted that the continuous flow reactor operating in batch mode does have the added benefit of a reflector behind the exposed tubes, which would increase its efficiency with respect to the experiments carried out in the bottle (this benefit is discussed in the next chapter). As can be seen from Table 4.6 above, the bottle experiments were shown to be more efficient when inactivation coefficients were calculated according to k_Q. It can be assumed that not all incident photons on the reflector are absorbed on their way through the suspension in the tubes i.e. the fluence on the absorber tube is less than that falling on the aperture area because the reflector will distinguish some of the radiation (as discussed in section 3).

During continuous flow experiments the contaminated water is constantly recirculating between the reactor where it is exposed to radiation and the reservoir, which is effectively a dark zone. These results suggest that in a large-scale once through system inactivation time would be much lower than in a batch system.

These results also compare favourably with previous research into batch process solar disinfection. Rincon and Pulgarin (2005) reported an inactivation rate constant of 0.399min-1 for *E. coli* K-12 exposed for similar experimental time and UV intensity, using a different type of solar simulator (Hanau). Most other research into the batch process and *E. coli* focuses on enhancing the process using a photocatalyst (Matsunga, 1995, Dunlop, 2002, Wist, 2002, Huang, 2000, Sunada, 2003, Ibanez, 2003),which is considered in Section 3.

4.8 Concluding Remarks

It is evident from the above experiments that solar disinfection is achievable in a sufficient time to explore the applicability for use under natural solar conditions.

Relatively little difference was found between the three different flow regimes tested, presumably due to the turning of the fluid at each bend in the reactor and the shallow water depths involved. Surprisingly, results indicated that turbulent conditions were slightly less efficient than laminar flow conditions, although this is thought to be due to the frequency of exposure to sunlight in each particular reactor configuration, which is discussed further in Section 8. RTD analysis shows that the turbulent flow regime would be most appropriate in the design of a once through flow system.

The results of the intensity experiments indicate that inactivation kinetics are similar after exposure to certain threshold irradiances. These results also indicate that there is a non-lineal dependence between bacterial inactivation rate and light intensity suggesting that inactivation is not based solely on intensity and time as is traditionally thought. This is particularly important in natural sunlight where the intensity is continually changing due to cloud cover, whereas when UV lamps are used there is no variation in intensity .

S. typhimurium is approximately twice as resistant as *E.coli* K-12 to solar radiation. And the relative resistance did not change at lower intensities. The relative resistances of other microorganisms were assessed from literature and found to be in order of least resistance to solar disinfection:

Sh.dysenteriae < P.aeruginosa < Sh.flexneri < E.clocae < S.enteriditis < E.coli < Ent.faecalis < coliforms< *S.Typhimurium < Sh.Sonnei < MS-2 bacteriophage< Poliovirus < C.albicans < A.polyphage < F.solani < V.cholerae < Enterococci sp.< B.subtilis*

Both tubing types-borosilicate and soda lime glass-performed equally under simulated solar conditions both having equal inactivation rate constants. After time a loss in transmission could occur due to impurities such as iron and therefore it is recommended that a low-iron content borosilicate glass be used in a full-scale reactor.

Continuous flow solar disinfection was found to be more efficient than batch process solar disinfection when inactivation rate constant are based either on dose or actual illumination time. In turn this enables a much bigger volume of water to be treated in the same amount of time.

CHAPTER 5

COMPARISON OF SOLAR DISINFECTION REACTORS

5.1 Introduction

The objective of the following experiments was to assess the efficiency of different solar disinfection reactors under a variety of conditions. This involved:

i. A comparison of four different shaped small-scale reactors under simulated solar conditions.

ii. A comparison of four different shaped small-scale reactors under natural solar conditions at a latitude where there is an abundance of solar radiation.

iii. A comparison of four different shaped small-scale reactors under natural solar conditions in Ireland.

iv. An assessment of the differences between simulated solar radiation and natural solar radiation with regard to the solar disinfection process.

v. A comparison of a small-scale compound parabolic reactor and a pilot-scale solar reactor.

vi. An assessment of the effect of reactor area on the disinfection process.

Throughout these experiments the four small-scale reactors described in Section 3.2.2 were used along with the pilot scale reactor described in Section 3.2.3.

5.2 Comparison of Small-scale Reactors under Simulated Solar Conditions

5.2.1 Introduction

The purpose of these experiments was to assess the efficiency of four different shaped small-scale solar disinfection reactors under simulated solar conditions. The reactors had three different reflector profiles: compound parabolic, parabolic, v-groove and one configured without a reflector, as described in Section 3.3.2.

5.2.2 Experimental Set-up

Each reactor was configured as a recirculating system with a turbulent flow regime and Pyrex tubing (96mm diameter) placed at the focal point of the reflector. The volume of water in each case was kept constant; each test using one litre of sterile water (Baxter) inoculated with a 1×10^6 CFU/ml concentration of *E. coli* K-12. All tests were carried out using simulated solar radiation in the laboratory using the 1000W Xenon arc lamp as described in Section 3.4.1, adjusted to give an optical irradiance of 31W/m^2 simulated solar UV radiation, which corresponds to a total global radiation of 900W/m^2.

Sampling was carried out every 15 minutes with controls left in the dark throughout the experiment. The samples were enumerated as outlined in Section 3.6.4 and inactivation kinetics determined as described in Section 3.7. All of the tests were repeated at least four times.

5.2.3   Results and Discussion

Representative data from the laboratory trials using the four different reactors are presented in Figure 5.1. All plots show an average of at least four experiments.

All experiments showed at least >2-log reduction of *E. coli* K-12 within the 120 minute experimental time. The inactivation rate constant calculated for the Compound Parabolic reactor was 0.125min^{-1} (±0.027, 95% CI), with rate constants calculated for the Parabolic, 0.067min^{-1} (±0.03, 95% CI), V-groove, 0.063min^{-1} (±0.02, 95% CI), and non-reflecting, 0.049min^{-1} (±0.005, 95% CI), reactors. Inactivation rate constants were also calculated using the actual illumination time, as described in Section 3.7.2, as well as the cumulative simulated solar UV dose, Q as described in Section 3.7.3. These calculated inactivation rate constants are shown in Table 5.1 below.

Reactor	k_Q (l.kJ^{-1})	k_t (min^{-1})	$k_{t illum.}$ (min^{-1})
Compound Parabola	1.15	0.13	0.66
Parabola	0.94	0.07	0.41
V-Groove	0.59	0.06	0.34
No Reflector	1.82	0.05	0.26

Table 5.1: Inactivation rate constants calculated for the four different reactors based on dose, experimental time and actual illumination time.

Simulated solar UV doses required to achieve 1-log inactivation were calculated for each of the four reactors and found to be 2kJ/l for the Compound Parabolic reactor, whereas 2.45kJ/l and 3.9kJ/l was required for the Parabolic and V-groove reactors respectively as would be expected. However, the non-reflecting reactor required just 1.26kJ/l to cause a 1-log reduction of *E. coli* K-12, which is illogical as the non-reflecting reactor takes the most amount of time to achieve inactivation, see Figure 4.1(a).

(a)

(b)
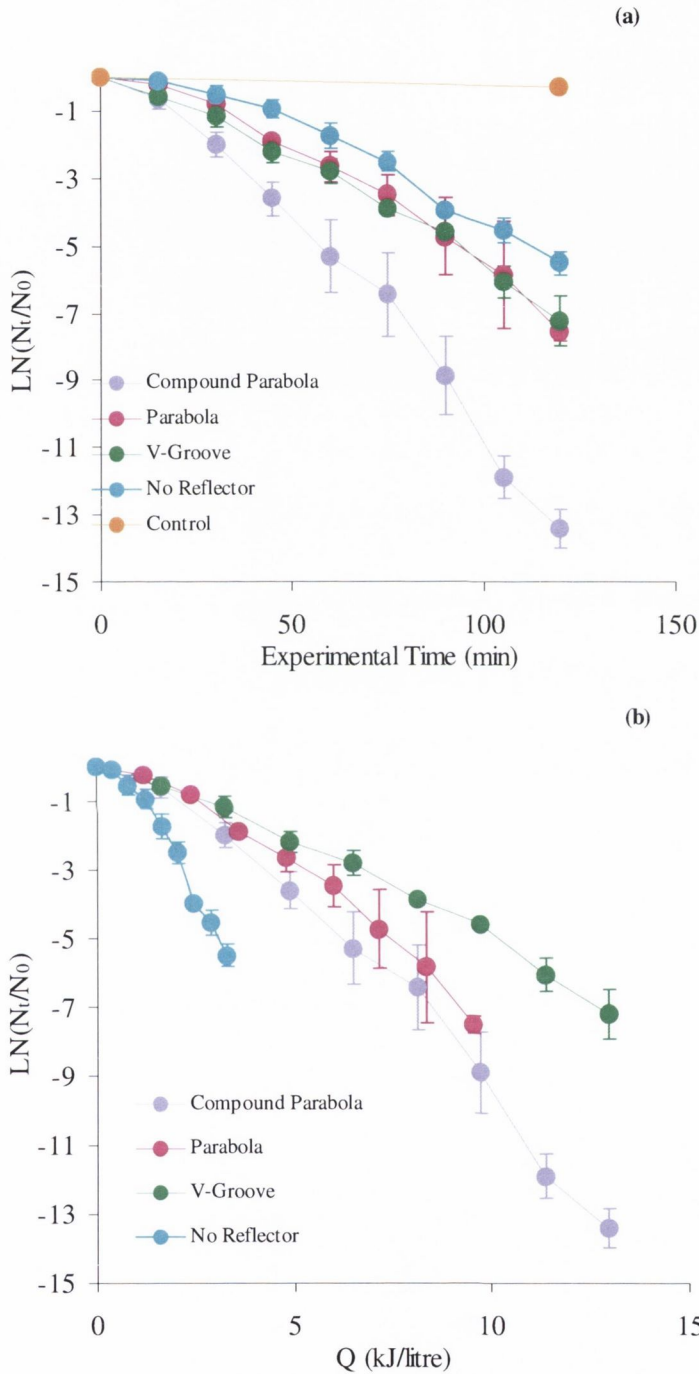
Figure 5.1:Comparison of four different reactors, Compound Parabolic, Parabolic, V-groove and non-reflecting, plotted as (a) inactivation of *E. coli* K-12 against experimental time (min) and (b) inactivation of *E. coli* K-12 against cumulative solar UV dose, Q, (kJ/l).

104

This arises due to the differing incident areas of the reactors (assumed in the calculation, Eq 3.9). It clearly demonstrates that the non-reflecting reactor makes the most efficient use of light per unit area. The kinetics for the non-reflecting reactor only take into account the sunlight falling directly on the absorber tube compared to the additional incident area of the reflectors in the other three reactors which also collect some diffuse radiation. However in terms of overall reactor efficiency, this definition of cumulative UV dose does not reflect the fact that the Compound Parabolic reactor is performing better than the others (inactivation achieved in a shorter amount of time). If the results are plotted according to the UV dose based only on the absorber area of each reactor (Eq. 3.10), the comparisons show that the Compound Parabolic reactor is more efficient than the Parabolic, V-groove and non-reflecting reactor, see Figure 5.2 below and a factor of efficiency depending on reflector type can be calculated.
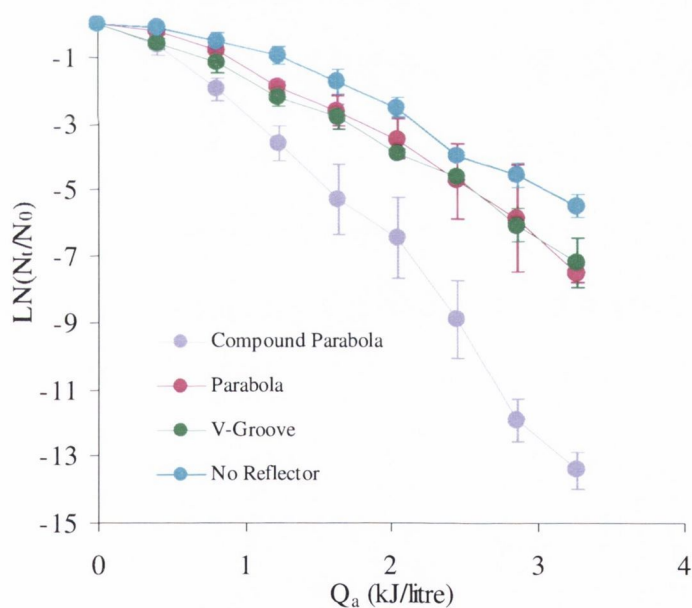
Figure 5.2: Comparison of four different reactors, Compound Parabolic, Parabolic, V-groove and non-reflecting plotted as inactivation of *E. coli* K-12 against cumulative solar UV dose, Q_a, (kJ/l), calculated by absorber area.

The dose, (Q_a, kJ/l), required to cause 1-log in the parabolic reactor was 0.5kJ/l, whereas 0.84kJ/l, 0.98kJ/l and 1.26kJ/l was required for the Parabolic, V-groove and non-reflecting reactors respectively. Therefore the absorber plan area should be taken as the incident area in order for valid comparisons to be made between reactors of different areas and thus a factor of efficiency can be established for each reflector shape. Calculated inactivation rate constants for Q_a are shown in Table 5.2.

Reactor	k_Q (l.kJ^{-1})	k_{Qa} (l.kJ^{-1})	k_t (min^{-1})	$k_{tillum.}$ (min^{-1})
Compound Parabola	1.15	4.59	0.13	0.66
Parabola	0.94	2.74	0.07	0.41
V-Groove	0.59	2.34	0.06	0.34
No Reflector	1.82	1.82	0.05	0.26

Table 5.2: Inactivation rate constants calculated for Q, Q_a, experimental time and illumination time.

It can clearly be seen from these results that the order of reactor efficiency was the Compound Parabolic reactor, the Parabolic, and the V-groove reactor with the non-reflecting reactor being least efficient. If the non-reflecting reactor is used as the baseline, efficiencies were increased by a factor of 2.5 with the Compound Parabolic reactor, 1.5 with the Parabolic reactor and 1.28 with the V-groove reactor. These ratios can be used to decide whether the additional cost of fabricating a Compound Parabolic reactor for a scaled up plant can be justified. The Compound Parabolic reactor has the capacity to collect both diffuse and direct radiation (Blanco and Malato, 2001), as discussed in Section 3.1.4. Direct solar radiation is that radiation which reaches ground level without being absorbed or scattered, radiation that has been dispersed but reaches ground level is called diffuse radiation and the addition of both is called global radiation, see Section 2.5.3. In general, the direct component of global radiation on cloudy days is at a minimum and the diffuse component is at a maximum, producing the opposite situation on clear days (Malato, 1999). Hence, the enhancement of 2.5 found when comparing the Compound Parabolic reactor with a non-reflecting reactor, which may justify the cost of fabricating the Compound Parabolic, a factor that must be considered when designing this process for developing countries.

5.3 Comparison of Small-scale Reactors under Natural Solar Conditions (PSA)

5.3.1 Introduction

The purpose of these experiments was to assess the efficiency of the four different shaped small-scale solar disinfection reactors under natural solar conditions. The four reactors tested above, Compound Parabolic, Parabolic, V-groove and non-reflecting were tested at Plataforma Solar de Almería in southern Spain.

5.3.2 Experimental Set-up

Each reactor was configured in an identical manner to Section 5.2.2. The volume of water in each case was kept constant; each test using one litre of water (MilliQ), which was tested for sterility, inoculated with a 1×10^6 CFU/ml concentration of *E. coli* K-12. All tests were carried out natural solar radiation at Plataforma Solar de Almería during June and July 2003. Reflector apertures were tilted to the local latitude angle (37°) to maximise sunlight capture as described in Section 3.4.2 and positioned so that the tubes were aligned in an east-west orientation. Sampling was carried out every 10 minutes with controls left in the dark throughout the experiment. The samples were enumerated as outlined in Section 3.6.4 and inactivation kinetics determined as described in Section 3.7. All of the tests were repeated at least four times.

5.3.3 Results and Discussion

Representative data from the laboratory trials using the four different reactors are presented in Figure 5.3. All plots show an average of at least four experiments.

The experiments performed in the Compound Parabolic reactor exhibited >4-log reduction in *E. coli* K-12, whereas the Parabolic and V-groove reactor experiments exhibited a 3-log and 2-log reduction in *E. coli* K-12 respectively. The non-reflecting reactor produced only > 1-log reduction in the 60 minute experimental time. The inactivation rate constant calculated for the Compound Parabolic reactor was 0.251min^{-1} (±0.09, 95% CI), with rate constants calculated for the Parabolic, 0.195min^{-1} (±0.08, 95% CI), V-groove, 0.134min^{-1} (±0.09, 95% CI), and non-reflecting, 0.066min^{-1} (±0.009, 95% CI), reactors.

(a)

(b)
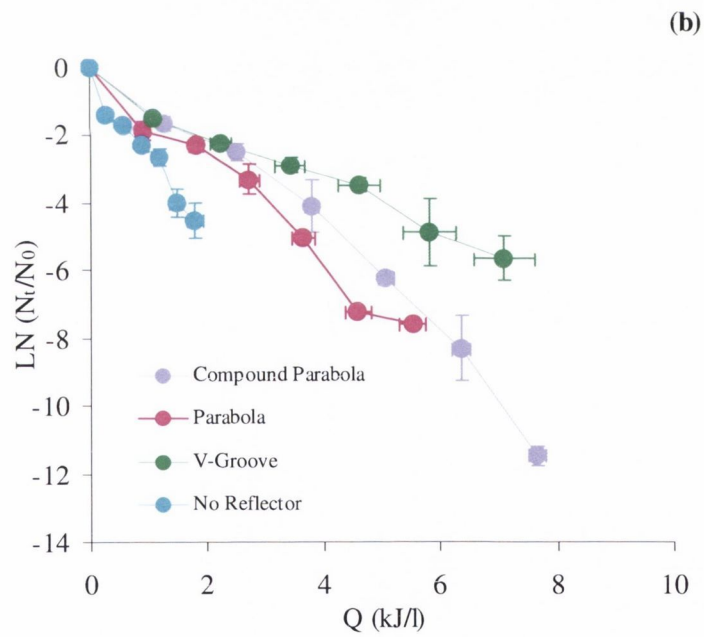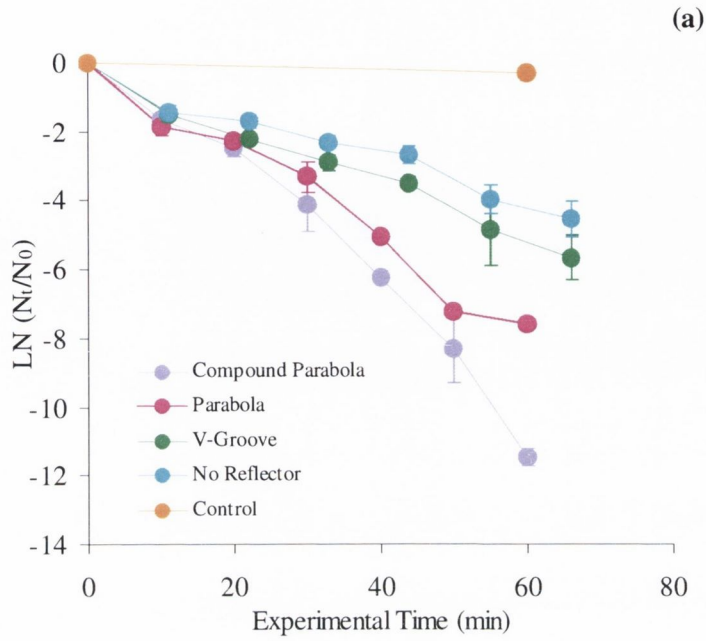
Figure 5.3: Comparison of four different reactors, Compound Parabolic, Parabolic, V-groove and non-reflecting, plotted as (a) inactivation of *E. coli* K-12 against experimental time (min) and (b) inactivation of *E. coli* K-12 against cumulative solar UV dose, Q, (kJ/l).

Inactivation rate constants were also calculated using the actual illumination time, as described in Section 3.7.2, as well as the cumulative simulated solar UV dose, Q as described in Section 3.7.3 and Q_a based on absorber area (Eq. 3.10). These calculated inactivation rate constants are shown in Table 5.3 below.

Reactor	k_Q (l.kJ^{-1})	k_{Qa} (l.kJ^{-1})	k_t (min^{-1})	$k_{tillum.}$ (min^{-1})
Compound Parabola	1.96	7.79	0.25	1.32
Parabola	2.08	6.08	0.20	1.03
V-Groove	1.19	4.71	0.13	1.19
No Reflector	2.46	2.46	0.07	2.46

Table 5.3: Inactivation rate constants calculated for the four different reactors based on dose, experimental time and actual illumination time.

Natural solar UV doses required to achieve 1-log inactivation were calculated for each of the four reactors. The dose required to achieve 1-log inactivation calculated for the Compound Parabolic reactor was 1.17kJ/l, whereas 1.10kJ/l and 1.94kJ/l was required for the Parabolic and V-groove reactors respectively. The non-reflecting reactor required just 0.936kJ/l to cause a 1-log reduction of *E. coli* K-12, again these were calculated as per Q, Eq. 3.9. When inaction of bacteria was plotted against dose as per Q_a, (Eq. 3.10). The calculated dose required to achieve 1-log reduction was 0.29kJ/l, 0.38kJ/l, 0.49kJ/l and 0.94kJ/l for the Compound Parabolic, Parabolic, V-groove and non-reflecting reactors respectively. The results are plotted as inactivation of *E. coli* K-12 against Q_a, kJ/l, in Figure 5.4 below.

The error bars in the x direction on the plots above indicate the variation in the dose term as the solar intensity was continually changing throughout the experiments (since these results are an average of four separate trials). Average solar intensities for the experiments were found to be 37.2W/m^2 (std. dev. 2.33), 36.4W/m^2 (std. dev. 2.36), 30.8W/m^2 (std. dev. 5.9) and 30.8W/m^2 (std. dev. 5.9) for the Compound Parabolic, Parabolic, V-groove and non-reflecting reactors respectively.
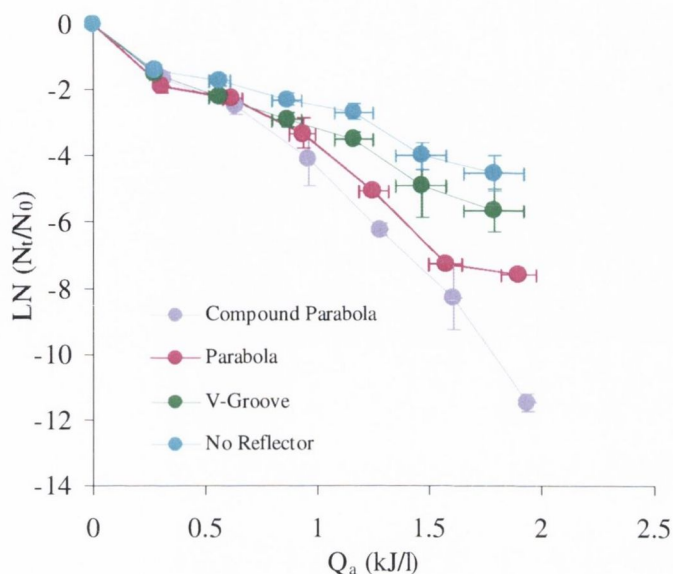
Figure 5.4: Comparison of four different reactors, compound parabolic, parabolic, v-groove and non-reflecting plotted as inactivation of *E.coli* K-12 against cumulative solar UV dose, Q_a, (kJ/l), calculated by absorber area.

It is evident from these results that the Compound Parabolic reactor performed the best in natural sunlight with the others performing in the same order as the experiments performed under simulated sunlight. If the non-reflecting reactor is used as the baseline, efficiencies were increased by a factor of 3.0 with the Compound Parabolic reactor, 2.5 with the Parabolic reactor and 1.9 with the V-groove reactor. It is also apparent that all reactors performed better in natural sunlight, which will be discussed in Section 5.5.

5.4 Comparison of Small-scale Reactors under Natural Solar Conditions (Ireland)

5.4.1 Introduction

The purpose of these experiments was to assess the efficiency of four different shaped small-scale solar disinfection reactors under natural solar conditions in Ireland in order to assess how a difference in intensity affects the dose kinetic. The four reactors tested above, Compound Parabolic, Parabolic, V-groove and non-reflecting were tested at Trinity College, Dublin.

5.4.2 Experimental Set-up

Each reactor was configured as a recirculating system with a turbulent flow regime and Pyrex tubing placed at the focal point of the reflector as before. The volume of water in each case was kept constant; each test using one litre of autoclaved water, inoculated with a 1×10^6 CFU/ml concentration of *E. coli* K-12. All tests were carried out in natural solar radiation at Trinity College, Dublin during August 2003. Reflector apertures were tilted to the local latitude angle (53°C) to maximise sunlight capture as described in Section 3.4.2 and positioned so that the tubes were aligned in an east-west orientation. Sampling was carried out every 15 minutes with controls left in the dark throughout the experiment. The samples were enumerated as outlined in Section 3.6.4 and inactivation kinetics determined as described in Section 3.7. All of the tests were repeated at least three times.

5.3.3 Results and Discussion

Representative data from the laboratory trials using the four different reactors are presented in Figure 5.5. All plots show an average of at least four experiments.

The experiments performed in the Compound Parabolic reactor exhibited >5-log reduction in *E. coli* K-12, whereas the Parabolic and V-groove reactor experiments exhibited a 4-log and 2-log reduction in *E.coli* K-12 respectively in the 180 minute experimental time. The inactivation rate constant calculated for the Compound Parabolic reactor was 0.108min^{-1} (±0.09, 95% CI), with rate constants calculated for the Parabolic, 0.067min^{-1} (±0.022, 95% CI), V-groove, 0.039min^{-1} (±0.025, 95% CI), and non-reflecting, 0.036min^{-1} (±0.009, 95% CI), reactors.
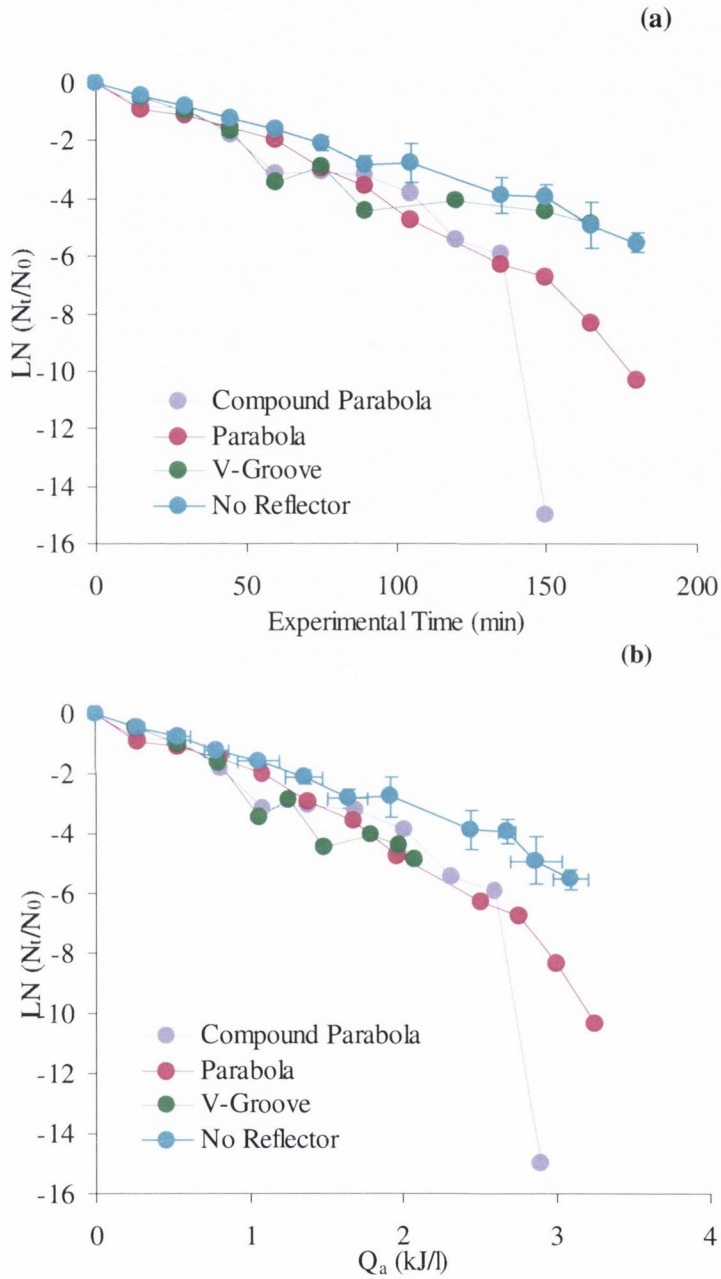
Figure 5.5:Comparison of four different reactors, compound parabolic, parabolic, v-groove and non-reflecting, plotted as (a) inactivation of *E. coli* K-12 against experimental time (min) and (b) inactivation of *E. coli* K-12 against cumulative solar UV dose, Q_a, (kJ/l). Note: error bars are plotted on one line only for clarity.

112

Inactivation rate constants were also calculated using the actual illumination time, as described in Section 3.7.2, as well as the cumulative simulated solar UV dose, Q_a as described in Section 3.7.3. These calculated inactivation rate constants are shown in Table 5.4 below.

Reactor	k_{Qa} (l.kJ^{-1})	k_t (min^{-1})	$k_{tillum.}$ (min^{-1})
Compound Parabola	3.92	0.11	0.57
Parabola	2.90	0.07	0.36
V-Groove	2.42	0.04	0.21
No Reflector	1.68	0.03	0.18

Table 5.4: Inactivation rate constants calculated for the four different reactors based on dose, experimental time and actual illumination time.

Natural solar UV doses required to achieve 1-log inactivation were calculated for each of the four reactors based on Q_a. The dose required to achieve 1-log inactivation calculated for the Compound Parabolic reactor was 0.58kJ/l, whereas 0.79kJ/l and 0.95kJ/l was required for the Parabolic and V-groove reactors respectively. The non-reflecting reactor required 1.37kJ/l to cause a 1-log reduction of *E. coli* K-12; again these were calculated as per Q_a, Eq. 3.10.

The error bars in the x direction on the plots above indicate the variation in the dose term as the solar intensity was continually changing throughout the experiments. Average solar intensities for the experiments were found to be 22.2W/m^2 (std. dev. 2.9), 20.9W/m^2 (std. dev. 3.2), 16.2W/m^2 (std. dev. 4.8) and 20W/m^2 (std. dev. 3.2) for the Compound Parabolic, Parabolic, V-groove and non-reflecting reactors respectively.

Once again it is evident from these results that the Compound Parabolic reactor performed the best in natural sunlight with a low intensity, as it was the only reactor to inactivate the bacteria to a level below detection for all three trials (see Figure 5.5). If the non-reflecting reactor is used as the baseline, efficiencies were increased by a factor of 2.33 with the Compound Parabolic reactor, 1.72 with the Parabolic reactor and 1.44 with the V-groove reactor. It is also apparent that all reactors performed better under high intensity solar conditions (PSA) than low intensity conditions (Ireland). Table 5.5 below summarises the inactivation constants for PSA and Ireland along with the average solar intensity of the trials performed.

Ireland			Spain		
Reactor	k_{Qa} (l.kJ^{-1})	Average Intensity (W/m^2)	Reactor	k_{Qa} (l.kJ^{-1})	Average Intensity (W/m^2)
Compound Parabola	3.92	22.2	Compound Parabola	7.79	37.2
Parabola	2.90	20.9	Parabola	6.08	36.2
V-Groove	2.42	16.2	V-Groove	4.71	30.8
No Reflector	1.68	20.0	No Reflector	2.46	30.8

Table 5.5: Comparison of Inactivation coefficients calculated for Ireland and Spain along with the average intensities during exposure time.

The average intensity during trials performed at PSA was approximately 15W/m^2 higher than those trials performed in Ireland (except for trials performed using the non reflecting reactor where the solar UV intensity was only 10W/m^2 higher). Reactors with reflectors all performed a factor of two times better when exposed to high intensity radiation than those exposed to lower intensity radiation in Ireland. This supports the theory that there is a non-linear relationship between intensity of exposure and inactivation of microorganisms as discussed in Section 4.3. The differences in the results could also be due to a synergistic effect between solar radiation and temperature. This effect is explored further in Section 7.2.

5.5 Comparison of Simulated and Natural Solar Conditions

5.5.1 Introduction

It is apparent from the experiments described above that there is a difference between the results found under natural solar conditions to those found in the laboratory under simulated conditions. Section 3.4.1 describes the solar simulator and its spectral output, whereas the output of natural solar radiation is described in Section 3.4.2. Figure 5.6 below compares the output from the solar simulator with the ASTM standard solar spectral irradiance, showing the difference between the spectral output of the solar simulator and natural sunlight.
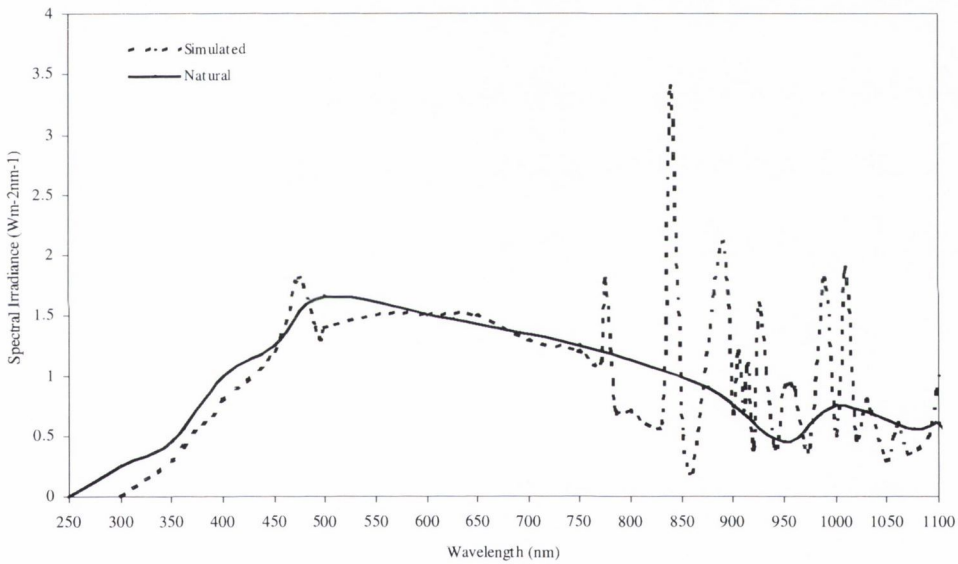
Figure 5.6: Comparison of Solar Simulator output and ASTM Reference Spectrum for a flat plate tilted at 37°

5.5.2 Results and Discussion

Representative data from the trials using the Compound Parabolic reactor in natural and simulated sunlight are presented in Figure 5.7 (a) and (b). The comparisons are made using the natural solar trials performed at PSA, as the average intensity during these trials was $37.2W/m^2$ (std. dev. 2.33). The simulated solar radiation intensity was kept at

31.6W/m2 whereas the average intensity during the Irish trials was almost 10W/m^2 less than the simulated intensity as discussed in the previous section.

Table 5.6 shows the inactivation rate constants for all reactors under simulated sunlight and natural sunlight for both the experimental time and cumulative solar UV dose, Q_a.

Source	Natural Solar Radiation			Simulated Solar Radiation		
Reactor	k_{Qa} (l.kJ^{-1})	k_t (min^{-1})	$k_{tillum.}$ (min^{-1})	k_{Qa} (l.kJ^{-1})	k_t (min^{-1})	$k_{tillum.}$ (min^{-1})
Compound Parabola	7.79	0.25	1.32	4.59	0.13	0.66
Parabola	6.08	0.20	1.03	2.74	0.07	0.41
V-Groove	4.70	0.13	0.71	2.34	0.06	0.34
No Reflector	2.46	0.07	0.35	1.82	0.05	0.26

Table 5.6: Inactivation rate constant for small-scale reactors under both simulated and natural conditions.

It is apparent from the results described above that there are discrepancies between the inactivation rate constants achieved during simulated and natural solar experiments. Dose inactivation rate constants were a factor of 2.2-1.35 greater for natural sunlight than for simulated sunlight, a trend that was consistent throughout the experiments.

The spectral irradiances emitted from the solar simulator (Oriel Corp) and those falling naturally on earth (Gueymard, 2004) are given in Table 5.7 below as percentages. This shows that there is a marked difference in the UV range where the proportional UV output of the sun is 2.54 times more than that of the solar simulator at the same measured intensity. The atmosphere absorbs most UVC radiation before reaching ground level and thus both simulator and natural outputs are <1% at this wavelength (<280nm). Thus, only UVB and UVA radiation play a role in terrestrial applications. It is radiation in this wavelength range (200-400nm) that causes major damage to microorganisms (Kalisvaart, 2001). The majority of biological effects are due to photochemical reactions in the nucleic acid DNA. The absorbed photons result in the formation of photoproducts, the most common of which is the thymine dimer. UV-A radiation is generally absorbed by photosensitisers, which can be present in contaminated water. These can react with oxygen molecules producing highly reactive oxygen species, which in turn react with DNA (Whitelam, 1986) as discussed in Section 2.7.2.
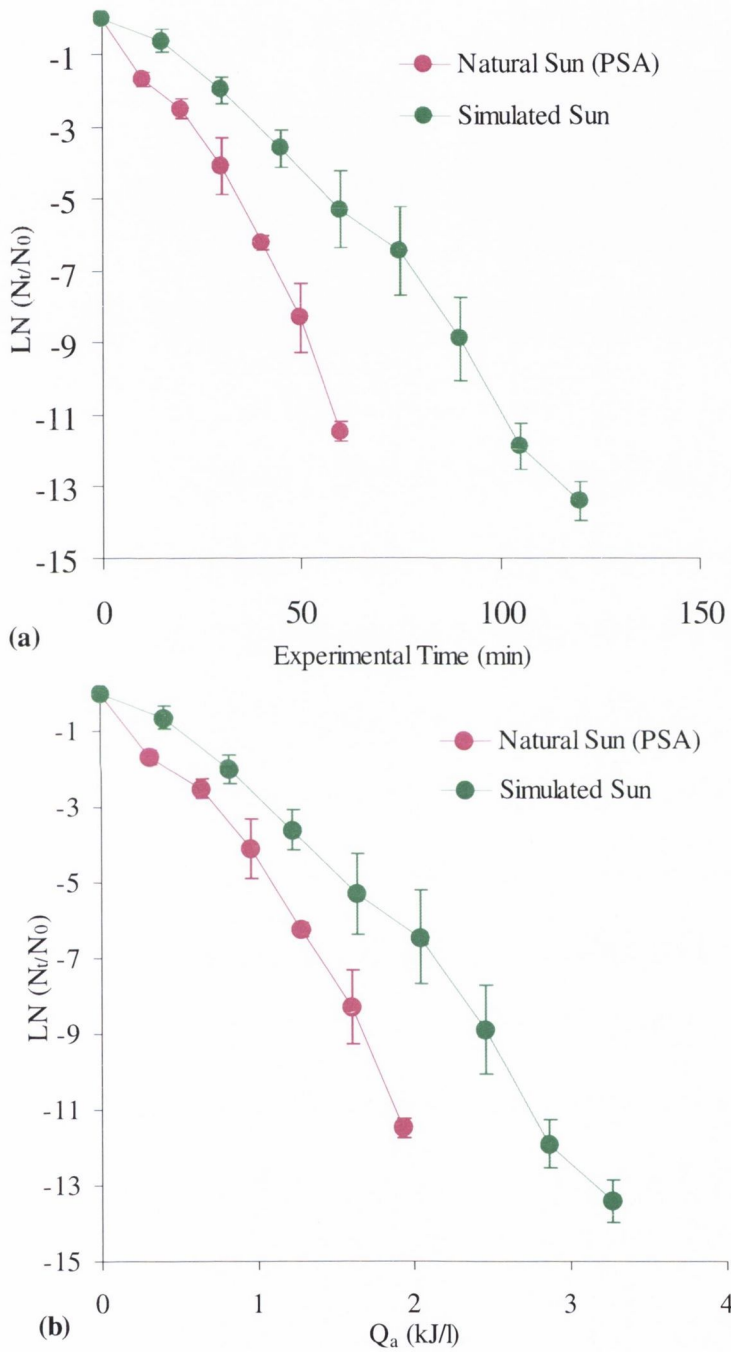
Figure 5.7: Comparison of the compound parabolic reactor under natural and simulated sunlight plotted as (a) inactivation of *E. coli* K-12 against experimental time (min) and (b) inactivation of *E. coli* K-12 against cumulative solar UV dose, Q_a, (kJ/l).

It can also be seen (Table 5.7) that there is proportionately 1.14 times more infrared radiation in the simulated solar output than that received at the earth's surface. It has been reported (Lage *et al.*, 2000) that exposure to infrared radiation can actually aid survival for bacteria on exposure to UV radiation. Samples of *E. coli* K-12 were pre-exposed to infrared or non-coherent visible radiation and in all cases the pre-exposed samples exhibited a resistance to UV radiation. Lage *et al.*, (2000) suggest that overall effects of UV-C and perhaps UV-B radiation may be significantly attenuated when they are simultaneously absorbed with the visible and infrared components of the solar spectrum. This phenomenon could explain the differences in inactivation kinetics between the experiments carried out under simulated solar radiation and natural solar radiation.

Radiation	% Output Solar Simulator	& Output Natural Solar	Natural/Simulated
UV	3.51	8.90	2.54
Visable	37.25	39.10	1.05
Infrared	59.25	52.00	0.88

Table 5.7: Factored spectral irradiances emitted by the Solar Simulator compared with those falling naturally at ground level.

Finally, information from the lamp manufactures indicates that there is a slight reduction in the UVA / Visible ratio in the output for Xenon Arc lamps over time. This is another factor which would only reduce the relative UV radiation with respect to intensity compared to natural solar light. It should be noted that the percentage outputs given in Table 5.7 are for a new lamp.

These differences between experiments performed in the laboratory as opposed to natural sunlight should be taken into account when comparing efficiencies of different reactors or when using the disinfection kinetics found during small-scale experiments to scale-up reactors to pilot level. These results suggest that the disinfection process will occur in less time and with a smaller radiation dose in natural sunlight than with simulated sunlight.

This could be looked at in two ways: either the kinetics found under simulated sunlight should be factored up for full-scale reactor design or the kinetics found in solar simulated experiments could be considered to include an inbuilt factor of safety which is always necessary when designing water treatment processes that have a direct impact on public health.

5.6 Comparison of Small-Scale and Pilot-Scale Solar Disinfection Reactors

5.6.1 Introduction

The following experiments compare the Compound Parabolic small-scale reactor $(0.057m^2)$ with a pilot-scale reactor installed at Plataforma Solar de Almería $(3m^2)$. The pilot-scale reactor is described in Section 3.3.3.

5.6.2 Experimental Set-up

Each reactor was configured as a recirculating system with a turbulent flow regime (~5000) and Pyrex tubing placed at the focal point of the reflector. The volume of water in each case was kept constant; during small-scale experiments one litre of water (MilliQ), tested for sterility, inoculated with a $1x10^6$ CFU/ml concentration of *E. coli* K-12. All tests were carried out natural solar radiation Plataforma Solar de Almería during June and July 2003. Reflector apertures were tilted to the local latitude angle (37°C) to maximise sunlight capture as described in Section 3.4.2 and positioned so that the tubes were aligned in an east-west orientation. During pilot-scale experiments 35 litres of solar-distilled water inoculated with *E. coli* K-12 was admitted into the reactor's reservoir. The reactor was kept covered for ten minutes to ensure a complete mix was achieved (confirmed by tracer study) and uniform concentrations of bacteria existed throughout the reactor. Sampling was carried out every 5 or 10 minutes with controls left in the dark throughout the experiment. The samples were enumerated as outlined in Section 3.6.4 and inactivation kinetics determined as described in Section 3.7. All of the tests were repeated at least four times.

5.6.3 Results and Discussion

Representative data from the laboratory trials using the four different reactors are presented in Figure 5.8. All plots show an average of at least four experiments.

The experiments performed in the small-scale compound parabolic reactor exhibited >5-log reduction in *E. coli* K-12, which was similar to the reduction found in the pilot-scale in the same experimental time. The inactivation rate constant calculated for the small-scale reactor was 0.25min^{-1} (±0.09, 95% CI), whereas the rate constant calculated for the pilot-scale reactor 0.35min^{-1} (±0.02, 95% CI), reactors. Inactivation rate

constants were also calculated using the actual illumination time, as described in Section 3.7.2, as well as the cumulative simulated solar UV dose, Q_a as described in section 3.7.3. These calculated inactivation rate constants are shown in Table 5.8 below.

Reactor	k_{Qa} (l.kJ^{-1})	k_Q (l.kJ^{-1})	k_t (min^{-1})	$k_{tillum.}$ (min^{-1})
Small-Scale	7.79	1.96	0.25	1.32
Pilot-Scale	5.73	1.86	0.35	0.55

Table 5.8: Inactivation rate constants calculated for small-scale and pilot-scale reactors based on dose Q_a, experimental time and actual illumination time.

Natural solar UV doses required to achieve 1-log inactivation were calculated for each reactors based on Q_a. The dose required to achieve 1-log inactivation calculated for the small-scale reactor was 0.3kJ/l, whereas a dose of 0.4kJ/l was required in the pilot-scale reactor.

The inactivation rate constants calculated for illuminated time suggest that the small-scale reactor is significantly more efficient than the pilot-scale reactor, whereas the calculated rate constants based on experimental time suggest that the pilot-scale reactor is more efficient. The pilot-scale reactor has a total volume of 35 litres, with an illuminated volume of 22 litres giving a light to dark ratio of 1.6:1. The small-scale reactor has a total volume of 1 litre with an illuminated volume of 0.2 litres giving a light to dark ratio of 0.2:1. Figure 5.9 shows a plot of bacterial inactivation against cumulative dose calculated by the actual illumination time, $Q_{a\ illum}$.

Calculated inactivation rate constants for the small-scale and pilot-scale reactors as a function of $Q_{a\ illum}$ are 41.0kJ/l and 9.0kJ/l respectively. This suggests that the ratio of light to dark time could have a significant effect on the solar disinfection process, which is investigated in Section 8. Other than this factor the depth of the water flowing through the pilot-scale reactor (29.4mm) could have an effect on the attenuation of solar radiation.
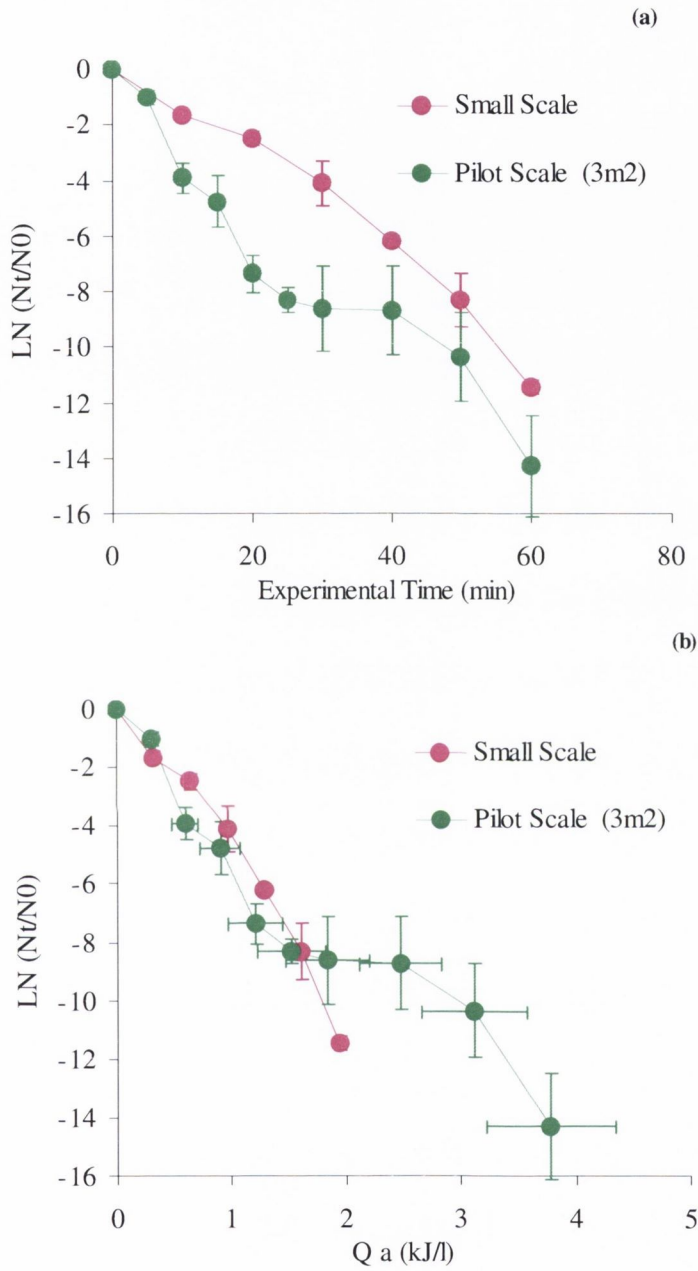
Figure 5.8: Comparison of the small-scale (CP) and pilot-scale reactors plotted as (a) inactivation of *E. coli* K-12 against experimental time (min) and (b) inactivation of *E. coli* K-12 against cumulative solar UV dose, Q_a, (kJ/l).
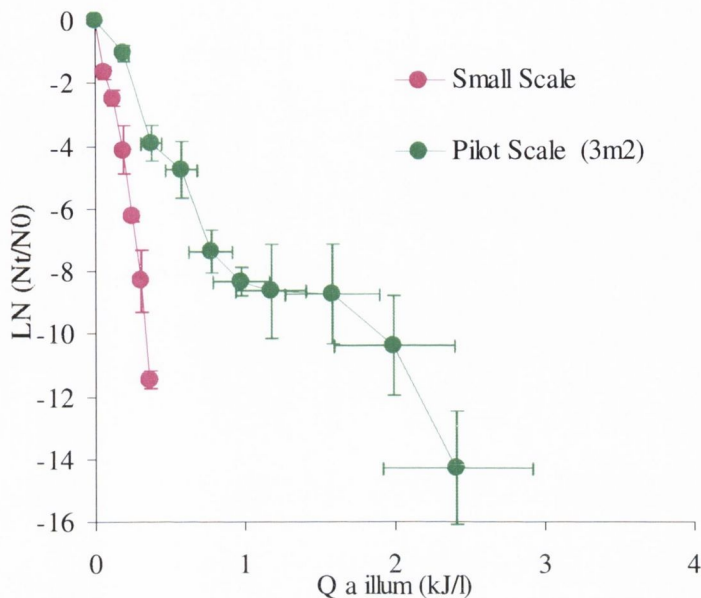
Figure 5.9: Comparison of the small-scale (CP) and pilot-scale reactors plotted as inactivation of *E. coli* K-12 against cumulative solar UV dose, $Q_{a,illum}$ (kJ/l).

5.7 Assessment of the Effect of Reactor Area

5.7.1 Introduction

The following experiment assesses the effect of reactor area on the continuous flow solar disinfection process. Experiments were carried out at Plataforma Solar de Almería using the pilot-scale reactor as described in Section 3.2.3 configured as a $3m^2$ (whole reactor exposed) and a $1m^2$ (by covering $2m^2$ of the total area) continuous flow recirculating reactor.

5.7.2 Experimental Set-up

Each reactor was configured as a recirculating system with a turbulent flow regime and Pyrex tubing placed at the focal point of the reflector. The volume of water in each case was kept constant at 35 litres. All tests were carried out natural solar radiation Plataforma solar de Almería during June and July 2003. At the beginning of each experiment a fresh batch of solar distilled water (checked for sterility) was inoculated

122

with *E. coli* K-12 to an initial concentration of 1×10^6CFU/ml. The reactor was kept covered for ten minutes to ensure a complete mix was achieved and uniform concentrations of bacteria existed throughout the reactor. Sampling was carried out every 5 minutes with controls left in the dark throughout the experiment. The samples were enumerated as out lined in Section 3.5.4 and inactivation kinetics determined as described in Section 3.6. All of the tests were repeated at least four times.

5.7.3   Results and Discussion

Representative data from the laboratory trials using the two different reactor configurations are presented in Figure 5.10. All plots show an average of at least four experiments.

Both configurations of reactor exhibited similar inactivation kinetics achieving >5-log removal during the experimental time. The inactivation rate constant calculated for the $3m^2$ reactor configuration was 0.349min^{-1} ($\pm$0.02, 95% CI), whereas for the $1m^2$ configuration it was 0.34min^{-1} ($\pm$0.09, 95% CI). Inactivation rate constants were also calculated using the actual illumination time, as described in Section 3.7.2, as well as the cumulative simulated solar UV dose, Q_a as described in Section 3.7.3. These calculated inactivation rate constants are shown in Table 5.9 below.

Reactor	k_{Qa} (l.kJ^{-1})	k_t (min^{-1})	$k_{tillum.}$ (min^{-1})	k_Q (l.kJ^{-1})
$1m^2$	16.16	0.34	1.63	2.50
$3m^2$	5.73	0.35	0.55	1.86

Table 5.9: Inactivation rate constants calculated for the $3m^2$ and $1m^2$ reactor configuration based on dose Q_a, experimental time and actual illumination time.

Natural solar UV doses required to achieve 1-log inactivation were calculated for each reactors based on Q_a. The dose required to achieve 1-log inactivation calculated for the $1m^2$ reactor was 0.14kJ/l, whereas a dose of 0.40kJ/l was required in the $3m^2$ configuration
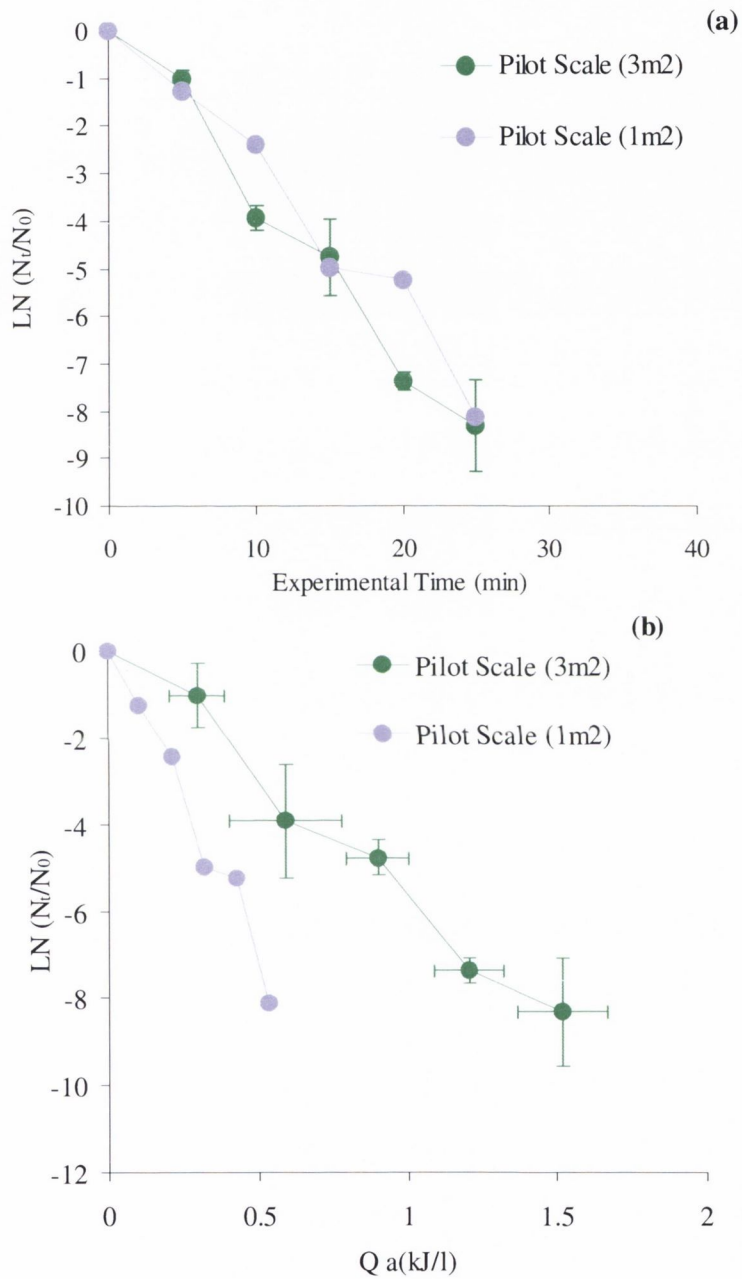
Figure 5.10: Comparison of the pilot-scale reactor with a reactor area of $3m^2$ and $1m^2$ plotted as (a) inactivation of *E. coli* K-12 against experimental time (min) and (b) inactivation of *E. coli* K-12 against cumulative solar UV dose, Q_a, (kJ/l).

The inactivation rate constants calculated for illuminated time and dose suggest that the $1m^2$ reactor is more efficient than the $3m^2$ reactor. The $3m^2$ reactor has a total volume of 35 litres, with an illuminated volume of 22 litres giving a light to dark ratio of 1.6:1. The small-scale reactor has a total volume of 35 litres with an illuminated volume of 7.3 litres giving a light to dark ratio of 0.3:1. Figure 5.11 shows a plot of bacterial inactivation against cumulative dose calculated by the actual illumination time, $Q_{a\ illum}$.
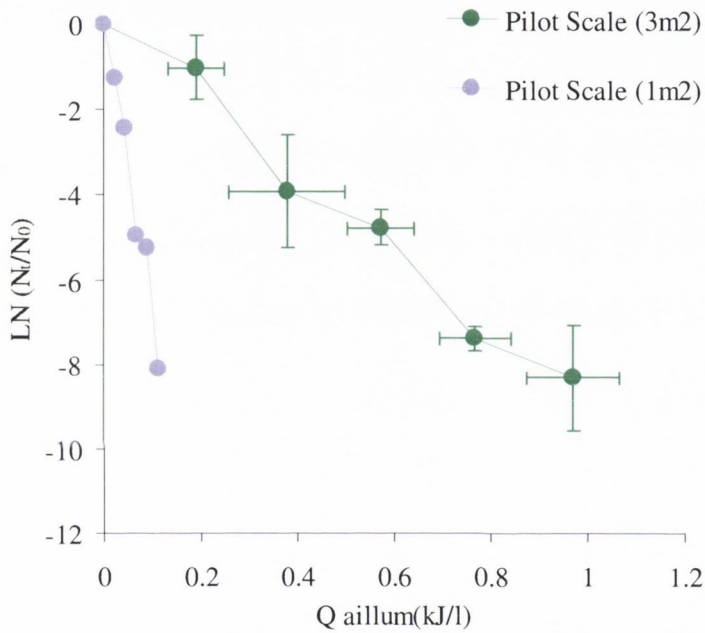
Figure 5.11: Comparison of the $1m^2$ and $3m^2$ reactor configurations plotted as inactivation of *E. coli* K-12 against cumulative solar UV dose, $Q_{a,illum}$ (kJ/l).

Calculated inactivation rate constants for the $1m^2$ and $3m^2$ reactor configurations as a function of $Q_{a\ illum}$ are 69.0kJ/l and 9.0kJ/l respectively. This also suggests that the ratio of light to dark time could have an effect on the solar disinfection process, as the results seem paradoxical due to greater dose received by the $3m^2$ reactor. One common feature in both experimental configurations however, is that on average each bacterium will make the same number of cycles per unit time and will also move across a dark to light interface for every revolution made of the reactor. This then provides the interesting hypothesis that another mechanism, apart from the presumed UV radiation dose, could be governing the disinfection kinetic at such a temporal scale of less than 10 minutes

illuminated time. This mechanism could be due to the stress associated with the bacteria moving from the dark into the light, possibly in conjunction with a threshold UV dose, and hence the inactivation kinetics could be primarily governed by the frequency of shock to the bacteria (i.e. a stroboscopic shock mechanism). Undoubtedly the UV dose disinfection mechanism, as witnessed in numerous other trials, will still be occurring, but the overall kinetics observed in these experiments could be revealing a much faster acting mechanism due to the frequency of intermittent illumination, which is totally swamping the slower, UV dose proportional mechanism. In these trials the average time per revolution of the pilot plant was 105 seconds, of which the time in the dark was 38 seconds and 83 seconds per revolution for the $3m^2$ and $1m^2$ illuminated areas. This gives a dark to light ratio of 0.36 and 0.79 respectively which may also be a critical parameter for such a stroboscopic shock mechanism. This theory has been investigated by a series of further trials as discussed in Section 8. Research into the effect of alternating bacteria between light and dark conditions was carried out in one previous study (Rincón and Pulgarin 2003) although the results provided contradictory findings depending on the type of microorganism used. It should also be noted however, that the stroboscopic frequency in those trials were typically at much lower values compared to the trials presented here.

5.8   Concluding Remarks

It is evident from the above experiments that solar disinfection is achievable in a reasonable amount of time under both simulated and natural solar conditions.

The Compound Parabolic reactor performed consistently better than the other three reactors, both under natural and simulated conditions as well as under low intensity natural conditions.

There was a marked different in performance under natural conditions compared with simulated conditions for all reactors. This could be due to spectral differences in the UV and Infrared regions of simulated and natural solar conditions.

There also seems to be a mechanism other than dose related contributing to the disinfection process when there is a dark phase in the continuous flow process.

Finally, the results from these studies suggest that inactivation kinetics should be calculated according to absorber area and actual exposure time when comparing continuous flow reactors of different areas and varying dark zones.

CHAPTER 6

SOLAR PHOTOCATALYTIC DISINFECTION

6.1 Introduction

The objective of the following experiments was to assess the efficiency of the solar photocatalytic disinfection process and compare this to the solar disinfection process. A number of experiments were carried out:

i. A comparison of the solar disinfection process and a low concentration of titanium dioxide (TiO$_2$) enhanced process using the catalyst in suspension.

ii. Assessment of the effect of a fixed photocatalyst on the solar disinfection process.

iii. Comparison of two different types of fixed catalyst and their effect on the disinfection process.

iv. An assessment of the potential for regrowth in a solar disinfection and solar photocatalytic disinfection system.

6.2 Titanium Dioxide in Suspension

6.2.1 Introduction

The purpose of these experiments was to investigate the effect of introducing a suspension of TiO$_2$ into the solar disinfection process. The enhancement of the solar disinfection process by photocatalytic oxidation was first demonstrated in Japan (Matsunga, 1985) with continuing research both in natural and simulated sunlight proving successful against a wide range of micro-organisms (McGuigan *et al*, 1999; Salih, 2003; Rincón and Pulgarin, 2003; Saito *et al*., 1992; Block *et al*., 1997; Pham *et al*., 1997) as described in Section 2.8. Such studies have used mainly TiO$_2$ that has an appropriate energetic separation between its valence and conduction bands, which can be surpassed by the energy content of a solar photon thus creating an electron-electron hole pair (Robert and Malato, 2002). This electron combines with dissolved oxygen in water to produce a hydroxyl radical ($^\cdot$OH) which is thought to damage microbial cells. In the following experiments TiO$_2$ is added to the solution as a suspension as described in Section 2.8.

6.2.2 Experimental Set-up

The pilot-scale reactor at PSA configured as in 1m^2 area recirculating reactor was used during these experiments. The volume of water in each case was kept constant at 35 litres. All tests were carried out natural solar radiation Plataforma Solar de Almería during June and July 2003. At the beginning of each experiment a fresh batch of solar

127

distilled water (checked for sterility) was inoculated with *E. coli* K-12 to an initial concentration of 1×10^6CFU/ml. The reactor was kept covered for ten minutes to ensure a complete mix was achieved and uniform concentrations of bacteria existed throughout the reactor. During TiO_2 experiments the photocatalyst was prepared as outlined in Section 3.5 and then added to the solution in the reactor to obtain the desired concentration of 3, 6 or 9 mg/l. The solution in the reactor was recirculated in the dark to allow a complete mix of water, bacteria and TiO_2. Sampling was carried out every 5 minutes with controls left in the dark throughout the experiment. The samples were enumerated as outlined in Section 3.6.4 and inactivation kinetics determined as described in Section 3.7. All of the tests were repeated at least once.

6.2.3 *Results and Discussion*

Representative data from the laboratory trials using four different concentrations of TiO_2 are presented in Figure 6.1. All plots show an average of at least four experiments. It is apparent from Figure 6.1(a) that all four experimental solutions required almost the same amount of exposure time in order for complete inactivation to take place, between 20 and 30 minutes, corresponding to an illumination time of 4 to 6 minutes. Inactivation rate constants are shown in Table 6.1 calculated for experimental time, illumination time, Q_a and $Q_{a\,illum}$.

Average solar intensities were calculated and found to be $38.28W_{uv}/m^2$ (std. dev. 1.59) for the trials using a zero concentration of TiO_2 and $27.48W_{uv}/m^2$ (std. dev. 2.35), $41.40W_{uv}/m^2$ (std. dev. 0.62), $39.55W_{uv}/m^2$ (std. dev. 1.29) for trials with a concentration of 3mg/l, 6mg/l and 9mg/l of TiO_2 added respectively.

(b)
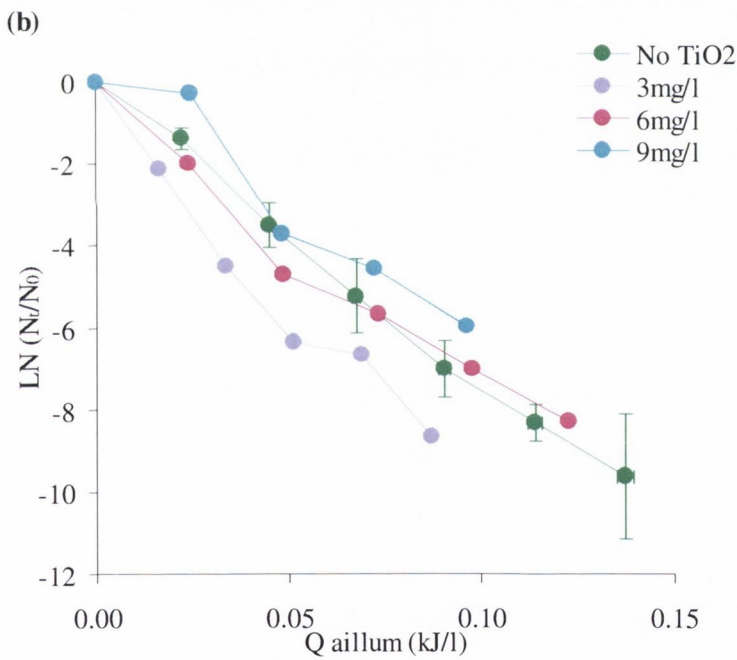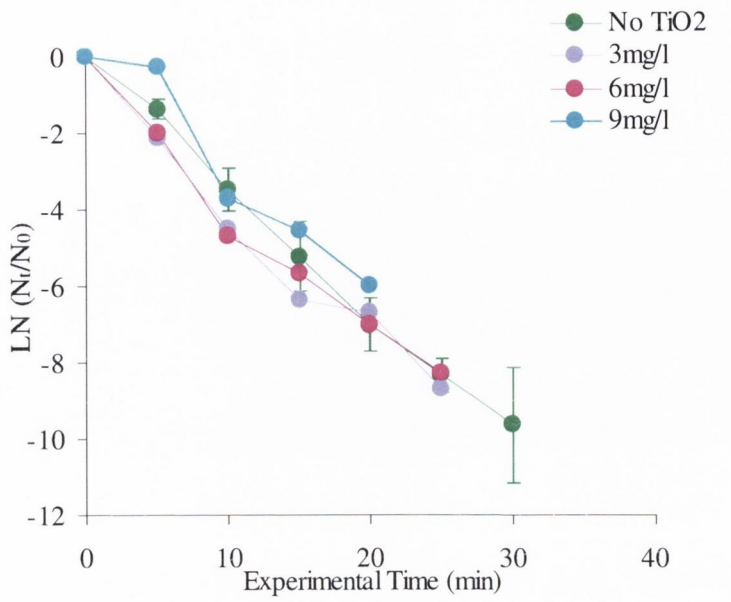
Figure 6.1: Comparison of the pilot-scale reactor with a reactor area of $1m^2$ with 4 concentrations of TiO_2 suspension added plotted as (a) inactivation of *E.coli* K-12 against experimental time and (b) inactivation of *E.coli* K-12 against cumulative solar UV dose, $Q_{a\,illum}$. Note: error bars only on one data set for clarity.

All experiments exhibited similar inactivation kinetics achieving >4-log removal during the experimental time. The inactivation rate constant calculated for the 0mg/l concentration of TiO$_2$ was 0.34min^{-1} (±0.02, 95% CI), similar to those experiments containing TiO$_2$ as shown in Table 6.1 below.

TiO$_2$	k_{Qa} (l.kJ^{-1})	$k_{Qa\ illum}$ (l.kJ^{-1})	k_Q (l.kJ^{-1})	k_t (min^{-1})	$k_{t illum.}$ (min^{-1})
0	16.16	75.73	5.26	0.34	1.68
3	20.55	96.32	5.62	0.34	1.68
6	14.27	66.91	4.01	0.33	1.54
9	14.42	67.57	4.29	0.33	1.52

Table 6.1: Inactivation rate constants calculated for different doses of suspended TiO$_2$ based on doses Q$_a$ and Q$_{a\ illum}$, experimental time and actual illumination time.

Natural solar UV doses required to achieve 1-log inactivation were calculated for each reactors based on Q$_a$. The dose required to achieve 1-log inactivation calculated for the 1m^2 reactor with no TiO$_2$ was 0.143kJ/l, whereas a dose of 0.161kJ/l and 0.159kJ/l was required during experiments containing a suspension in concentrations of 6mg/l and 9mg/l TiO$_2$ respectively. Perhaps surprisingly the experiments performed with a 3mg/l suspension performed most efficiently with only 0.112kJ/l solar UV radiation required to produce 1-log reduction of bacteria.

Doses required to achieve 1-log reduction were also calculated based on Q$_{a\ illum}$ as shown in Figure 6.1(b). Both the systems with 6 and 9mg/l concentration of TiO$_2$ required a higher dose than the system with no TiO$_2$ added, with calculated doses equal to 0.034kJ/l as opposed to 0.030kJ/l. Again during the experiments with only 3mg/l added, the least dose was required to inactivate 1-log of bacteria, 0.023kJ/l.

At first sight it may seem counter intuitive that the concentration of 3mg/l is most effective whereas higher concentrations of TiO$_2$ only produced results of approximately the same efficiency as the 0mg/l concentration solar disinfection experiments. The 3mg/l result could be due the fact that increasing the dose of TiO$_2$ also increases the opaqueness of the water which thus reduces the overall UV dose throughout the process water, a phenomenon which has been noticed before in batch processes (Salih, 2002). Hence, any enhancement due to the extra photocatalytic mechanism is being muted by a reduction in the solar UV disinfection mechanism due to lower intensities. For example, a concentration of 9 mg/l TiO$_2$ at a path length of 30 mm will reduce the sum of absorbed and scattered light by around 15-20% (Malato et al., 2004). Whilst such

photocatalytic mechanisms have proved particularly effective at high concentrations (up to 200mg/l) of TiO_2 against recalcitrant organics (pesticides etc) (Hancapié et al., 2005), it may be that its benefit to the overall disinfection efficiency is minimal if the photocatalytic inactivation kinetic is of a similar order to the UV light inactivation kinetic whereby an increase in one inevitably leads to a decrease in the other. Further tests could be carried out at lower ranges of TiO_2 concentrations in order to optimise the chemical dose, although the results presented here do not indicate that the addition of TiO_2 as a photocatalyst will prove particularly attractive for a low cost, disinfection process for developing countries. It should also be noted that if the stroboscopic shock (or mechanic stress) mechanism aired in Section 8 is significant, it could also be swamping the true differences between the photocatalytic and UV radiation mechanism as discussed in Section 8.

The results indicate that it could be beneficial to add a small amount of TiO_2 to the system in order to increase efficiency, here 3mg/l added was found to be 27% more efficient than a zero dose of TiO_2. This benefit does not appear to be significant enough to justify adding the photocatalyst as a suspension into the water as a sustainable solution for developing countries with its inherent requirement for an extra separation process before water consumption. One benefit of using TiO_2 that has been reported however, is that any re-growth of bacteria is hindered much more effectively compared to normal UV disinfection, due to the destruction of the cellular structure by photocatalytic mechanisms (Rincón and Pulgarin, 2003; Sunada et al.; 1998, Ibáñez et al., 2003). A low cost method of fixing the TiO_2 within the tubes of the reactor would enable both the photocatalytic and UV light disinfection mechanisms to act on the pathogens although in general, fixed catalysts tend to have lower reaction rates than suspensions, which may constrain the feasibility of such a method.

6.3 Fixed Titanium Dioxide (PSA)

6.3.1 Introduction

In order to test the effectiveness of using TiO_2 as a photocatalyst in the reactors, it was decided to evaluate a design whereby a stable coating of TiO_2 could be fixed in the reactor. These experiments look at the concept of coating small 2mm diameter glass rods with TiO_2, which were then fixed along the centre of each reactor tube. A stable coating of TiO_2 onto the glass rods was achieved using the technique described in Section 3.5.3. Fixed catalysts have proven to be less successful than suspensions of TiO_2 at enhancing the disinfection process as the contact area between the TiO_2 and the contaminated water needs to be very small (Salih, 2002) but have been considered in a few batch studies (Sunada *et al.*, 2003; Rincón and Pulgarin, 2004; Dunlop *et al.*, 2002; Wist *et al.*, 2002).

6.3.2 Experimental Set-up

Each of the four small-scale reactors described in Section 3.3.2 was configured as a recirculating system with a turbulent flow regime and Pyrex tubing placed at the focal point of the reflector as before. TiO_2 coated rods were fixed into position at the centre of the Pyrex tubes in each reactor before exposure to sunlight. The rods were typically exposed to water velocities in the tubes of up to 0.67 m/s which would promote high localised shear stresses on the coating. However, during all trials the coating appeared to be stable. The amount of photocatalyst attached to the rods per unit illuminated volume was found by removing the rods after use, drying in an oven at 105°C and weighing them. These rods were then cleaned of all traces of TiO_2, dried in an oven again and then reweighed to calculate the difference in mass. The appropriate calculations return a concentration of TiO_2 coating per unit illuminated volume to be 94 mg/l.

The volume of water in each experiment was kept constant; each test using one litre of water (MilliQ), which was tested for sterility, inoculated with a 1×10^6 CFU/ml concentration of *E. coli* K-12. All tests were carried out in natural solar radiation at Plataforma Solar de Almería during June and July 2003. Reflector apertures were tilted to the local latitude angle (37°) to maximise sunlight capture as described in Section 3.4.2 and positioned so that the tubes were aligned in an east-west orientation. Sampling was carried out every 10 minutes with controls left in the dark throughout the experiment. The samples were enumerated as outlined in Section 3.6.4 and inactivation

kinetics determined as described in Section 3.7. All of the tests were repeated at least three times.

6.3.3   Results and Discussion

Representative data from the laboratory trials using the compound parabolic reactor with fixed TiO_2 are presented in Figure 6.2. All plots show an average of at least four experiments. Inactivation rate constants are shown in Table 6.2 calculated for experimental time, illumination time, Q_a and $Q_{a\ illum}$ for the Compound Parabolic, Parabolic and V-groove reactors.

Average solar intensities were calculated and found to be $38.17W_{uv}/m^2$ (std. dev. 6.33) for the trials using the compound parabolic reactor with fixed TiO_2 and $30.44W_{uv}/m^2$ (std. dev. 7.08) and $37.55W_{uv}/m^2$ (std. dev. 3.29) for trials with the Parabolic and V-groove reactors respectively.

Inactivation kinetics were similar for all experiments with a 3-5-log reduction in bacteria during the 60 minute experimental time. Inactivation rate constants calculated from the experimental time were found to be $0.199min^{-1}$, $0.12min^{-1}$ and $0.83min^{-1}$ for the Compound Parabolic, Parabolic and V-groove reactors respectively. When the effect of different experimental solar UV radiation intensities is taken into account and the results are plotted as survival against cumulative UV radiation dose, $Q_{a\ illum}$, (see Figure 6.2(b)), calculated inactivation rate constants were found to be $47.27\ l.kJ^{-1}$ for the Compound Parabolic reactor and $28.9\ l.kJ^{-1}$ and $32.39\ l.kJ^{-1}$ for the Parabolic and V-groove reactors.

The average temperature during the experiments was 36°C for the Compound Parabolic reactor experiments and 34°C and 36°C for the Parabolic and V-groove reactor experiments respectively.
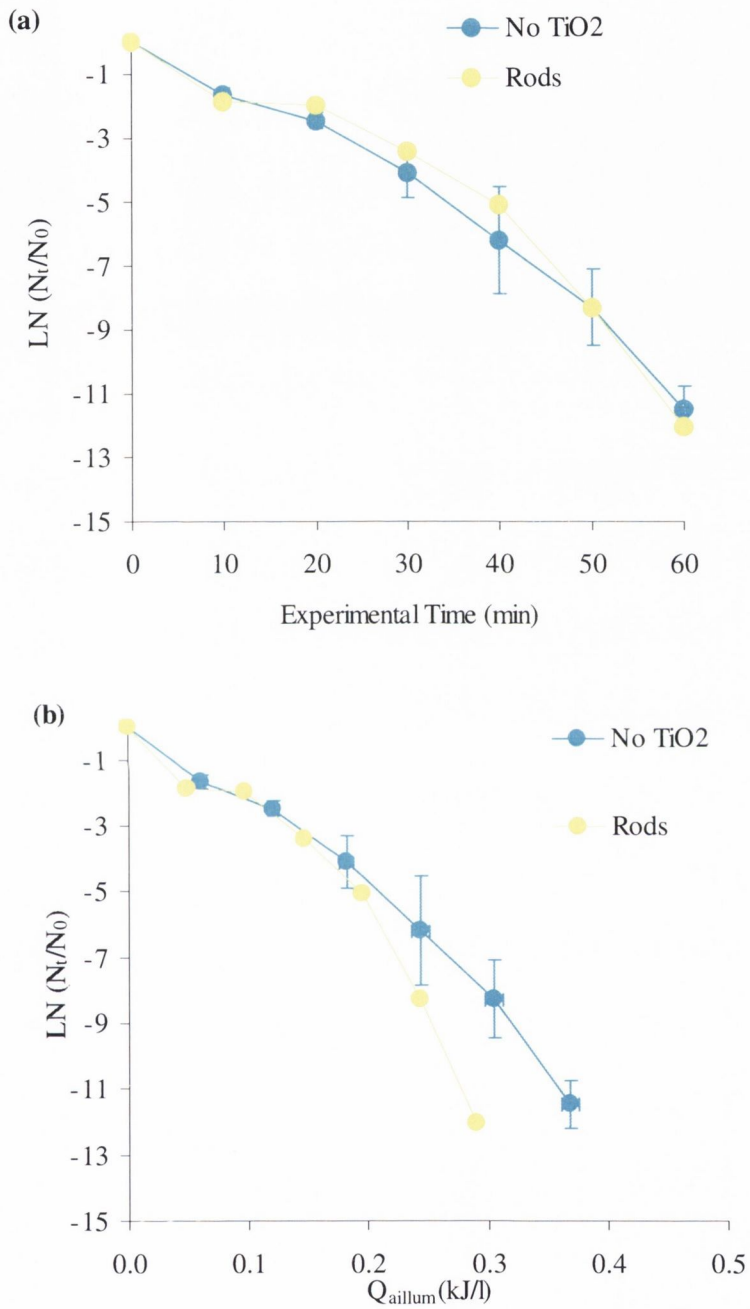
Figure 6.2: Comparison of the compound parabolic reactor with and without fixed TiO_2 plotted as (a) inactivation of *E. coli* K-12 against experimental time and (b) inactivation of *E. coli* K-12 against cumulative solar UV dose, $Q_{a\,illum}$.

Reactor	TiO$_2$	k$_{Qa}$ (l.kJ^{-1})	k$_{Qa\,illum}$ (l.kJ^{-1})	k$_Q$ (l.kJ^{-1})	k$_t$ (min^{-1})	k$_{t\,illum.}$ (min^{-1})
CP	N	7.79	41.00	1.96	0.25	1.32
	Y	8.88	47.27	1.77	0.20	1.05
P	N	6.08	32.01	2.08	0.19	1.02
	Y	5.49	28.90	1.19	0.12	0.63
V	N	4.71	24.80	1.19	0.13	0.71
	Y	6.06	32.29	1.52	0.16	0.83

Table 6.2: Inactivation rate constants calculated for different solar disinfection reactors with and without fixed TiO$_2$ based on doses Q$_a$ and Q$_{a\,illum}$, experimental time and actual illumination time.

Natural solar UV doses required to achieve 1-log inactivation were calculated for each of the reactors based on Q$_a$. The dose required to achieve 1-log inactivation calculated for the Compound Parabolic reactor with no TiO$_2$ was 0.30kJ/l, whereas a dose of 0.26kJ/l was required during experiments containing the fixed TiO$_2$ rods. Calculated doses required for 1-log reduction in bacteria for experiments carried out using the Parabolic reactor were 0.37kJ/l whereas surprisingly when TiO$_2$ rods were added to the system the dose required was the greater value of 0.41kJ/l. An enhancement in the efficiency of the process was found with the V-groove reactor with calculated required doses of 0.48kJ/l and 0.38kJ/l for the system without TiO$_2$ and with TiO$_2$ rods respectively.

Doses required to achieve 1-log reduction were also calculated based on Q$_{a\,illum}$ as shown for the compound parabola in Figure 6.1(b). The dose required to achieve 1-log inactivation calculated for the Compound Parabolic reactor with no TiO$_2$ was 0.056kJ/l, whereas a dose of 0.048kJ/l was required during experiments containing the fixed TiO$_2$ rods. Calculated doses required for 1-log reduction in bacteria for experiments carried out using the Parabolic reactor were 0.071kJ/l whereas when TiO$_2$ rods were added to the system the dose required was the greater value of 0.078kJ/l. An enhancement in the efficiency of the process was found with the V-groove reactor with calculated required doses of 0.093kJ/l and 0.071kJ/l for the system without TiO$_2$ and with TiO$_2$ rods respectively.

Hence, when TiO$_2$ was added as a fixed catalyst, the inactivation rate constants from the trials (where the kinetics have been calculated with respect to dose) demonstrate that there does seem to be evidence of an enhancement of 13-16% using the Compound Parabolic reactor and 26-30% using the V-groove reactor although no such enhancement was measured in the Parabolic reactor, which actually only performed at

90% of its efficiency when run containing the TiO_2 rods. A hypothesis to explain the apparent lack of photocatalytic response in the parabolic rector could be that any augmentation of the disinfection by the photocatalyst is being cancelled out by the shading of the direct UV light by the small 2mm rod supporting the TiO_2, this effect would be most prominent in the parabolic reactor as the reflector area is smaller. This was not the case for the CP reactor since it is a much more efficient reflector particularly with respect to focusing the incident solar radiation behind the rod.

Hence, the results do not show a particularly large benefit at this scale using fixed TiO_2 concentrations when taking into account the extra costs of fabrication required for such a continuous flow system. It may be that the concentration of the TiO_2 per illuminated litre was not high enough to promote much photocatalytic disinfection with respect to a dominant solar UV disinfection mechanism. It should be noted that the concentration of TiO_2 coating used (94 mg/l) is low when compared to typical doses that have been used in other fixed TiO_2 research trials. Where researchers have used TiO_2 fixed to an inert media, concentrations of 250–2000 mg/l have been used for disinfection applications (Salih, 2002; Rincón and Pulgarin 2003). In these cases, however, the attached photocatalyst has been used in batch processes, which makes direct comparison with the TiO_2 coated rods used in this research difficult since they are located in turbulent flow conditions. It should be noted that this is a surface effect and therefore the contaminated water has to be in contact with the photocatalyst meaning that every effort should be made to increase the contact area between the fixed catalyst and the contaminated water. Another factor to be considered is the dissolved oxygen (DO) level, not monitored during these trials, as it is reported to have an effect on photocatalytic efficiency but due to the agitation caused by the pump of each system a reasonable DO level is assumed. Photocatalytic reactions require the presence of molecular oxygen; lack of sufficient supply will stop the reaction completely (Sagwe *et al.*, 2005). Every effort should be made to ensure that the solution is kept as close as possible to DO saturation level. Hence, future research should be targeted to find improved methods of fixing higher concentrations of photocatalyst within the tubes of the reactor or alternatively maximizing the TiO_2 area to liquid volume ratio.

6.4 Fixed Titanium Dioxide (Ireland)

6.4.1 *Introduction*

These experiments compare the 2mm diameter glass rods coated with TiO_2 used in Section 6.3 with a commercially available TiO_2 coated paper. The coated paper (Ahlstrom[©]) was fixed in the reactor by wrapping it around 2mm diameter glass tubes as described in Section 3.5.3. These experiments were carried out in Trinity College Ireland.

6.3.2 *Experimental Set-up*

Again the small-scale compound parabolic reactor described in Section 3.2.4 was configured as a recirculating system with a turbulent flow regime and Pyrex tubing placed at the focal point of the reflector. TiO_2 coated rods were fixed into position at the centre of the Pyrex tubes in each reactor before exposure to sunlight as before or the rods that had been wrapped in TiO_2 paper were fixed into the centre of the tubes. The amount of TiO_2 photocatalyst attached to the rods per unit illuminated volume was found to be 94 mg/l as before. The paper was wrapped around the same 2mm glass rods and was calculated to give 147 mg/l TiO_2 photocatalyst per unit illuminated volume. Similar photocatalysts were used in both the rod and paper systems. The rods were coated with Degussa P-25 TiO_2 (anatase: rutile ratio 3:1, surface area=50m2/g, non-porous particles) by the technique described in Section 3.5.4. The paper consisted of Degussa P-25 coated on glass fibre paper using an organic (SiO_2) binder as described in Section 3.5.3.

The volume of water in each experiment was kept constant; each test using one litre of autoclaved water, which was tested for sterility, inoculated with a 1×10^5 CFU/ml concentration of *E. coli* K-12. All tests were carried out in natural solar radiation at Trinity College, Dublin during August 2004. Reflector apertures were tilted to the local latitude angle (53°) to maximise sunlight capture as described in Section 3.4.2 and positioned so that the tubes were aligned in an east-west orientation. Sampling was carried out every 10 minutes with controls left in the dark throughout the experiment. The samples were enumerated as out lined in Section 3.6.4 and inactivation kinetics determined as described in Section 3.7. All of the tests were repeated at least three times.

6.4.3 Results and Discussion

Representative data from the laboratory trials using the Compound Parabolic reactor with the two types of fixed TiO_2 are presented in Figure 6.3. All plots show an average of at least four experiments. Inactivation rate constants are shown in Table 6.3 calculated for experimental time, illumination time, Q_a and $Q_{a\ illum}$ for the Compound Parabolic reactor containing two different types of fixed TiO_2.

Average solar intensities were calculated and found to be $22.23W_{uv}/m^2$ (std. dev. 2.90) for the trials using the Compound Parabolic reactor without TiO_2 and $26.94W_{uv}/m^2$ (std. dev. 9.46) and $33.75W_{uv}/m^2$ (std. dev. 12.92) for trials with the TiO_2 coated rods and paper wrapped rods respectively.

Inactivation kinetics were similar for all experiments with >4-log reduction in bacteria during the 150 minute experimental time. Inactivation rate constants calculated from the experimental time were found to be $0.076min^{-1}$ (±0.04, 95% CI), $0.054min^{-1}$ (±0.04, 95% CI) and $0.076min^{-1}$ (±0.09, 95% CI) for the rods, paper and no TiO_2 respectively. When the effect of different experimental solar UV radiation intensities is taken into account and the results are plotted as survival against cumulative UV radiation dose, $Q_{a\ illum}$, (see Figure 6.2(b)), calculated inactivation rate constants were found to be $22.28 l.kJ^{-1}$ for the Compound Parabolic reactor containing the coated rods and $17.36 l.kJ^{-1}$ and $20.63 l.kJ^{-1}$ for the paper and no TiO_2. These results are summarised in Table 6.3 below

TiO_2	k_{Qa} ($l.kJ^{-1}$)	$k_{Qa\ illum}$ ($l.kJ^{-1}$)	k_Q ($l.kJ^{-1}$)	k_t (min^{-1})	$k_{t\ illum.}$ (min^{-1})
None	3.92	20.63	1.15	0.08	0.40
Rods	4.19	22.28	0.80	0.08	0.40
Paper	3.26	17.36	0.51	0.06	0.32

Table 6.3: Inactivation rate constants calculated for the Compound Parabolic solar disinfection reactor for two types of fixed TiO_2 based on doses Q_a and $Q_{a\ illum}$, experimental time and actual illumination time.
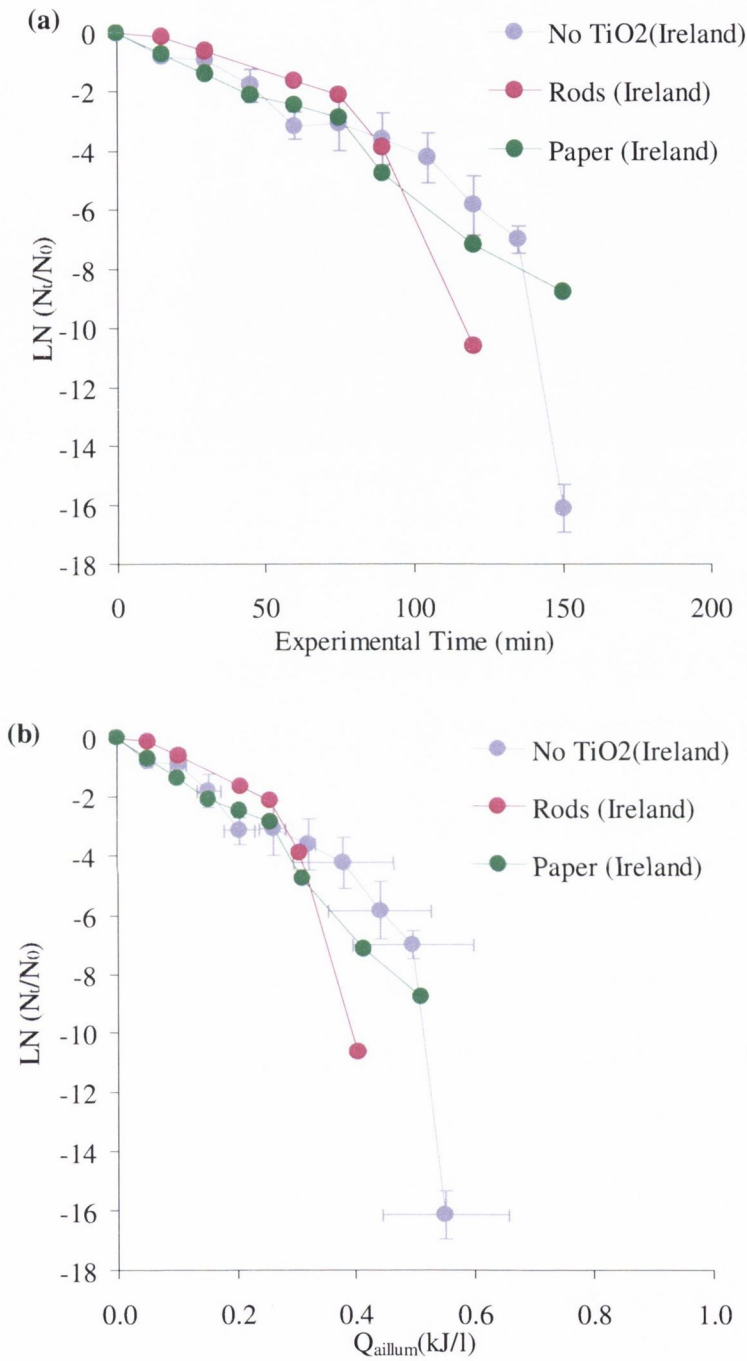
Figure 6.3: Comparison of the compound parabolic reactor with two different methods of fixed TiO_2 plotted as (a) inactivation of *E. coli* K-12 against experimental time and (b) inactivation of *E. coli* K-12 against cumulative solar UV dose, $Q_{a\,illum}$. Note: Error bars are shown on one plot only for clarity.

Natural solar UV doses required to achieve 1-log inactivation were calculated for each of the experiments based on Q_a. The dose required to achieve 1-log inactivation calculated for the Compound Parabolic reactor with no TiO_2 was 0.58kJ/l, whereas a dose of 0.55kJ/l was required during experiments containing the fixed TiO_2 rods. Calculated doses required for 1-log reduction in bacteria for experiments carried out using the paper were 0.71kJ/l where the system was surprisingly found to be less efficient.

Doses required to achieve 1-log reduction were also calculated based on $Q_{a\ illum}$ as shown for these experiments in Figure 6.1(b). The dose required to achieve 1-log inactivation calculated for the Compound Parabolic reactor with no TiO_2 was 0.112kJ/l, whereas a dose of 0.103kJ/l was required during experiments containing the fixed TiO_2 rods. Calculated doses required for 1-log reduction in bacteria for experiments carried out using the paper were 0.133kJ/l.

The TiO_2 rods enhanced the inactivation process (where the kinetics have been calculated with respect to dose) by up to 8%. When a performance comparison is made between systems in Ireland and Spain the process was found to be ~2 times more efficient in Spain, which is similar to the previous results found with the reactors and no photocatalyst as discussed in Section 5.4. The rods that were coated in the paper caused the system to be 18% less efficient, which could be due to a number of reasons. The average solar intensity was much higher during the paper experiments, the non-linear relationship between light intensity and deactivation of bacteria could be due to excessive •OH radical generation at this higher solar radiation intensity leading to self-recombination which leads to a decrease in the attack of target organisms (Rincón and Pulgarin, 2003) and a less efficient process. Moreover, when a high photonic flux is applied high concentrations of electrons and holes are generated in the semiconductor, which results in a high recombination rate. The method of fixing the paper into the tubes could also be modified in order to promote greater contact with the contaminated water. The surface texture of the paper is uneven which would promote a boundary layer at the flow rates used in the reactor and hence, the majority of the flow would not pass close enough to the photocatalyst surface to be within range of the transitory hydroxyl radicals. The absorber area was also less when the paper was attached to the rods as the thickness of the TiO_2 coated paper is ~1mm (which was taken into account when calculating Q_{aillum}).

Hence, the results do not show a particularly large benefit at this scale using fixed TiO_2 concentrations when taking into account the extra costs of fabrication required for such a continuous flow system.

6.5 Post Irradiation Regrowth (Ireland)

6.5.1 Introduction

One of the potential benefits of using a photocatalyst reported by some authors is that the photocatalytic disinfection mechanism prevents any regrowth of the sample microorganism post-irradiation if the water is subsequently stored in the dark (Rincón and Pulgarin, 2003a,b; Rincón and Pulgarin, 2004; Dunlop *et al.*, 2002; Wist *et al.*, 2002). This is a particularly attractive characteristic for continuous flow reactor design where the disinfected water is likely to be stored in a closed reservoir for some time before consumption.

6.5.2 Experimental Set-up

Experiments were carried out in Ireland using *E. coli* K-12 on the same small-scale reactors and same procedure as described above (Section 6.3). The same small-scale reactors were used as in Section 4.2 experiments were carried out in Ireland in summer again using *E. coli* K-12. This time, however, at each time step, 3 parallel samples were taken: one was plated immediately; one sample was left for two hours in dark before being plated and the third sample for 24 hours before plating. This procedure was carried out for each of 12 samples. Samples were enumerated as outlined in Section 3.6.4.

6.5.3 Results and Discussion

Representative data from the experiments are shown in Figure 6.4. In all cases no significant regrowth occurred between samples plated after 0, 2 or 24 hours. Sample 7 in the experiments carried out with no TiO_2 (Figure 6.4(a)) and Sample 1 in the experiments carried out with the TiO_2 rods (Figure 6.4(b)) showed slight regrowth but this is within expected experimental error. The experiments carried out with TiO_2, either rods or paper did show an appreciable reduction in concentration of culturable cells after 24 hours suggesting that the addition of a photocatalyst may damage cells in such a way that they are inactivated after a period in the dark.
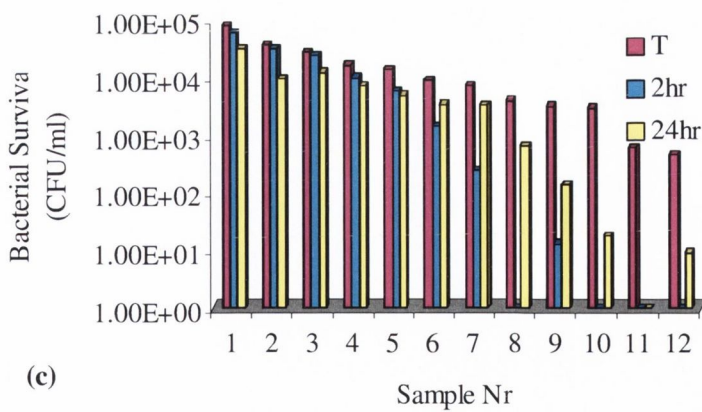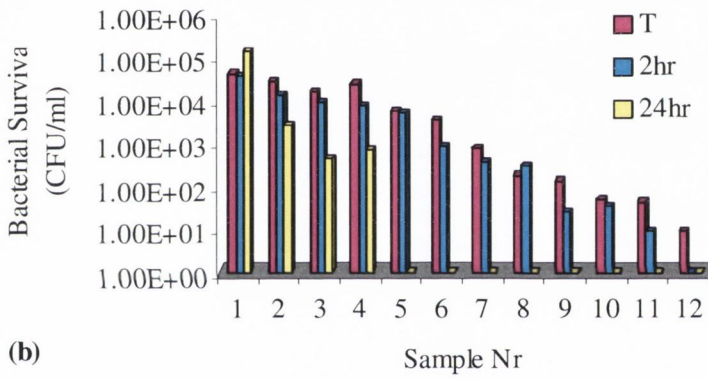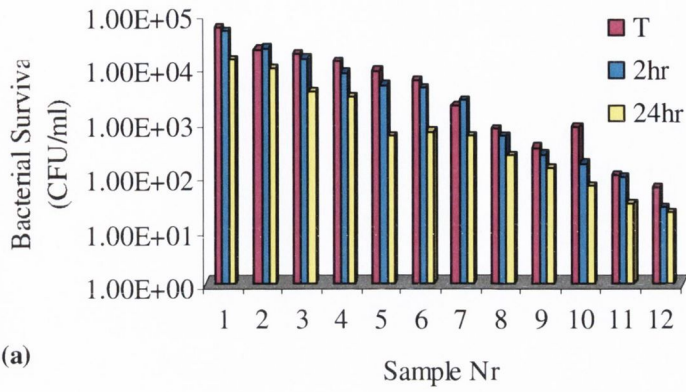
Figure 6.4: Bacterial Survival after 0, 2 and 24 hours for the small-scale solar disinfection reactors with (a) no fixed catalyst, (b) TiO_2 coated rods and (c) TiO_2 coated paper.

6.6   CONCLUDING REMARKS

A slight enhancement of the disinfection process was found on addition of a low concentration (3mg/l) of TiO_2 to the pilot-scale solar disinfection reactor. However, these results do not indicate that an addition of a TiO_2 solution can be justified as a sustainable solution for developing countries with its inherent requirement for an extra separation process before water consumption.

The technique of using low concentrations of TiO_2 fixed to a glass rod within the reactors demonstrated a moderate enhancement to overall disinfection efficiency in the Compound Parabolic and V-groove reactors.

TiO_2 coated paper did not improve reactor performance, which could be due to a number of reasons including, excessive •OH radical generation, method of fixing and surface texture. TiO_2 coated glass rods showed a slight enhancement under lower intensity Irish sun.

Post-irradiation regrowth was also examined for both solar disinfection and solar photocatalytic disinfection. After 24 hours there was no appreciable regrowth in either system but a loss in culturable cell in samples of the photocatalytic systems suggests that an addition of TiO_2 could produce a residual effect. It should be noted that these experiments were carried out using sterile water and during disinfection in a real situation, rather than the laboratory, organics present in raw water sources could affect regrowth in an undesirable way.

OTHER FACTORS WHICH EFFECT THE SOLAR DISINFECTION PROCESS

7.1 Introduction

The aim of this study was to

i.   Investigate the influence of temperature on the continuous flow disinfection process

ii. Compare the solar disinfection kinetics calculated for different volumes of contaminated water

Throughout these experiments the Parabolic and Compound Parabolic collector was used to compare the different parameters.

7.2 Effect of Temperature

7.2.1 Introduction

The objective of the following experiments is to assess the influence of temperature on the continuous flow solar disinfection process. Batch process solar disinfection is based on the synergistic effect of both water temperature and UVA radiation (EAWAG, 2005), where the water temperature in the bottles increases to above 40°C during exposure. During the continuous flow experiments described previously water temperatures did not increase above 40°C, so the following experiments were carried out by increasing the temperature by an artificial input of heat.

7.2.2 Experimental Set-up

The first set of trials investigated the disinfection efficiency of the solar reactor in natural sunlight with no artificial increase in temperature. A second set of trials repeated the first but with an artificial increase in temperature up to 45°C. A third set investigated the effect of a temperature increase alone with no exposure to sunlight. Temperatures used in this set of trials were 40°, 45° and 50°C.

The experiments in which the reactor was exposed to natural sunlight were carried out during June and July 2003 at Plataforma Solar de Almería, Spain. At the beginning of each experiment 1litre of filtered MilliQ water inoculated with *E. coli* K-12, was admitted into the reservoir. After this inoculation the water was circulated through the solar reactor tubes in the dark until a complete mix and a uniform concentration of bacteria was achieved throughout the reactor. The initial bacterial concentrations were approximately 1×10^6CFU/ml. At the start of each experiment a sample was taken at t=0 and the reactor was uncovered. This sample was enumerated and then kept in the dark as a control during the experiment. Samples were taken at 10 minute intervals and each

experiment was repeated at least three times. The flowrate through the Pyrex tubes was 2.8litre/min equating to Reynolds numbers of >4000 with temperatures not exceeding 36°C. Solar radiation measurements were made using a 300-400nm broadband UV radiometer (CUV3 Kipp and Zonen, Netherlands) located on site, as described in Section 3.3.2. Global UV intensity ranged between 30.3 and 40.8 W/m^2 with the average UV intensity during the first set of trials calculated to be $37.2W/m^2$.

This procedure was repeated for the second set of trials but for these experiments the reservoir was insulated and placed onto a hotplate in order to increase the temperature to 45°C during irradiation. Samples were taken from the reservoir every 5 or 10 minutes. During this set of trials the global UV intensity measured was in the range 22.7 to $42.3W/m^2$ with an average calculated at $31.6W/m^2$.

For the third set of trials the reactor was kept in the dark with the reservoir insulated and once again placed on a hotplate. This dark environment ensured that temperature increase alone was the cause of bacterial inactivation. An initial sample was taken before the beginning of the experiment and then the heat was applied gradually, so as not to induce a thermal shock in the bacteria. When the required temperature was reached a second sample was taken and used to calculate the initial bacterial concentration (approximately $1x10^6CFU/ml$). Both samples were used as controls. Further samples from the reservoir were taken every fifteen minutes. Three different temperatures were investigated: 40°, 45° and 50°C. Water temperature measurements were made throughout all experiments with a thermocouple-based digital thermometer as described in Section 3.4.1 at the system's reservoir.

7.2.3   Results and Discussion

Solar Disinfection (UVA alone)

Data from the first set of trials using the small-scale Parabolic continuous flow solar reactor is presented in Figure 7.1, which shows the survival of bacteria within the reactor as a function of experimental time. In all experiments at least a 3-4-log reduction occurred within the 60-minute experimental time. In this case 60 minutes total experimental time equates to 12 minutes illumination time.
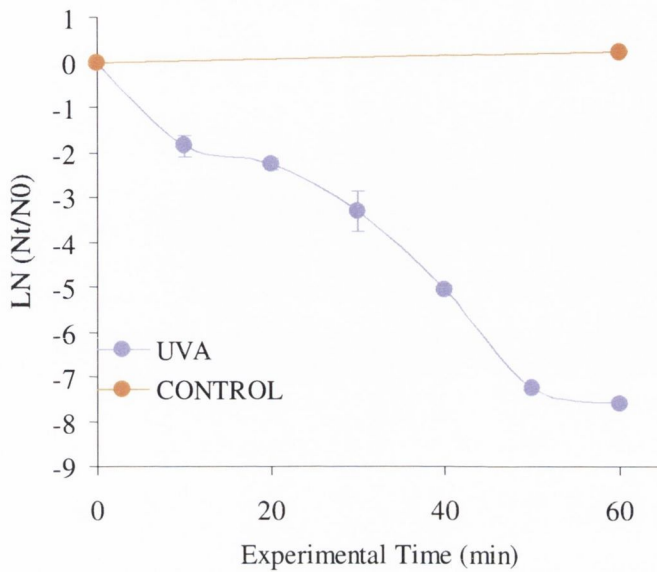
Figure 7.1: Inactivation of *E. coli* K-12 by UVA alone against experimental time with temperature ranging from 30-36°C.

The inactivation rate constant for UVA radiation alone was 0.19±0.08min^{-1} (95% CI), which equates to 1.02 (illuminated min)$^{-1}$. This result has been discussed previously in Section 5.3.3; it is included here for clarity.

Solar Disinfection with Addition of Heat (UVA + Temperature)

Data from the second set of trials is presented in Figure 7.2 above showing bacterial survival as a function of experimental time. In all experiments a 6-log reduction of bacteria occurred within the 60-minute experiment time, which once again equates to 12 minutes illumination time. The temperature was maintained at 45°C throughout the experiment. Inactivation rate constants were calculated to be 0.31±0.06min^{-1} (95% CI) or 1.57 (illuminated min)$^{-1}$. Comparing this result to the inactivation rate constants achieved using solar disinfection alone indicates that at this temperature there is a synergistic effect of radiation and temperature that enhances disinfection efficiency by 63%. The power of the difference between the two experiments was statistically shown to be 77%.

146
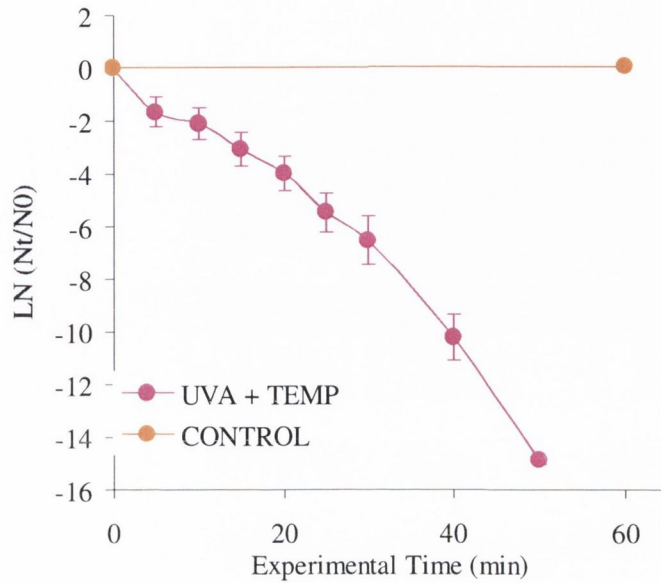
Figure 7.2: Inactivation of *E. coli* K-12 by UVA with temperature kept constant at 45°C.

The effect of the combination of both stress factors (UVA and temperature) can be seen clearly in Figure 7.3 below where the results for both sets of experiments are plotted as bacterial survival against UV dose, $Q_{a \text{ illum}}$ (kJ/litre). As discussed previously, the results above do not account for the fact that the solar intensity received by the reactor during the trials was changing constantly. This is taken into account by calculating the accumulated UV radiation dose by using Eq. 3.11 (Section 3.6.7).

Inactivation rate constants calculated using dose ($Q_{a \text{ illum}}$) are $32.0kJ^{-1}$ and $55.3kJ^{-1}$ for inactivation by UVA alone and UVA and temperature respectively. The standard deviation of intensity during the UVA alone trials was $2.33W/m^2$ with an average intensity of $37.19W/m^2$ while for the trials with an increase in temperature the average intensity was $32.63W/m^2$ with a standard deviation of $5.60 W/m^2$. When results are calculated in this way (by UVA dose) an enhancement of 72% for the system with temperature at 45°C is apparent. These results show that a dose of $0.04kJ_{UV}/litre$ was required to achieve 1-log reduction when temperature was increased to 45°C while a dose of $0.072kJ_{UV}/litre$ produced a 1-log reduction under normal temperature conditions.
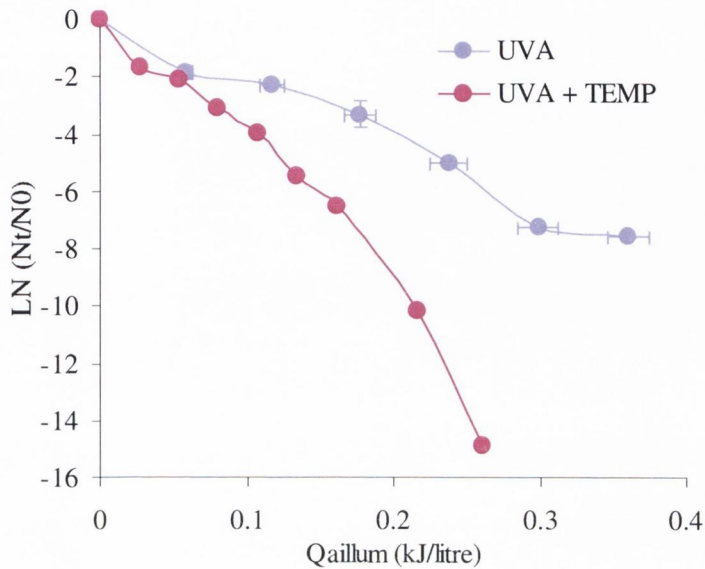
Figure 7.3: Survival of *E. coli* K-12 as a function of UV radiation dose, $Q_{a\ illum}$ (kJ/l).

These results indicate a clear advantage of increasing the temperature of the water to 45°C, which could be achieved by a concentrated reactor system using an oversized reflector. These results confirm the SODIS batch system theory where the synergistic effect of temperature and UVA can reduce exposure times by 4 hours (EAWAG). All major cellular components of gram (-) bacteria are affected by high temperatures, namely the outer cell layers, especially the outer membrane, proteins, enzymes, RNA and DNA. Thus extra stress is placed on the same cell components that are targeted by UVA. Some UV radiation repair-defective mutants of *E. coli* are also sensitive suggesting that synergistic systems could be more effective in causing inactivation of *E. coli* (Russell, 2003).

The Effect of Temperature on E.coli K-12

Figure 7.4 below shows the results of the third set of trials plotted as bacterial survival against experimental time for three separate temperatures, 40°, 45° and 50°C. Inactivation rate constants were calculated to be 0.046min^{-1} (R^2=0.9), 0.230min^{-1} (R^2=0.97) and 0.900min^{-1} for 40°, 45° and 50°C respectively.

148

This concurs with the previous results as an additional stress (UVA) increases the inactivation rate by 34% showing a clear synergistic effect between UVA and temperature at 45°C. After 1 hour at 40°C only 1-log removal was apparent whereas at 50°C a 6-log removal of *E. coli* K-12 was achieved in just 15 minutes.
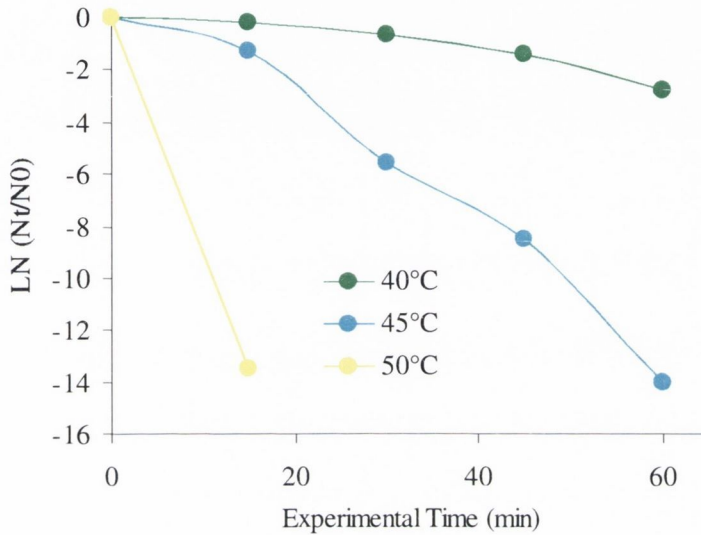
Figure 7.4: Inactivation of E.coli K-12 at 40°, 45° and 50°C

Safapour and Metcalf, (1999), reported complete inactivation of *E. coli* after 1 hour when temperatures reached 60°C in a batch solar disinfection system whereas lower temperatures have been reported for complete inactivation of *E. coli* (55°C) as well as other microorganisms such as *Vibrio cholera* (45°C) (EAWAG, 2005; Joyce *et al.*, 1996).

All results are summarised in Figure 7.5 and Table 7.1 below.

Experiment	$k_{Qa\,illum}$ (kJ^{-1})	k_Q (kJ^{-1})	k_t (min^{-1})	$k_{t\,illum.}$ (min^{-1})
UVA	32.0	2.1	0.19	1.02
UVA + 45°C	55.3	3.1	0.31	1.57
40°C	-	-	0.05	-
45°C	-	-	0.23	-
50°C	-	-	0.90	-

Table 7.1: Inactivation Rate constants calculated for experimental time, illumination time and dose, $Q_{a\,illum}$.
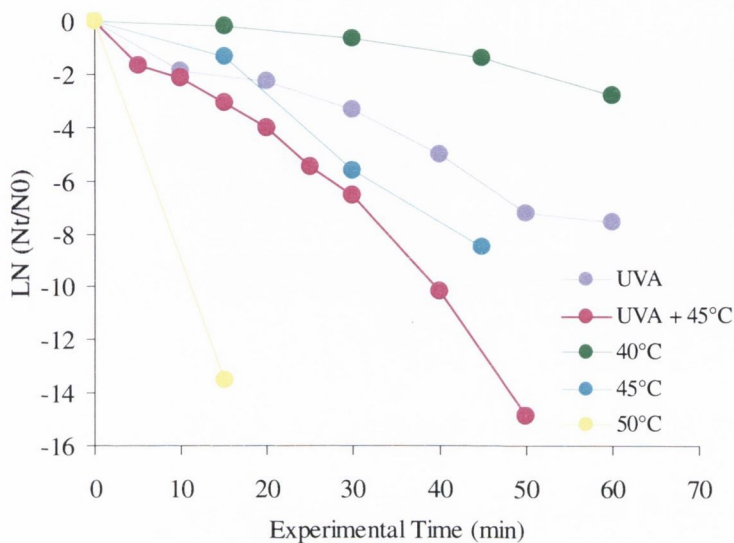
Figure 7.5: Comparison of *E. coli* K-12 inactivation at different temperatures.

These trials reveal a clear advantage of increasing temperature to at least 45°C in order to enhance the solar disinfection process. This confirms that while solar disinfection by UVA alone is a realistic process for use in countries with an abundance of sunlight, an optimised process incorporating this synergistic effect would be more efficient than a traditional solar disinfection system. Many systems have concentrated on the effect of increasing temperature (>65°) alone on pathogenic organisms (Simate, 2001; Safapour and Metcalf, 1998; Jorgenson *et al*., 1998) as discussed in Section 2.6.2. These results show that for a combined UVA and temperature system the temperature needs to increase to 45°C in order to demonstrate a synergistic effect. Hence, future research should be targeted on concentrating systems or insulated systems (Casalake *et al*., 2004) which promote increased temperatures within solar reactors.

7.3 Effect of Volume

7.3.1 Introduction

The objective of the following experiments is to assess the influence of volume on the solar disinfection process. During continuous flow experiments the solution is constantly recirculated between the reactor and the reservoir, which is effectively a dark zone. As the volume of the solution increases the amount of time the solution spends exposed to solar radiation is decreased.

7.3.2 Experimental Set-up

The experiments were carried out during June and July 2003 at Plataforma Solar de Almería, Spain using the small-scale Compound Parabolic reactor. At the beginning of each experiment the required volume (1litre or 0.4 litres) of filtered MilliQ water inoculated with *E. coli* K-12, was admitted into the reservoir. After this inoculation the water was circulated through the solar reactor tubes in the dark until a complete mix and a uniform concentration of bacteria was achieved throughout the reactor. The initial bacterial concentrations were approximately 1×10^6CFU/ml. At the start of each experiment a sample was taken at t=0 and the reactor was uncovered. This sample was enumerated and then kept in the dark as a control during the experiment. Samples were taken at 5 or 10 minute intervals and each experiment was repeated at least three times. Solar radiation measurements were taken as described in Section 3.4.2 and samples were enumerated as described in Section 3.6.4. The average intensity during the 0.4 litre experiments was 34.5W/m^2 (std. dev. 4.25), while during the 1 litre experiments was 37.2W/m^2 (std. dev. 2.33).

7.3.3 Results and Discussion

Representative data from the laboratory trials using the Compound Parabolic reactor and three different volumes of solution are presented in Figure 7.6. All plots show an average of at least four experiments.

All experiments showed at least a >4-log reduction of *E. coli* K-12 within the 60-minute experimental time. Inactivation rate constants were calculated according to the standard principles of disinfection kinetics as described in Section 3.6.
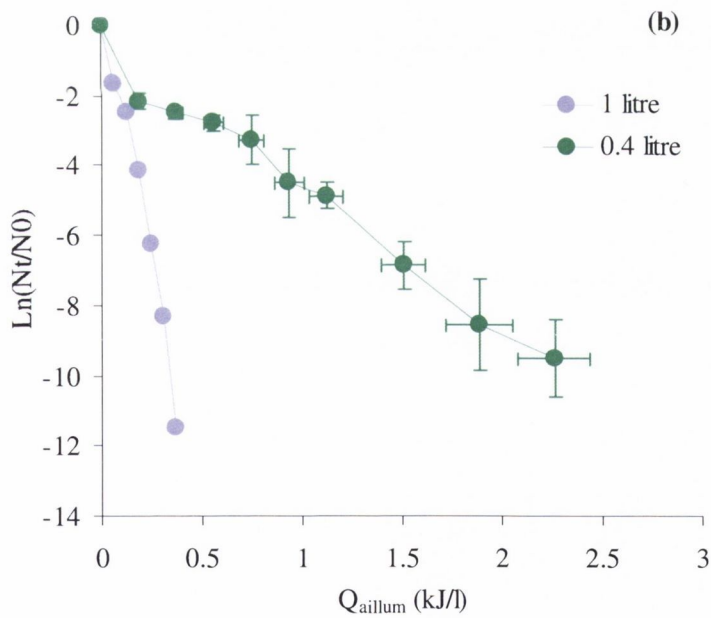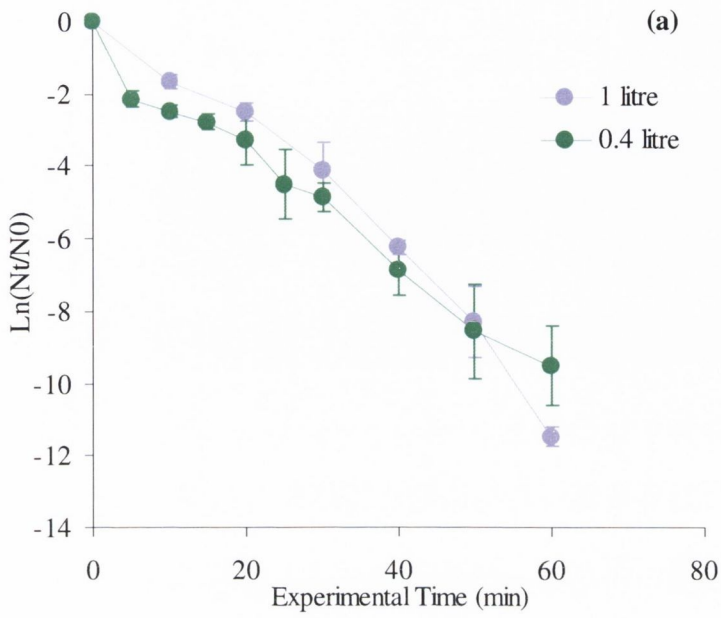
Figure 7.6: Comparison of two different volumes plotted as (a) inactivation of *E. coli* K-12 against experimental time (min) and (b) inactivation of *E. coli* K-12 against cumulative simulated solar UV dose, Q, (kJ/l).

The inactivation rate constant calculated for the 0.4 litre solution was $0.23min^{-1}$ (±0.17, 95% CI), with a rate constant of $0.25min^{-1}$ (±0.09, 95% CI) for the 1 litre solution. Inactivation rate constants were also calculated using the actual illumination time, as described in Section 3.6, as well as the cumulative simulated solar UV dose, Q as described in Section 3.6. These calculated inactivation rate constants are shown in Table 7.2 below.

Volume	$k_{Qa\ illum}$ (kJ^{-1})	k_Q (kJ^{-1})	k_t (min^{-1})	$k_{t illum.}$ (min^{-1})
1 litre	41.0	1.96	0.25	1.32
0.4 litre	6.23	1.98	0.23	0.45

Table 7.2: Inactivation Rate constants calculated for experimental time, illumination time and dose, $Q_{a\ illum}$.

When the results are assessed using experimental time very similar inactivation kinetics are apparent, however, when actual solar UV dose is considered there is a significant difference between the kinetics. The dose (calculated by absorber area and illumination time) required to achieve a 1-log reduction in the 1 litre sample was 0.056kJ/l whereas that required for a similar reduction in the 0.4 litre sample was 0.37kJ/l with calculated dose inactivation rate constants 41 $litre.kJ^{-1}$ and 6.23 $litre.kJ^{-1}$ respectively. Previous research concerned with volume effects has focused on batch process solar disinfection both with and without TiO_2 enhancement (Kehoe et al., 2001; Duffy et al, 2005). No significant difference was found with varying volumes of water, however during these batch experiment studies both volume of water and reactor size were reduced, while during these trials the reactor areas were kept constant and only the volume of contaminated water was varied.

The major difference between the two sets of experiments described above was the amount of time spent in the reservoir and fittings, effectively dark zones. The 0.4 litre sample spent significantly more experimental time exposed to solar radiation, 30 minutes (50%), while the 1 litre sample spent only 12 minutes (20%) of the total experimental time exposed. Figure 7.7 shows a plot of bacterial inactivation against illumination time.

It is evident from this plot and the calculated inactivation rate constants, 0.45 and $1.32min^{-1}$ for the 0.4 litre sample and 1 litre sample respectively, that the 1 litre system is more efficient.

153
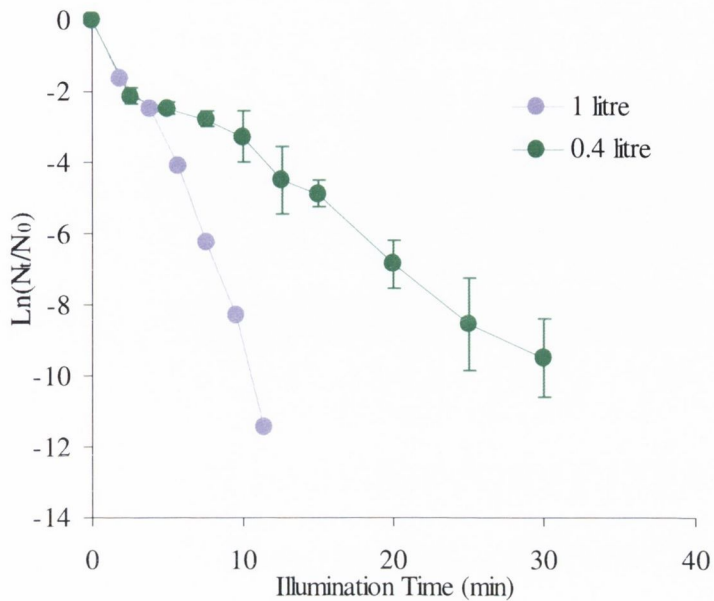
Figure 7.7: Comparison of two different volumes plotted as inactivation of *E.coli* K-12 against illumination time (min).

This suggests that there is possibly a photo effect that continues when the bacteria are in a dark phase (the reservoir in the case of the I litre sample). The effect of reactor components themselves (such as the pump) was investigated by a series of trials carried out in darkness, which showed no effect on bacteria. This suggests that there may be another mechanism involved in the solar disinfection process, which is dependent on both light and dark zones within the reactor as suggested in Section 5.7, and investigated in Section 8.

7.4   CONCLUDING REMARKS

There is a clear advantage on having increased temperatures within the solar disinfection reactor. The additional stress of water temperature at 45°C caused up to a 73% increase in the efficiency of the parabolic reactor.

The change in volume in the Compound Parabolic reactor caused a decrease in solar disinfection efficiency. This is predominantly due to the absence of a dark zone, which suggests that solar disinfection is not solely dose dependent and that possible other mechanisms could exist.

CHAPTER 8

THE STROBOSCOPIC MECHANISM

8.1 Introduction

The objective of the following experiments was to assess the effect of alternating illuminated and dark phases on the solar disinfection process. This was achieved by:

i.   Assessing the effect of introducing dark phases of various lengths into the batch solar disinfection process

ii. Assessing the effect of varying the ratio of illuminated phase and dark phases in batch process solar disinfection

iii. Assessing the effect of the introduction of illuminated and dark phases in the pilot-scale solar disinfection reactor.

8.2 Dark Phases in Batch Process Solar Disinfection

8.2.1 Introduction

The purpose of these experiments was to investigate the effect of introducing a dark phase into the batch solar disinfection process. The results discussed in Section 5.7 and Section 7.3 suggest that changing the illuminated area in a continuous flow reactor has an impact on the solar disinfection process, which is contrary to the expected results. Reduced illuminated areas ($1m^2$) produced more effective disinfection results per unit solar dose than larger areas ($3m^2$). This suggests that a dark phase in a solar disinfection reactor should lead to a beneficial effect on the solar disinfection process in terms of efficiency and hence the size of the reflector required in a full-scale solar disinfection system could be reduced with a consequential reduction in manufacturing cost. If such an effect exists it should also be apparent on the introduction of dark phases in batch process solar disinfection. It does not appear that other researchers have not explicitly studied this effect.

8.2.2 Experimental Set-up

During these experiments a one-litre bottle made of borosilicate glass (Duran$^©$) was filled with water and then inoculated with *E. coli* K-12 with an initial concentration of $1 \times 10^6 CFU/ml$. The bottles were then placed under the solar simulator and exposed for up to 5 hours. The simulated solar UV intensity was kept constant at $31.6 W/m^2$. Samples were taken at discrete time intervals and all experiments were repeated at least twice.

Experiments were carried out under four different illumination conditions, continuous illumination ($\diamond$), intermittent illumination of 4 seconds (4 $\diamond$) with 8-second dark

phases (8 ●), intermittent illumination of 4 seconds (4 ☼) with 16-second dark phases (16 ●), intermittent illumination of 4 seconds (4 ☼) with 32-second dark phases (32 ●). The shutter of the solar simulator was connected to a signal generator as described in Section 3.3.1 in order to create the four different regimes.

Control samples were left in the dark throughout all experiments to ensure inactivation was due to exposure to simulated solar radiation alone. The samples were enumerated as outlined in Section 3.6.4 and inactivation kinetics determined as described in Section 3.7.

8.2.3   Results and Discussion

Representative data from the laboratory trials using four different illumination regimes are presented in Figure 8.1. All plots show an average of at least two experiments.

From Figure 8.1(a) it can be seen that the most efficient illumination regime (when inactivation was plotted for experimental time) is the experiments carried out under continuous illumination. Calculated inactivation rate constants were calculated to be 0.069min^{-1} (±0.04, 95% CI), 0.023 min^{-1} (±0.002, 95% CI), 0.020 min^{-1} (±0.02, 95% CI) and 0.013 min^{-1} (±0.02, 95% CI), for the (☼), (4☼: 8●), (4☼: 16●) and (4☼: 32●) regimes respectively. These results would obviously agree with conventional solar disinfection theory i.e. the higher the solar dose the higher the rate of disinfection.

When these results are plotted against actual illumination time it seems that the experiments in which there were longer dark phases are more efficient per minute of illuminated time. Inactivation rate constants were calculated to be 0.069min^{-1}, 0.070 min^{-1}, 0.100 min^{-1} and 0.120 min^{-1}, for the (☼), (4☼: 8●), (4☼: 16●) and (4☼: 32●) regimes respectively. These results are summarised in Table 8.1 below along with the inactivation rate constants calculated for dose ($Q_{a\ illum}$).

Regime	$k_{Qa\ illum}$ (l.kJ^{-1})	k_Q (l.kJ^{-1})	k_t (min^{-1})	$k_{t illum.}$ (min^{-1})
☼	2.32	2.32	0.07	0.07
4☼ : 8●	2.35	0.78	0.02	0.07
4☼ : 16●	3.32	0.66	0.02	0.10
4☼ : 32●	3.86	0.43	0.01	0.12

Table 8.1: Inactivation rate constants calculated for different illumination regimes based on dose $Q_{a\ illum}$, experimental time and actual illumination time.
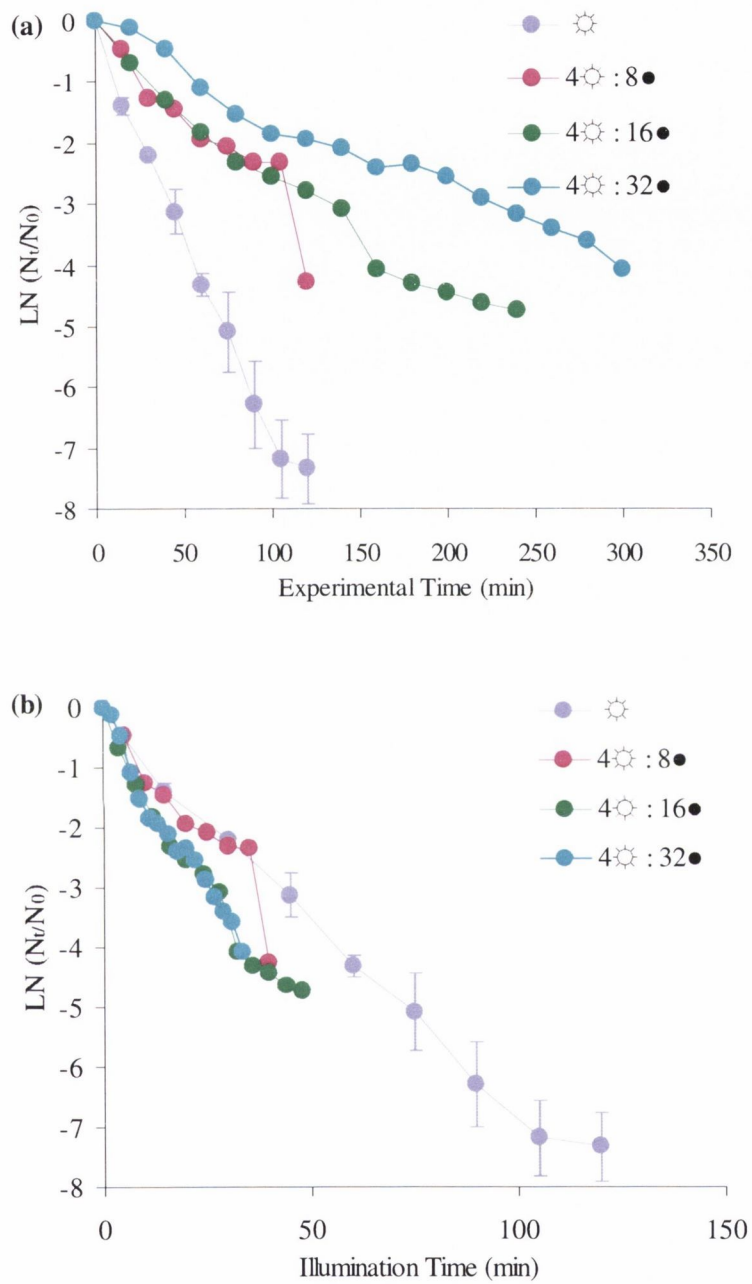
Figure 8.1: Comparison of four different illumination regimes plotted as (a) inactivation of *E. coli* K-12 against experimental time and (b) inactivation of *E. coli* K-12 against actual illumination time. Note: error bars are only shown on one line for clarity.

Simulated solar UV doses required to achieve 1-log inactivation were calculated for each illumination regime based on $Q_{a\ illum}$. The dose required to achieve 1-log inactivation calculated for the continuously illuminated sample ($\lozenge$) was 0.99kJ/l, whereas a similar dose of 0.97kJ/l was required for samples during the (4$\lozenge$: 8$\bullet$) regime. The experiments that had longer dark phases required only 0.69kJ/l and 0.6kJ/l ((4$\lozenge$: 16$\bullet$) and (4$\lozenge$: 32$\bullet$) respectively). The results are presented in Figure 8.2 below.
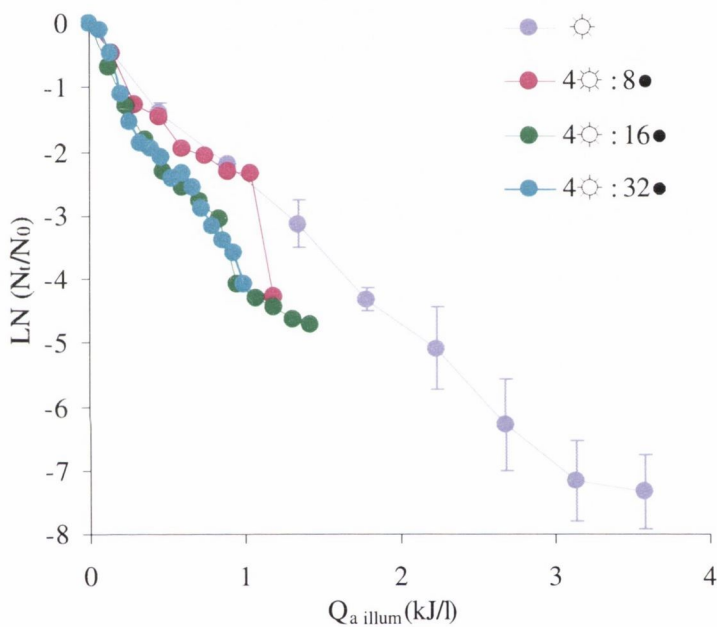
Figure 8.2: Comparison of four different illumination regimes plotted as inactivation of *E. coli* K-12 against Cumulative simulated solar UV dose, $Q_{a\ illum}$.

These results suggest that a mechanism of inactivation may be taking place which continues in a dark phase. The interruption of illumination has been investigated with conflicting results; intermittent illumination has been reported to reduce *B. pumilus* spores and MS2 bacteriophage more effectively than continuous exposure to UV radiation (Pham *et al.*, 1995; Laot *et al.*, 1999) but *Bacteriodies fragilis* requires more illumination time when exposed to intermittent illumination (Laot *et al.*, 1999). The main advantage of this mechanism is that the solar disinfection reactor would require less reflective material (i.e. more dark zones).

8.3 Illuminated-Dark Ratio in Batch Process Solar Disinfection

8.3.1 Introduction

The purpose of these experiments was to investigate the effect of introducing a variety of different illumination regimes with relatively short illuminated or dark phases into the batch solar disinfection process. Illuminated phases consisted of short bursts of between 1 and 4 seconds with intervening dark periods. These experiments were also carried out using batch process solar disinfection under simulated solar radiation.

8.3.2 Experimental Set-up

During these experiments a one-litre bottle made of borosilicate glass (Duran©) was filled with water and then inoculated with *E. coli* K-12 with an initial concentration of 1×10^4 CFU/ml. The bottles were then placed under the solar simulator and exposed for up to 6 hours. The simulated solar UV intensity was kept constant at 31.6W/m^2. Samples were taken at discrete time intervals and all experiments were repeated at twice.

Experiments were carried out initially under four different illumination conditions, continuous illumination (☼), intermittent illumination of 1 second with 1-second dark phases (1☼: 1●), intermittent illumination of 2 seconds with 2-second dark phases (2☼: 2●) and intermittent illumination of 4 seconds with 4-second dark phases (4☼: 4●). During each regime the total illumination was kept at one half of the total experimental time.

Second sets of experiments were carried out with illumination time being a total of one third of the total experimental time. Experiments were carried out under three different illumination conditions, continuous illumination (☼), intermittent illumination of 1 second with 2-second dark phases (1☼: 2●) and intermittent illumination of 2 seconds with 4-second dark phases (2☼: 4●).

The shutter of the solar simulator was connected to a signal generator as described in Section 3.4.1 in order to create the different regimes.

Control samples were left in the dark throughout all experiments to ensure inactivation was due to exposure to simulated solar radiation alone. The samples were enumerated as outlined in Section 3.6.4 and inactivation kinetics determined as described in Section 3.7.

8.3.3 Results and Discussion

Representative data from the laboratory trials using four different illumination regimes are presented in Figure 8.3. All plots show an average of at least two experiments.

From Figure 8.3(a) it can be seen that when the results are plotted as inactivation against experimental time the continuous illumination regime seems to be most efficient in terms of solar disinfection with a calculated inactivation rate constant of $0.033 min^{-1}$. The intermittent regimes were less efficient with a calculated inactivation rate constant of $0.02 min^{-1}$ for all regimes. When these results are plotted against actual illumination time the order of efficiency of the experiments was intermittent illumination of (4☼: 4●), (2☼: 2●) with both (☼) and the (1☼: 1●) being least efficient. Inactivation rate constants were calculated to be $0.033 min^{-1}$ (±0.01, 95% CI), $0.032 min^{-1}$ (±0.0002, 95% CI), $0.040 min^{-1}$ (±0.003, 95% CI) and $0.050 min^{-1}$ (±0.01, 95% CI), for the (☼), (1☼: 1●), (2☼: 2●) and (4☼: 4●) regimes respectively. These results are summarised in Table 8.2 below along with the inactivation rate constants calculated for dose ($Q_{a\ illum}$).

Regime	$k_{Qa\ illum}$ $(l.kJ^{-1})$	k_Q $(l.kJ^{-1})$	k_t (min^{-1})	$k_{t\ illum.}$ (min^{-1})
☼	1.11	1.11	0.03	0.03
1☼ : 1●	1.15	0.57	0.02	0.03
2☼ : 2●	1.33	0.67	0.02	0.04
4☼ : 4●	1.51	1.23	0.02	0.05

Table 8.2: Inactivation rate constants calculated for different illumination regimes based on dose $Q_{a\ illum}$, experimental time and actual illumination time.

Simulated solar UV doses required to achieve 1-log inactivation were calculated for each illumination regime based on $Q_{a\ illum}$. The dose required to achieve 1-log inactivation calculated for the (☼) sample was 2.07kJ/l, whereas a similar dose of 2.01kJ/l was required for samples illuminated under the (1☼: 1●) regime. The experiments that had longer dark phases required only 1.53kJ/l and 1.72kJ/l ((4☼: 4●) and (2☼: 2●) respectively).
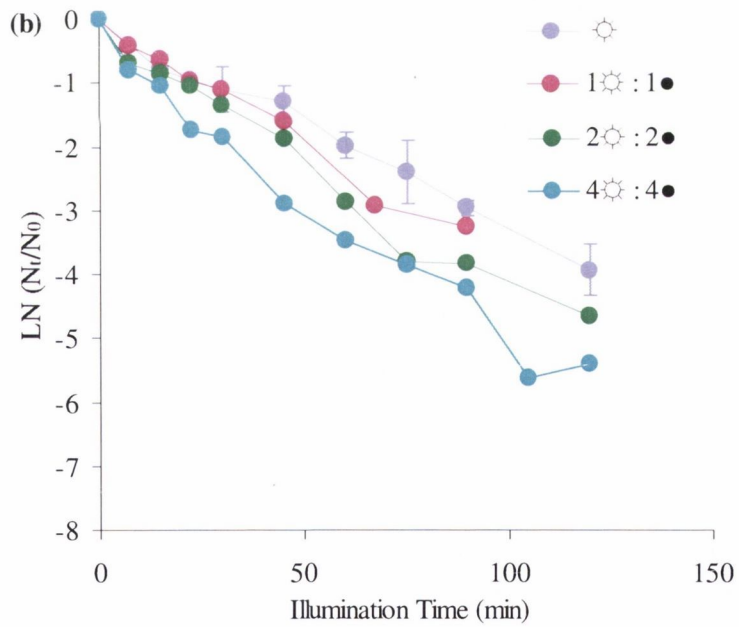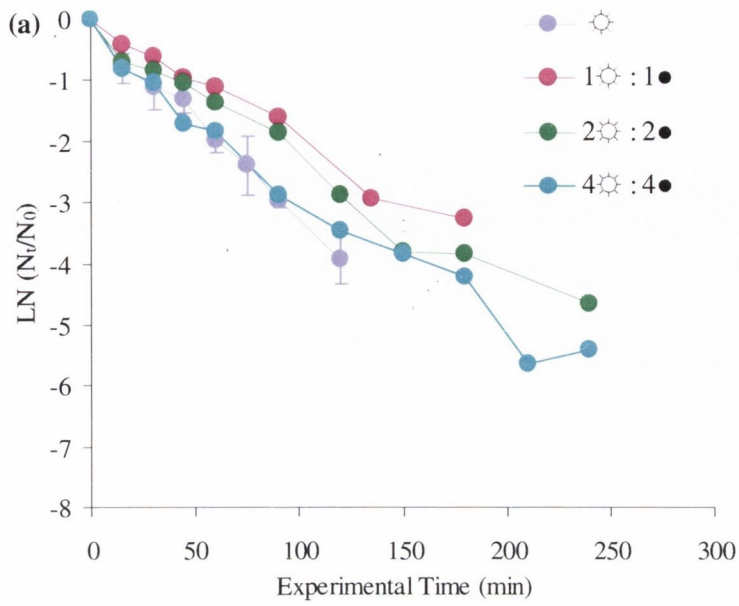
Figure 8.3: Comparison of batch process solar disinfection subjected to four different illumination regimes plotted as (a) inactivation of *E. coli* K-12 against experimental time and (b) inactivation of *E. coli* K-12 against actual illumination time.
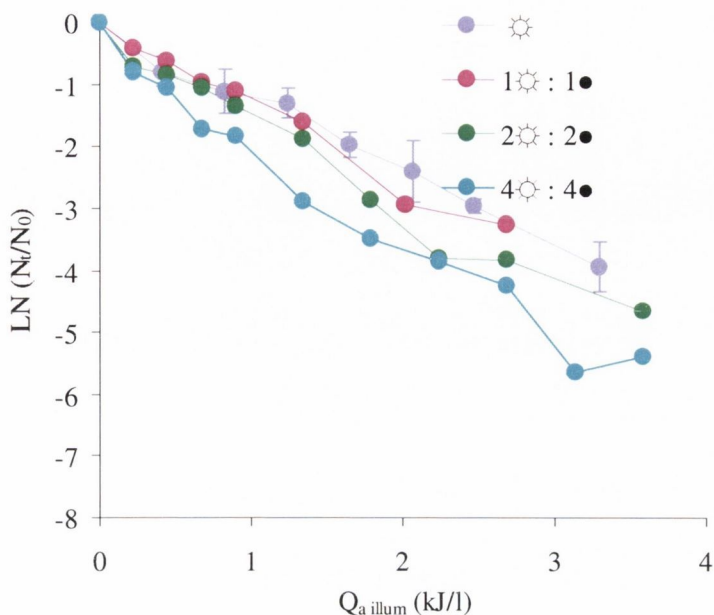
Figure 8.4: Comparison of four different illumination regimes plotted as inactivation of *E. coli* K-12 against cumulative simulated solar UV dose, $Q_{a\ illum}$.

These results suggest that the intermittent regimes are more efficient than a system that is exposed continually to solar radiation. The (1☼: 1●) regime promoted almost the same disinfection kinetics as that for continuous radiation suggesting that either the "flash" was too short for the bacteria to be affected by this mechanism i.e. that this 1 second dark period was so short that it approximated a continuous illumination regime. Representative data from the laboratory trials using the second three illumination regimes are presented in Figure 8.5. All plots show an average of at least two experiments.

From Figure 8.5(a) it can be seen that when the results are plotted as inactivation against experimental time, the (☼) regime seems to be most efficient in terms of solar disinfection with a calculated inactivation rate constant of 0.033min⁻¹. The intermittent regimes were less efficient with a calculated inactivation rate constant of 0.014min⁻¹ for the (1☼: 2●) regime and 0.015min⁻¹ for the (2☼: 2●).
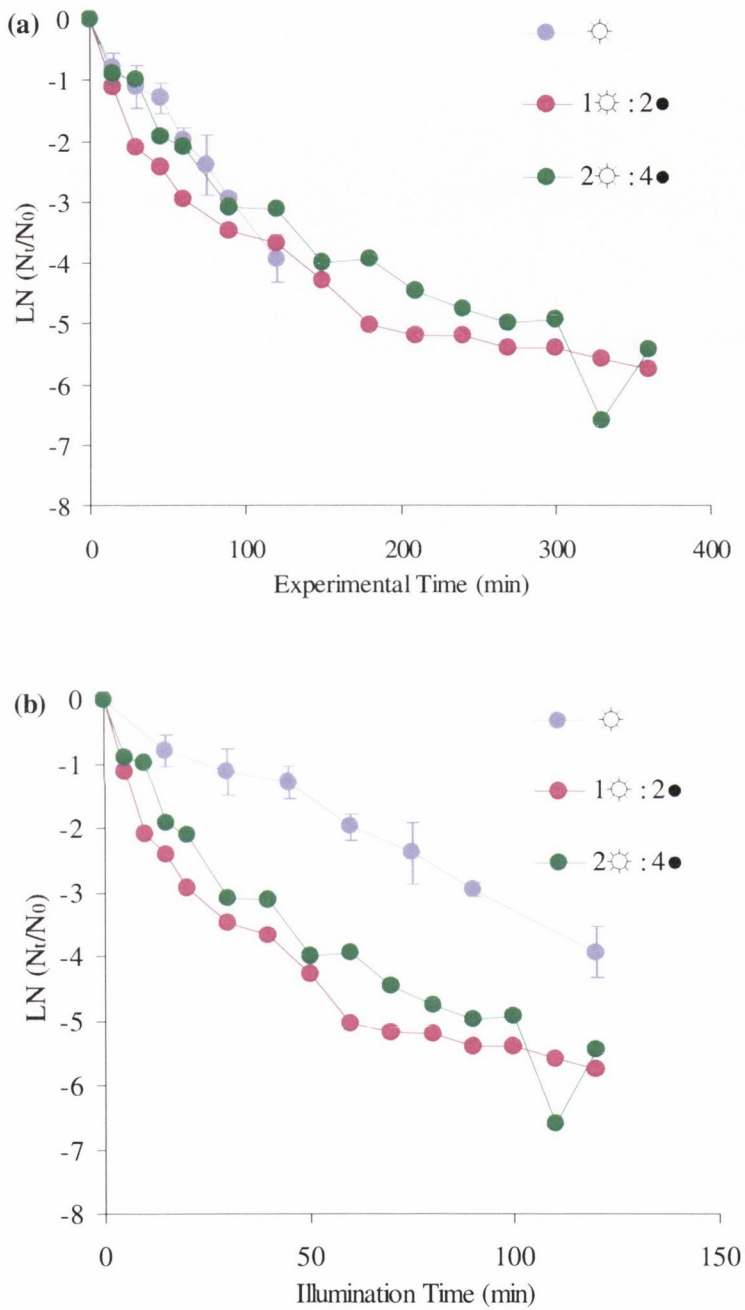
Figure 8.5: Comparison of batch process solar disinfection subjected to three different illumination regimes plotted as (a) inactivation of *E. coli* K-12 against experimental time and (b) inactivation of *E. coli* K-12 against actual illumination time.

When these results are plotted against actual illumination time the order of efficiency of the experiments once again changes with the intermittent illumination experiments performing better. Inactivation rate constants were calculated to be 0.033min^{-1} (±0.01, 95% CI), 0.04 min^{-1} (±0.0006, 95% CI) and 0.045 min^{-1} (±0.0027, 95% CI) for the (☼), (1☼: 2●) and (2☼: 4●) regimes respectively. These results are summarised in Table 8.3 below along with the inactivation rate constants calculated for dose ($Q_{a\,illum}$).

Regime	$k_{Qa\,illum}$ $(l.kJ^{-1})$	k_Q $(l.kJ^{-1})$	k_t (min^{-1})	$k_{tillum.}$ (min^{-1})
☼	1.11	1.11	0.03	0.03
1☼ : 2●	1.37	0.46	0.01	0.04
2☼ : 4●	1.49	0.49	0.02	0.05

Table 8.3: Inactivation rate constants calculated for different illumination regimes based on dose $Q_{a\,illum}$, experimental time and actual illumination time.

Simulated solar UV doses required to achieve 1-log inactivation were calculated for each illumination regime based on $Q_{a\,illum}$. The dose required to achieve 1-log inactivation calculated for the (☼) sample was 2.07kJ/l, whereas a dose of 1.68kJ/l was required for samples illuminated for (1☼: 2●). The experiments which were carried out with the (2☼: 4●) regime had a calculated inactivation rate constant of 1.49l/kJ and required only 1.55kJ/l to achieve 1-log inactivation.

These results suggest that the intermittent regimes are more efficient than a system that is exposed continually to solar radiation. The (2☼: 4●) regime promoted the most efficient disinfection kinetics of the three illumination regimes, 1.3 times more efficient than the (☼) sample. The (1☼: 2●) regime proved to be 1.2 times as efficient as the (☼) sample. In theory intermittent regimes should promote more efficient inactivation kinetics in all types of solar disinfection processes not just batch process solar disinfection on which these trials are based. The effect of intermittent illumination on continuous flow solar disinfection is explored in the next section.
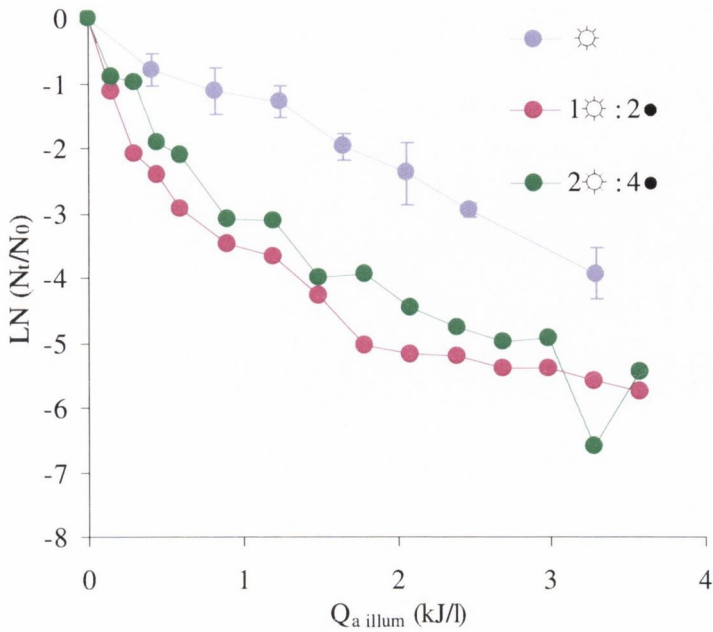
Figure 8.6: Comparison of three different illumination regimes plotted as inactivation of *E. coli* K-12 against cumulative simulated solar UV dose, $Q_{a\ illum}$.

8.4 Intermittent Illumination and Continuous Flow Solar Disinfection

8.4.1 Introduction

The purpose of these experiments was to investigate the effect of introducing a variety of different illumination regimes with relatively short illuminated or dark phases into the continuous flow solar disinfection process. The pilot scale solar continuous flow reactor at PSA (as described in Section 3.3.3) was used in a number of configurations with $1.5m^2$ and $1m^2$ of the reactor exposed at any one time. These experiments were carried out at PSA during June 2004.

8.4.2 Experimental Set-up

During these experiments 35 litres of distilled water was inoculated with *E. coli* K-12 in a concentration of $1 \times 10^4 CFU/ml$ and admitted into the reactor. The reactor was kept completely covered for ten minutes to ensure a complete mix was achieved and uniform concentrations of bacteria existed in the reactor. Sampling was carried out every 5

minutes with controls left in the dark throughout the experiments to ensure inactivation was due to exposure to simulated solar radiation alone. The samples were enumerated as outlined in Section 3.6.4 and inactivation kinetics determined as described in Section 3.7.

Two separate sets of experiments were carried out, one set using $1.5m^2$ of reactor and one using $1m^2$ of reactor. Four systems of "flashes" were set up in the reactor for each set of experiments by covering parts of the reactor in black plastic in order to introduce dark phases. Figures 8.7 and 8.8 show the reactor configurations for the $1.5m^2$ and $1m^2$ reactor configurations. The "flashes" ranged for 1 second to 15 seconds and are described in Table 8.4 below. The time spent in the reservoir was not included as a flash as this was common to all experiments. The flowrate was kept constant at 20l/min in all experiments. The time spent in the reservoir was not included as a flash as this was common to all experiments (Table 8.4).

Area	Regime	Light (secs)	Dark (secs)	Nr. of Flashes	Reservoir (secs)
$1.5m^2$	☼	34.0	34.0	1	38.0
	2.8☼ : 2.8●	2.8	2.8	12	38.0
	5.7☼ : 5.7●	5.7	5.7	6	38.0
	8.5☼ : 8.5●	8.5	8.5	4	38.0
$1m^2$	☼	22.7	45.3	1	38.0
	2.8☼ : 5.7●	2.8	5.7	8	38.0
	0.9☼ : 1.9●	0.9	1.9	24	38.0
	7.6☼ : 15.1●	7.6	15.1	3	38.0

Table 8.4: Intermittent Illumination regimes for the pilot-scale reactor.
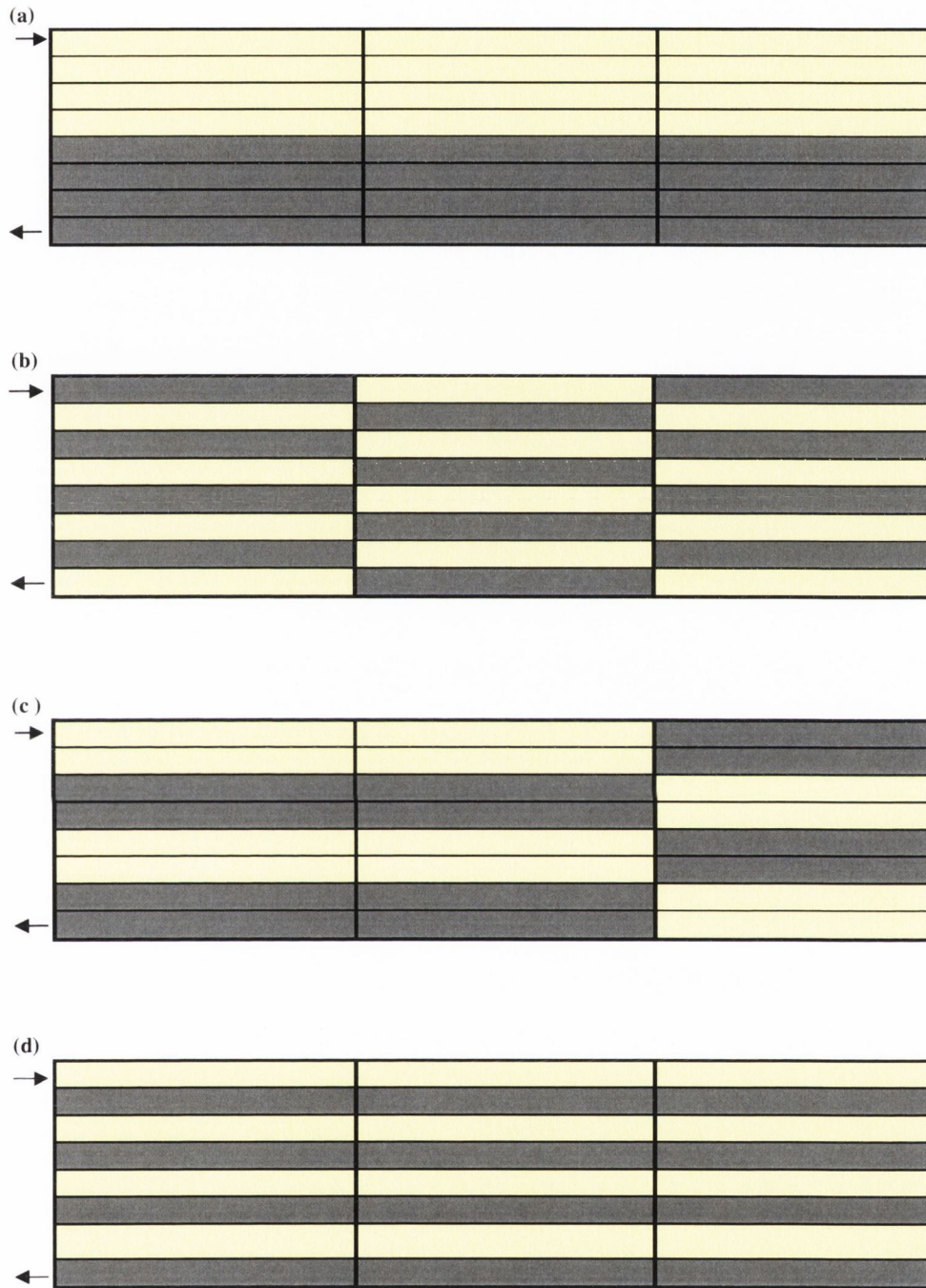
Figure 8.7: Pilot-scale reactor configurations for the 1.5m^2 experiments (yellow=light, grey=dark). Regime (a) (34☼: 34●)[☼], (b) (2.8☼: 2.8●), (c) (5.7☼: 5.7●) and (d) (8.5☼: 8.5●).
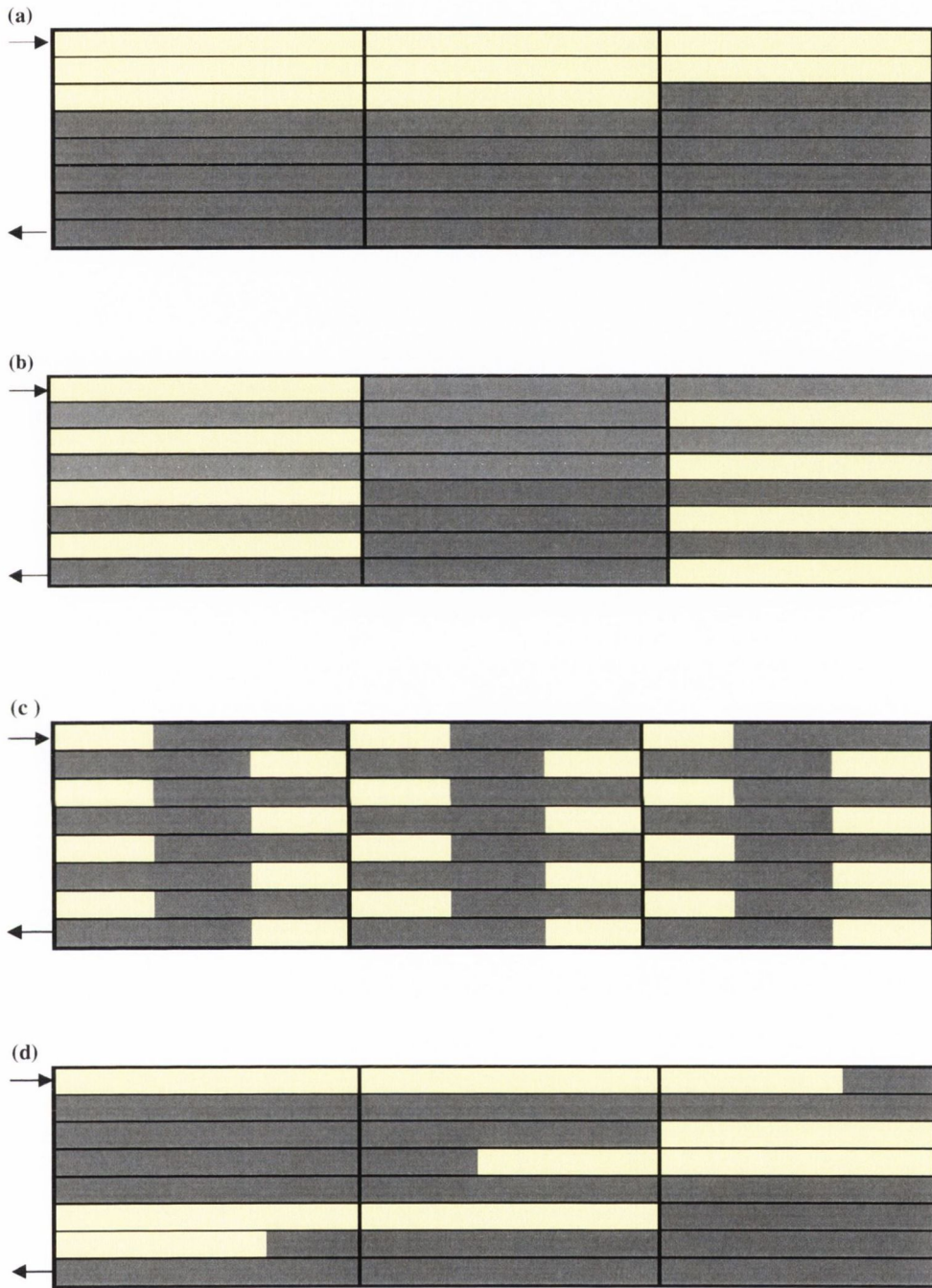
Figure 8.8: Pilot-scale reactor configurations for the $1m^2$ experiments (yellow=light, grey=dark). Regime (a) (22.7☼: 45.3●) [☼], (b) (2.8☼: 5.7●), (c) (0.9☼: 1.9●) and (d) (7.6☼: 15.1●).

8.4.3   Results and Discussion

Representative data from the laboratory trials using four different illumination regimes and $1.5m^2$ of reactor are presented in Figures 8.9 and 8.10. All plots show an average of at least two experiments.

From Figure 8.9(a) it can be seen that when the results are plotted as inactivation against experimental time the $(2.8\unicode{x263C}: 2.8\bullet)$ regime (as described in Figures 8.7 (b)) seems to be most efficient in terms of solar disinfection with a calculated inactivation rate constant of $0.16min^{-1}$. The $(8.5\unicode{x263C}: 8.5\bullet)$ regime, (c), was least efficient with a calculated inactivation rate constant of $0.066min^{-1}$ with the $(\unicode{x263C})$, (a), and $(5.7\unicode{x263C}: 5.7\bullet)$, (c), being in the middle with calculated inactivation rate constants of $0.075min^{-1}$ and $0.11min^{-1}$ respectively. This order of efficiency was preserved when the results were plotted as inactivation of *E. coli* K-12 against illumination time (Figure 8.9(b)). Inactivation rate constants were calculated to be $0.233min^{-1}$ (±0.01, 95% CI), $0.514\ min^{-1}$ (±0.001, 95% CI), $0.33\ min^{-1}$ (±0.01, 95% CI) and $0.205\ min^{-1}$ (±0.01, 95% CI), for the $(\unicode{x263C})$, $(2.8\unicode{x263C}: 2.8\bullet)$, $(5.7\unicode{x263C}: 5.7\bullet)$ and $(8.5\unicode{x263C}: 8.5\bullet)$ regimes respectively.

These results are summarised in Table 8.5 below along with the inactivation rate constants calculated for dose ($Q_{a\ illum}$) and dose (Q_a).

Regime	$k_{Qa\ illum}$ $(l.kJ^{-1})$	k_{Qa} $(l.kJ^{-1})$	k_Q $(l.kJ^{-1})$	k_t (min^{-1})	$k_{t\ illum.}$ (min^{-1})
$\unicode{x263C}$	7.72	2.47	0.80	0.08	0.23
$2.8\unicode{x263C}: 2.8\bullet$	16.09	5.15	1.67	0.16	0.51
$5.7\unicode{x263C}: 5.7\bullet$	11.56	3.70	1.20	0.11	0.33
$8.5\unicode{x263C}: 8.5\bullet$	6.71	2.14	0.70	0.07	0.21

Table 8.5: Inactivation rate constants calculated for different illumination regimes based on dose $Q_{a\ illum}$ and Q_a, experimental time and actual illumination time.

Simulated solar UV doses required to achieve 1-log inactivation were calculated for each illumination regime based on $Q_{a\ illum}$. The dose required to achieve 1-log inactivation calculated for the $(\unicode{x263C})$ sample was 0.30kJ/l, whereas a dose of 0.14kJ/l was required for the $(2.8\unicode{x263C}: 2.8\bullet)$ regime, which consisted of the shortest flash time. The $(5.7\unicode{x263C}: 5.7\bullet)$ and $(8.5\unicode{x263C}: 8.5\bullet)$ regimes required 0.20kJ/l and 0.34kJ/l of solar radiation respectively in order to achieve results. Therefore the $(2.8\unicode{x263C}: 2.8\bullet)$ regime seemed to promote the most efficient results. These results are shown in Figure 8.9(b) along with results plotted for dose calculated as Q_a, (a).
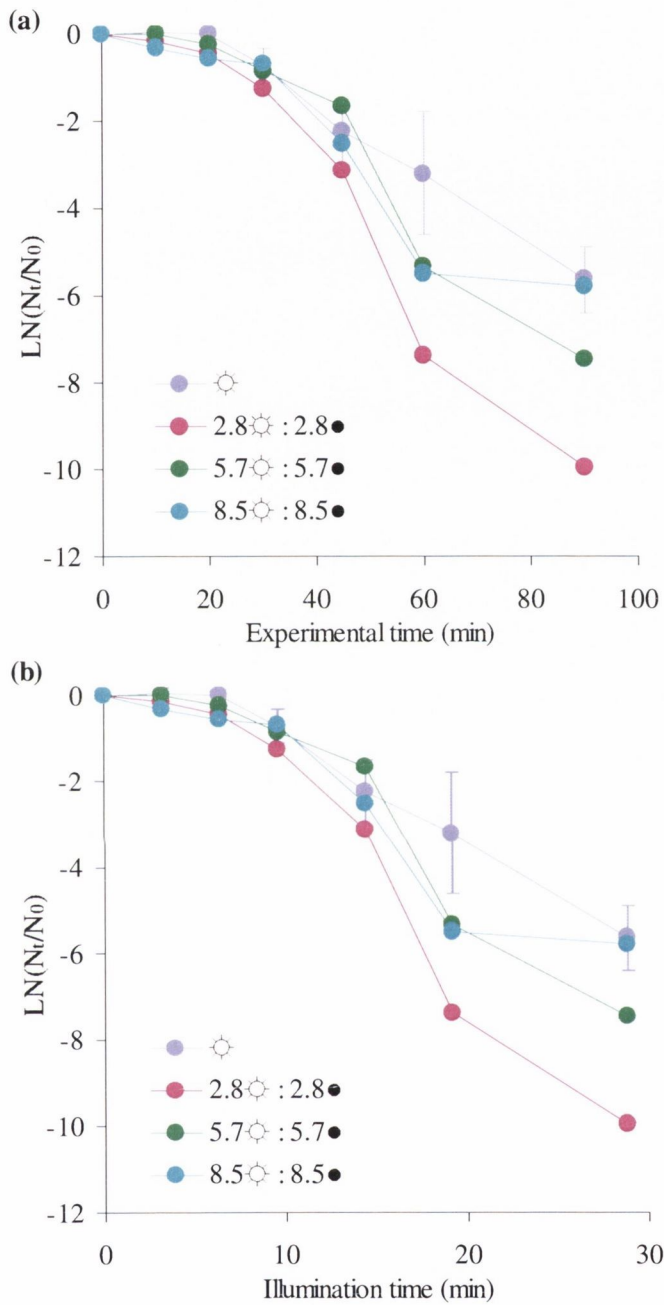
Figure 8.9: Comparison of continuous flow solar disinfection subjected to four different illumination regimes plotted as (a) inactivation of *E. coli* K-12 against experimental time and (b) inactivation of *E. coli* K-12 against actual illumination time, for the 1.5m^2 reactor.
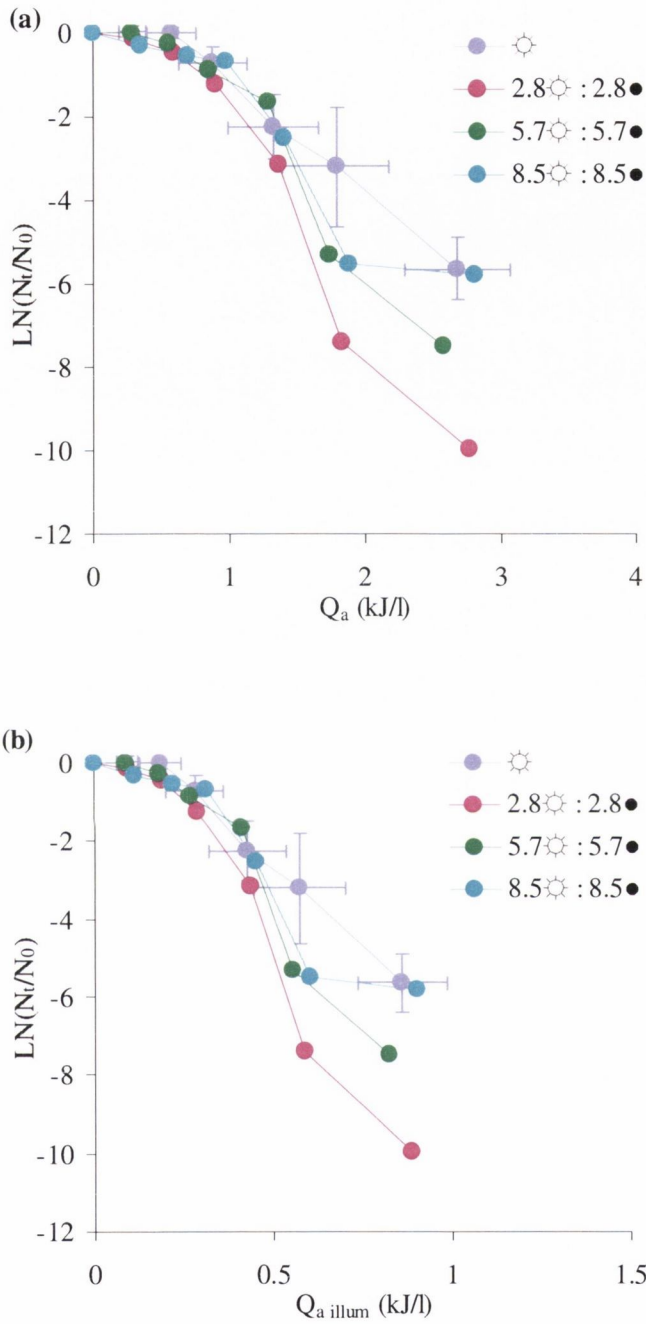
Figure 8.10: Comparison of continuous flow solar disinfection subjected to four different illumination regimes plotted as (a) inactivation of *E. coli* K-12 against Q_a and (b) inactivation of *E. coli* K-12 against $Q_{a\,illum}$, for the 1.5m^2 reactor.

These results agree with Section 8.2 where intermittent illumination over the 1.5m^2 area promoted more efficient solar disinfection than a continuously illuminated 1.5m^2 area reactor. From these results it seems that the shorter the "flash" period the more effect the intermittent illumination has on the disinfection process, the 2.83 second "flash" producing the most efficient results.

These experiments were repeated using a 1m^2 illuminated area and varying intermittent illumination regimes as described in Table 8.4. The results are presented in Figures 8.11 and 8.12 below. Inactivation rate constants were calculated for experimental time, illumination time, Q_a and $Q_{a\,illum}$ and are presented in Table 8.6 below.

Regime	$k_{Qa\,illum}$ (l.kJ^{-1})	k_Q (l.kJ^{-1})	k_t (min^{-1})	$k_{t\,illum.}$ (min^{-1})
☼	27.95	1.94	0.11	0.53
2.8☼ : 5.7●	34.57	2.40	0.13	0.61
0.9☼ : 1.9●	52.62	3.70	0.21	0.97
7.6☼ : 15.1●	35.43	2.50	0.15	0.71

Table 8.6: Inactivation rate constants calculated for different illumination regimes based on dose $Q_{a\,illum}$ and Q_a, experimental time and actual illumination time.

From Figure 8.11(a) it can be seen that when the results are plotted as inactivation against experimental time the (0.9☼: 1.9●) regime (as described in Figure 8.7 (c)) seems to be most efficient in terms of solar disinfection with a calculated inactivation rate constant of 0.207min^{-1}. The (☼) regime which consisted of 1m^2 of continuous illumination was least efficient with a calculated inactivation rate constant of 0.114min^{-1} with the (2.8☼: 5.6●),(b) and (7.5☼: 15.1●), (d) being in the middle with calculated inactivation rate constants of 0.13min^{-1} and 0.15min^{-1} respectively. This order of efficiency was preserved when the results were plotted as inactivation of *E. coli* K-12 against illumination time (Figure 8.11 (b)). Inactivation rate constants were calculated to be 0.53min^{-1}(±0.06, 95% CI), 0.61 min^{-1} (±0.18, 95% CI), 0.97 min^{-1} (±0.05, 95% CI) and 0.71 min^{-1} (±0.18, 95% CI), for the (☼), (2.8☼: 5.7●), (0.9☼: 1.9●) and (7.6☼: 15.1●) regimes respectively. These results are summarised in Table 8.6 above along with the inactivation rate constants calculated for dose ($Q_{a\,illum}$) and dose (Q_a).
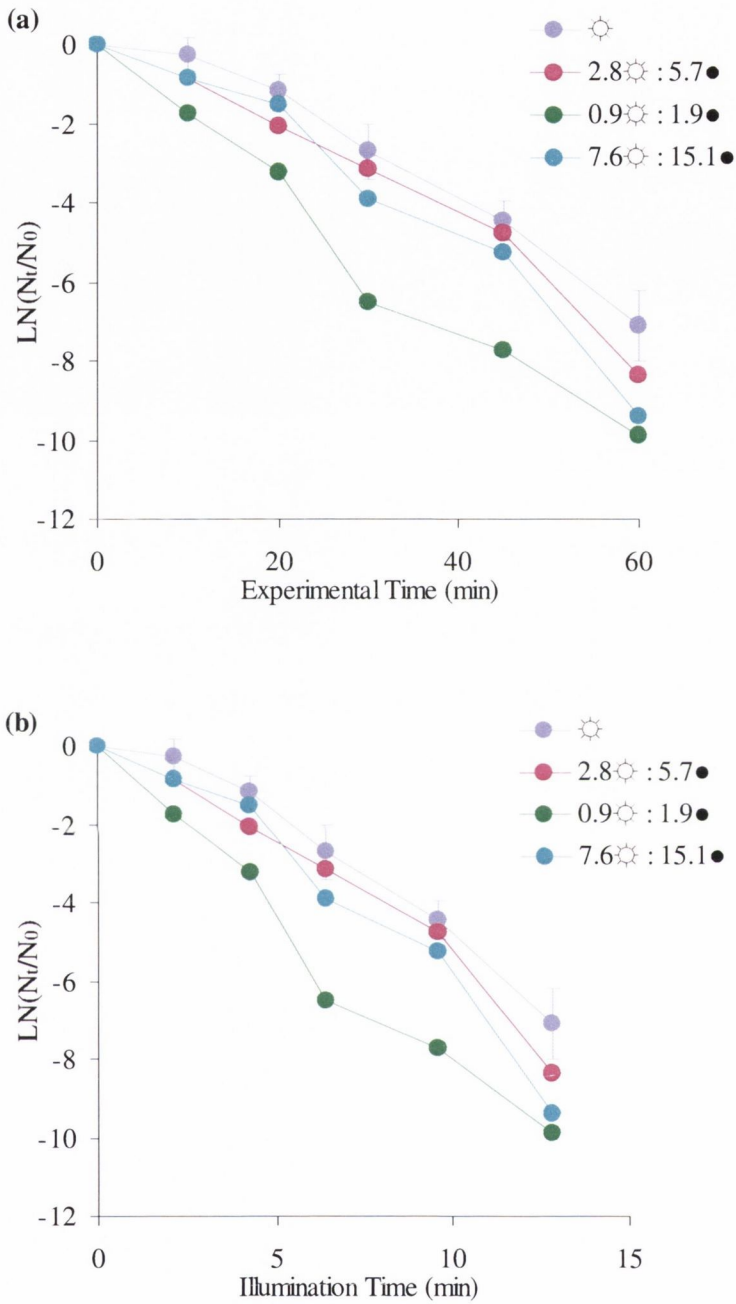
Figure 8.11: Comparison of continuous flow solar disinfection subjected to four different illumination regimes plotted as (a) inactivation of *E. coli* K-12 against experimental time and (b) inactivation of *E. coli* K-12 against actual illumination time, for the 1m^2 reactor.
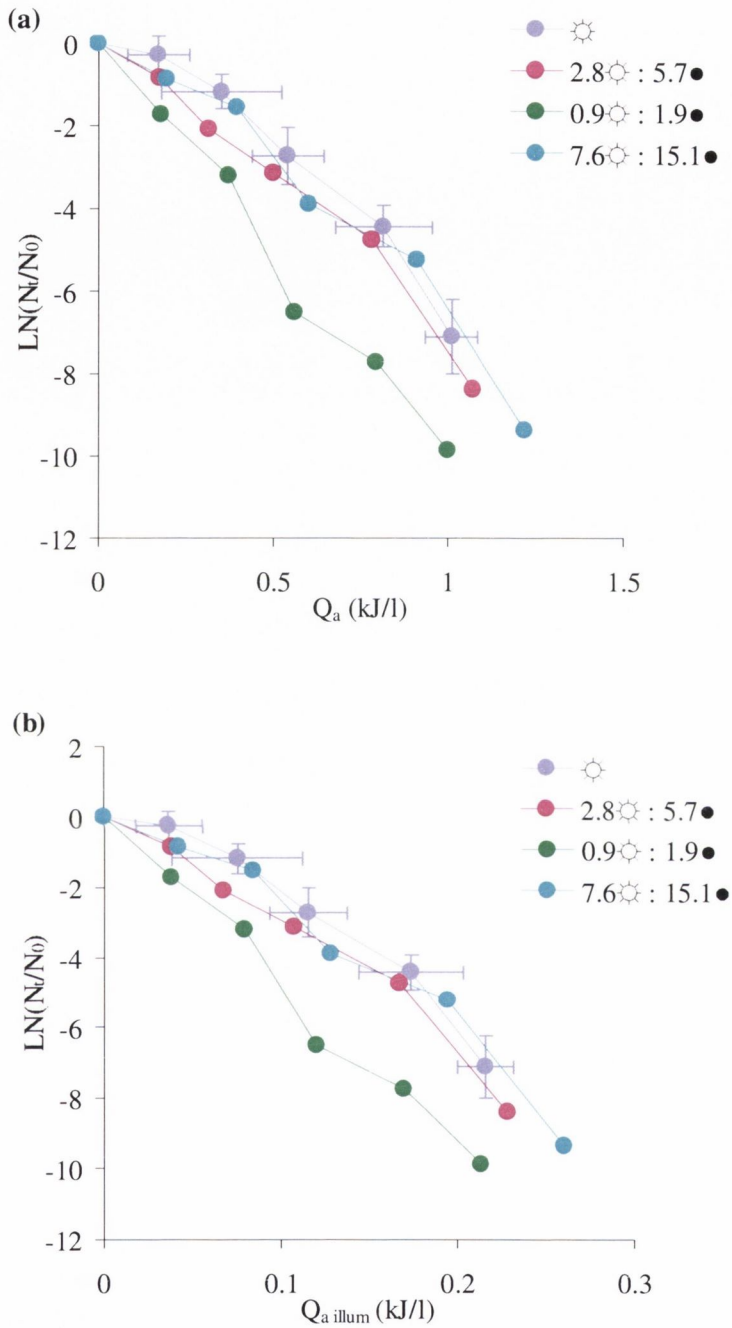
Figure 8.12: Comparison of continuous flow solar disinfection subjected to four different illumination regimes plotted as (a) inactivation of *E. coli* K-12 against Q_a and (b) inactivation of *E. coli* K-12 against $Q_{a\ illum}$, for the $1m^2$ reactor.

Simulated solar UV doses required to achieve 1-log inactivation were calculated for each illumination regime based on $Q_{a\ illum}$. The dose required to achieve 1-log inactivation calculated for the (☼) sample was 0.39kJ/l, whereas a dose of 0.205kJ/l was required for illumination regime (0.9☼: 1.9●), which consisted of the shortest flash time. Regimes (2.8☼: 5.7●) and (7.6☼: 15.1●) both required 0.31kJ/l of solar radiation in order to achieve similar results. Therefore the (0.9☼: 1.9●) regime seemed to promote the most efficient results. These results are shown in Figure 8.12(b) along with results plotted for dose calculated as Q_a, (Figure 8.1(a)).

These results agree with the previous sections where intermittent illumination promoted more efficient solar disinfection than a continuously illuminated sample. From these results it also seems that the shorter the "flash" period the more effect the intermittent illumination has on the disinfection process, the 1 second "flash" producing the most efficient results.

It is interesting to note that experiments carried out using $1m^2$ of the reactor produced more efficient results than those carried out using $1.5m^2$ of reactor. Average solar intensities were similar during both sets of experiments - $32W/m^2$ and $35W/m^2$ respectively. Examining the continuously illuminated experiments (negating the reservoir) the $1m^2$ configuration was 1.5 times more efficient than the $1.5m^2$ configuration when comparing inactivation coefficients based on experimental time and 2.2 times more efficient when compared using actual illumination time. This contradicts other research which suggests that having an interruption during illumination favours defence mechanisms and therefore increases time required for inactivation (Rincón and Pulgarin, 2003). This supports the theory that a longer dark period following illumination aids bacterial inactivation (Section 8.2). It is also important to reiterate that the effect of the reservoir is not taken into account as it is common to all experiments and would have a dampening effect on inactivation, so it is reasonable to assume that the disinfection efficiency of all experiments would increase if the reservoir was not present. It is also important to note that during control experiments carried out under no illumination no bacterial inactivation took place discounting the theory that system elements themselves, for example, the pump, play a part in inactivation.

The results presented above suggests that the shorter the "flash" the more efficient the disinfection capacity. Disinfection using pulsed light or flash lamps is not a new idea but previous research has concentrated on exposing samples to very intense UVC or

broad-spectrum light (0.25-2 J/cm^2) for short durations of approximately 200 µs. This has two effects: the standard germicidal action of UVC and rupture and disintegration of micro-organisms through overheating after absorption of all the incident UV photons emitted in the light pulse (Wekhof *et al.*, 2001; Marquenie *et al.*; 2003a,b, McDonald *et al.*, 2000; Roberts and Hope, 2003; Takeshita *et al.*, 2003). In the experiments described above the "flashes" are much longer at 1 or 2 seconds which has not been reported to produce this overheating effect in bacteria. If this phenomenon was occurring the total experimental time would be much less as according to the literature only a short amount of pulses are required. 1 pulse has been reported to achieve 2-12 log reduction in *E. coli* depending on pulse intensity (Wekhof, 2000). It is interesting to note that in the research described above pulse intensity ranged from 4×10^2 to 3×10^3 times more intense than those intensities used in this study. It is therefore assumed that a shock mechanism occurs in the above experiments where the alternating light/dark regimes add an additional stress to the bacteria making them more susceptible to the effect of solar UV radiation. This additional stress when added causes behaviour similar to the addition of heat where the combination of stresses promotes more effective disinfection efficiency. Shorter flash times allow less recovery time between flashes and therefore more effective disinfection. In the 1.5m^2 experiments the shortest flash was 2.8 seconds of illumination and 2.8 seconds of darkness which proved to be 2.1 times more efficient than the continuously irradiated area experiments when compared using experimental time and 2.2 times more efficient when compared using illuminated time. In the 1m^2 experiments the shortest flash was 0.9 seconds of illumination and 1.9 seconds of darkness, which proved to be 1.8 times more efficient than the continuously irradiated area experiments when compared using experimental time and illuminated time.

From these results it seems that an optimum balance exists between frequency of flash, length of flash and a following dark period. During continuous flow experiments the most efficient light regimes were those consisting of the shortest flash times, which agreed with the batch experiments described in Section 8.3. However, the results of the batch trials described in Section 8.2 suggest that a longer dark period after illumination aids bacterial inactivation suggesting that inactivation carries on in the dark, possibly to a greater extent than during illumination (it is important to note that the batch trials only examined illuminated periods of up to 4 seconds). It is important to remember that the time spent in the reservoir during continuous flow experiments was effectively

mimicking this dark period in earlier batch experiments, suggesting that a series of short flashes followed by a longer dark period as one cycle would provide the most efficient disinfection kinetics.

8.5 Concluding Remarks

Intermittent illumination regimes have a positive effect on the solar disinfection process. The efficiency of batch process disinfection is enhanced up to 1.3 times by introducing a flash of illumination into the disinfection process. During batch process experiments shorter flashes of illumination followed by short dark periods produced the best results.

During continuous flow experiments an illuminated area of $1m^2$ produced better results than illuminating an area of $1.5m^2$ suggesting that a dark period is beneficial in the disinfection process. These results agreed with batch experiments.

When flashes were introduced in continuous flow disinfection experiments both $1.5m^2$ and $1m^2$ experiments showed an improved disinfection capacity. Shorter flash times proved to be most efficient in both reactor configurations. In all experiments flash times of between 1 and 4 seconds produced the most efficient results. It is suggested that the flashes cause a shock mechanism to the bacteria, which enhances normal solar disinfection mechanisms.

9.1 Introduction

The aim of this research is to provide a safe water supply for communities in developing countries. This chapter attempts to use the results found in previous chapters to produce a scaled-up design to supply drinking water for a small community in a developing country. Here the results from the $3m^2$ pilot-scale reactor and the small-scale parabolic reactor are used in order to provide a basis for a scaled-up design. The pilot-scale reactor is a compound parabolic collector system as described in Section 3.2.3 and the small-scale compound parabolic reactor is described in Section 3.3.2 (the compound parabolic reactor was found to be the most efficient collector type during the experimental trials). The results have been based upon the dose parameter Q_{aillum} but can be adjusted for experimental time or illumination time if necessary. The aim is to provide a series of charts suitable for field use in developing countries.

9.2 Designing from the Experimental Results

For the design of a full-scale system a number of parameters need to be considered:

- The population to be served with drinking water, the quantity of water required per person per day and hence, the total volume of water required per day.
- The operating hours of the solar disinfection system per day and the flowrate through the system.
- The required pathogenic removal.
- The required residence time of the contaminated water with the solar disinfection system to achieve this removal, i.e. insuring that the contaminated water receives the necessary dose to achieve this desired pathogenic removal, based on the incident radiation.
- The physical dimensions of the system:
  - Absorber diameter, d,
  - Absorber length, L_a,
  - Aperture area, A_{ap}.

It should be noted that the CPC unit used to obtain the experimental results had a half acceptance angle of $\theta_a = 90°$ (as discussed in Section 3.2.4) and therefore systems designed using the following method should also be limited to systems with a half acceptance angle of 90°. Also as an essential prerequisite the source of the water should

be considered to determine whether flowrates are feasible (i.e. from a handpump or river source).

9.2.1 Population Water Requirements and Operating Hours

Each person needs a minimum of five litres of water per day in order to survive. For basic needs this figure increases from five to fifteen litres per day. Basic water requirements are summarised in Table 9.1 below. However, it is also assumed that each person needs 20-60 litres of water per day in order to eradicate water washed diseases. It is important to note that the quantities of water needed for domestic use may vary according to the climate, the sanitation facilities available, people's normal habits, their religious and cultural practices, the food they cook, the clothes they wear and so on. Water consumption generally increases the nearer the water source is to the dwelling (Cairncross and Feachem, 2000, The Sphere Project, 2004).

Survival Needs	Quantity	Other Factors
Water intake: drinking and food	2.5-3 litres per day	Depends on: the climate and individual physiology
Basic hygeine practices	2-6 litres per day	Depends on: social and cultural norms
Basic cooking needs	3-6 litres per day	Depends on: food type, social as well as cultural norms
Total basic water needs	7.5-15 litres per day	

Table 9.1: Basic Water Requirements (The Sphere Project, 2004).

As well as deciding on the required quantity of water per head of population the operating hours of the system must be known in order to decide on the flowrate of the system. For the purposes of this design it was decided to hold the operating hours of the system constant at 6 hours per day. Therefore the value of incident solar radiation used for calculations must be exceeded for the entire duration of the operation. Figure 9.1 relates to a study carried out in Haiti (Oates *et al.*, 2003) where a solar intensity of $470W/m^2$ would be taken as the incident intensity over six operating hours from 9am to 3pm. The peak solar intensity over this time is $800W/m^2$, demonstrating that this is a

conservative estimate as well as taking into account that bacterial inactivation is not linearly proportional to solar intensity, as discussed in Section 4.3.   A six-hour operating time also controls the flowrate within the system as a shorter operational time will promote larger flowrates, which could cause problems with system size as well as the rate of supply possible from the water source.
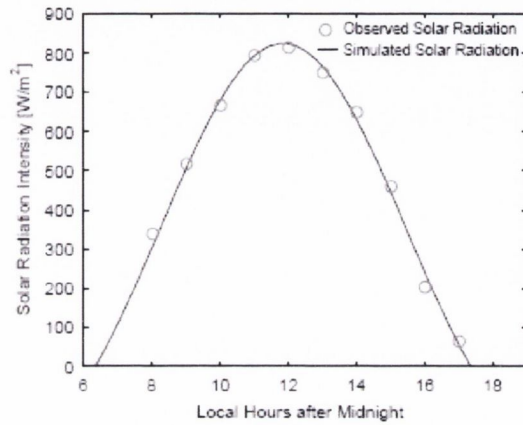
Figure 9.1: Variation of Solar Radiation Intensity throughout the day- Haiti (Oates *et al.*, 2003).

The first design chart is a plot of population against required flowrate through the reactor depending on the volume of water required per person per day.
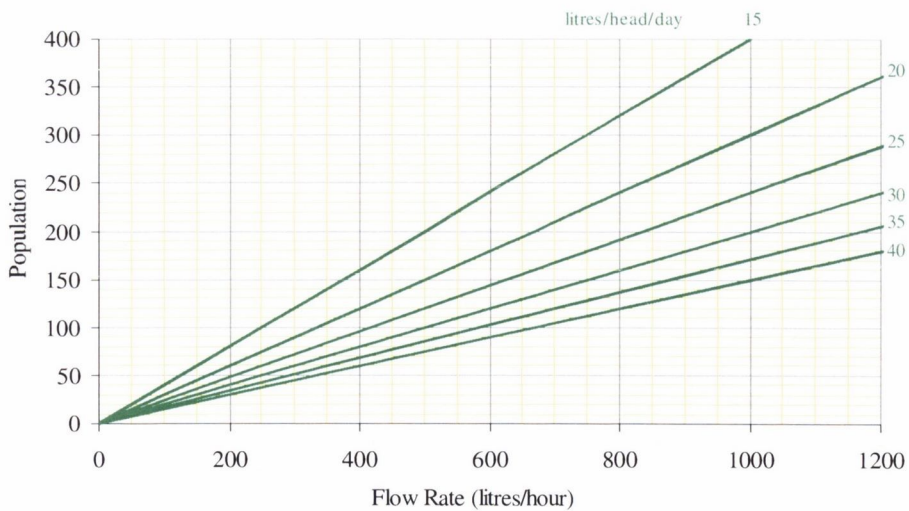
Figure 9.2: Determination of flowrate depending on water requirements and population for a six-hour operation time.

When a flowrate has been calculated a second chart could be used to incorporate a factor of safety in order to account for water spillage or wastage.
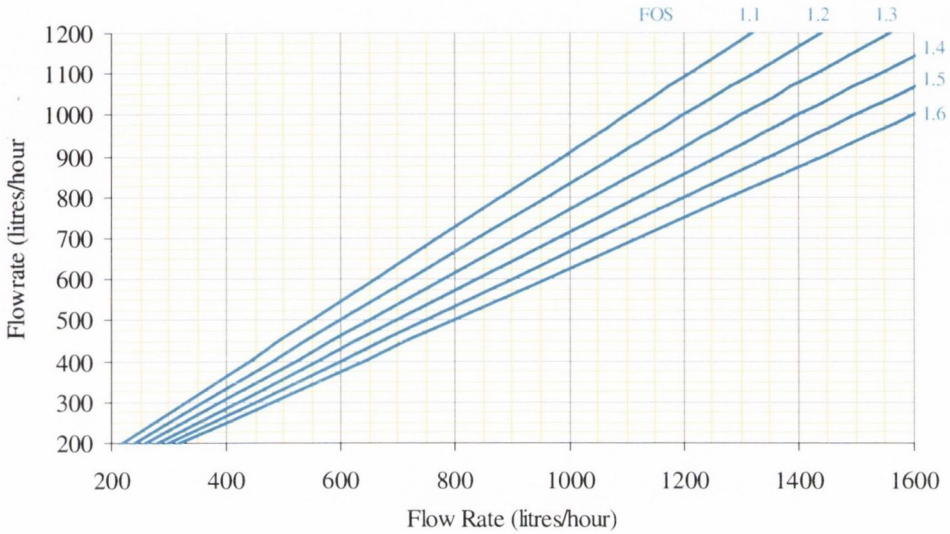
Figure 9.3: Determination of a new flowrate depending on the required factor of safety.

From Section 4.2 it was decided that the flow regime of the system should be kept turbulent in order to ensure complete mixing within the system and promote an even dose distribution to the bacteria present. Therefore the Reynolds number should be kept above 4000. The Re number is calculated using Eq. 9.1 and the design chart shows the smallest diameter of absorber necessary to achieve a turbulent flow regime for a particular flowrate.

$$Re = \frac{vd}{v} \qquad\qquad (9.1)$$

Where v is the velocity within the absorber, m/s, d is the absorber diameter, m, and v is the kinematic viscosity, m^2/s.
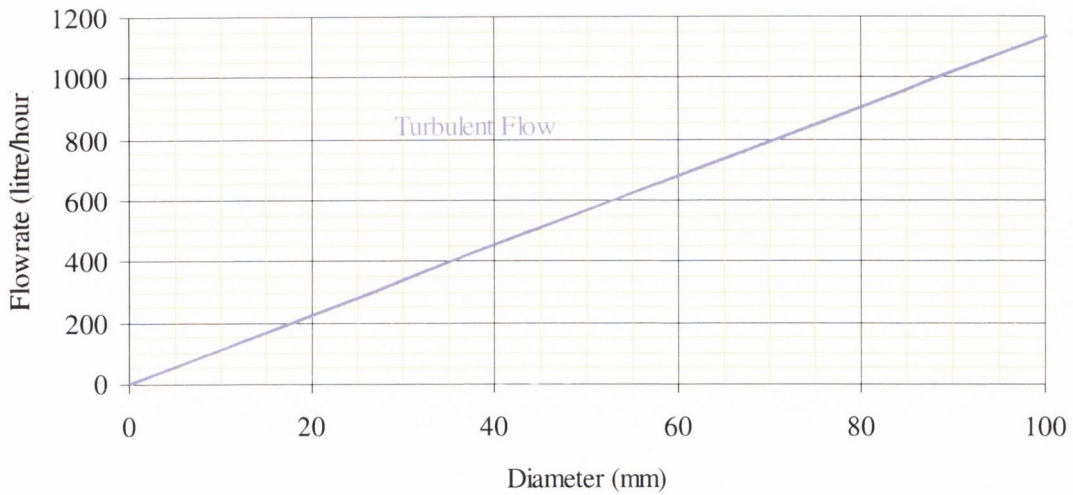
Figure 9.4: Determination of a diameter based on a turbulent flow regime.

9.2.2 Pathogenic Removal and Dose

In order to design a system where a specific bacterial removal is required some correlation between the results obtained in the experimental trials and a complete system must be obtained. The inactivation rate constant ($k_{qaillum}$) describes the disinfection kinetics and was plotted against intensity for all experiments involving the pilot-scale reactor and the small-scale parabolic reactor. The inactivation rate constants were determined by calculating the individual rate constants for each cumulative dose step relative to the initial bacterial concentration in order to obtain a relationship with which a complete system of varying size could be designed. The main difference between the two reactors was the diameter of their absorber tubes (pilot-scale= 29.4mm; small-scale=9.6mm). The relationship between the two regression lines (Figure 9.5) reveals that the shallower depth of water in the small-scale reactor promoted much better disinfection kinetics than the deeper water in the pilot-scale reactor. Hence, a relationship between the inactivation rate constant and intensity has been developed based on a linear relationship between absorber diameter (i.e. water depth) and the dose kinetic, ($k_{Qaillum}$), (Eq. 9.2).

$$k_{Qaillum} = \frac{I \times \dfrac{d_{ps}}{d_{ss}}}{\dfrac{x_2}{x_1} \times \dfrac{d}{d_{ss}}}$$

(9.2)

where, I is the intensity of the incoming radiation, d is the absorber tube diameter, d_{ps} is the diameter of the absorber tube in the pilot scale reactor, d_{ss} is the diameter of the absorber tube in the small-scale reactor, x_1 is the relationship between $k_{Qaillum}$ and intensity for the small-scale diameter line in Figure 9.5 and x_2 is the relationship between $k_{Qaillum}$ and intensity for the pilot-scale line as show in Figure 9.5. The scatter of the results for the small-scale system can be mitigated by apply factors of safety during the design process
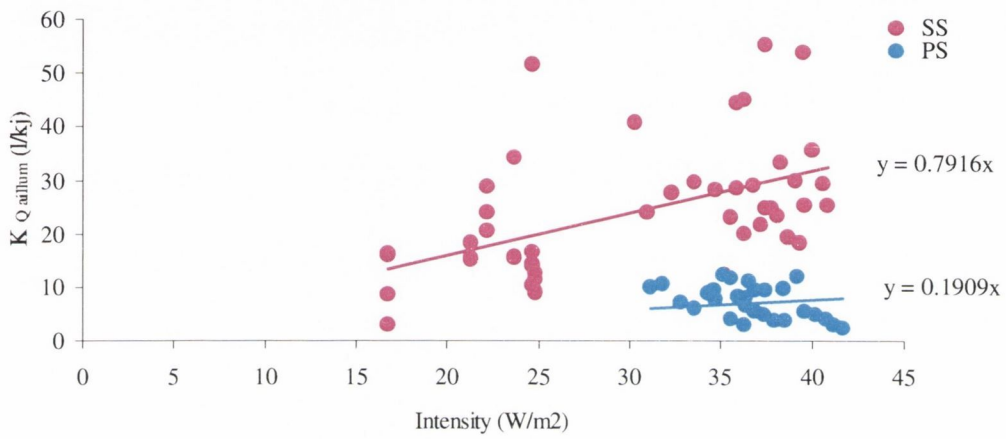
Figure 9.5: A comparison of the small-scale compound parabolic reactor and pilot scale reactor as a function of dose kinetic $k_{qaillum}$ and intensity.

From Figure 9.5 and Eq. 9.2, a graph of $k_{qaillum}$ against intensity can be plotted for different diameter absorbers (Figure 9.6).
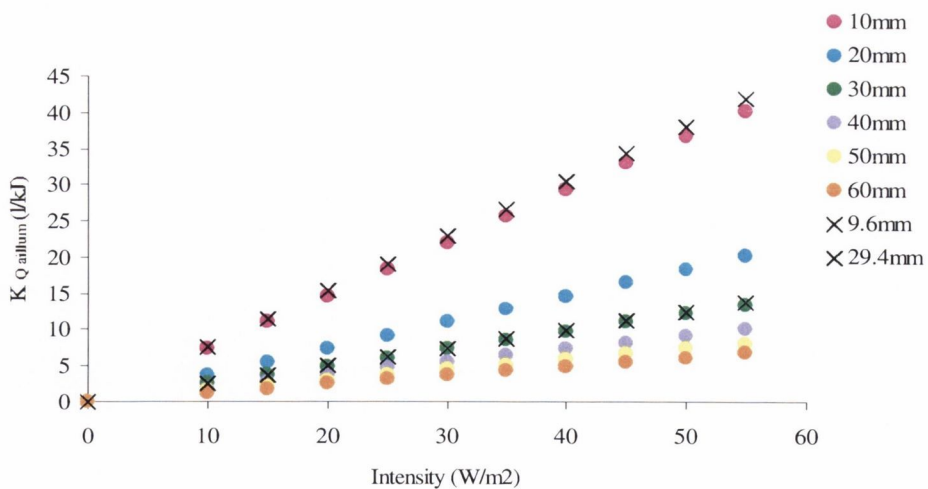
Figure 9.6: Dose kinetic $k_{qaillum}$ against intensity for different absorber diameters.

The slope of the regression line gives an empirical formula created between $k_{qaillum}$ and the solar radiation intensity.

$$K_{Qaillum} = xI \tag{9.3}$$

From Figure 9.6 above it can be seen that for each diameter a value for x can be evaluated. This equation (9.3) can then be used with Eq 9.4 below to calculate the dose (Q_{aillum}) required for a specific log-removal. Here the design charts have been formulated to remove 6-log of *E. coli* K-12. It should be noted therefore that this does not necessarily ensure a 6-log removal of all pathogenic organisms as each organism has a different resistance to solar radiation. The relative resistance of other organisms to solar radiation has been discussed in Section 4.5 and this method could then be adapted to suit any of these organisms. It is also unlikely that a water source would contain higher concentrations than 1×10^6 CFU/ml of any organism and so this estimate is considered to be fairly conservative as typical surface water contamination would be more in the order 10^3CFU/ml faecal coliforms (Conroy *et al.*, 1996).

The dose required to achieve the requisite log removal is calculated from the following equations:

$$LN\left[\frac{N_t}{N_0}\right] = kQ_{aillum} \tag{9.4}$$

$$(I \times x) = k_{Qaillum} \tag{9.5}$$

Substituting for k,

$$Q_{aillum} = \frac{LN\dfrac{N_t}{N_0}}{x \times I} \tag{9.6}$$

Therefore the dose required at a specific solar intensity for each specific diameter can be calculated as shown on Figure 9.7.
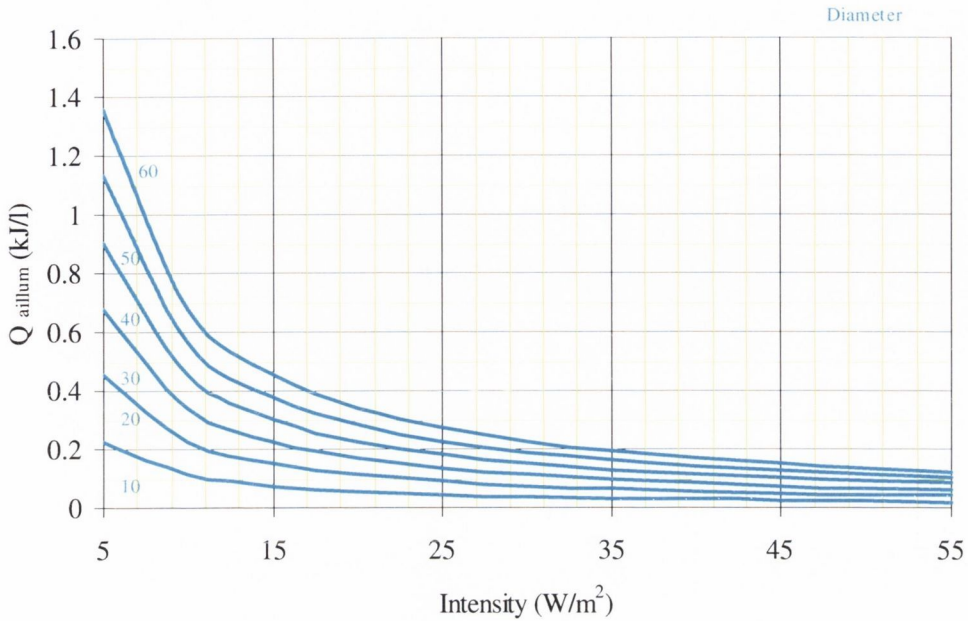
Figure 9.7: Determination of the required dose, Q_{aillum} , for a 6-log removal of *E. coli* K-12.

The residence time required in the reactor can then be determined using Eq. 9.7 and Figure 9.8 below.

$$Q_{aillum} = \Delta t I \left[\frac{A_{ab}}{V} \right] \tag{9.7}$$

where Δt is the time required for inactivation, A_{ab} is the plan area of the absorber and V is the volume of the absorber.

When determining the residence time from the chart, if a value falls in between two divisions (e.g. 8 minutes), the number of the next largest should be taken as a design value (e.g. 10 minutes), which provides an extra factor of safety in the design. These FOS will also take the varying resistances of different microorganisms and varying initial concentrations into account as the required exposure time is increased to ensure complete removal of all pathogenic organisms.
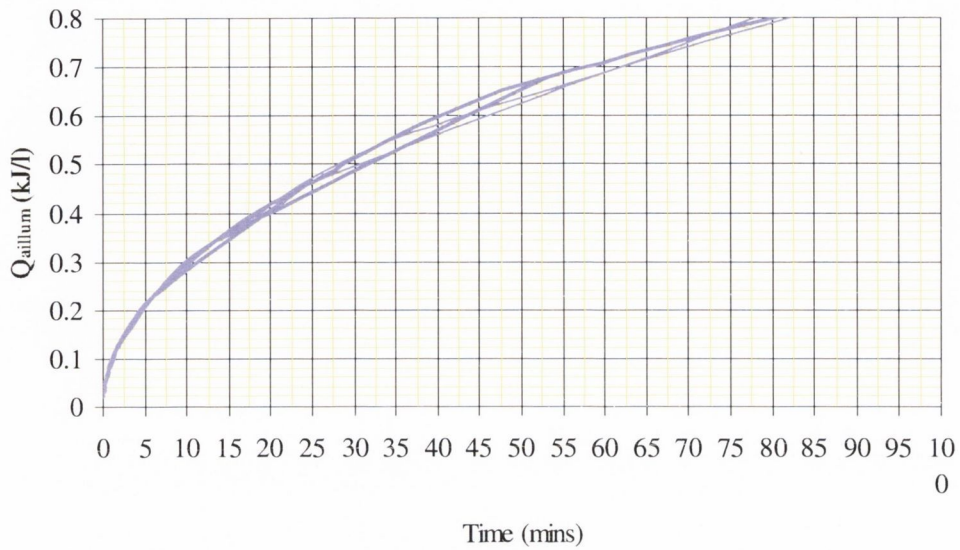
Figure 9.8: Determination of require residence time (min)

9.2.3 Physical Parameters

The physical parameters of the system, such as absorber diameter, absorber length and aperture area can now be calculated. The total system volume, V, can then be calculated using the flowrate, Q, and a specific residence time, t, from Eq. 9.8.

$$V = Q \times t \qquad (9.8)$$
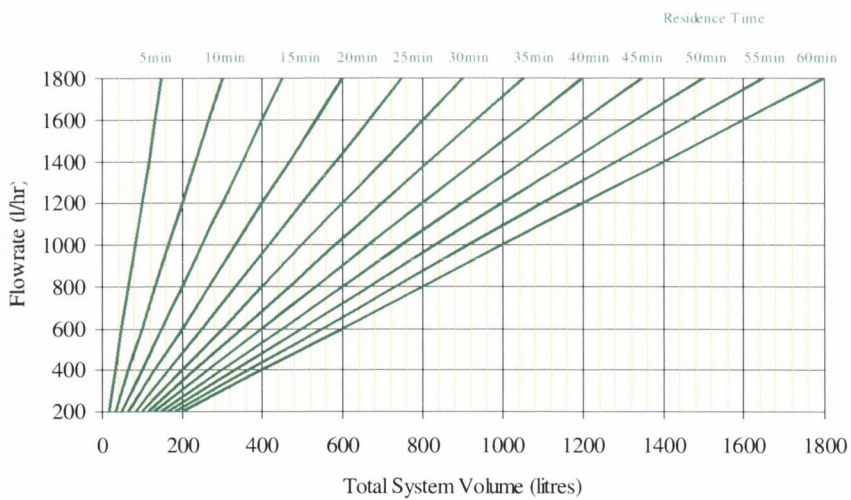
Figure 9.9: Determination of total system volume based on the flowrate and the required residence time.

The absorber length, L_a, can then be calculated for specific absorber diameters using the total volume, V, (Eq. 9.9).

$$L_a = \frac{V}{A_{ab}}$$ (9.9)
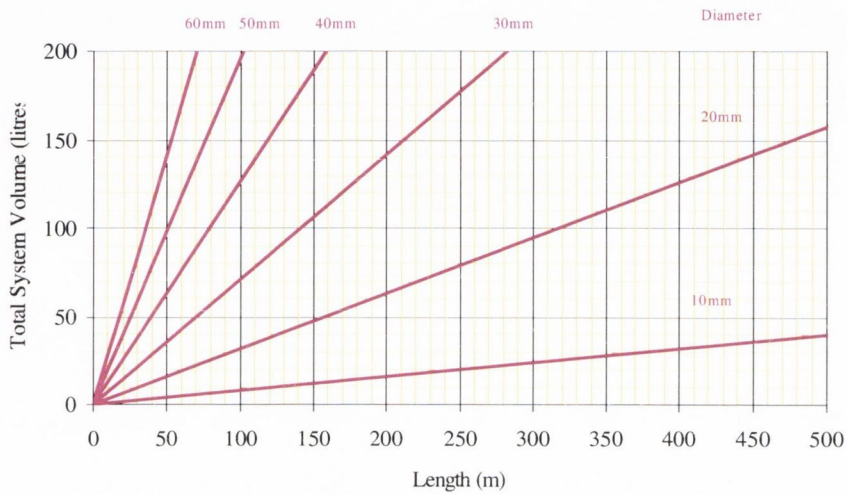
Figure 9.10: Determination of absorber length based on the total system volume for specific absorber diameters.

Finally, the aperture area, A_{ap}, of the collector can then be calculated for specific absorber diameters based on the required absorber length using Equation 9.10 below.

$$A_{ap} = (d + 3mm) \times \pi \times L_{ab}$$ (9.10)
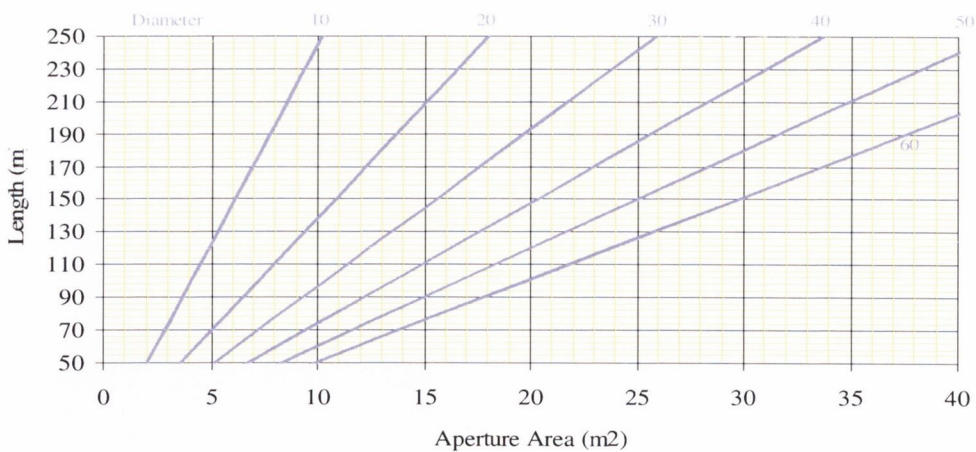
Figure 9.11: Determination of collector aperture area based on the absorber length for specific absorber diameters.

9.3 Using the Design Charts

This section goes through the step-by-step design of a solar disinfection system for a village in a developing country. The following parameter details have been assumed for a typical location at a tropical latitude:

- The village has a population of 200 people.
- Each person requires 15 litres of water a day for drinking, washing and cooking.
- Recordings of daily solar intensity were taken and found to exceed a value of $600W/m^2$ ($30W_{UV}/m^2$) for the peak 6 hours of the day

Step 1

For a population of 200 people at 15 l/head/day a value of 500 litres/hour is obtained for the flowrate, as shown in Figure 9.12.
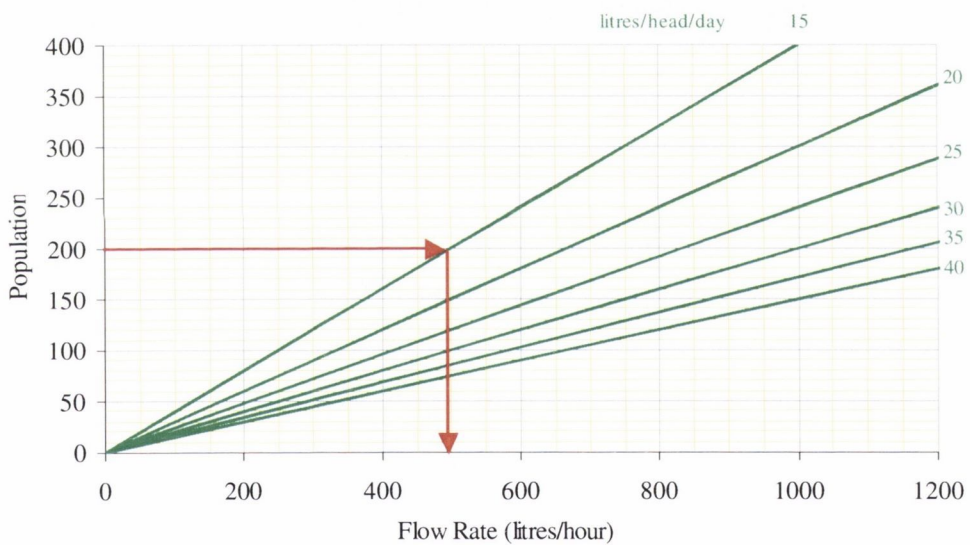
Figure 9.12: Obtaining the flowrate

A factor of safety of 1.2 is applied to the design and so the design flowrate to be used is 600 litres/hour (Figure 9.11).
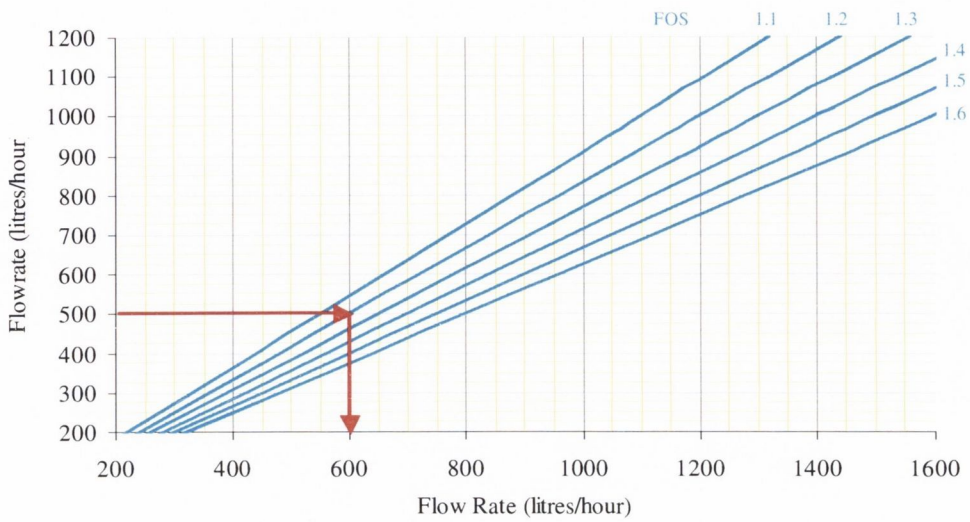
Figure 9.13: Obtaining the design flowrate

Step 2

The required diameter to achieve turbulent flow is found to be 55mm so a diameter of 50mm will be used for design. (Note: the next largest diameter according to standard sizes should be adopted).
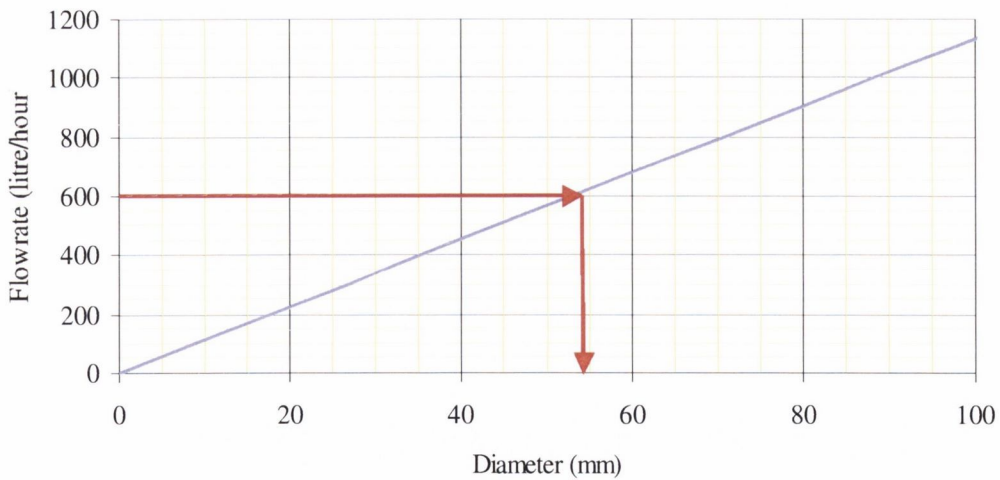
Figure 9.14: Obtaining the diameter

189

Step 3

The required dose for 6-log removal is found to be 0.2kJ/l for a diameter of 60mm and an intensity of $30W_{UV}/m^2$.
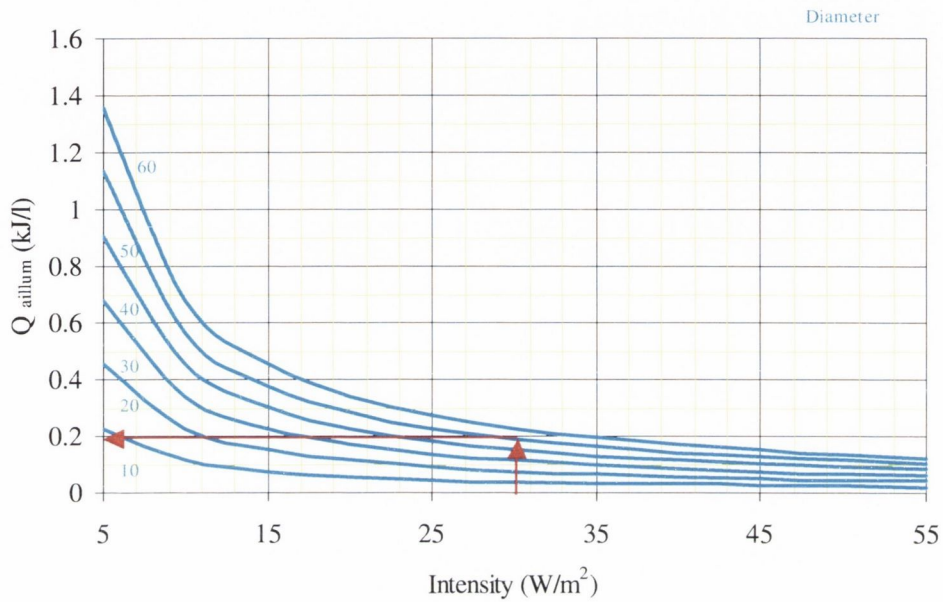
Figure 9.15: Obtaining the required dose

Step 4

The required residence time to achieve a dose of 0.20kJ/l is found to be 6 minutes, so a design residence time of 10 minutes is used.
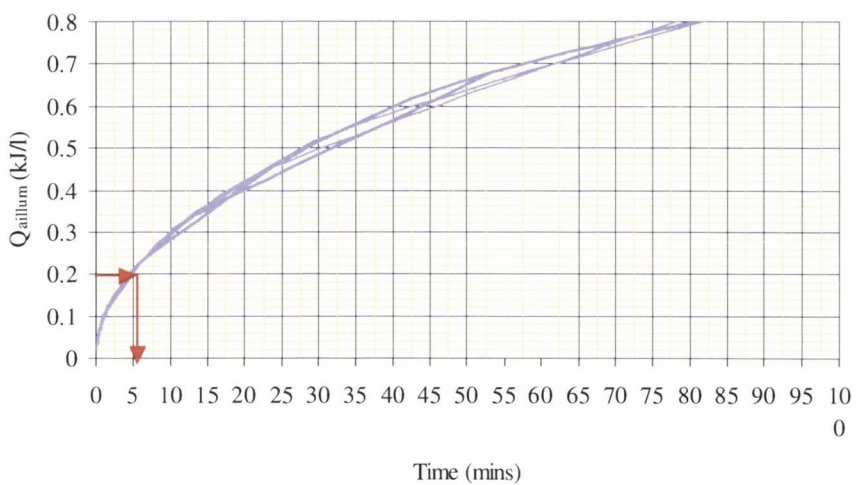
Figure 9.16: Obtaining the residence time

Step 5

A total system volume of 100 litres is obtained from Figure 9.17 and the required residence time of 10 minutes
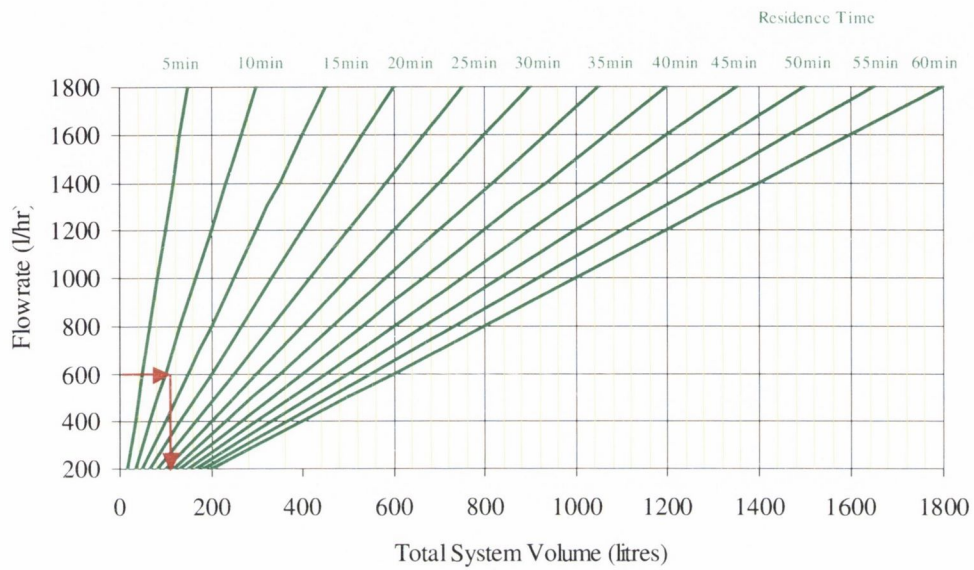
Figure 9.17: Obtaining the total system volume.

Step 6

An absorber length of 50m is obtained from Figure 9.18 for a system volume of 100 litres and a diameter of 60mm.
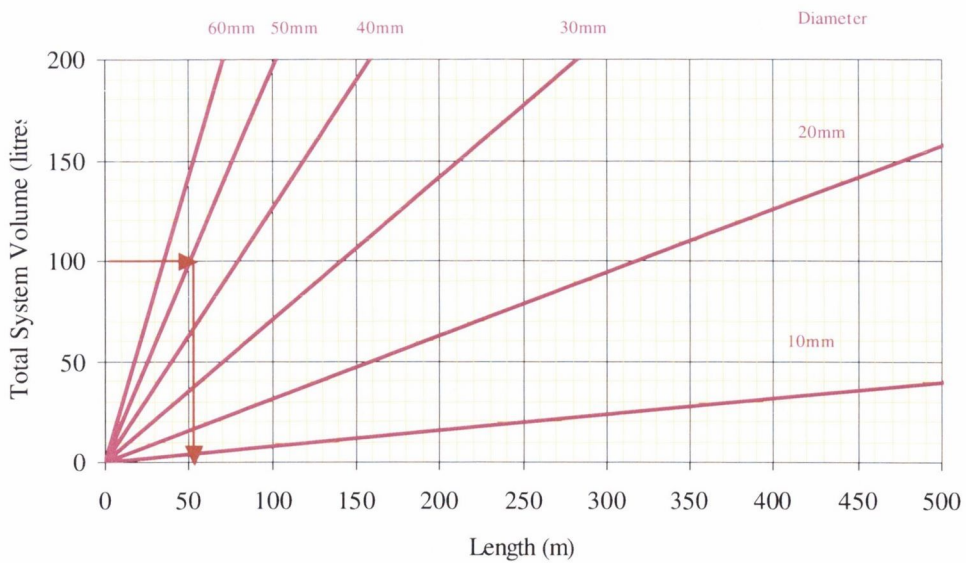
Figure 9.18: Obtaining absorber length.

Step 7

An aperture area of 8m^2 is obtained from Figure 9.19 for a system length of 50m and a diameter of 50mm.
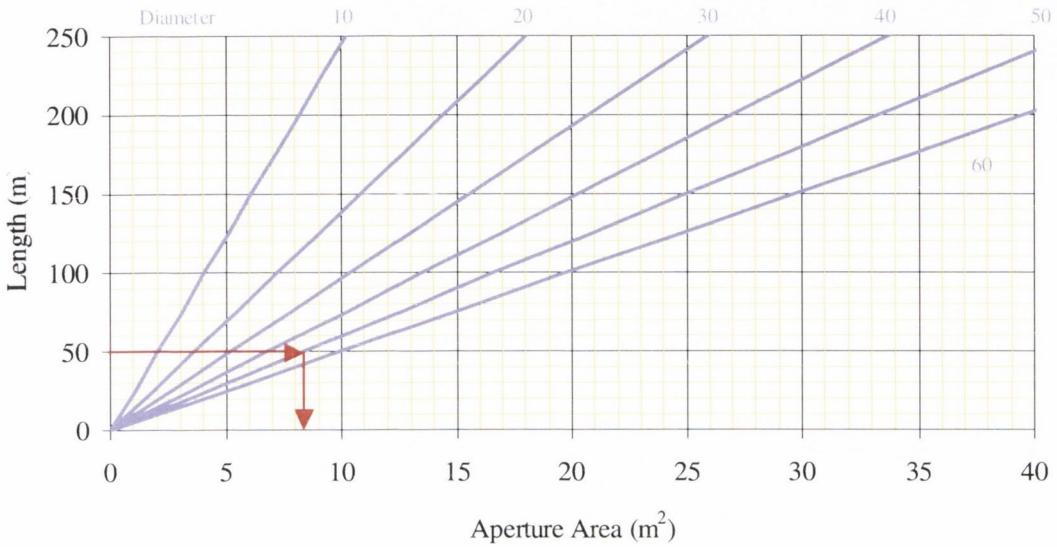
Figure 9.19: Obtaining the aperture area.

So the system needed to supply 15 litres of clean water per person per day to 200 people in a village with a solar intensity of 600W/m^2 has the following specifications:

- Aperture Area= 8m^2
- Absorber diameter= 50mm
- Absorber Length= 50m

These are the main parameters necessary for sizing the system but after this stage other factors must be considered in order to assess the exact footprint of the system. For example, in this case two possible scenarios would be to have one 50 metre length of pipe or five 10m length pipes connected in series. The total headloss across the system also needs to be determined to achieve the design flowrate which will depend on the reactor configuration. Once this headloss is defined, balancing tanks will be required t maintain the head across the system if it is to be operated under gravity feed-the most suitable solution for such a technology.

9.4 Concluding Remarks

A series of design charts have been produced in order to provide a simplified method of designing solar disinfection reactors for specific situations.

In the worked example an area of $16m^2$ does not seem prohibitive in terms of ground space to provide clean water for a village of 200 people. Therefore, from these calculations it would appear that full-scale solar disinfection reactors could be a realistic option for the provision of drinking water in developing countries.

CHAPTER 10

CONCLUDING REMARKS & RECOMMENDATIONS

10.1 Conclusions

It is evident from the experiments carried out that solar disinfection is achievable in a sufficient time to explore the applicability for use in a full-scale system in a developing country.

- Relatively little difference was found between the three different flow regimes tested, presumably due to the turning of the fluid at each bend in the reactor and the shallow water depths involved. Surprisingly results indicated that turbulent conditions were slightly less efficient than laminar flow conditions, although this is thought to be more due to the frequency of exposure to sunlight in each particular reactor configuration than the actual flow regime. RTD analysis shows that the turbulent flow regime has a better mixing capacity, which also would be more critical in the design of a once-through flow system.

- The results of the intensity experiments indicate that inactivation kinetics are similar on exposure to certain threshold irradiances. These results also agree with the literature that there is a non-lineal dependence between bacterial inactivation rate and light intensity.

- *Salmonella Typhimurium* was found to be approximately twice as resistant as *E. coli* K-12 to solar radiation and the relative difference between resistances did not change at lower intensities. The relative resistances of other microorganisms were assessed from literature and found to be, as follows, in order of least to greatest resistance to solar disinfection:

  Sh. dysenteriae < P. aeruginosa < Sh. flexneri < E. clocae < S. enteriditis < E. coli < Ent. faecalis < coliforms< S. Typhimurium < Sh. Sonnei < MS-2 bacteriophage< Poliovirus < C. albicans < A. polyphage < F. solani < V. cholerae < Enterococci sp.< B. subtilis

- Both tubing types, borosilicate and soda lime glass performed equally under simulated solar conditions having equal inactivation rate constants. After time a loss in transmission could occur due to impurities such as iron and hence it is recommended that a low-iron content borosilicate glass is used in a full-scale reactor.

- Continuous flow solar disinfection was found to be more efficient than batch process solar disinfection due to the actual exposure time being much shorter in the continuous flow reactor than in the bottle i.e. during continuous flow experiments the contaminated water was recirculated through a reservoir which was effectively a dark zone, reducing the total illumination time of the solution.

- The reactor with the Compound Parabolic reflector performed consistently better than the other three reactors with Parabolic, V-groove and no reflectors, both under natural and simulated conditions as well as under low intensity natural conditions.

- There was a marked different in performance under natural conditions compared with simulated conditions for all reactors. This could be due to spectral differences in the UV and Infrared regions of simulated and natural solar conditions.

- There also seems to be a mechanism other than the assumed UV dose mechanism related contributing to the disinfection process due to the presence of a dark phase in the continuous flow process.

- It is suggested that inactivation kinetics be calculated according to absorber area and actual exposure time when comparing reactors of different areas and varying dark zones.

- A slight enhancement of the disinfection process was found on addition of a low concentration (3mg/l) of TiO_2 to the pilot-scale solar disinfection reactor. However, these results do not indicate that an addition of a TiO_2 suspension can be justified as a sustainable solution for developing countries with its inherent requirement for an extra separation process before water consumption.

- The technique of using low concentrations of TiO_2 fixed to a glass rod within the reactors demonstrated a moderate enhancement to overall disinfection efficiency in the Compound Parabolic and V-groove reactors under both Spanish and Irish intensities. However, TiO_2 coated paper did not improve reactor performance, which could be due to a number of reasons including, excessive ˙OH radical generation leading to recombination, method of fixing and surface texture.

- Post-irradiation regrowth was also examined for both solar disinfection and solar photocatalytic disinfection. After 24 hours although there was no appreciable

regrowth in either system, a loss in culturable cells in samples of the photocatalytic systems suggests that an addition of TiO_2 could produce a residual effect.

- A clear advantage on having increased temperatures within the solar disinfection reactor was demonstrated. The additional stress of water temperature at 45°C caused a 20% increase in the efficiency of the Parabolic reactor.

- The change in volume in the Compound Parabolic reactor caused a decrease in solar disinfection efficiency. This is predominantly due to the absence of a dark zone, which suggests that solar disinfection is not solely dose dependent and that possible other mechanisms could exist.

- Intermittent illumination regimes have a positive effect on the solar disinfection process in terms of efficiency per unit dose received. The efficiency of batch process disinfection is enhanced up to 1.3 times by introducing a flash of illumination into the disinfection process. During batch process experiments shorter flashes of illumination followed by short dark periods produced the best results.

- During continuous flow experiments an illuminated area of $1m^2$ produced better results than illuminating an area of $1.5m^2$ suggesting that a dark period is beneficial to the disinfection process. This phenomenon was also observed with the batch experiments.

- When flashes were introduced in continuous flow disinfection experiments both $1.5 m^2$ and $1m^2$ experiments showed an improved disinfection efficiency with respect to dose. Shorter flash times proved to be most efficient in both reactor configurations- in all experiments discrete flash periods of between 1 and 4 seconds produced the most efficient results. It is therefore suggested that the flashes cause an additional stress to the bacteria which enhances the normal solar disinfection mechanisms.

- A simplified design protocol for solar disinfection reactors based on these results has been developed which shows that reasonably sized solar disinfection reactors have a realistic potential for use in a developing country.

Overall, therefore, the experimental work carried out during this project shows that solar disinfection of contaminated water could be a valid solution for developing countries.

10.2   Recommendations

It is evident from experimental work that there are additional factors which can affect the solar disinfection process in a positive manner. It is suggested that a new method of fixing TiO_2 to an inert surface which ensures that the contaminated water is in contact with a high dose of TiO_2 should be examined. This would ensure that the positive effects of suspended TiO_2 could be employed in a continuous flow reactor. The potential benefit of a residual photocatalytic disinfection effect on the bacteria using TiO_2 should also be examined further. This would be particularly important if the solar disinfected water is to be stored in a reservoir prior to use.

The results suggest that the design of an oversized concentrating reactor could enhance the solar disinfection process by a synergistic solar UV and temperature effect. These types of reactors should be examined further in order to assess their overall benefit against the increased cost of a more complex reactor. Alternatively an insulated reactor employing the greenhouse effect could be used to promote the same temperature increase.

The non-lineal dependence between bacterial inactivation and solar radiation intensity should be explored further in order to more accurately rationalise the disinfection kinetics of bacteria exposed to many different solar intensities.

The stroboscopic mechanism results indicate that an additional stress is placed on *E. coli* K-12 when a series of flashes is inbuilt into the disinfection system. Future work should focus on determining the optimum light to dark ratio. The required dark phases in a reactor would translate into a decrease in collector area which could therefore result in a decrease in the overall cost of a system.

It is also recommended that a full-scale system be built in a developing country in order to carry out full-scale trials in a gravity-fed once-through system. This would assess the validity of such a technology under realistic water quality and operating conditions.

References

Acra, A., Jurdi, M., Mu'allem, H., Karahagopian, Y., Raffoul, Z., (1989). Water Disinfection by Solar Radiation : Assessment and Application. Technical Study 66e IRDC.

Acra, A., Raffoul, Z., Karahagopian, Y., (1984). Solar Disinfection of Drinking Water and Oral Rehydration Solutions-guidelines for household application in developing countries. UNICEF, Beirut.

Alexandris, D., Varotsos, C., YaKondratyev, K., Chronopoulos, G., (1999). On the altitude dependence of solar effective UV. *Physics and Chemistry of the Earth, Part C: Solar, Terrestrial and Planetary Science*, **24**, 5, pp515-517.

Alfano, O.M., Bahnemann, D., Cassano, A.E., Dillert, R, Goslich, R., (2000). Photocatalysis in water environments using artificial and solar light. *Catalysis Today*, **58**, 2-3, pp199-230.

APHA, 1999, Standard Methods for the Exanimation of Water and Wastewater, 20th ed. American Public Health Association, Washington, DC.

Axelsson-Olsson, F., Waldenstrom, J., Broman, T., Olsen, B., Holmberg, M., (2005). Prozotoan Acanthamoeba polyphaga as a potential reservoir for *Campylobacter jejuni. Applied and Environmental Microbiology*, 71, 2, pp987-992.

Barker, J., Brown, M.R.W., (1994). Trojan Horses of the Microbial world: protozoa and the survival of bacterial pathogens in the environment. *Microbiology*, **140**, pp1253-1259.

Bell M. and Franceys, R. (1995) Improving Human Welfare through Appropriate Technology: Government Responsibility, Citizen Duty or Customer Choice. *Social Science Med.*, **40**, 9, pp1169-1179.

Blanco Galvez, J., Malato Rodriguez, S., (ed) (2003) Solar Detoxification. UNESCO Publishing Renewable Energy Series, ISBN: 9231039164.

Blanco, J., Malato, S., Fernandez, P., Vidal, A., Morales, A., Trincado, P., Oliviera, J.C., Minero, C., Musci, M., Casalle, C., Brunotte, M., Tratzky, S., Dischinger, N., Funken, K.H., Sattler, C., Vincent, M., Collares-Pereira, M., Mendes, J.F., Rangel, C.M., (1999). Compound Parabolic Concentrator Technology Development to Commercial Solar Detoxification Applications. *Solar Energy*, **67**, 4-6, pp317-330.

Block, S.S., Seng, V.P. and Goswani, D.W., (1997). Chemically enhanced sunlight for killing bacteria, *Journal of Solar Energy Engineering*, ASME, **119**(1), pp.85-91.

Cairncross, S., Feachim, R., Environmental Health Engineering in the Tropics: an introductory text. Wiley and Son, 2nd Edition, ISBN 0471938858

Caslake, L.F., Connolly, D.J., Menon, V., Duncanson, C.M. Rojas, R. and Tavakoli, J., (2004). Disinfection of Contaminated Water by Using Solar Irradiation, *Applied and Environmental Microbiology*, **70**(2), pp. 1145-1150.

Chen, D., Wangberg, S.A., Wulff, A., Borne, K., (2004). Attenuation of biologically effective UV doses under overcast skies: a case study form the eastern Atlantic sector of the Southern Ocean. *Deep-Sea Research II*, **51**, pp2673-2682.

Chick, H., 1908, An investigation into the laws of disinfection, *Journal of Hygiene*, **8**, pp.92-158.

CIEMAT, (2005). Solar Photochemistry technology, Plataforma Solar de Almeria. Available from www.psa.es.

Conroy, R.M., Elmore-Meegan, M., Joyce, T., McGuigan, K.G., Barnes, J., (1996) Solar Disinfection of Drinking Water and Diarrhoea in Maasai Children: A Controlled Field Trial. *The Lancet*, **348**, Dec 21/28.

Cooper, A.T., Goswami, D.Y., (1998). Solar photochemical detoxification and disinfection for water treatment in tropical countries. *Journal of Advance Oxidation Technologies*, **3**, 2, pp151-154.

Downes, A., Blunt, T.P. (1877) The Influence of Light Upon the Development of Bacteria. *Nature*, **20**, p218.

Duffy E.F., Al Touati F., Kehoe S.C., McLoughlin O.A., Gill L.W., Gernjak W., Oller I., Maldonado M.I., Malato S., Cassidy J., Reed R.H. and McGuigan K.G., (2004). A novel TiO$_2$-assisted solar photocatalytic batch-process disinfection reactor for the treatment of biological and chemical contaminants in domestic drinking water in developing countries, *Solar Energy* **77**(5), pp.649-655.

Dunlop, P.S.M., Byrne, J.A., Manga, N. and Eggins, B.R., (2002). The photocatalytic removal of bacterial pollutants from drinking water. *Journal of Photochemistry and Photobiology A: Chemistry*, **148**, pp355-363.

Dvorkin, A.Y., Steinberger, E.H., (1999). Modelling the Altitude Effect on Solar UV Radiation. *Solar Energy*, **65**, 3, pp181-187.

Eawag/SANDEC, (2005). SODIS Technical Notes. Available from www.sodis.ch

Eicher, T.S. (1999) Training Adverse Selection and Appropriate Technology Development and Growth in a Small Open Economy. *Journal of Economic Dynamics and Control*, **23**, pp727-746.

Falkenmark, M. (1998) Preparing for the Future: Water for a Growing Population. *Journal of Water Supply Research and Technology- Aqua*, **43**, 4, pp161-166

Fallmann, H., Krutzler, T., Bauer, R., Malato, S., Blanco, J., (1999). Applicability of the Photo-Fenton method for treating water containing pesticides. *Catalysis Today*, **54**, 2-3, pp309-319.

Farr, S., Kogoma, T., (1991) Oxidative Stress Responses in *Escherichia coli* and *Salmonella Typhimurium*. *Microbiological Reviews*, Dec, p561-585.

Fend, T., Jorgensen, G., Bohmer, M., Kramer, T., Rietbrock, P., (1998). First surface aluminium mirrors an assessment for outdoor applications. Proc. Eurosun 1998,

Slovenia.

Geraghty, P. and Temnewo, G. (2000) Water Resource Development & Management in Eritrea. Proc. of IWRA's Xth World Water Congress, Melbourne, March 2000.

Goswami, D.Y., (1995). Engineering of Solar Photocatalytic Detoxification and Disinfection. In: Karl, W. Böer (Ed.), Advances in Solar Energy, vol. 10. ASES, pp165-210, September, Chapter 3.

Gueymard, C.A. (2004) The sun's total and spectral irradiance for solar energy applications and solar radiation models. *Solar Energy*, **76**, pp423-453

Hamill, L., (2001). Understanding Hydraulics. 2nd edition Palgrave.

Harm (1980) Biological Effects of Ultraviolet Radiation. Cambridge Press 1st Ed. Chapter 1.

Hockberger, P.E., (2000) The Discovery of the Damaging Effect of Sunlight on Bacteria. *Journal of Photochemistry and Photobiology B: Biology*, **58**, p185-191.

Ibanez, J., Litter, M. I., Pizarro, R.A. (2003) Photocatalytic bactericidal effect of TiO_2 on *Enterobacter clocae* Comparative study with Other Gram (-) bacteria. *Journal of Photochemistry and Photobiology A: Chemistry*, **157**, p81-85.

Jagger (1967) Introduction to Research in Ultraviolet Radiation. Prentice-Hall, Englewood Cliffs, 1st Edition.

Jorgensen, Fjendbo, A.J., Nohr, K., Sorensen, H., Boisen, F., (1998) Decontamination of Drinking Water by Direct Heating in Solar Panels. *Journal of Applied Microbiology*, **853**, 441-447.

Joyce, T.M, McGuigan, K.G., Elmore-Meegan, M. and Conroy, R.M., (1996). Inactivation of faecal bacteria in drinking water by solar heating, *Applied Environmental Microbiology*, **62**, pp.399-402.

Kalisvaart, B.F., (2001)., Photobiological Effects of Polychromatic Medium Pressure UV Lamps. *Water Science and Technology*, **43**, 4, p191-197.

Kehoe, S.C., Barer, M.R., Devlin, L.O. and McGuigan K.G., (2004). Batch process solar disinfection is an efficient means of disinfecting water contaminated with *Shigella dysenteriae* type I. *Letters in Applied Microbiology*, **38**, pp.410-414.

Kehoe, S.C., Joyce, T.M., Ibrahim, P., Gillespie, J.B., Shahar, R.A., McGuigan, K.G., (2001) Effect of Agitation, Turbidity, Aluminium Foil Reflectors and Container Volume on the Inactivation Efficiency of Batch Process Solar Disinfectors. *Water Research*, **35**, 4, p1061-1065.

Kohen, E., Santus, R., Hirschberg, J.G., (1995) Photobiology. Academic Press Ltd, London, ISBN 0124177557.

Konstantinou I.K. and Albanis T.A., (2003). Photocatalytic transformation of pesticides in aqueous titanium dioxide suspensions using artificial and solar light: intermediates and degradation pathways. *Applied Catalysis B: Environmental*, **42**, pp.319-335.

Lage, C., Teixeira, P.C.N., Leitão, A.C., (2000). Non-coherent visable and infrared radiation increase survival to UV (254nm) in *Escherichia coli* K-12. *Journal of Photochemistry and Photobiology B: Biology*, **54**, pp155-161.

Laot, N., Narkis, N., Neeman, I., Bilanovic, D., Armo, R., (1998). TiO_2 Photocatalytic Inactivation of Selected Microorganisms under Various Conditions: Sunlight, Intermittent and Variable Irradiation Intensity, Cds Augmentation and Entrapment of TiO_2 into Sol gel. *Journal of Advanced Oxidation*, **4**, pp97.

Lewin, B., (1997). Restriction and Repair, pp505-528. In B. Lewin (ed.) Genes VI. Oxford University Press. New York.

Linnell, C.C. (1995) Appropriate Technology in the Technology Curriculum. *Journal*

of Industrial Teacher Education, **32**, 3, pp83-86.

Lonen, J., Kilvington, S., Kehoe, S.C., Al-Touati, F. and McGuigan, K.G., (2005). Solar and photocatalytic disinfection of protozoan, fungal and bacterial microbes in drinking water. *Water Research*, **39**, 877-833.

Malato-Rodriguez, S., Blanco Galvez, J., Maldonado Rubio, M.I., Fernandez-Ibanez, J., Correira de Oliverira, J., (2004). Engineering of solar photocatalytic collectors. *Solar Energy*, **77**, 5, pp513-524.

Malato, S., Blanco, J., Caceres, J.,, Fernandez-Alba, A.R., Aguera, A. and Rodriguez, A., (2002). Photocatalytic treatment of water-soluble pesticides by photo-fenton and TiO_2 using solar energy. *Catalysis Today*, **76**, pp.209-220.

Malato, S. (1999). Solar Photocatalytic Decomposition of Pentachlorophenol Dissolved in Water. Editorial CIEMAT, ISBN: 84-7834-336-9.

Marquenie, D., Michiels, C.W., Van Impe, J.F., Schrevens, E., Nicolai, B.N. (2003). Pulsed white light in combination with UV-C and heat to reduce storage rot o strawberry. *Postharvest Biology and Technology*, **28**, 3, pp455-461.

Marquenie, D., Geeraerd, A.H., Lammertyn, J., Soonjens, C., Van Impe, J.F., Michiels, C.W., Nicolai, B.M. (2003). Copmbinations of pulsed white light and UV-C or mild heat treatment to inactivate *condida* of *Botrytic cinerea* and *monilia fructigena*. *International Journal of Food Microbiology*, **85**, 1-2, pp185-196.

Martin-Dominguez, A., Alarcon-Herrara, M.T., Martin-Dominguez, I.R., Gonzalez-Herrara, A., (2005) Efficiency in the Duisinfection of Water for Human Consumption in Rural Communities Using Solar Radiation. *Solar Energy*, **78**, 1, p31-40.

Matsunga, T., (1985). Sterilization with particulate photosemiconductor. *Journal of Antibacterial and Antifungal Agents*, **13**, pp211-220.

McGuigan, K.G., Joyce, T.M. and Conroy, R.M., (1999). Solar Disinfection: use of sunlight to decontaminate drinking water in developing countries. *Journal of Medical Microbiology*, **48**(9), pp.765-787.

Méndez-Hermida, F., Castro-Hermida, J.A., Ares-Mazás, E., Kehoe, S.C. and McGuigan, K.G., (2005). Effect of batch-process solar disinfection on survival of *Cryptosporidium parvum* oocysts in drinking water. *Applied and Environmental Microbiology*, **71**(3), pp.1653-1654.

Metcalf and Eddy (2003) Wastewater Engineering- Treatment, Disposal, Reuse. 4th Edition, Chapter 7, p301-352.

Mihelic, J.R., (1999) Photochemistry and the Atmosphere. In Fundamentals of Environmental Engineering, Wiley and Son, Chapter 3, p123-129.

Monke, D., Ehrt, D., (2004). Irradiation induced defects in glasses resulting in the photoionisation of polyvalent dopants. *Optical Materials*, **25**, pp425-437.

NASA, 2005. Surface Meteorology and Solar Energy. Available from: http://eosweb.larc.nasa.gov/sse/.

Oates, P.M., Shanahan, P., Poltz, M.F. (2003). Solar Disinfection (SODIS): simulation of solar radiation for global assessment and application for point-of-use water treatment in Haiti. *Water Research*, **37**, 1, pp47-54.

Pham, H.N., McDowell, T., Wilkin, E., (1995). Photocatalytically-mediated disinfection of water using TiO_2 as a catalyst and spore-forming *Bacillus pumilus* as a model. *Journal of Environmental Science and Health-Part A: Environmental Science and Engineering and Toxic and Hazardous Substance Control*, **30**, 3, pp627-636.

Pham, H.N., Wilkins, E., Heger, A.S. and Kauffman, D., (1997). Quantitative analysis of variations in initial Bacillus pumilus spore densities in aqueous TiO_2 suspension and design of a photocatalytic reactor. *Journal of Environmental Science and Health*, **A32**(1), pp.153-163.

Play-pump (2005). Information available from www.roundabout.co.za.

Reed, R.H., (1997) Solar Inactivation of Faecal Bacteria in Water: the Critical Role of Oxygen. *Letters in Applied Microbiology*, **24**, p276-280.

Reed, R.H., Mani, S.K., Meyer, V., (2000) Solar Photo-oxidative Disinfection of Drinking Water: Preliminary Field Observations. *Letters in Applied Microbiology*, **30**, p432-436.

Rincon, A.G., Pulgarin, C. (2003) Photocatalytical Inactivation of *E.coli*: effect of (continuous-intermittent) light intensity and of (suspended-fixed) TiO_2 concentration. *Applied Catalysis B: Environmental*, **44**, p263-284.

Rincón, A.G. and Pulgarin, C., (2004). Bactericidal action of illuminated TiO_2 on pure *E.coli* and natural bacterial consortia: post-irradiation events in the dark and assessment of the effective disinfection time. *Applied Catalysis B: Environmental*, **49**, pp.99-112.

Rincón, A.G. and Pulgarin, C., (2004). Field solar *E.coli* inactivation in the absence and presence of TiO_2: is UV solar dose an appropriate parameter for standardization of water solar disinfection?. Solar Energy, **77**, pp.635-648.

Robert, D. and Malato, S., (2002). Solar photocatalysis : a clean process for water detoxification. *Science of the Total Environment*, **291**, pp.85-97.

Roberts, P., Hope, A., (2003). Virus inactivation by high intensity broad spectrum pulsed light. *Journal of Virological Methods*, **110**, 1, pp61-65.

Rolla, T.C., (1998) Sun and Water: An Overview of Solar Water Treatment Devices. *Journal of Env. Health*, **60**, 10, p30-33.

Rottier, E., Ince, M., Controlling and Preventing Disease, The Role of Water and Environmental Sanitation Interventions. WEDC, Loughborough University, UK,

ISBN: 0906055903.

Russell, A.D. (2003), Lethal Effects of Heat on Bacterial Physiology and Structure. *Science Progress*, 86, 1/2, p115-137

Safapour, N., Metcalf, R.H., (1999) Enhancement of Solar Water Pasteurisation with Reflectors. *Applied and Environmental Microbiology*, 65, 2, p859-861.

Saito, T., Iwase, T., Horie, J. and Morioka, T., (1992). Mode of photocatalytic bactericidal of powdered semiconductor TiO_2 on *Mutans Streptococci*. *Journal of Photochemistry and Photobiology B: Biology*, **14**, pp.369-379.

Salih, F.M. (2002) Enhancement of solar inactivation of *Escherichia coli* by titanium dioxide photocatalytic oxidation. *Journal of Applied Microbiology*, **92**, p920-226.

Salih, F.M., (2003). Formulation of a mathematical model to predict solar water disinfection. *Water Research*, **37**, pp.3921-3927.

Sansonetti, P., (1999). *Shigella* plays dangerous games. *ASM news*, **65**, pp.611-617.

Şen, Z., (2004). Solar energy in progress and future research trends. *Progress in Energy and Combustion Science*, **30**, pp367-416.

Serpone, N., Emeline, A.V., (2002). Suggested terms and definitions in photocatalysis and radiocatalysis. *International Journal of Photoenergy*, **4**, pp91-138.

Simate, I.N. (2001) Solar Water Distillation-Zambian Perspective. Proc. 27th WEDC Conference, Lusaka, Zambia.

Sinha, P.R., Hader, D.P., (2002). UV-induced damage and repair: a review. *Photochem. Photobiol. Science*, **1**, pp225-236.

Sommer, B, Marino, A., Solarte, Y., Salas, M.L., Dierolf, C., Valiente, C., Mora, D., Reichsteiner, R., setter, P., Wriojanagud, W., Ajarmeh, H., Al-Hassan, A., Wegelin,

M., (1997) SODIS-An Emerging Water Treatment Process. *Journal of Water Supply Research and Technology- Aqua,* **46**, 3, p127-137.

Smith, R., Kehoe, S., McGuigan, K.G., and Barer, M., (2000). Effects of simulated solar disinfection on infectivity of *Salmonella typhimurium.* *Letters in Applied Microbiology,* **31**, pp.284-288.

Spikes, J., (1977) Photosensitisation. In The Science of Photobiology, K. Smith (ed), Plenum, New York.

Sunada, K., Watanabe, T. and Hashimoto, K., (2003). Studies on photokilling of bacteria on TiO_2 thin film. *Journal of Photochemistry Photobiology A: Chemistry,* **156**, pp.227-233.

Takeshita, K., Shibato, J., Sameshima, T., Fukunaga, S., Isobe, S., Arihara, K., Itoh, M., (2003). Damage to yeast cells induced by pulsed light irradiation. *International Journal of Food Microbiology,* **85**, 1-2, pp151-158.

Tatiestse, T.T. and Rodriguez, M. (2001) A Method to Improve Population Access to Drinking Water Networks in Cities of Developing Countries. *Journal of Water Supply Research and Technology- Aqua,* **50**, 1, pp47-48.
Thom, S.W.D., Drasser, B.S., (1992). Association of *Vibrio cholerae* with fresh water amoebae. *Journal of Medical Microbiology,* 36, pp303-306.

Tortora (1995) Microbiology- An Introduction. The Benjamin-Cummings Publishing Company, 5th Edition.

Twort, A.C., Ratnayaka, D.D., Brandt, M.J., (2000). Water Supply. IWA Publishing, 5th ed. ISBN 0 340 72018 2.

UNESCO (2003) The UN World Water Development Report: Water for People, Water for Life. UNESCO Publishing.

USEPA (1999) Alternative Disinfectants and Oxidants Guidance Manual. EPA 815-

R-99-014, USEPA, April 1999.

USEPA (1993). Preventing Waterborne Disease, A focus on EPA's research. Office of Research and Development, Washington, DC 20460, EPA 640-K-93-001, April 1993.

Vidal, A., Diaz, A.I., (2000) High Performance Low Cost Solar Collectors for Disinfection of Contaminated Water. *Wat. Environ. Res.*, **72**, 3, p271—276

Von Sonntag (1986) Disinfection by Free Radicals and UV Radiation. International Workshop on Water Disinfection, Companie Generale des Eaux, Mulhouse.

Watts, R.J., Kong, S., Orr, M.P., Miller, G.C. and Henry, B.E., (1994). Photocatalytic Inactivation of coliform bacteria and viruses in secondary effluent. Water Research, **29**, 1, pp95-100.

Walker, D.C, Len, S-V. and Sheehan, B., (2004). Development and evaluation of a reflective solar disinfection pouch for the treatment of drinking water. *Applied and Environmental Microbiology*, **70**(4), pp.2545-2550.

Wekhof, A., Trompeter, F.J., Franken, O., (2001). Pulsed UV Disintegration (PUVD): a new sterilisation mechanism for packaging and broad medical-hospital applications. Proc. The First International Conference on Ultraviolet Technologies, Washington D.C., USA.

Wekhof, A., (2000). Disinfection with Flash Lamps. *PDA Journal of Pharmaceutical Science and Technology*, **54**, 3, pp264-276.

Whitelam, G., Codd, G., (1986) Damage to Microorganisms by Light. *Spec. Publ. Soc Gen Microbiology*, **17**, 129-169.

WHO (2000) Millennium Development Goals. Available from www.who.int/mdg/en

WHO (2003) Emerging Issues in Water and Infectious Diseases. World Health

Organisation, 2003, ISBN 92 4 1590823.

Wicklein R.C. (1998) Designing for Appropriate Technology in Developing Countries. *Technology in Society*, **20**, pp371-375.

Wist, J., Sanabria, J., Dierolf, C., Torres, W. and Pulgarin, C., (2002). Evaluation of photocatalytic disinfection of crude water for drinking-water production. *Journal of Photochemistry and Photobiology A: Chemistry*, **147**, pp.241-246.

Wolfe, R.L., (1990) Ultraviolet disinfection of potable water. *Environmental Science Technology*, **24**, 6.

APPENDIX A

STATISTICAL METHODS

A.1 Statistical Methods

1. Mean

The mean is the average of all observed values. To calculate the mean the observed values are added and then divided by the number of values.

$$\bar{x} = \frac{(\sum x)}{n}$$

where,

$\bar{x}$ = the mean

x = each of the observed values

n = number of values

Mean values of inactivation kinetic constants are used throughout this thesis as well as plots showing the mean value of observed values in repeated experiments.

2. Standard Deviation

The standard deviation indicates the spread of deviations around a mean value. The standard deviation is defined as the square root of the variance of a data set (sum of squares of deviations from the mean divided by the number of observations minus one).

$$SD = \sqrt{\frac{\sum (x - \bar{x})^2}{n - 1}}$$

3. Standard Error of the Mean

The standard error of the mean of a sample is the estimate of the standard deviation that would be obtained from the means of a large number of samples drawn from that population.

$$SE = \frac{SD}{\sqrt{n}}$$

The error bars shown on all plots represent the standard error of the mean for each sample.

4. Confidence Interval

The 95% confidence interval is constructed such that 95% of the intervals will include the true mean.

$$95\% CI : \bar{x} \pm z \left[\frac{SD}{\sqrt{n}} \right]$$

where z is dependent on the number of samples and is found using the t-distribution tables.

B.1 Simulated Solar Radiation

B.1.1 Small-Scale Parabolic Reactor: Simulated Solar Radiation (Flowrate)

Flow Regime	k_Q (kJ^{-1})	k_t (min^{-1})	$k_{tillum.}$ (min^{-1})
Laminar	1.13	0.08	0.44
Transitional	1.09	0.07	0.43
Turbulent	0.94	0.07	0.32

B.1.2 Small-Scale Parabolic Reactor: Simulated Solar Radiation (Intensity)

Intensity (W/m^2)	k_Q (kJ^{-1})	k_t (min^{-1})	$k_{tillum.}$ (min^{-1})
9.5	1.93	0.050	0.21
17.5	1.42	0.062	0.30
35.6	0.94	0.067	0.32

B.1.3 Small-Scale Parabolic Reactor: Simulated Solar Radiation (Indicator)

Indicator	Intensity (W/m^2)	k_Q (kJ^{-1})	k_t (min^{-1})	$k_{tillum.}$ (min^{-1})
E. coli	31.6	0.94	0.067	0.32
S. typhimurium	31.6	0.54	0.043	0.19
E. coli	9.5	1.93	0.050	0.21
S. typhimurium	9.5	0.88	0.020	0.10

B.1.4 Small-Scale Parabolic Reactor: Simulated Solar Radiation (Tubing)

Tubing Type	k_Q (kJ^{-1})	k_t (min^{-1})	$k_{tillum.}$ (min^{-1})
Pyrex	0.94	0.07	0.32
Soda Lime	0.94	0.07	0.32

B.1.5 Small-Scale Parabolic Reactor: Simulated Solar Radiation (Batch/Continuous)

Process	k_{Qa} (kJ^{-1})	k_t (min^{-1})	$k_{tillum.}$ (min^{-1})
Batch	2.23	0.066	0.07
Continuous	2.74	0.067	0.31

B.2   Comparison of Solar Disinfection Reactors

B.2.1   *Small-Scale Reactors under Simulated Solar Conditions*

Reactor	k_Q (l.kJ^{-1})	k_t (min^{-1})	$k_{tillum.}$ (min^{-1})
Compound Parabola	1.15	0.13	0.66
Parabola	0.94	0.07	0.41
V-Groove	0.59	0.06	0.34
No Reflector	1.82	0.05	0.26

B.2.2   *Small-Scale Reactors under Natural Solar Conditions (PSA)*

Reactor	k_Q (l.kJ^{-1})	k_{Qa} (l.kJ^{-1})	k_t (min^{-1})	$k_{tillum.}$ (min^{-1})
Compound Parabola	1.15	4.59	0.13	0.66
Parabola	0.94	2.74	0.07	0.41
V-Groove	0.59	2.34	0.06	0.34
No Reflector	1.82	1.82	0.05	0.26

B.2.3   *Small-Scale Reactors under Natural Solar Conditions (Ireland)*

Reactor	k_Q (l.kJ^{-1})	k_{Qa} (l.kJ^{-1})	k_t (min^{-1})	$k_{tillum.}$ (min^{-1})
Compound Parabola	1.96	7.79	0.25	1.32
Parabola	2.08	6.08	0.20	1.03
V-Groove	1.19	4.71	0.13	1.19
No Reflector	2.46	2.46	0.07	2.46

B.2.4   *Compound Parabolic Small-Scale Reactor and Pilot-Scale Reactor 3m^2*

Reactor	k_{Qa} (l.kJ^{-1})	k_t (min^{-1})	$k_{tillum.}$ (min^{-1})
Compound Parabola	3.92	0.11	0.57
Parabola	2.90	0.07	0.36
V-Groove	2.42	0.04	0.21
No Reflector	1.68	0.03	0.18

C.2.5   *Pilot-Scale Reactor 3m^2 and 1m^2*

Reactor	k_{Qa} (l.kJ^{-1})	k_t (min^{-1})	$k_{tillum.}$ (min^{-1})
1m^2	16.16	0.34	1.63
3m^2	5.73	0.35	0.55

B.3   Solar Photocatalytic Disinfection

B.3.1   *Pilot-Scale Reactor (1m^2) with Suspended TiO$_2$*

TiO$_2$ (mg/l)	k_{Qa} (l.kJ^{-1})	$k_{Qa\,illum}$ (l.kJ^{-1})	k_t (min^{-1})	$k_{tillum.}$ (min^{-1})
0	16.16	75.73	0.34	1.68
3	20.55	96.32	0.34	1.68
6	14.27	66.91	0.33	1.54
9	14.42	67.57	0.33	1.52

B.3.2   *Small-Scale Reactor (Compound Parabolic) with Fixed TiO$_2$ (PSA)*

Reactor	TiO$_2$	k_{Qa} (l.kJ^{-1})	$k_{Qa\,illum}$ (l.kJ^{-1})	k_t (min^{-1})	$k_{tillum.}$ (min^{-1})
CP	N	7.79	41.00	0.25	1.32
	Y	8.88	47.27	0.20	1.05
P	N	6.08	32.01	0.19	1.02
	Y	5.49	28.90	0.12	0.63
V	N	4.71	24.80	0.13	0.71
	Y	6.06	32.29	0.16	0.83

B.3.3   *Small-Scale Reactor (Compound Parabolic) with Fixed TiO$_2$ (Ireland)*

TiO$_2$	k_{Qa} (l.kJ^{-1})	$k_{Qa\,illum}$ (l.kJ^{-1})	k_t (min^{-1})	$k_{tillum.}$ (min^{-1})
None	3.92	20.63	0.08	0.40
Rods	4.19	22.28	0.08	0.40
Paper	3.26	17.36	0.06	0.32

B.4 Other Factors which Effect the Solar Disinfection Process

B.4.1   Small Scale Reactor (Parabolic) and Effect of Temperature

Experiment	$k_{Qa\,illum}$ (kJ^{-1})	k_t (min^{-1})	$k_{t\,illum.}$ (min^{-1})
UVA	32.0	0.19	1.02
UVA + 45°C	55.3	0.31	1.57
40°C	-	0.05	-
45°C	-	0.23	-
50°C	-	0.90	-

B.4.2   Small Scale Reactor (Compound Parabolic) and Effect of Volume

Volume	$k_{Qa\,illum}$ (kJ^{-1})	k_t (min^{-1})	$k_{t\,illum.}$ (min^{-1})
1 litre	41.0	0.25	1.32
0.4 litre	6.23	0.23	0.45

B.5 The Stroboscopic Mechanism

B.5.1   Dark Phases in Batch Process Solar Disinfection

Regime	$k_{Qa\,illum}$ $(l.kJ^{-1})$	k_t (min^{-1})	$k_{t\,illum.}$ (min^{-1})
☼	2.32	0.07	0.07
4☼ : 8●	2.35	0.02	0.07
4☼ : 16●	3.32	0.02	0.10
4☼ : 32●	3.86	0.01	0.12

B.5.2   Illuminated-Dark Ratio in Batch Process Solar Disinfection

Regime	$k_{Qa\,illum}$ $(l.kJ^{-1})$	k_t (min^{-1})	$k_{t\,illum.}$ (min^{-1})
☼	1.11	0.03	0.03
1☼ : 1●	1.15	0.02	0.03
2☼ : 2●	1.33	0.02	0.04
4☼ : 4●	1.51	0.02	0.05

B.5.3   *Intermittent Illumination and Continuous Flow Solar Disinfection 1.5m²*

Regime	$k_{Qa\ illum}$ (l.kJ^{-1})	k_{Qa} (l.kJ^{-1})	k_t (min^{-1})	$k_{tillum.}$ (min^{-1})
☼	7.72	2.47	0.08	0.23
2.8☼ : 2.8●	16.09	5.15	0.16	0.51
5.7☼ : 5.7●	11.56	3.70	0.11	0.33
8.5☼ : 8.5●	6.71	2.14	0.07	0.21

B.5.4   *Intermittent Illumination and Continuous Flow Solar Disinfection 1m²*

Regime	$k_{Qa\ illum}$ (l.kJ^{-1})	k_t (min^{-1})	$k_{tillum.}$ (min^{-1})
☼	27.95	0.11	0.53
2.8☼ : 5.7●	34.57	0.13	0.61
0.9☼ : 1.9●	52.62	0.21	0.97
7.6☼ : 15.1●	35.43	0.15	0.71

APPENDIX C

EXPERIMENTAL RESULTS: PLATE COUNTS

C.1 Simulated Solar Radiation

C.1.1 Small-Scale Parabolic Reactor: Simulated Solar Radiation (Flowrate)

Parabolic Small-Scale Reactor (Simulated Sunlight)

Trial A	4th December 2002	Laminar		Trial A	6th December 2002	Transitional
Trial B	5th December 2002	Laminar		Trial B	6th December 2002	Transitional
Trial C	5th December 2002	Laminar		Trial C	6th December 2002	Transitional
Trial D	5th December 2002	Laminar		Trial D	6th December 2002	Transitional

Laminar

Trial A

Time	0		-1		-2		-3		Temp	CFU/ml
0							39	33	24	1800000
15							22	30	25	1300000
30					105	101	12	8	27	515000
45					42	51	8	1	28	233000
60			65	69	8	12			29	33500
75			5	9					30	3500
90	5	1							30	150
105	1	0							30	25
120	3	(250)							30	6

Trial B

Time	0		-1		-2		-3		Temp	CFU/ml
0							24	27	21	1280000
15					107	98	13	13	23	650000
30					31	25	8	5	25	140000
45					22	19	5	0	26	103000
60			46	59	3	12			27	26300
75			18	22	1	4			28	10000
90	48	41							29	2230
105	101	58	(250)						29	318
120	11	14	(250)						29	50

Trial C

Time	0		-1		-2		-3		Temp	CFU/ml
0							19	19	24	950000
15							13	12	25	625000
30					49	49	7	6	27	245000
45					18	17	3	1	28	87500
60			30	29	5	3			29	14800
75			12	14					29	6500
90	39	31	7	7					29	1750
105			1	0					29	250
120	8	7	(250)						30	30

Trial D

Time	0		-1		-2		-3		Temp	CFU/ml
0							14	15	27	725000
15					79	82	6	7	28	403000
30					39	35	11	7	29	185000
45					23	13	3	0	30	90000
60			39	43	11	5			30	20500
75			9	8	2	2			30	3700
90	31	33	3	8					30	1600
105	115	109	(250)						30	448
120	19	16	(250)						30	70

Transitional

Trial A

Time	0		-1		-2		-3		Temp	CFU/ml
0							19	21	22	1000000
15							12	19	27	775000
30							12	21	25	825000
45					35	31	4	5	26	165000
60			82	70					27	38000
75			28	22					28	12500
90	23	48							28	1780
105	17	15	(250)						29	64
120	4	2	(250)						29	12

Trial B

Time	0		-1		-2		-3		Temp	CFU/ml
0							35	42	25	1930000
15							25	33	26	1450000
30							19	14	27	825000
45					33	40	3	9	28	183000
60					18	20			29	95000
75			40	27					30	16800
90	70	70							30	3500
105	10	11							30	525
120	5	18	(250)						30	66

Trial C

Time	0		-1		-2		-3		Temp	CFU/ml
0							32	34	26	1650000
15							18	27	28	1130000
30					70	68	9	13	29	345000
45					22	24			29	115000
60			61	72	12	13			29	33300
75			26	24					29	12500
90	62	54	11	7					29	2900
105	159	151	(250)						30	620
120	14	9	(250)						30	46

Trial D

Time	0		-1		-2		-3		Temp	CFU/ml
0							22	38	26	1500000
15					110	89	13	9	27	498000
30					46	52	6	7	29	245000
45					12	14	2	1	29	65000
60			57	48	4	7			29	26300
75			24	17	1	5			30	10300
90	58	57	5	5					30	2880
105	11	14							30	625
120	3	20	(250)						30	66

Trial A   19th November 2002   Turbulent
Trial B   22nd November 2002   Turbulent
Trial C   26th November 2002   Turbulent
Trial D   27th November 2002   Turbulent

Trial A										
Time	0		-1		-2		-3		Temp	CFU/ml
0							51	48		2480000
15							42	31		1830000
30							25	20		1130000
45					67	88	4	11		388000
60					49	37				215000
75					16	24				100000
90			74	73						36800
105			26	19						11300
120	10	17								675

Trial B										
Time	0		-1		-2		-3		Temp	CFU/ml
0							39	49		2200000
15							24	30		1350000
30							23	13		900000
45					62	64	5	6		315000
60					30	32	7	3		155000
75			87	89	18	10	1	0		70000
90			30	29	4	5				14800
105	100	99	9	15						2730
120	34	27								1530

Trial C										
Time	0		-1		-2		-3		Temp	CFU/ml
0							33	37		1750000
15							32	39		1780000
30							16	18		850000
45					80	70	6	14		375000
60					34	44	2	3		195000
75			103	98	17	14	2	0		77500
90			41	43	2	6				21000
105	77	80								3930
120	23	22								1130

Trial D										
Time	0		-1		-2		-3		Temp	CFU/ml
0							37	40		1930000
15							36	30		1650000
30							17	16		825000
45					42	32	6	5		185000
60			67	50	4	10	2	0		29300
75			14	12						6500
90	6	3								225
105										
120	2	0	(250)							8

C.1.2   Small-Scale Parabolic Reactor: Simulated Solar Radiation (Intensity)

Parabolic Small-Scale Reactor (Simulated Sunlight)

Trial A	10th December 2002	9.5W/m2	Trial A	11th December 2002	17.5W/m2
Trial B	10th December 2002	9.5W/m2	Trial B	12th December 2002	17.5W/m2
Trial C	11th December 2002	9.5W/m2	Trial C	12th December 2002	17.5W/m2
Trial D	11th December 2002	9.5W/m2	Trial D	27th November 2002	17.5W/m2

Trial A (9.5W/m2)

Time	0		-1		-2		-3		Temp	CFU/ml
0					101	95	10	9	23	490000
15					76	84	13	6	25	400000
30					57	45	6	5	25	255000
45					45	44	4	6	25	223000
60					23	24			26	118000
75			77	118	7	8			26	48800
90			49	48	8	5			27	24300
105			20	17	2	3			28	9250
120	56	52	11	12					28	2700

Trial B (9.5W/m2)

Time	0		-1		-2		-3		Temp	CFU/ml
0					124	121	17	11	21	613000
15					87	77	14	12	22	410000
30					66	72	12	6	23	345000
45					47	40	5	1	24	218000
60			129	125	23	16	1	2	25	63500
75			42	36	5	2			26	19500
90			24	18	1	0			26	10500
105	30	25	6	8					27	1380
120	15	16							27	775

Trial C (9.5W/m2)

Time	0		-1		-2		-3		Temp	CFU/ml
0							24	29	23	1330000
15							22	19	23	1030000
30							15	14	24	725000
45					50	56			25	265000
60					39	37	5	3	26	190000
75					20	20			26	100000
90					12	15			26	67500
105			62	75	7	12			26	34300
120			43	39					26	20300

Trial D (9.5W/m2)

Time	0		-1		-2		-3		Temp	CFU/ml
0							38	30	20	1700000
15							19	22	22	1030000
30					81	79	13	14	23	400000
45					50	52	8	11	24	255000
60					40	44			24	210000
75					10	15			25	62500
90			55	56	5	3			27	27800
105			23	32	4	2			27	13800
120			13	11					27	6000

Trial A (17.5W/m2)

Time	0		-1		-2		-3		Temp	CFU/ml
0							18	23	25	1030000
15					69	65	13	5	25	335000
30					63	68	8	10	26	328000
45					33	27	4	3	28	150000
60					16	16			30	80000
75			52	58	4	12			30	27500
90			19	27	4	7			31	11500
105	62	64	9	9					32	3150
120	17	17							33	850

Trial B (17.5W/m2)

Time	0		-1		-2		-3		Temp	CFU/ml
0							29	44	21	1830000
15					119	132	30	23	24	6280000
30					60	65			25	313000
45					37	13			28	125000
60			65	57					27	30500
75			34	44					29	19500
90	54	55							29	2750
105	20	12							29	800
120	6	9							29	375

Trial C (17.5W/m2)

Time	0		-1		-2		-3		Temp	CFU/ml
0							27	25	28	1300000
15							17	25	28	1050000
30							10	15	28	625000
45					45	39	11	4	28	210000
60					18	17			28	87500
75			77	62	11	8			29	34800
90			40	30					29	17500
105			15	10					29	6250
120	32	30							30	1630

Trial D (17.5W/m2)

Time	0		-1		-2		-3		Temp	CFU/ml
0							29	33	26	1550000
15							20	28	28	1200000
30							10	10	28	500000
45					38	46			28	210000
60					15	14			29	72500
75			46	62	4	8			29	27000
90			19	23					29	10500
105	47	49							30	2400
120	16	11							30	675

Trial A								
Time	0		-1		-2		-3	Temp	CFU/ml
0							51	48		2480000
15							42	31		1830000
30							25	20		1130000
45					67	88	4	11		388000
60					49	37				215000
75					16	24				100000
90			74	73						36800
105			26	19						11300
120	10	17								675

Trial B								
Time	0		-1		-2		-3	Temp	CFU/ml
0							39	49		2200000
15							24	30		1350000
30							23	13		900000
45					62	64	5	6		315000
60					30	32	7	3		155000
75			87	89	18	10	1	0		70000
90			30	29	4	5				14800
105	100	99	9	15						2730
120	34	27								1530

Trial C								
Time	0		-1		-2		-3	Temp	CFU/ml
0							33	37		1750000
15							32	39		1780000
30							16	18		850000
45					80	70	6	14		375000
60					34	44	2	3		195000
75			103	98	17	14	2	0		77500
90			41	43	2	6				21000
105	77	80								3930
120	23	22								1130

Trial D								
Time	0		-1		-2		-3	Temp	CFU/ml
0							37	40		1930000
15							36	30		1650000
30							17	16		825000
45					42	32	6	5		185000
60			67	50	4	10	2	0		29300
75			14	12						6500
90	6	3								225
105										
120	2	0	(250)							8

Parabolic Small-Scale Reactor (Simulated Sunlight, 9.5W/m^2)

Trial A	10th December 2002	*E. coli*	Trial A	15th January 2003	*S. Typhimurium*
Trial B	10th December 2002	*E. coli*	Trial B	15th January 2003	*S. Typhimurium*
Trial C	11th December 2002	*E. coli*	Trial C	17th January 2003	*S. Typhimurium*
Trial D	11th December 2002	*E. coli*	Trial D	17th January 2003	*S. Typhimurium*

Trial A (E. coli)

Time	0		-1		-2		-3		Temp	CFU/ml
0					101	95	10	9	23	490000
15					76	84	13	6	25	400000
30					57	45	6	5	25	255000
45					45	44	4	6	25	223000
60					23	24			26	118000
75			77	118	7	8			26	48800
90			49	48	8	5			27	24300
105			20	17	2	3			28	9250
120	56	52	11	12					28	2700

Trial B (E. coli)

Time	0		-1		-2		-3		Temp	CFU/ml
0					124	121	17	11	21	613000
15					87	77	14	12	22	410000
30					66	72	12	6	23	345000
45					47	40	5	1	24	218000
60			129	125	23	16	1	2	25	63500
75			42	36	5	2			26	19500
90			24	18	1	0			26	10500
105	30	25	6	8					27	1380
120	15	16							27	775

Trial C (E. coli)

Time	0		-1		-2		-3		Temp	CFU/ml
0							24	29	23	1330000
15							22	19	23	1030000
30							15	14	24	725000
45					50	56			25	265000
60					39	37	5	3	26	190000
75					20	20			26	100000
90					12	15			26	67500
105			62	75	7	12			26	34300
120			43	39					26	20300

Trial D (E. coli)

Time	0		-1		-2		-3		Temp	CFU/ml
0							38	30	20	1700000
15							19	22	22	1030000
30					81	79	13	14	23	400000
45					50	52	8	11	24	255000
60					40	44			24	210000
75					10	15			25	62500
90			55	56	5	3			27	27800
105			23	32	4	2			27	13800
120			13	11					27	6000

Trial A (S. Typhimurium)

Time	0		-1		-2		-3		Temp	CFU/ml
0					60	70			23	325000
15					75	54			25	323000
30					36	49			26	213000
45					37	38			26	188000
60					35	34			27	173000
75					32	28			28	150000
90					22	22			28	110000
105					18	16			29	85000
120					17	11			29	70000

Trial B (S. Typhimurium)

Time	0		-1		-2		-3		Temp	CFU/ml
0					63	79	8	6	21	355000
15					72	73	13	8	23	363000
30					51	56	5	8	24	268000
45					48	45	4	8	25	233000
60					34	31	3	3	25	163000
75					28	24	1	4	26	130000
90					15	19	4	2	27	85000
105					19	19			27	95000
120					15	11	2	1	28	65000

Trial C (S. Typhimurium)

Time	0		-1		-2		-3		Temp	CFU/ml
0							13	13	24	650000
15							12	11	24	575000
30					63	63			25	315000
45					35	33			25	170000
60					30	35			26	163000
75					15	19			26	85000
90					19	22			26	103000
105			107	70					27	44300
120			50	51					27	25300

Trial D (S. Typhimurium)

Time	0		-1		-2		-3		Temp	CFU/ml
0					77	94	12	6	26	428000
15					63	45	8	3	26	270000
30					38	50			27	220000
45							5	3	27	200000
60					20	16			28	90000
75					18	11			28	72500
90			57	38	10	5			29	23800
105			44	36					29	20000
120			27	30					30	14300

Parabolic Small-Scale Reactor (Simulated Sunlight, 31.6W/m²)

Trial A	19th November 2002	*E. coli*	
Trial B	22nd November 2002	*E. coli*	
Trial C	26th November 2002	*E. coli*	
Trial D	27th November 2002	*E. coli*	

Trial A	21st January 2003	*S. Typhimurium*	
Trial B	21st January 2003	*S. Typhimurium*	
Trial C	22nd January 2003	*S. Typhimurium*	
Trial D	22nd January 2003	*S. Typhimurium*	

Trial A (E. coli)

Time	0		-1		-2		-3		Temp	CFU/ml
0							51	48		2480000
15							42	31		1830000
30							25	20		1130000
45					67	88	4	11		388000
60					49	37				215000
75					16	24				100000
90			74	73						36800
105			26	19						11300
120	10	17								675

Trial B (E. coli)

Time	0		-1		-2		-3		Temp	CFU/ml
0							39	49		2200000
15							24	30		1350000
30							23	13		900000
45					62	64	5	6		315000
60					30	32	7	3		155000
75			87	89	18	10	1	0		70000
90			30	29	4	5				14800
105	100	99	9	15						2730
120	34	27								1530

Trial C (E. coli)

Time	0		-1		-2		-3		Temp	CFU/ml
0							33	37		1750000
15							32	39		1780000
30							16	18		850000
45					80	70	6	14		375000
60					34	44	2	3		195000
75			103	98	17	14	2	0		77500
90			41	43	2	6				21000
105	77	80								3930
120	23	22								1130

Trial D (E. coli)

Time	0		-1		-2		-3		Temp	CFU/ml
0							37	40		1930000
15							36	30		1650000
30							17	16		825000
45					42	32	6	5		185000
60			67	50	4	10	2	0		29300
75			14	12						6500
90	6	3								225
105										
120	2	0	(250)							8

Trial A (S. Typhimurium)

Time	0		-1		-2		-3		Temp	CFU/ml
0							20	27	23	1180000
15							16	16	25	800000
30							16	15	25	775000
45					94	78	13	4	27	430000
60					55	43			28	245000
75					25	23			29	120000
90					15	14			29	72500
105			72	77	12	8			30	3730
120			27	33					30	1500

Trial B (S. Typhimurium)

Time	0		-1		-2		-3		Temp	CFU/ml
0							20	21	22	1030000
15							18	17	25	875000
30			67	93					27	400000
45			55	65					28	300000
60			35	39					30	185000
75			21	17					30	95000
90		83	90						31	43300
105		88	65						32	38300
120		46	35						33	20300

Trial C (S. Typhimurium)

Time	0		-1		-2		-3		Temp	CFU/ml
0							20	16	27	900000
15			109	72	7	13			30	453000
30					7	8			30	375000
45			34	33					31	168000
60			20	17					31	92500
75		100	104	6	14				31	51000
90		68	68						32	34000
105		40	35						32	18800
120		31	29						32	15000

Trial D (S. Typhimurium)

Time	0		-1		-2		-3		Temp	CFU/ml
0							13	12	27	625000
15					34	36			29	175000
30					20	17			30	92500
45			51	62					32	28300
60			39	38					33	19300
75			18	19					33	9250
90			10	17					33	6750
105	57	58							33	2880
120	32	28							33	1500

Parabolic Small-Scale Reactor (Tubing)

Trial A	19th November 2002	Pyrex		Trial A	21st January 2003	Soda Lime
Trial B	22nd November 2002	Pyrex		Trial B	21st January 2003	Soda Lime
Trial C	26th November 2002	Pyrex		Trial C	22nd January 2003	Soda Lime
Trial D	27th November 2002	Pyrex		Trial D	22nd January 2003	Soda Lime

Trial A (Pyrex)

Time	0		-1		-2		-3		Temp	CFU/ml
0							51	48		2480000
15							42	31		1830000
30							25	20		1130000
45					67	88	4	11		388000
60					49	37				215000
75					16	24				100000
90			74	73						36800
105			26	19						11300
120	10	17								675

Trial B (Pyrex)

Time	0		-1		-2		-3		Temp	CFU/ml
0							39	49		2200000
15							24	30		1350000
30							23	13		900000
45					62	64	5	6		315000
60					30	32	7	3		155000
75			87	89	18	10	1	0		70000
90			30	29	4	5				14800
105	100	99	9	15						2730
120	34	27								1530

Trial C (Pyrex)

Time	0		-1		-2		-3		Temp	CFU/ml
0							33	37		1750000
15							32	39		1780000
30							16	18		850000
45					80	70	6	14		375000
60					34	44	2	3		195000
75			103	98			2	0		77500
90			41	43	2	6				21000
105	77	80								3930
120	23	22								1130

Trial D (Pyrex)

Time	0		-1		-2		-3		Temp	CFU/ml
0							37	40		1930000
15							36	30		1650000
30							17	16		825000
45					42	32	6	5		185000
60			67	50	4	10	2	0		29300
75			14	12						6500
90	6	3								225
105										
120	2	0	(250)							8

Trial A (Soda Lime)

Time	0		-1		-2		-3		Temp	CFU/ml
0					57	55	6	6	21	280000
15					45	35	8	6	23	200000
30			64	64	7	11			25	32000
45			36	26					27	15500
60			21	23					27	11000
75			11	9					28	5000
90			7	4					28	2750
105	7	2							29	225
120	1	1							29	50

Trial B (Soda Lime)

Time	0		-1		-2		-3		Temp	CFU/ml
0							13	13	24	650000
15					77	72	14	8	26	373000
30					31	38			28	173000
45										
60			15	29					30	11000
75			4	10					30	3500
90			5	3					30	2000
105	6	8							30	350
120	1	1							30	50

Trial C (Soda Lime)

Time	0		-1		-2		-3		Temp	CFU/ml
0							23	23	24	1150000
15					56	64	4	8	28	305000
30					27	36			30	158000
45					12	14			30	65000
60			31	45					30	19000
75			16	11					30	6750
90			5	5					30	2500
105	22	23							30	1130
120	3	1							30	100

Trial D (Soda Lime)

Time	0		-1		-2		-3		Temp	CFU/ml
0							23	16	25	975000
15					39	42			28	203000
30					13	15			29	70000
45			27	26					30	13300
60			2	4					30	1500
75			1	1					30	500
90									30	
105									31	
120									31	

Parabolic Small-Scale Reactor (Simulated Sunlight, 31.6W/m²)

Trial A	19th November 2002	CF		Trial A	5th April 2004	Batch
Trial B	22nd November 2002	CF		Trial B	5th April 2004	Batch
Trial C	26th November 2002	CF				
Trial D	27th November 2002	CF				

Trial A

Time	0		-1		-2		-3		Temp	CFU/ml
0							51	48		2480000
15							42	31		1830000
30							25	20		1130000
45					67	88	4	11		388000
60					49	37				215000
75					16	24				100000
90			74	73						36800
105			26	19						11300
120	10	17								675

Trial B

Time	0		-1		-2		-3		Temp	CFU/ml
0							39	49		2200000
15							24	30		1350000
30							23	13		900000
45					62	64	5	6		315000
60					30	32	7	3		155000
75			87	89	18	10	1	0		70000
90			30	29	4	5				14800
105	100	99	9	15						2730
120	34	27								1530

Trial C

Time	0		-1		-2		-3		Temp	CFU/ml
0							33	37		1750000
15							32	39		1780000
30							16	18		850000
45					80	70	6	14		375000
60					34	44	2	3		195000
75			103	98	17	14	2	0		77500
90			41	43	2	6				21000
105	77	80								3930
120	23	22								1130

Trial D

Time	0		-1		-2		-3		Temp	CFU/ml
0							37	40		1930000
15							36	30		1650000
30							17	16		825000
45					42	32	6	5		185000
60			67	50	4	10	2	0		29300
75			14	12						6500
90	6	3								225
105										
120	2	0	(250)							8

Trial A

Time	0		-1		-2		-3		Temp	CFU/ml
0							22	24		1150000
15					65	60	8	10		313000
30					24	25				123000
45					15	10				62500
60			39	30						17300
75			18	22						10000
90			6	9						3750
105	2		4							1500
120	3		2							1250

Trial B

Time	0		-1		-2		-3		Temp	CFU/ml
0							22	24		1150000
15					50	51	6	8		253000
30					27	24	1	1		128000
45			74	75	8	12	2	2		37300
60			31	22	7	3				13300
75			8	8	0	3				4000
90			1	1						500
105			1	0						250
120	1		0							250

C.2 Comparison of Solar Disinfection Reactors

C.2.1 Small-Scale Reactors under Simulated Solar Conditions

Small-Scale Reactors (Simulated Sunlight)

Trial A	17th October 2002	Compound Parabolic	Trial A	19th November 2002	Parabolic
Trial B	22nd October 2002	Compound Parabolic	Trial B	22nd November 2002	Parabolic
Trial C	23rd October 2002	Compound Parabolic	Trial C	26th November 2002	Parabolic
Trial D	25th October 2002	Compound Parabolic	Trial D	27th November 2002	Parabolic
Trial E	31st October 2002	Compound Parabolic			

Trial A

Time	0		-1		-2		-3		Temp	CFU/ml
0					46	58	5	8		325000
15					47	46				232000
30					28	25				133000
45			94	87	13	7				45250
60			54	48	2	0				25500
75			21	22						10750
90	57	67	11	7						3100
105	8	4	2	0						300
120										1

Trial B

Time	0		-1		-2		-3		Temp	CFU/ml
0					70	76	9	7		365000
15					37	39				19000058500
30			107	122	13	9				15800
45			29	34						2880
60	55	60	26	11						2100
75	54	30	6	7						176
90	37	16	2	13	(250)					4
105	1	0								6
120										1

Trial C

Time	0		-1		-2		-3		Temp	CFU/ml
0					112	77	10	11		473000
15			125	115	14	8	5	9		60000
30			29	33	4	6	2	3		15500
45			7	3	2	0	5	0		2500
60	5	4	5	1						225
75	1	0								25
90										1
105										
120										

Trial D

Time	0		-1		-2		-3		Temp	CFU/ml
0							39	34		1830000
15					66	59	40	28		1700000
30			148	13	9	18				313000
45			36	28						70000
60			13	6						16000
75	81	86								4180
90	10	17								348
105	2	0								34
120										1

Trial E

Time	0		-1		-2		-3		Temp	CFU/ml
0							70	53		3080000
15							22	20		1050000
30					61	64				313000
45	63	57	12	10						30000
60	5	13								142
75										28
90										8
105										1

Trial A

Time	0		-1		-2		-3		Temp	CFU/ml
0							51	48		2480000
15							42	31		1830000
30							25	20		1130000
45					67	88	4	11		388000
60					49	37				215000
75					16	24				100000
90			74	73						36800
105			26	19						11300
120	10	17								675

Trial B

Time	0		-1		-2		-3		Temp	CFU/ml
0							39	49		2200000
15							24	30		1350000
30							23	13		900000
45					62	64	5	6		315000
60					30	32	7	3		155000
75			87	89	18	10	1	0		70000
90			30	29	4	5				14800
105	100	99	9	15						2730
120	34	27								1530

Trial C

Time	0		-1		-2		-3		Temp	CFU/ml
0							33	37		1750000
15							32	39		1780000
30							16	18		850000
45					80	70	6	14		375000
60					34	44	2	3		195000
75			103	98	17	14	2	0		77500
90			41	43	2	6				21000
105	77	80								3930
120	23	22								1130

Trial D

Time	0		-1		-2		-3		Temp	CFU/ml
0							37	40		1930000
15							36	30		1650000
30							17	16		825000
45					42	32	6	5		185000
60			67	50	4	10	2	0		29300
75			14	12						6500
90	6	3								225
105										
120	2	0	(250)							8

Trial A (V-Groove)

Time	0		-1		-2		-3		Temp	CFU/ml
0							39	34		1880000
15							24	16		1000000
30					105	109	13	10		535000
45					45	38	6	5		208000
60					24	9				82500
75			70	83	14	12				38300
90			27	33						15000
105	20	30	3	4						1250
120	1	2								124

Trial B (V-Groove)

Time	0		-1		-2		-3		Temp	CFU/ml
0							37	35		1800000
15							12	14		650000
30					47	40	10	6		218000
45					15	15	2	1		75000
60			90	78	15	13	3	0		42000
75			64	64	10	6	2	0		32000
90			39	41	2	7				20000
105			19	27						11500
120	94	79								4330

Trial C (V-Groove)

Time	0		-1		-2		-3		Temp	CFU/ml
0							39	41		2000000
15							33	30		1580000
30					178	151	17	25		1050000
45					68	74	10	10		355000
60					42	62	6	5		260000
75			101	117	11	18	4	1		54500
90			54	50	6	4				2600
105	54	62	6	8						590
120	156	139	(250)							

Trial D (V-Groove)

Time	0		-1		-2		-3		Temp	CFU/ml
0							55	36		2280000
15							23	28		1280000
30							16	11		675000
45					37	58	7	4		238000
60					17	23	4	3		100000
75			62	75	13	6	3	1		34300
90					6	1				17500
105	56	52								2700
120	13	19								800

Trial A (No Reflector)

Time	0		-1		-2		-3		Temp	CFU/ml
0							48	52		2500000
15							33	29		1550000
30							23	7		750000
45							14	11		625000
60					35	32				168000
75					17	16				82500
90			78	89						41800
105	155	176								8280
120	86	84								4250

Trial B (No Reflector)

Time	0		-1		-2		-3		Temp	CFU/ml
0							57	42		2480000
15							44	48		2300000
30							33	28		1530000
45							25	27		1300000
60							15	12		675000
75					54	65	4	9		298000
90			55	111						41500
105			61	99						40000
120			29	43						18000

Trial C (No Reflector)

Time	0		-1		-2		-3		Temp	CFU/ml
0							34	27		1530000
15							38	39		1930000
30							34	34		1700000
45							17	21		950000
60					89	80	4	7		423000
75					38	33	2	8		178000
90			82	79	11	15				40300
105			46	49	7	4				23800
120			14	17						7750

Trial D (No Reflector)

Time	0		-1		-2		-3		Temp	CFU/ml
0							41	37		1950000
15							35	32		1680000
30							18	19		925000
45					87	70	5	13		393000
60					43	33	5	8		190000
75					25	24	2	0		123000
90			66	73	11	10				34800
105			24	43						16800
120	99	73								4300

C.2.2 Small-Scale Reactors under Natural Solar Conditions (PSA)

Small-Scale Reactors (Natural Sunlight PSA)

Trial A	19th June 2003	Compound Parabolic	Trial A	18th June 2003	Parabolic
Trial B	19th June 2003	Compound Parabolic	Trial B	19th June 2003	Parabolic
Trial C	20th June 2003	Compound Parabolic	Trial C	20th June 2003	Parabolic
Trial D	18th June 2003	Compound Parabolic	Trial D	18th June 2003	Parabolic
Trial E	19th June 2003	Compound Parabolic	Trial E	19th June 2003	Parabolic

Trial A (Compound Parabolic)

Time	0		-1		-2		-3		Temp	CFU/ml
0							14	11	35	625000
10					57	65			35	305000
20			103	62	7	1			35	41250
30	1	7	1	0					35	200
40	0	0							35	1
50									35	
60									36	

Trial B (Compound Parabolic)

Time	0		-1		-2		-3		Temp	CFU/ml
0							67	79	28	3650000
10					139	130			32	672500
20					67	64			33	327500
30			135	142					34	69250
40			21	13					35	8500
50	3	2							36	125
60	2	0							36	50

Trial C (Compound Parabolic)

Time	0		-1		-2		-3		Temp	CFU/ml
0							55	66	28	3025000
10					69	83			31	380000
20					49	52			33	252500
30			82	68	36	32			35	37500
40	104	95							35	4975
50	26	27							36	1325
60									36	1

Trial D (Compound Parabolic)

Time	0		-1		-2		-3		Temp	CFU/ml
0							25	25	31	1250000
10					49	44			30	232500
20			54	50					30	26000
30	25	19							36	1100
40	0	0							36	1
50									36	
60									37	

Trial E (Compound Parabolic)

Time	0		-1		-2		-3		Temp	CFU/ml
0							74	76	30	3750000
10					140	150			34	725000
20					65	83			36	370000
30			193	177					37	92500
40			22	21					37	10750
50	36	27							38	1575
60	2	1							38	75

Trial A (Parabolic)

Time	0		-1		-2		-3		Temp	CFU/ml
0					40	38	8	7	35	195000
10					31	22			35	133000
20					1	0			35	2500
30									35	1
40									35	
50									35	
60									35	

Trial B (Parabolic)

Time	0		-1		-2		-3		Temp	CFU/ml
0							50	55	28	2630000
10					47	58			32	263000
20					43	48			33	228000
30			111	97					34	52000
40	50	54							35	2600
50	2	0							36	50
60									36	1

Trial C (Parabolic)

Time	0		-1		-2		-3		Temp	CFU/ml
0							62	56	28	2950000
10					69	122			31	478000
20					59	63			33	305000
30					33	42			34	188000
40			97	90					34	46800
50	119	105							35	5600
60	80	82							35	4050

Trial D (Parabolic)

Time	0		-1		-2		-3		Temp	CFU/ml
0							8	11	31	475000
10			88	81	9	13			30	42200
20			1	0					30	250
30									36	1
40									37	
50									37	
60									38	

Trial E (Parabolic)

Time	0		-1		-2		-3		Temp	CFU/ml
0							42	45	29	2430000
10					83	113			34	490000
20					57	62			36	298000
30			104	95					36	49800
40	51	29							36	2000
50	1	1							37	50
60									37	1

Trial A

Time	0		-1		-2		-3		Temp	CFU/ml
0							47	50	29	2430000
10					103	107			34	525000
20					60	51			36	278000
30			113	82					39	48800
40	30	41							40	1780
50	2	1							40	75
60	0	1							41	25

Trial B

Time	0		-1		-2		-3		Temp	CFU/ml
0							80	77	32	3930000
10					134	132			26	665000
20					95	88			26	458000
30					63	57			32	300000
40					50	45			33	238000
50			148	148					33	74000
60			82	97					33	44800

Trial C

Time	0		-1		-2		-3		Temp	CFU/ml
0							72	58	26	3250000
10							30	24	28	1350000
20					77	78			30	388000
30					37	28			32	163000
40					30	22			34	130000
50			14	16					35	7500
60			18	20					35	9500

Trial D

Time	0		-1		-2		-3		Temp	CFU/ml
0							73	95	29	4200000
10					148	142			33	725000
20					75	105			35	450000
30					61	61			36	305000
40					26	24			36	125000
50			89	80					36	42300
60	47	47	6	16					36	2350

Trial E

Time	0		-1		-2		-3		Temp	CFU/ml
0							48	50	29	2450000
10					67	68			35	338000
20					44	37			36	203000
30					15	16			37	77500
40	26	27							38	1330
50	2	2							38	100
60									39	1

Trial A

Time	0		-1		-2		-3		Temp	CFU/ml
0							37	32	28	1725000
10					124	156			34	707500
20					11	137			36	637500
30					63	71			39	360000
40			162	185	36	35			40	177500
50			69	57					40	31500
60			55	39					41	23500

Trial B

Time	0		-1		-2		-3		Temp	CFU/ml
0							76	56	32	3300000
10					122	101			29	558000
20					122	129			31	628000
30					63	62			32	313000
40					62	53			33	288000
50			203	194					34	99300
60			150	114					34	66000

Trial C

Time	0		-1		-2		-3		Temp	CFU/ml
0							68	66	26	3350000
10							24	26	30	1250000
20					106	114			31	550000
30					66	50			32	290000
40			138	99	44	50			35	235000
50			62	60					35	30500
60			28	32					35	15000

Trial D

Time	0		-1		-2		-3		Temp	CFU/ml
0							78	84	29	4050000
10					170	151			33	803000
20					126	110			35	590000
30					88	80			36	420000
40					55	53			36	270000
50			173	189					36	90500
60			94	91					36	46300

Trial E

Time	0		-1		-2		-3		Temp	CFU/ml
0							69	83	29	3800000
10					122	112			35	585000
20					77	111			36	470000
30					42	56			37	245000
40			136	75	28	35			38	158000
50			105	82					39	46800
60			44	50					39	23500

Small-Scale Reactors (Natural Sunlight Ireland)

Trial A	9th September 2004	Compound Parabolic
Trial B	16th September 2004	Compound Parabolic
Trial C	17th September 2004	Compound Parabolic

Trial A	11th September 2003	Parabolic
Trial B	16th September 2003	Parabolic
Trial C	17th September 2003	Parabolic

Trial A

Time	0		-1		-2		-3		Temp	CFU/ml
0							50	72	23	3050000
15							32	31	23	1575000
30							51	46	23	2425000
45							23	20	23	1075000
60					44	43	9	11	20	210000
75					87	87			21	435000
90					54	43			23	242500
105					28	25			23	132500
120			54	62					25	29000
135			14	22					24	9000
150			0	0					24	1
165			1	0					24	25
180			0	0					24	1

Trial B

Time	0		-1		-2		-3		Temp	CFU/ml
0							85	64	24	3725000
15							25	32	24	1425000
30							15	15	25	750000
45					71	69			26	350000
60					22	39			27	152500
75					4	7			27	27500
90			49	50					28	24750
105			16	20					29	9000
120			0	0					29	1
135									29	
150									29	
165									29	
180									29	

Trial C

Time	0		-1		-2		-3		Temp	CFU/ml
0							62	70	29	3300000
15							25	32	30	1425000
30							22	16	30	950000
45					42	54			30	240000
60					13	11			30	60000
75			0	0					30	1
90									30	
105									29	
120									29	
135									29	
150									30	
165									31	
180									32	

Trial A

Time	0		-1		-2		-3		Temp	CFU/ml
0							80	96	24	4400000
15							37	28	23	1625000
30							37	43	23	2000000
45							25	29	23	1350000
60							17	17	20	850000
75					80	75			21	387500
90					42	44			23	215000
105			124	101	12	7			23	56250
120			37	27					25	16000
135			32	45					24	19250
150			23	25					24	12000
165			5	5					24	2500
180									24	1

Trial B

Time	0		-1		-2		-3		Temp	CFU/ml
0							64	66	24	3250000
15							18	20	24	950000
30							12	18	25	750000
45							19	13	26	800000
60							7	12	26	500000
75					30	32			27	155000
90					14	17			27	77500
105			60	53	13	9			28	28300
120									29	
135	22	20							29	1050
150	10	12							29	550
165	2	0							29	50
180	10	4							29	350

Trial C

Time	0		-1		-2		-3		Temp	CFU/ml
0							57	75	29	3300000
15							33	35	30	1700000
30							16	19	30	875000
45					48	52			30	250000
60					29	31			30	150000
75			48	53	8	10			30	25300
90			25	17					29	10500
105			18	12					28	7500
120									29	
135	5	6							2	275
150	2	2							29	100
165									29	
180									29	1

Trial A										
Time	0		-1		-2		-3		Temp	CFU/ml
0							45	27	20	1800000
15							20	18	19	950000
30							15	8	19	575000
45					49	55			18	260000
60					19	14			17	82500
75			56	47					18	25750
90			30	21					16	20250
105									16	
120									16	
135									16	
150									16	
165									16	
180									17	

Trial B										
Time	0		-1		-2		-3		Temp	CFU/ml
0							23	22	28	1130000
15							22	8	23	750000
30					112	89			23	503000
45					27	24			23	128000
60					3	8			22	27500
75					42	38			21	200000
90									17	
105									19	
120			76	66					19	35000
135									19	
150			38	42					18	21300
165	138	131							18	13450
180									18	

Trial C										
Time	0		-1		-2		-3		Temp	CFU/ml
0							41	55	27	2400000
15							29	33	24	1550000
30							21	14	24	875000
45							15	10	22	625000
60									23	
75					15	13			23	70000
90					32	32			24	160000
105									24	
120					4	6			23	25000
135									22	
150									21	
165									21	
180									21	

Trial A										
Time	0		-1		-2		-3		Temp	CFU/ml
0							33	40	20	1825000
15							32	28	19	1500000
30							20	17	19	925000
45							12	10	19	550000
60					66	64	6	8	18	325000
75					49	38			16	2.17ee5
90					28	30			17	145000
105									16	
120									16	
135									16	
150	36	46							15	20500
165	23	18							16	1025
180									17	

Trial B										
Time	0		-1		-2		-3		Temp	CFU/ml
0							37	39	28	1900000
15							23	19	24	1050000
30							23	20	23	1080000
45							16	10	22	650000
60							9	10	21	475000
75					63	68			20	328000
90									17	
105					45	34			19	198000
120			105	46					19	62800
135									19	
150			117	107					17	56000
165									18	
180			6	12					18	4300

Trial C										
Time	0		-1		-2		-3		Temp	CFU/ml
0							47	50	27	2430000
15							29	27	24	1400000
30							18	15	24	825000
45									22	
60							10	7	23	425000
75					40	38			23	195000
90					13	25			23	95000
105					6	18			22	60000
120			39	43					21	20500
135			45	50					21	23800
150			36	23					21	14800
165			23	23					21	11500
180			7	10					21	4250

C.2.4 *Compound Parabolic Small-Scale Reactor and Pilot-Scale Reactor 3m²*

Compund ParabolicSmall-Scale Reactor Pilot-Scale Reactor 3m²

Trial A	19th June 2003	Compound Parabolic	Trial A	24th June 2003	Pilot Scale 3m²
Trial B	19th June 2003	Compound Parabolic	Trial B	25th June 2003	Pilot Scale 3m²
Trial C	20th June 2003	Compound Parabolic	Trial C	2nd July 2003	Pilot Scale 3m²
Trial D	18th June 2003	Compound Parabolic			
Trial E	19th June 2003	Compound Parabolic			

Trial A (Compound Parabolic)

Time	0		-1		-2		-3		Temp	CFU/ml
0							14	11	35	625000
10					57	65			35	305000
20			103	62	7	1			35	41250
30	1	7	1	0					35	200
40	0	0							35	1
50									35	
60									36	

Trial B (Compound Parabolic)

Time	0		-1		-2		-3		Temp	CFU/ml
0							67	79	28	3650000
10					139	130			32	672500
20					67	64			33	327500
30			135	142					34	69250
40			21	13					35	8500
50	3	2							36	125
60	2	0							36	50

Trial C (Compound Parabolic)

Time	0		-1		-2		-3		Temp	CFU/ml
0							55	66	28	3025000
10					69	83			31	380000
20					49	52			33	252500
30			82	68	36	32			35	37500
40	104	95							35	4975
50	26	27							36	1325
60									36	1

Trial D (Compound Parabolic)

Time	0		-1		-2		-3		Temp	CFU/ml
0							25	25	31	1250000
10					49	44			30	232500
20			54	50					30	26000
30	25	19							36	1100
40	0	0							36	1
50									36	
60									37	

Trial E (Compound Parabolic)

Time	0		-1		-2		-3		Temp	CFU/ml
0							74	76	30	3750000
10					140	150			34	725000
20					65	83			36	370000
30			193	177					37	92500
40			22	21					37	10750
50	36	27							38	1575
60	2	1							38	75

Trial A (Pilot Scale 3m²)

Time	0		-1		-2		-3		Temp	CFU/ml
0							20	23	41.7	1075000
10			86	61	8	11	1	0	42.5	36750
20			2	1					42.8	750
30	9	14							42.8	575
40	4	5							42.8	225
50									43.2	1
60	5	4							43.5	225
80	2	4							43.7	250
100	1	0							43.8	25
120	1	0							44	25
140									44.3	

Trial B (Pilot Scale 3m²)

Time	0		-1		-2		-3		Temp	CFU/ml
0							48	45	32.1	2325000
5					86	96			38.1	455000
10			91	78	18	11			38.9	72500
15									39.6	2300
20	47	45							40.4	350
25	6	8							40.9	1000
30	21	19							41.6	250
40	1	9							42.6	650
50	10	16							43.6	175
60	3	4							44.6	300
80	5	7							46	25
100	1	0							46.4	25
120	1	0							46.3	25

Trial B (Pilot Scale 3m²)

Time	0		-1		-2		-3		Temp	CFU/ml
0							42	45	39.5	2175000
5					117	125			40.2	605000
10			53	56					40.5	27250
15			14	21					40.8	8750
20	27	24							41.2	1275
25	3	2							41.5	125
30	0	0							42.4	1
40	5	7							42.3	300
50	1	3							43.2	100
60	4	1							43.9	125
80	1	5							44.6	150
100	1	0							44.7	25
120									45.8	1

C.2.4   *Pilot-Scale Reactor 3m² and 1m²*

Pilot-Scale Reactor 3m² and 1m²

Trial A	3rd July 2003	Pilot Scale 1m²	
Trial B	8th July 2003	Pilot Scale 1m²	
Trial C	9th July 2003	Pilot Scale 1m²	

Trial A	24th June 2003	Pilot Scale 3m²	
Trial B	25th June 2003	Pilot Scale 3m²	
Trial C	2nd July 2003	Pilot Scale 3m²	

Trial A (1m²)

Time	0		-1		-2		-3		Temp	CFU/ml
0							8	13	36.9	525000
5					21	19			37.9	100000
10			13	16					38.7	7250
15	27	20							39.2	1175
20	11	2							39.8	325
25	1	2							40	75
30	7	4							40.5	1
40	2	0							41.5	50
50	1	1							42.3	50
60	1	2							42.8	75
80	2	1							44.8	75
100	0	0							46	1

Trial B (1m²)

Time	0		-1		-2		-3		Temp	CFU/ml
0							7	13	38.6	500000
5					34	41			39.2	187500
10			55	70	9	8			39.6	31250
15			11	15					39.9	6500
20	17	20							40.2	925
25	4	5							40.6	225
30	2	1							41	75
40	1	2							41.4	75
50	3	0							41.8	75
60	6	0							42.4	150
80	1	0							43.2	25
100	2	0							44	50
120	0	0							44.7	1

Trial C (1m²)

Time	0		-1		-2		-3		Temp	CFU/ml
0							14	7	37.7	525000
5					17	24			38.6	102500
10			14	18	9	2			39.4	8000
15	11	8							40	475
20	4	1							40.7	125
25	3	0							41.5	75
30	1	0							42	25
40	0	0							43	1
50	0	0							43.6	1
60	0	0							44	1
80	1	0							44.5	25
100	0	0							45	1
120									45.5	
40			22	21					37	10750
50	36	27							38	1575
60	2	1							38	75

Trial A (3m²)

Time	0		-1		-2		-3		Temp	CFU/ml
0							20	23	41.7	1075000
10			86	61	8	11	1	0	42.5	36750
20			2	1					42.8	750
30	9	14							42.8	575
40	4	5							42.8	225
50									43.2	1
60	5	4							43.5	225
80	2	4							43.7	250
100	1	0							43.8	25
120	1	0							44	25
140									44.3	

Trial B (3m²)

Time	0		-1		-2		-3		Temp	CFU/ml
0							48	45	32.1	2325000
5					86	96			38.1	455000
10			91	78	18	11			38.9	72500
15									39.6	2300
20	47	45							40.4	350
25	6	8							40.9	1000
30	21	19							41.6	250
40	1	9							42.6	650
50	10	16							43.6	175
60	3	4							44.6	300
80	5	7							46	25
100	1	0							46.4	25
120	1	0							46.3	25

Trial B (3m²)

Time	0		-1		-2		-3		Temp	CFU/ml
0							42	45	39.5	2175000
5					117	125			40.2	605000
10			53	56					40.5	27250
15			14	21					40.8	8750
20	27	24							41.2	1275
25	3	2							41.5	125
30	0	0							42.4	1
40	5	7							42.3	300
50	1	3							43.2	100
60	4	1							43.9	125
80	1	5							44.6	150
100	1	0							44.7	25
120									45.8	1

C.3.1 Pilot-Scale Reactor ($1m^2$) with Suspended TiO_2

Pilot-Scale Reactor ($1m^2$)

Trial A	3rd July 2003	
Trial B	8th July 2003	
Trial C	9th July 2003	

Trial A	10th July 2003	3mg/l TiO_2
Trial B	10th July 2003	6mg/l TiO_2
Trial C	10th July 2003	9mg/l TiO_2

Trial A (3rd July 2003)

Time	0		-1		-2		-3		Temp	CFU/ml
0							8	13	36.9	525000
5					21	19			37.9	100000
10			13	16					38.7	7250
15	27	20							39.2	1175
20	11	2							39.8	325
25	1	2							40	75
30	7	4							40.5	1
40	2	0							41.5	50
50	1	1							42.3	50
60	1	2							42.8	75
80	2	1							44.8	75
100	0	0							46	1

Trial B (8th July 2003)

Time	0		-1		-2		-3		Temp	CFU/ml
0							7	13	38.6	500000
5					34	41			39.2	187500
10			55	70	9	8			39.6	31250
15			11	15					39.9	6500
20	17	20							40.2	925
25	4	5							40.6	225
30	2	1							41	75
40	1	2							41.4	75
50	3	0							41.8	75
60	6	0							42.4	150
80	1	0							43.2	25
100	2	0							44	50
120	0	0							44.7	1

Trial C (9th July 2003)

Time	0		-1		-2		-3		Temp	CFU/ml
0							14	7	37.7	525000
5					17	24			38.6	102500
10			14	18	9	2			39.4	8000
15	11	8							40	475
20	4	1							40.7	125
25	3	0							41.5	75
30	1	0							42	25
40	0	0							43	1
50	0	0							43.6	1
60	0	0							44	1
80	1	0							44.5	25
100	0	0							45	1
120									45.5	

Trial A (10th July 2003, 3mg/l TiO_2)

Time	0		-1		-2		-3		Temp	CFU/ml
0					90	139	30	17	33.8	1175000
5					30	26			34.4	140000
10			27	25					34.4	13000
15	44	38							36.3	2050
20	29	30							35.8	1475
25	3	5							36.2	200
30	7	5							36.6	300
40	4	7							37.5	275
50	7	6							38.5	325
60	4	0							39.5	100

Trial B (10th July 2003, 6mg/l TiO_2)

Time	0		-1		-2		-3		Temp	CFU/ml
0					31	48	2	8	38.5	197500
5			54	55	0	6			39.2	27250
10	43	28	1	4					39.8	1775
15	11	16	2	1	2	0			40.3	675
20	3	4							40.9	175
25	2	0							41.4	50
30	1	1							41.7	50
40	0	0							42.6	1
50	0	0							42.9	1
60	1	0							43.2	25

Trial C (10th July 2003, 9mg/l TiO_2)

Time	0		-1		-2		-3		Temp	CFU/ml
0					12	16	1	1	36	50000
5			94	102	8	7			37.8	37500
10	19	30	2	3					38.6	1225
15	12	9							39.3	525
20	4	1							39.3	125
25	0	0							40	1
30	0	1							40.7	25
40	0	0							41.6	1
50	0	0							42.5	1
60	0	0							43.2	1

C.3.2   *Small-Scale Reactor (Compound Parabolic) with Fixed TiO$_2$ (PSA)*

Compound Parabolic Small-Scale Reactor (PSA)

Trial A	19th June 2003		Trial A	25th June 2003 TiO$_2$ Rods
Trial B	19th June 2003		Trial B	24th June 2003 TiO$_2$ Rods
Trial C	20th June 2003			
Trial D	18th June 2003			
Trial E	19th June 2003			

Trial A

Time	0		-1		-2		-3		Temp	CFU/ml
0							14	11	35	625000
10					57	65			35	305000
20			103	62	7	1			35	41250
30	1	7	1	0					35	200
40	0	0							35	1
50									35	
60									36	

Trial B

Time	0		-1		-2		-3		Temp	CFU/ml
0							67	79	28	3650000
10					139	130			32	672500
20					67	64			33	327500
30			135	142					34	69250
40			21	13					35	8500
50	3	2							36	125
60	2	0							36	50

Trial C

Time	0		-1		-2		-3		Temp	CFU/ml
0							55	66	28	3025000
10					69	83			31	380000
20					49	52			33	252500
30			82	68	36	32			35	37500
40	104	95							35	4975
50	26	27							36	1325
60									36	1

Trial D

Time	0		-1		-2		-3		Temp	CFU/ml
0							25	25	31	1250000
10					49	44			30	232500
20			54	50					30	26000
30	25	19							36	1100
40	0	0							36	1
50									36	
60									37	

Trial E

Time	0		-1		-2		-3		Temp	CFU/ml
0							74	76	30	4.E+06
10					140	150			34	7.E+05
20					65	83			36	4.E+05
30			193	177					37	9.E+04
40			22	21					37	1.E+04
50	36	27							38	2.E+03
60	2	1							38	8.E+01

Trial A

Time	0		-1		-2		-3		Temp	CFU/ml
0							64	69	31	3325000
10					80	84			36	410000
20					62	76			39	345000
30					16	7			40	57500
40			33	34					40	16750
50	16	11							41	675
60	0	0							41	1

Trial B

Time	0		-1		-2		-3		Temp	CFU/ml
0							19	29	35	1200000
10					50	63			35	282500
20					44	62			37	265000
30					20	16			37	90000
40			19	24					39	10750
50	5	12							38	425
60	0	0							38	25

C.3.3   *Small-Scale Reactor (Compound Parabolic) with Fixed TiO₂ (Ireland)*

Compound Parabolic Small-Scale Reactor (Ireland)

Trial A	9th September 2004	
Trial B	16th September 2004	
Trial C	17th September 2004	

Trial A	21st July 2004	TiO₂ Rods
Trial B	22nd July 2004	TiO₂ Rods
Trial C	31st August 2004	TiO₂ Paper
Trial D	9th September 2004	TiO₂ Paper

Trial A

Time	0		-1		-2		-3		Temp	CFU/ml
0							50	72	23	3050000
15							32	31	23	1575000
30							51	46	23	2425000
45							23	20	23	1075000
60					44	43	9	11	20	210000
75					87	87			21	435000
90					54	43			23	242500
105					28	25			23	132500
120			54	62					25	29000
135			14	22					24	9000
150			0	0					24	1
165			1	0					24	25
180			0	0					24	1

Trial B

Time	0		-1		-2		-3		Temp	CFU/ml
0							85	64	24	3725000
15							25	32	24	1425000
30							15	15	25	750000
45					71	69			26	350000
60					22	39			27	152500
75					4	7			27	27500
90			49	50					28	24750
105			16	20					29	9000
120			0	0					29	1
135									29	
150									29	
165									29	
180									29	

Trial C

Time	0		-1		-2		-3		Temp	CFU/ml
0							62	70	29	3300000
15							25	32	30	1425000
30							22	16	30	950000
45					42	54			30	240000
60					13	11			30	60000
75			0	0					30	1
90									30	
105									29	
120									29	
135									29	
150									30	
165									31	
180									32	

Trial A

Time	0		-1		-2		-3		Temp	CFU/ml
0					3	5				20000
15					3	2				12500
30			5	4						2250
45			3	3						1500
60			5	3						2000
75			1	2						750
90	8	1								225
105	0	0								1
120										
135										
150										
165										
180										

Trial B

Time	0		-1		-2		-3		Temp	CFU/ml
0					14	11				62500
15					14	9				57500
30					7	10				42500
45					9	9				45000
60			30	25						13800
75			22	14						9000
90	26	30								1400
105	0	0								1
120										
135										
150										
165										
180										

Trial C

Time	0		-1		-2		-3		Temp	CFU/ml
0			22	25	0	2				11800
15			18	19						9250
30			3	1						1000
45			2	1						750
60			2	2						1000
75			4	0						1000
90	13	15								700
105	0	0								1
120										
135										
150										
165										
180										

Trial D

Time	0		-1		-2		-3		Temp	CFU/ml
0					24	37				153000
15					12	16				70000
30					10	6				40000
45			36	40						19000
60			29	23						13000
75			16	17						8250

C.4 Other Factors which Effect the Solar Disinfection Process

C.4.1 *Small Scale Reactor (Parabolic) and Effect of Temperature*

Parabolic Small-Scale Reactor (Temperature)

Trial A 19th June 2003
Trial B 20th June 2003
Trial C 19th June 2003

Trial A 8th July 2003 UVA + 45°
Trial B 8th July 2003 UVA + 45°
Trial C 9th July 2003 UVA + 45°
Trial D 9th July 2003 UVA + 45°
Trial E 25th June 2003 UVA + 45°
Trial F 24th June 2003 UVA + 45°

Trial A

Time	0		-1		-2		-3		Temp	CFU/ml
0							55	50	28	2625000
10					47	58			32	262500
20					43	48			33	227500
30			111	97					34	52000
40	50	54							35	2600
50	2	0							36	50
60	0	0							36	1

Trial B

Time	0		-1		-2		-3		Temp	CFU/ml
0							67	79	28	2950000
10					139	130			31	477500
20					67	64			33	305000
30			135	142					34	187500
40			21	13					34	46750
50	3	2							35	5600
60	2	0							35	4050

Trial C

Time	0		-1		-2		-3		Temp	CFU/ml
0							55	66	29	2425000
10					69	83			34	490000
20					49	52			36	297500
30			82	68	36	32			36	49750
40	104	95							36	2000
50	26	27							37	50
60									37	1

Trial A 28th January 2004 40°
Trial B 5th February 2004 45°
Trial C 5th February 2004 50°

Trial A

Time	0		-1		-2		-3		Temp	CFU/ml
0							79	76	40	3875000
15							60	70	40	3250000
30							43	34	40	1925000
45							16	22	40	950000
60					45	47			40	230000

Trial B

Time	0		-1		-2		-3		Temp	CFU/ml
0							25	24	45	1250000
15					37	40	5	8	45	192500
30			6	12					45	4500
45			0	0					45	1
60									45	

Trial C

Time	0		-1		-2		-3		Temp	CFU/ml
0							23	6	50	725000
15					0	0			50	1
30									50	
45									50	
60									50	

Trial A

Time	0		-1		-2		-3		Temp	CFU/ml
0							55	53	44	2700000
5			54	51	2	11			45	26250
10			27	15					45	10500
15			6	2					45	2000
20	22	16							45	950
25	5	1							45	150
30	1	0							45	25
40	4	0							45	100
50	0	0							45	1
60									46	

Trial B

Time	0		-1		-2		-3		Temp	CFU/ml
0							22	36	44	1450000
5					78	87			44	412500
10					34	35			45	172500
15			46	60	11	15			45	28000
20			23	24					45	11750
25	29	24							45	1325
30	2	0							45	50
40	0	0							45	1
50									45	
60									45	

Trial C

Time	0		-1		-2		-3		Temp	CFU/ml
0							51	38	42	2225000
5									44	
10					52	81			45	332500
15					41	38			45	197500
20					12	13			45	62500
25			26	18					45	11000
30	20	19							45	975
40	1	0							45	25
50	0	0							45	1
60									46	

Trial D

Time	0		-1		-2		-3		Temp	CFU/ml
0							34	27	45	1525000
5					69	75			45	360000
10					37	27			45	160000
15			54	66	8	8			45	30000
20			28	32	1	4			45	15000
25			11	10					46	5250
30	20	21	1	0					46	1025
40	0	0							46	1
50									46	
60									46	

Trial E										
Time	0		-1		-2		-3		Temp	CFU/ml
0							61	64	45	3125000
5					107	109			45	540000
10					92	59			45	377500
15					34	23			45	142500
20					20	9			45	72500
25			42	34					45	19000
30			17	16					45	8250
40	2	6							46	200
50	0	0							45	1
60									46	

Trial F										
Time	0		-1		-2		-3		Temp	CFU/ml
0							37	31	45	1700000
5					70	55			44	312500
10					33	23			45	140000
15					15	19			45	85000
20			50	51	5	5			45	25250
25			17	19					45	9000
30	36	35	4	14					45	1775
40	3	5							46	200
50	0	0							46	1
60									46	

Compound Parabolic Small-Scale Reactor (Volume)

Trial A	19th June 2003		
Trial B	19th June 2003		
Trial C	20th June 2003		
Trial D	18th June 2003		
Trial E	19th June 2003		

Trial A	8th July 2003	0.4 litres
Trial B	8th July 2003	0.4 litres
Trial C	9th July 2003	0.4 litres
Trial D	9th July 2003	0.4 litres

Trial A

Time	0		-1		-2		-3		Temp	CFU/ml
0							14	11	35	625000
10					57	65			35	305000
20			103	62	7	1			35	41250
30	1	7	1	0					35	200
40	0	0							35	1
50									35	
60									36	

Trial B

Time	0		-1		-2		-3		Temp	CFU/ml
0							67	79	28	3650000
10					139	130			32	672500
20					67	64			33	327500
30			135	142					34	69250
40			21	13					35	8500
50	3	2							36	125
60	2	0							36	50

Trial C

Time	0		-1		-2		-3		Temp	CFU/ml
0							55	66	28	3025000
10					69	83			31	380000
20					49	52			33	252500
30			82	68	36	32			35	37500
40	104	95							35	4975
50	26	27							36	1325
60									36	1

Trial D

Time	0		-1		-2		-3		Temp	CFU/ml
0							25	25	31	1250000
10					49	44			30	232500
20			54	50					30	26000
30	25	19							36	1100
40	0	0							36	1
50									36	
60									37	

Trial E

Time	0		-1		-2		-3		Temp	CFU/ml
0							74	76	30	3750000
10					140	150			34	725000
20					65	83			36	370000
30			193	177					37	92500
40			22	21					37	10750
50	36	27							38	1575
60	2	1							38	75

Trial A

Time	0		-1		-2		-3		CFU/ml
0							60	52	2800000
5					29	39			170000
10					28	28			140000
15					18	16			85000
20			11	21	2	4			8000
25	22	12							850
30	0	0							1

Trial B

Time	0		-1		-2		-3		CFU/ml
0							46	58	2600000
5					60	66			315000
10					40	50			225000
15					28	35			158000
20			103	85	23	21			110000
25			77	77	11	12			38500
30			34	32					16500
40	16	15							775

Trial C

Time	0		-1		-2		-3		CFU/ml
0							58	52	2750000
5					64	86			375000
10					48	52			250000
15					46	51			243000
20			150	177	38	40			195000
25			115	119					58500
30			103	89					48000
40			12	12					6000
50	16	19							875
60	6	7							325

Trial C

Time	0		-1		-2		-3		CFU/ml
0							40	39	1980000
5					67	64			328000
10					42	48			225000
15					23	33			140000
20					13	14			67500
25			19	40					14800
30			26	25					12800
40	23	23							1150
50	2	2							100
60	2	0							50

C.5 The Stroboscopic Mechanism

C.5.1 *Dark Phases in Batch Process Solar Disinfection*

Batch Reactor Dark Phases

Trial A 5th April 2004 Continuous
Trial B 5th April 2004 Continuous

Trial A 6th April 2004 4 sec light- 8 sec dark
Trial B 6th April 2004 4 sec light- 8 sec dark

Test A					
Time	0	-1	-2	-3	CFU/ml
0				22/24	1150000
15			65/60	8/10	312500
30			24/25		122500
45			15/10		62500
60		39/30			17250
75		18/22			10000
90		6/9			3750
105		2/4			1500
120		3/2			1250
Test B					
Time	0	-1	-2	-3	CFU/ml
0				22/24	1150000
15			50/51	6/8	252500
30			27/24	1/1	127500
45		74/75	8/12	2/2	37250
60		31/22	7/3		13250
75		8/8	0/3		4000
90		1/1			500
105		1/0			250
120		1/0			250

Test A					
Time	0	-1	-2.00	-3	CFU/ml
0				41/43	2100000
15				28/25	1325000
30				11/16	675000
45				10/16	650000
60		75/76		9/12	377500
75		59/61			300000
90		51/44			237500
105		48/49			242500
120					
Test B					
Time	0	-1	-2	-3	CFU/ml
60			45/42		2175000
75			24/31		1375000
90			14/7		525000
105		63/72			337500
120		41/50			227500
0		48/46			235000
Trial A		37/35			180000
Trial B		34/34			170000
0	117/120				59250

Trial A 7th April 2004 4 sec light- 16 sec dark
Trial B 7th April 2004 4 sec light- 16 sec dark

Trial A 28th April 2004 4 sec light- 32 sec dark
Trial B 28th April 2004 4 sec light- 32 sec dark

Test A					
Time	0	-1	-2	-3	CFU/ml
0				28/28	1400000
20				11/11	550000
40				10/9	475000
60			47/42		222500
80			27/32		147500
100			21/23		110000
120			22/15		92500
140			10/16		65000
160		37/48			21250
180		34/44			19500
200		35/30			16250
220		28/34			15500
240		26/22			12000
Test B					
Time	0	-1	-2	-3	CFU/ml
0				31/32	1575000
20				17/21	950000
40			69/67	13/6	340000
60			53/51		260000
80			29/29		145000
100			25/22		117500
120			20/16		90000
140			14/15		72500
160		61/65			29000
180		44/38			20500
200		38/36			18500
220		24/29			13250
240		27/30			14250

Test A					
Time	0	-1	-2	-3	CFU/ml
0				37/30	1650000
20				28/31	1475000
40				21/18	975000
60			83/76	15/7	397500
80			75/62	9/6	342500
100			48/47		237500
120			42/42		210000
140			29/37		165000
160			31/27		145000
180			32/22		135000
200			24/27		127500
220			20/14		85000
240			12/22		85000
260			13/13		65000
280			11/10		52500
300		49/54			25750
Test B					
Time	0	-1	-2	-3	CFU/ml
0				23/25	1200000
20				24/18	1050000
40				15/17	800000
60				11/11	550000
80			58/51	10/3	272500
100			35/47		205000
120			42/36		195000
140		37/36			182500
160			24/20		110000
180			29/25		135000
200			19/18		92500
220			16/13		72500
240		68/64	10/7		33000
260		56/65			30250
280		53/49			25500
300		44/55			22250

Illuminarted-Dark Ratio Batch Reactor

Trial A	17th November 2004	Continuous	
Trial B	17th November 2004	Continuous	

Trial A	6th April 2004	1 sec light- 1 sec dark
Trial B	6th April 2004	1 sec light- 1 sec dark

Test A

Time	0	-1	-2	-3	CFU/ml
0		62/55	8/9		29250
15		27/39			16500
30		30/23			13250
45		23/17			10000
60	67/64				3275
75	33/30				1575
90	32/22				1350
105					
120	8/7				375

Test B

Time	0	-1	-2	-3	CFU/ml
0			13/13		65000
15		52/52			26000
30		39/32			17750
45		32/31			15750
60		19/20			9750
75		13/15			7000
90	68/73				3525
105					
120	28/29				1473

Test A

Time	0	-1	-2	-3	CFU/ml
0					
15					87500
30					47500
45					52500
60					36500
90					33000
120					19750
150					
180					4850
210					3675
240					

Test B

Time	0	-1	-2	-3	CFU/ml
0					
15					92500
30					72500
45					44000
60					32750
90					26250
120					
150					16250
180					4750
210					3200
240					

Trial A	1 sec light- 2 sec dark
Trial B	1 sec light- 2 sec dark

Trial A	2 sec light- 2 sec dark
Trial B	2 sec light- 2 sec dark

Test A

Time	0	-1	-2	-3	CFU/ml
0			50/44		235000
15			11/10		52500
30		45/45			22500
45		34/28			15500
60		21/17			9500
90		12/9			5250
120		9/7			4000
150		5/3			2000
180		1/4			1250
210	25/18				1075
240	23/18				1025
270	22/12				850
300	18/12				750
330	18/9				675
360	13/13				650

Test B

Time	0	-1	-2	-3	CFU/ml
0			26/18		110000
0			12/12		60000
0		36/44			20000
0		35/27			15500
0		19/16			8750
0		11/11			5500
0		9/10			4750
0		7/4			2750
0		2/2			1000
0	11/23				850
0	18/17				875
0	17/11				700
0	12/20				800
0	18/7				625
0	6/12				450

Test A

Time	0	-1	-2	-3	CFU/ml
0					55000
15					20750
30					17500
45					12750
60					10000
90					5750
120					2250
150					1050
180					950
210					125
240					350

Test B

Time	0	-1	-2	-3	CFU/ml
0					29750
15					21250
30					18500
45					16750
60					11750
90					7250
120					2575
150					850
180					875
210					400
240					450

Illuminarted-Dark Ratio Batch Reactor

Trial A	2 sec light- 4 sec dark	
Trial B	2 sec light- 4 sec dark	

Trial A	4 sec light- 4 sec dark
Trial B	4 sec light- 4 sec dark

Test A					
Time	0	-1	-2	-3	CFU/ml
0			32/35		167500
15			12/15		67500
30			8/12		50000
45		50/53			25750
60		35/34			17250
90		25/25			12500
120		13/15			7000
150		3/3			1500
180		9/4			3250
210	37/35				1800
240	28/29				1425
270	24/20				1100
300	17/24				1025
330	2/7				225
360	13/17				750
Test B					
Time	0	-1	-2	-3	CFU/ml
0			31/27		145000
15			8/15		57500
30			14/12		65000
45		35/46			20250
60		42/40			20500
90		5/1			1500
120		10/15			6875
150		12/15			4250
180		6/5			2750
210	33/40				1825
240	25/24				1225
270	18/23				1025
300	22/27				1225
330	3/5				200
360	12/12				600

Test A					
Time	0	-1	-2	-3	CFU/ml
0		27/17	12/2		35000
15		41/33			18500
30		28/25			13250
45		4/5			2250
60		4/10			3500
90	14/20				850
120	2/4				150
150	1/0				25
180	1				1
210	1				1
240	1				1
Test B					
Time	0	-1	-2	-3	CFU/ml
0		56/60	8/9		42500
15		34/30			16000
30		24/31			13750
45		24/22			11500
60		24/11			8750
90	70/68				3450
120	45/45				2250
150	30/35				1625
180	20/25				1125
210	4/7				275
240	6/8				350

Intermittent Illumination Continuous Flow 1.5m^2

| Trial A | 18th May 2004 | | Continuous | Trial A | 19th May 2004 | | 2.83 sec light- 2.83 sec |
| Trial B | 18th May 2004 | | Continuous | Trial B | 19th May 2004 | | 2.83 sec light- 2.83 sec |

Test A					
Time	250µl	0	-1	CFU/ml	Temp
-10	1			4	18.4
0			27/38	16250	20.4
10			29/33	15500	23
20			40/31	17750	24
30			17/26	10750	25.3
45		70/80		3750	26.8
60		33/34		1675	28.1
90		1/4		125	30.4

Test B					
Time	250µl	0	-1	CFU/ml	Temp
-10	ng			-	29.89
0			51/55	26500	30
10			71/48	29750	31.5
20			51/46	24250	32.5
30			17/23	10000	33.4
45		13/16		725	34.4
60		2/-		50	34.7
90		1/-		25	33.8

Test A					
Time	250ml	0	-1	CFU/ml	Temp
-10	2			8	23.8
0			44/55	24750	24
10			42/44	21500	25.1
20			44/32	19000	26
30			27/14	10250	27.1
45		35/38		1825	28.7
60		1/0		25	30.1
90				1	32

Test B					
Time	250ml	0	-1	CFU/ml	Temp
-10	-			-	24.6
0			35/37	18000	26.3
10			29/33	15500	28.4
20			17/15	8000	30.2
30		47/35	3/5	2050	31.7
45				1	33.2
60				1	34.3
90				1	34.8

| Trial A | 20th May 2004 | | 5.67 sec light- 5.67 sec dark | Trial A | 19th May 2004 | | 2.83 sec light- 2.83 sec |
| Trial B | 20th May 2004 | | 5.67 sec light- 5.67 sec dark | | | | |

Test A					
Time	250ml	0	-1	CFU/ml	Temp
-10	ng			-	18.1
0			34/61	23750	19.3
10			43/42	21250	21
20			30/38	17000	22.6
30			44/19	15750	24.1
45			16/19	8750	25.9
60		5/3		200	27.6
90		1/-		25	30.3

Test B					
Time	250ml	0	-1	CFU/ml	Temp
-10	ng			-	29.5
0			47/44/	22750	30.6
10			50/50	25000	32.5
20			33/43	19000	33.6
30		72/74	9/7	3650	34.5
45		1		1	35.6
60		1/-		25	36.4
90		1		1	35.8

Test A					
Time	250ml	0	-1	CFU/ml	Temp
-10	32			128	21.2
0			55/44	24750	23.8
10			43/39	18000	26.9
20			33/24	14250	27.9
30			24/26	12500	28.2
45		46/34		2000	29.7
60		3/1		100	31.2
90		1/2		75	34.1
120		1/0		25	35.2

Batch Reactor Dark Phases

Trial A	27th May 2004	Continuous	Trial A	24th May 2004	2.83 sec light- 5.6 sec dark
Trial B	27th May 2004	Continuous	Trial B	24th May 2004	2.83 sec light- 5.6 sec dark

Test A					
Time	250ml	0	-1	CFU/ml	Temp
-10					18.3
0			61/47	27000	19.8
10			52/60	28000	21.3
20			22/23	11250	22.5
30			10/14	6000	23.9
45		17/14		775	26.4
60		6/5		275	29.3
90		2/3		125	32.2

Test B					
Time	250ml	0	-1	CFU/ml	Temp
-10					20.5
0			36/25	15250	23.4
10			15/20	8750	27.5
20			7/7	3500	33.2
30		9/3	4/-	300	33.3
45		2/1		75	36.4
60		ng		1	35
90		ng		1	25.5

Test A					
Time	250µl	0	-1	CFU/ml	Temp
-10	tn			-	25.80
0			1.18	6000	27.10
10			1.60	3250	29.10
20			3/-	750	31.20
30		1.75		275	32.70
45		1.00		50	34.90
60		ng		1	37.00
90		ng		1	40.50

Test B					
Time	250µl	0	-1	CFU/ml	Temp
-10	1			4	28.50
0		62/44		2650	33.40
10			2/1	500	35.50
20					37.60
30		2/2		100	39.10
45		1/0		25	40.70
60		ng		1	42.30
90		ng		1	43.50

Trial A	28th May 2004	0.94 sec light- 1.89 sec dark	Trial A	1st June 2004	7.55 sec light- 15.11 sec dark
Trial B	28th May 2004	0.94 sec light- 1.89 sec dark	Trial B	1st June 2004	7.55 sec light- 15.11 sec dark

Test A					
Time	250µl	0	-1	CFU/ml	Temp
-10	tnbc			-	22.5
0			28/30	14500	23.9
10			9/13	5500	26
20			4/-	1250	28
30		5/5		250	29.5
45		ng		25	31.4
60		ng		1	31.9
90		ng		1	35.9

Test B					
Time	250µl	0	-1	CFU/ml	Temp
-10	tnbc				32.6
0			23/15	9500	34.3
10			11/13	6000	35.9
20			2/-	500	38.1
30		ng	ng	1	39
45		ng	ng	1	37
60		ng	ng	1	34.5
90		ng	ng	1	34.2

Test A					
Time	250µl	0	-1	CFU/ml	Temp
-10	tn				32.1
0			33/34	16750	34
10			11/17	7000	35.3
20			4/5	2250	36.7
30		3/6		225	38.4
45		1/1		50	40.4
60		ng		1	42
90		ng		1	45

Test B					
Time	250µl	0	-1	CFU/ml	Temp
-10	tn				27.7
0			11/16	6750	31.2
10			9/3	3000	34.6
20			6/5	2750	38.3
30		6/4		250	40.3
45		3/-		75	42.6
60		ng		1	43.7
90		ng		1	44.4

APPENDIX D

SOLAR RADIATION INTENSITY DATA

D.1 Comparison of Solar Disinfection Reactors

D.1.1 *Small-Scale Reactors (PSA)*

Small-Scale Reactors Natural Solar Radiation PSA

Intensity W/m^2

Compound Parabola				
Test A	Test B	Test C	Test D	Test E
35.2	35.86	30.3	40.82	39.63
35.53	36.31	31.03	40.58	39.35
36.31	37.24	32.35	40.03	38.7
37.46	37.83	33.57	39.5	38.09
38.32	38.3	34.7	38.76	37.45
39.09	39.14	35.87	37.87	36.82
39.9	39.75	36.9	36.99	35.96
Parabola				
Test A	Test B	Test C	Test D	Test E
35.2	35.86	30.3	40.82	39.63
35.53	36.31	31.03	40.58	39.35
36.31	37.24	32.35	40.03	38.7
37.46	37.83	33.57	39.5	38.09
38.32	38.3	34.7	38.76	37.45
39.09	39.14	35.87	37.87	36.82
39.9	39.75	36.9	36.99	35.96
V-Groove				
Test A	Test B	Test C	Test D	Test E
32.9	22.23	20.4	21.77	41.34
33.59	22.95	21.56	25.81	41.07
34.69	24.49	23.78	27.21	40.53
35.76	25.94	25.99	31.54	39.89
36.85	27.31	28.08	26.36	39.136
37.57	28.7	30.23	24.67	38.32
37.99	30.06	32.09	32.07	37.38
No Reflector				
Test A	Test B	Test C	Test D	Test E
32.9	22.23	20.4	21.77	41.34
33.59	22.95	21.56	25.81	41.07
34.69	24.49	23.78	27.21	40.53
35.76	25.94	25.99	31.54	39.89
36.85	27.31	28.08	26.36	39.136
37.57	28.7	30.23	24.67	38.32
37.99	30.06	32.09	32.07	37.38

Compound Parabola		
Test A	Test B	Test C
16.725	21.32	24.72
16.725	21.32	24.72
16.725	21.32	24.72
16.725	21.32	24.72
16.725	21.32	24.72
24.855	23.68	19.72
24.855	23.68	19.72
24.855	23.68	19.72
24.855	20.83	19.72
22.219	20.83	14.72
22.219	20.83	14.72
22.219	20.83	14.72
22.219		
Parabola		
16.725	21.32	24.72
16.725	21.32	24.72
16.725	21.32	24.72
16.725	21.32	24.72
16.725	21.32	24.72
24.855	23.68	19.72
24.855	23.68	19.72
24.855	23.68	19.72
22.219	20.83	19.72
22.219	20.83	14.72
22.219	20.83	14.72
22.219	20.83	14.72
V-Groove		
19.58	19.585	22.845
19.58	19.585	22.845
19.58	19.585	22.845
19.58	19.585	22.845
19.58	19.585	16.665
17.91	11.595	16.665
17.91	7.135	16.665
	7.135	
	7.135	
No Reflector		
16.725	21.32	24.72
16.725	21.32	24.72
16.725	21.32	24.72
16.725	21.32	24.72
16.725	21.32	19.72
24.855	23.68	19.72
24.855	23.68	19.72
22.219	20.83	19.72
22.219	20.83	14.72
	20.83	14.72
		14.72

D.1.3   *Comparison of Small-Scale and Pilot-scale Reactors*

Small-scale Compound Parabola				
Test A	Test B	Test C	Test D	Test E
35.2	35.86	30.3	40.82	39.63
35.53	36.31	31.03	40.58	39.35
36.31	37.24	32.35	40.03	38.7
37.46	37.83	33.57	39.5	38.09
38.32	38.3	34.7	38.76	37.45
39.09	39.14	35.87	37.87	36.82
39.9	39.75	36.9	36.99	35.96
Pilot Scale Reactor 3m^2				
Test A	Test B	Test C		
31.14	34.33	36.38		
31.835	34.61	36.535		
32.835	35.125	36.895		
33.53	35.545	37.48		
34.7	35.94	38.425		
35.59	36.4	39.225		
36.335	36.875	39.635		
36.63	37.41	40.17		
37.63	37.99	40.74		
37.9	38.5	41.156		
	39.3	41.724		
	40.112	42.334		

D.1.3   *Assessment of the Effect of Reactor Area*

Pilot Scale Reactor 3m^2			Pilot Scale Reactor 1m^2		
Test A	Test B	Test C	Test A	Test B	Test C
31.14	34.33	36.38	37.135	38.04	36.13
31.835	34.61	36.535	37.575	38.3	36.36
32.835	35.125	36.895	37.92	38.77	36.79
33.53	35.545	37.48	38.27	39.13	37.216
34.7	35.94	38.425	38.545	39.475	37.62
35.59	36.4	39.225	38.96	39.83	38.01
36.335	36.875	39.635	39.61	40.19	38.39
36.63	37.41	40.17	40.1425	40.6	38.74
37.63	37.99	40.74	40.6125	41.23	39.185
37.9	38.5	41.156		41.7	39.65
	39.3	41.724		42.254	40.31
	40.112	42.334			40.976

D.2 Solar Photocatalytic Disinfection

D.2.1 *Titanium Dioxide in Suspension*

Pilot Scale Reactor 1m^2					
Test A	Test B	Test C	3mg/l	6mg/l	9mg/l
37.135	38.04	36.13	27.48	40.56	41.13
37.575	38.3	36.36	27.84	40.696	40.98
37.92	38.77	36.79	28.55	40.9	40.07
38.27	39.13	37.216	29.246	41.2	40.35
38.545	39.475	37.62	29.92	41.42	40.02
38.96	39.83	38.01	30.58	41.65	39.69
39.61	40.19	38.39	31.216	41.8	39.36
40.1425	40.6	38.74	32.17	42.03	38.81
40.6125	41.23	39.185	33.385	42.2175	37.995
	41.7	39.65	34.5275	42.28	37.04
	42.254	40.31			
		40.976			

D.2.2 *Fixed Titanium Dioxide PSA*

Compound Parabola					Fixed Titanium Dioxide (Rods)		
Test A	Test B	Test C	Test D	Test E	Test A	Test B	Test C
35.2	35.86	30.3	40.82	39.63	22.16	39.28	37.275
35.53	36.31	31.03	40.58	39.35	22.79	39.113	37.11
36.31	37.24	32.35	40.03	38.7	24	38.75	36.77
37.46	37.83	33.57	39.5	38.09	25.273	40.01	36.2975
38.32	38.3	34.7	38.76	37.45	26.726	39.87	35.6675
39.09	39.14	35.87	37.87	36.82	27.94	39.82	35.105
39.9	39.75	36.9	36.99	35.96	28.99	39.55	33.92

D.2.3 *Fixed Titanium Dioxide Ireland*

Compound Parabola			Fixed Titanium Dioxide (Rods)			Fixed Titanium Dioxide (Paper)		
Test A	Test B	Test C	Test A	Test B	Test C	Test A	Test B	Test C
16.725	21.32	24.72	5.9	29.51	24.375	36.805	6.667	30.69
16.725	21.32	24.72	5.9	29.51	24.375	36.805	6.667	30.69
16.725	21.32	24.72	5.9	29.51	24.375	36.805	6.667	30.69
16.725	21.32	24.72	5.9	29.51	24.375	36.805	6.667	30.69
16.725	21.32	24.72	5.97	25.49	25.69	36.805	6.667	30.69
24.855	23.68	19.72	5.97	25.49	25.69	36.52	5.902	32.08
24.855	23.68	19.72	6.18	25.49	25.69	36.52	5.902	32.08
24.855	23.68	19.72	6.18	25.56	29.86	36.52	5.902	32.08
24.855	20.83	19.72	12.15	25.56	29.86	32.36	6.736	31.11
22.219	20.83	14.72	12.15	19.72	30.76	32.36	6.736	31.11
22.219	20.83	14.72	12.15	19.72	30.76	30.41	5.27	28.05
22.219	20.83	14.72				30.41	5.27	28.05
22.219								

D.3 Other Factors that Effect the Solar Disinfection Process

D.3.1   *Temperature*

UVA					UVA +45			
Test A	Test B	Test C	Test D	Test E	Test A	Test B	Test C	Test D
35.2	35.86	30.3	40.82	39.63	29.275	39.815	25.15	40.583
35.53	36.31	31.03	40.58	39.35	29.95	39.395	26.623	40.4
36.31	37.24	32.35	40.03	38.7	30.615	38.95	27.336	40.2
37.46	37.83	33.57	39.5	38.09	31.245	38.55	28.706	39.96
38.32	38.3	34.7	38.76	37.45	31.845	38.125	29.34	39.68
39.09	39.14	35.87	37.87	36.82	32.45	37.655	30.02	39.377
39.9	39.75	36.9	36.99	35.96	33.9	37.185	31.715	38.62

D.3.2   *Volume*

1 litre					0.4 litres			
Test A	Test B	Test C	Test D	Test E	Test A	Test B	Test C	Test D
35.2	35.86	30.3	40.82	39.63	29.275	39.815	25.15	40.583
35.53	36.31	31.03	40.58	39.35	29.95	39.395	26.623	40.4
36.31	37.24	32.35	40.03	38.7	30.615	38.95	27.336	40.2
37.46	37.83	33.57	39.5	38.09	31.245	38.55	28.706	39.96
38.32	38.3	34.7	38.76	37.45	31.845	38.125	29.34	39.68
39.09	39.14	35.87	37.87	36.82	32.45	37.655	30.02	39.377
39.9	39.75	36.9	36.99	35.96	32.45	37.185	31.715	38.62
						36.47	32.315	37.975
							32.895	37.55
							32.31	37.1175

D.4 The Stroboscopic Mechanism

D.4.1   Intermittent Illumination and Continuous Flow Solar Disinfection 1.5m^2

Continuous		2.83:2.83		5.67:5.67		8.5:8.5
Test A	Test B	Test A	Test B	Test A	Test B	Test A
25.8	42.52	28.19	39.76	23.75	41.95	41.37
26.59	42.485	28.95	40.99	24.6	41.68	41.38
27.8	42.26	30.26	42.05	26.2	41.38	41.4
29.41	41.74	31.28	41.65	26.97	41.18	33.52
31.2	40.7	32.93	40.95	28.91	41.07	34.29
33.12	39.52	34.75	39.54	31.56	40.3	37.75
35.6	35.35	37.25	37.41	34.27	32.51	37.08

D.4.2   Intermittent Illumination and Continuous Flow Solar Disinfection 1m^2

Continuous		2.83:5.6		0.94:1.89		7.55:15.11	
Test A	Test B	Test A	Test B	Test A	Test B	Test A	Test B
19.13	41.85	22.85	40.17	24.7	39.36	28.605	41.46
19.91	41.87	23.58	40.24	25.6	35.22	29.31	41.14
21.48	43.14	25.04	39.52	26.9	38.21	30.69	40.88
23.11	44.52	26.53	38.74	28.07	33.35	32.01	40.64
25.08	39.98	28.3	37.83	24.39	19.67	33.54	40.12
27.398	19.09	30.32	35.85	20.51	12.68	35.19	38.8
30.75	9.18	33.12		31.75	22.43	37.19	37.12

E.1 Peer-Reviewed Articles

O.A.McLoughlin, S.C.Kehoe, K.G.McGuigan, E.F. Duffy, F. Al Toutati, W.Gernjak, I. Oller, S.Malato, L.W. Gill (2004) Solar disinfection of contaminated water: a comparison of three small-scale reactors. *Solar Energy* 77(5), 657-664.

O.A.McLoughlin, P. Fernandez, W.Gernjak, S.Malato, L.W.Gill (2004) Photocatalytic disinfection of water using low cost compound parabolic collectors. *Solar Energy* 77(5), 625-633.

E.F. Duffy, F. Al Touati, S.C. Kehoe, O.A. McLoughlin, L.W. Gill, W. Gernjak, I. Oller, M.I. Maldonado, S. Malato, J. Cassidy, R.H. Reed, K.G. McGuigan (2004) A novel TiO$_2$-assisted solar photocatalytic batch-process disinfection reactor for the treatment of biological and chemical contaminants in domestic drinking water in developing countries. *Solar Energy* 77(5), 649-655.

L.W. Gill, O.A. McLoughlin (2005) Solar Disinfection Kinetic Design Parameters for Continuous Flow Reactors. *Journal of Solar Energy Engineering*, In Press.

L.W. Gill, O.A. McLoughlin (2005) The Influence of Temperature on Continuous Flow Solar Disinfection. *Solar World Congress*, Orlando, Florida, 8th-12th August 2005.

E.2 Articles under Review

O.A. McLoughlin, L.W. Gill (2005) A Comparison of Three Small-scale Solar Disinfection Reactors using both Natural and Simulated Sunlight.

E.3 Conference Papers and Posters

O. A. McLoughlin, P. Fernandez, W. Gernjak, S. Malato, L.W. Gill (2003) Feasibility of solar disinfection using low cost compound parabolic collectors. *3rd Scientific Meeting of the Spanish Society of Chromatography and Related Techniques.* Almería, Spain 19-21 November 2003.

O. A. McLoughlin, S. Kehoe, K. McGuigan, L.W. Gill (2004). Parameters needed for the design of low cost continuous flow solar disinfection systems. In, *Proceedings of the IWA Specialist Group Conference on Water & Wastewater Management for Developing Countries (IWA)*. Victoria Falls, Zimbabwe: 28-30th July 2004.

O. A. McLoughlin, L.W. Gill (2004). Photocatalytic disinfection of drinking water : a comparison of three small-scale reactors. In, *Proceedings of the3rd European Meeting on Solar Chemistry and Solar Photocatalysis: Environmental Applications (SPEA 3)*. Barcelona, Spain. 30 June-2 July 2004.

O. A. McLoughlin, S.C. Kehoe, K. McGuigan, L.W. Gill (2004) A Comparison of Three Small-scale Solar Disinfection Reactors using both Natural and Artificial Sunlight. *International Water Association 4th World Water Congress*, Marrakesh, Morroco 19-23 September 2004.

O.A. McLoughlin, L.W. Gill (2005) Continuous Flow Solar Disinfection. *Solar Disinfection of Drinking Water Workshop*, Dublin, Ireland, 1st and 2nd April 2005.

E.4   Other Publications

L.W. Gill, O.A.McLoughlin, K.G.McGuigan, E.F. Duffy, S.C.Kehoe, F. Al Touati, W.Gernjak, I. Oller, P. Fernandez, S.Malato (2004). Solar disinfection of contaminated water: a comparison of three small-scale continuous flow reactors. *Improving Human Potential Programme access to the research infrastructures activity – transnational access to the Plataforma Solar de Almería*. Research results at Plataforma Solar de Almería within the Year 2003 access campaign. Serie Ponencias. [ISBN 84-7834-474-8].

K.G. McGuigan, E.F. Duffy, F. Al Touati, S.C. Kehoe, O.A. McLoughlin, L.W. Gill, W.Gernjak, I. Oller, M.I. Maldonado, S. Malato, R.H. Reed (2004). Inactivation of bacterial contaminants in drinking water using a novel batch-process TiO_2-assisted solar photocatalytic disinfection (SPC-DIS) reactor for use in developing countries. *Improving Human Potential Programme access to the research infrastructures activity – transnational access to the Plataforma Solar de Almería*. Research results at

Plataforma Solar de Almería within the Year 2003 access campaign. Serie Ponencias [ISBN 84-7834-474-8].